

The image shows a cross-section of soil. The top layer is dark brown and appears to be a topsoil layer. Below it is a layer of soil that has cracked and is tinted with a vibrant blue color. The cracks are irregular and form a network across the surface. The bottom layer is a darker, more textured material, possibly a subsoil or a layer of organic matter. The overall appearance is that of a soil profile with a distinct blue-tinted layer.

**Dissertation**

**Modelling the role of temperature and  
soil moisture on soil organic carbon  
decomposition**

**Marleen Pallandt  
2024**

# **Modelling the role of temperature and soil moisture on soil organic carbon decomposition**

## **Dissertation**

With the aim of achieving the degree of  
Doctor of Natural Sciences (Dr. rer. nat.)  
at the Faculty of Biology, Chemistry and Earth Sciences

Submitted by  
Marga Helene Pallandt  
born Marga Helene Vermeulen in Scherpenzeel, the Netherlands

Bayreuth, 2024



The work described in this thesis was prepared from April 2018 to March 2024 under the supervision of Prof. Dr. Holger Lange at the University of Bayreuth and the Norwegian Institute for Bioeconomy Research. The research was carried out at the Max Planck Institute for Biogeochemistry in Jena and was co-supervised by Bernhard Ahrens, Marion Schrumpf, Sönke Zaehle and Markus Reichstein.

This work was supported by funding from the Norwegian Research Council through grant no. RCN 255 061 (MOisture dynamics and CARbon sequestration in BOREal Soils).

This is a full reprint of the thesis submitted to obtain the academic degree of Doctor of Natural Sciences (Dr. rer. nat.) and approved by the Faculty of Biology, Chemistry and Geosciences of the University of Bayreuth.

Form of the thesis: cumulative thesis

Date of submission: 02.04.2024

Date of defence: 25.09.2024

Acting Dean: Prof. Dr. Cyrus Samimi

Doctoral Committee:

Prof. Dr. Holger Lange	(reviewer)
Prof. Dr. Eva Lehndorff	(reviewer)
JProf. Dr. Lisa Hülsmann	(Chairman)
Prof. Dr. Werner Borke	



Cover art generated using Midjourney v6.0 generative artificial intelligence with the following prompt: “A soil profile with red elements indicating heat and blue elements indicating water, soil earth”. Only the cover art image was generated using generative artificial intelligence, which was not used in any other part of this thesis.



# Acknowledgements

---

Writing a PhD thesis is never an easy journey. But after many years, full of challenges and (personal) growth, I am relieved to finally submit this PhD thesis. Many, many people supported me along the way, and while I cannot possibly mention you all individually, please know I appreciate your contribution no matter how small it seemed.

My PhD supervision team consisted of five members, and I want to express my gratitude to them all. First of all, I am very grateful for the continuous support and encouragement I received from my direct mentor and supervisor, Bernhard. Thank you for your reliability and expertise, and for making me laugh while doing science together. Even when I felt completely stuck, you kept a positive attitude, encouraged me, and helped me to find the answers on my own. I am proud to be your first PhD student, and very confident that those who follow will have an equally positive experience! Together with Marion and Holger, you intensely supervised my work during the final months to ensure I kept on track towards a tight deadline. Thank you for everything! Marion, thank you for your wonderful person-oriented supervision, discussions, help editing manuscripts, and warm inclusion in your working group. You inspire me and other women in STEM with your science and leadership. Thank you for being there all the way, and for sharing your (love of) chocolate with me. Holger, I highly appreciate visiting you in Norway multiple times. Thank you for your great hospitality and sharing your scientific expertise, for including me in fieldwork, your group activities and family life. Thank you Markus and Sönke for initially inviting me to join your groups as a guest researcher, for being a member of my PhD advisory committee, and your overall support and constructive feedback during meetings. Markus, thank you for always supporting my participation in (international) workshops and conferences, it helped me build a great scientific network over the years.

Throughout my PhD, the guidance and support from Steffi, John and Stefanie at the IMPRS-gBGC graduate school was amazing, thank you so much for everything. Supplementing the financial support from the MPI for Biogeochemistry, I am grateful for funding I received from the Norwegian Research Council through grant no. RCN 255 061 (MOisture dynamics and CARbon sequestration in BOREal Soils).

While quite some time has passed since leaving Wageningen, I would never have started my career in science if it wasn't for my earlier mentor Bart Kruijt. Bart, thank you for believing in me as a qualified scientist, for always standing by me when things got bad, and for helping me develop a wide research network. I still have many scientist friends from these first meetings! And although we were unable to complete our journey together, I feel your initial encouragement still positively resonates in my current career.

To my dearest vriendinnetjes, thank you so much! Although you live far away our friendship remains strong. Thank you for your love, support, cards & chocolate supplies by mail, and (long!) video calls. Many friends and social groups helped me relax and unwind after long



work days: A big hug and thank you to all my (former) volleyball team members and trainers at WaHo/SV Schott/SV Pädagogick, various tabletop RPG groups, as well as my wonderful, quirky, smart friends and colleagues from Jena and Wageningen incl. the amazing international Koskesh ladies, Unitas members, and many, many more. I (will) miss you all so much!

I also want to thank my family. Mam, pa, my brothers and sister, as well as Fons and Mathilda, my brothers and sisters in law, Inky and Paul, my cool and cute nieces and nephews. You were there for me during this long journey and never wavered your support. I love you all very much.

So... It has come to this, Martijn ;) I cannot accurately express in words just how wonderful it is to have you as my amazing partner. You love and fully accept me, understand my needs (sometimes even before I do), and support both my personal and scientific ambitions. Thank you for being my rock, for believing in me, and for sometimes reminding me that yes, I can do it! You and Alex mean the absolute world to me, and I am so proud we finally completed this chapter of our lives together, while we grew as a loving family.

# Table of contents

---

<b>Abstract</b> .....	<b>1</b>
<b>Zusammenfassung</b> .....	<b>3</b>
<b>Chapter 1 – General introduction</b> .....	<b>5</b>
1.1 Importance of SOC stocks for the terrestrial C cycle.....	5
1.2 Importance of temperature and soil moisture for microbial SOC decomposition.....	5
1.3 Process representation in SOC decomposition models.....	7
1.3.1 Traditional SOC decomposition models.....	8
1.3.2 Microbially explicit SOC models.....	8
1.3.3 Depth-dependent process representation of SOC dynamics.....	9
1.4 Research objectives and questions.....	11
<b>Chapter 2 – Study design and key findings</b> .....	<b>12</b>
2.1 Study I: Modelling soil moisture controls on soil respiration through substrate and oxygen availability.....	12
2.2 Study II: Vertically divergent responses of SOC decomposition to soil moisture in a changing climate.....	15
2.3 Study III: Drought counteracts soil warming more strongly in the subsoil than in the topsoil according to a vertical microbial SOC model.....	19
<b>Chapter 3 – Discussion and outlook</b> .....	<b>23</b>
3.1 Changes in soil moisture can mitigate or accelerate SOC decomposition rates.....	23
3.2 Interactions between temperature, soil moisture and substrate availability in a dynamic system.....	26
3.3 Importance of vertical process-representation in SOC decomposition models.....	28
3.4 Conclusions.....	29
3.5 Outlook.....	30
<b>References</b> .....	<b>33</b>
<b>Individual and co-author contributions to each study</b> .....	<b>42</b>
<b>Study I</b> .....	<b>44</b>
<b>Study II</b> .....	<b>64</b>
<b>Study III</b> .....	<b>104</b>
<b>List of publications</b> .....	<b>132</b>
<b>Eidesstattliche Versicherungen und Erklärungen</b> .....	<b>133</b>

# Abstract

---

Soil organic carbon (SOC) is the largest terrestrial carbon (C) pool, and even small relative changes in SOC stocks have large consequences for the future carbon-climate feedback. Microbes are the main actors in the decomposition of litter and SOC, and microbial decomposition rates are strongly affected by soil temperature and soil moisture. Yet, large-scale model representations of the sensitivity of SOC to soil moisture, through microbial decomposition and interactions with mineral surfaces, are largely empirical to semi-empirical and uncertain. Therefore, there is a strong need for soil biogeochemistry models that reflect current process understanding to accurately represent the response of SOC to environmental change. Higher temperatures can promote microbial decomposition and increase soil respiration rates, but the response to soil moisture is less certain. Soil moisture variations confound temperature effects on soil respiration, lowering the high apparent temperature sensitivity values that can be observed under optimal soil moisture conditions as soils dry out or get wetter. Additionally, many soil properties such as SOC content, microbial biomass and organo-mineral associations vary with depth, while soil columns may not evenly dry out or become wetter under a changing climate. This vertical heterogeneity in soils is largely ignored in most current model SOC decomposition modelling approaches and warrants further research.

This thesis investigates how soil moisture and soil temperature changes can affect microbial SOC decomposition by applying a mechanistic model that disentangles their combined effects along a vertical soil gradient. In the first study, a simple model (the DAMM model) is introduced to describe the interactions between soil moisture, soil temperature and microbial decomposition and apply it to site-level soil respiration measurements. We show that in addition to soil temperature, the inclusion of soil moisture controls are vital to correctly model observed soil respiration rates, especially after rewetting events, and discuss which soil moisture control is dominant under different soil moisture conditions. The second study investigates differences in top- and subsoil moisture changes as simulated by global land surface models and how these changes affect respiration rates under a warming climate. The key finding is that the inclusion of soil moisture controls can have diverging effects on both the speed and direction of projected decomposition rates (up to  $\pm 20\%$ ), compared to a temperature-only approach. In the topsoil, the majority of these changes is driven by substrate availability. In deeper soil layers, oxygen availability plays a relatively stronger role. The research illustrates that vertical model representations of SOC dynamics will be crucial, due to the diverging responses of top- and subsoil layers to climatic drivers.

The third study of this thesis describes the dynamic interactions between soil moisture, soil temperature and substrate within a vertically explicit microbial SOC decomposition model. We focus on the depolymerisation of litter and microbial residues at different soil depths, and its sensitivities to soil warming and different drought intensities. The main finding is that soil warming leads to long-term SOC losses, but that depending on SOC composition and its

associated temperature sensitivities, these losses can be either reduced or further accelerated, especially in the subsoil. Droughts can alleviate the effects of soil warming and reduce SOC losses, and even lead to SOC gains. Furthermore, a combination of drought and the use of different temperature sensitivities for the half-saturation constants associated with the breakdown of litter or microbial residues can have counteracting effects on the overall SOC decomposition rates. While absolute SOC changes driven by soil warming and drought are highest in the topsoil, SOC in the subsoil is more sensitive to change through the interactions between the half-saturation constant, temperature and soil moisture changes, and mineral-associated SOC.

Summarising, this thesis provides new insights into the complex feedback between climate change and SOC dynamics to aid the further development of process-based soil models. In particular, the workI demonstrates that the next generation of models would benefit from including vertical representations of soil processes, with microbial dynamics and moisture functions that reflect our mechanistic understanding of the effects of soil drying and wetting. Incorporating such models into coupled climate or land surface models will enable us to study the effects and potential feedbacks of climate change on SOC stocks and CO<sub>2</sub>-release to the atmosphere.

# Zusammenfassung

---

Organischer Bodenkohlenstoff (SOC) ist der größte terrestrische Kohlenstoffpool, und selbst kleine relative Veränderungen der SOC-Bestände haben große Auswirkungen auf die künftige Kohlenstoff-Klima-Rückkopplung. Mikroben sind die Hauptakteure bei der Zersetzung von Streu und SOC, und die mikrobiellen Zersetzungsraten werden stark von Bodentemperatur und Bodenfeuchtigkeit beeinflusst. Dennoch sind großmaßstäbliche Modelldarstellungen der Empfindlichkeit von SOC gegenüber der Bodenfeuchtigkeit durch mikrobielle Zersetzung und Wechselwirkungen mit mineralischen Oberflächen weitgehend empirisch bis halbempirisch und unsicher. Daher besteht ein dringender Bedarf an biogeochemischen Bodenmodellen, die das aktuelle Prozessverständnis widerspiegeln, um die Reaktion von SOC auf Umweltveränderungen genau darzustellen. Höhere Temperaturen können die mikrobielle Zersetzung fördern und die Atmungsrate des Bodens erhöhen, aber die Reaktion auf die Bodenfeuchtigkeit ist weniger sicher. Schwankungen der Bodenfeuchtigkeit vermindern die Auswirkungen der Temperatur auf die Bodenatmung und senken die scheinbar hohen Werte für die Temperaturempfindlichkeit, die bei optimaler Bodenfeuchtigkeit beobachtet werden können, wenn die Böden austrocknen oder feuchter werden. Darüber hinaus variieren viele Bodeneigenschaften wie der SOC-Gehalt, die mikrobielle Biomasse und die organisch-mineralischen Assoziationen mit der Tiefe, während die Bodensäulen unter einem sich ändernden Klima nicht gleichmäßig austrocknen oder feuchter werden. Diese vertikale Heterogenität in Böden wird in den meisten aktuellen Modellierungsansätzen für den SOC-Abbau weitgehend ignoriert und bedarf weiterer Forschung.

In dieser Arbeit wird untersucht, wie sich Änderungen der Bodenfeuchte und der Bodentemperatur auf den mikrobiellen SOC-Abbau auswirken können. Dazu wird ein mechanistisches Modell angewandt, das ihre kombinierten Auswirkungen entlang eines vertikalen Bodengradienten entschlüsselt. In der ersten Studie wird ein einfaches Modell (das DAMM-Modell) zur Beschreibung der Wechselwirkungen zwischen Bodenfeuchte, Bodentemperatur und mikrobiellem Abbau eingeführt und auf Messungen der Bodenatmung an einem Standort angewendet. Wir zeigen, dass neben der Bodentemperatur die Einbeziehung der Bodenfeuchte entscheidend ist, um die beobachteten Bodenatmungsraten korrekt zu modellieren, insbesondere nach Wiederbefeuchtungseignissen, und erörtere, welcher Prozess bei unterschiedlichen Bodenfeuchtebedingungen dominiert. Die zweite Studie untersucht die Unterschiede in den von globalen Landoberflächen-Modellen simulierten Veränderungen der Feuchte im Ober- und Unterboden und wie sich diese Veränderungen auf die Atmungsraten in einem wärmeren Klima auswirken. Das wichtigste Ergebnis ist, dass die Einbeziehung der Bodenfeuchte sowohl die Geschwindigkeit als auch die Richtung der prognostizierten Zersetzungsraten unterschiedlich beeinflussen kann (bis zu  $\pm 20\%$ ), verglichen mit einem reinen Temperaturansatz. Im Oberboden wird der Großteil dieser Veränderungen durch die Substratverfügbarkeit bestimmt. In tieferen Bodenschichten spielt die Sauerstoffverfügbarkeit eine relativ stärkere Rolle. Die Untersuchung zeigt, dass

vertikale Modelldarstellungen der SOC-Dynamik aufgrund der unterschiedlichen Reaktionen der oberen und unteren Bodenschichten auf klimatische Faktoren von entscheidender Bedeutung sind.

Die dritte Studie dieser Arbeit beschreibt die dynamischen Wechselwirkungen zwischen Bodenfeuchte, Bodentemperatur und Substrat in einem vertikal expliziten mikrobiellen SOC-Umsatzmodell. Wir konzentrieren uns auf die Depolymerisation von Streu und mikrobiellen Resten in verschiedenen Bodentiefen und ihre Sensitivität in Bezug auf Bodenerwärmung und unterschiedlichen Trockenheitsintensitäten. Das Hauptergebnis ist, dass die Bodenerwärmung zu langfristigen SOC-Verlusten führt, dass aber je nach SOC-Zusammensetzung und den damit verbundenen Temperaturempfindlichkeiten diese Verluste entweder verringert oder weiter beschleunigt werden können, insbesondere im Unterboden. Dürren können die Auswirkungen der Bodenerwärmung abmildern und die SOC-Verluste verringern und sogar zu SOC-Gewinnen führen. Darüber hinaus kann eine Kombination aus Trockenheit und der Verwendung unterschiedlicher Temperaturempfindlichkeiten für die mit dem Abbau von Streu oder mikrobiellen Rückständen verbundenen Halbsättigungskonstanten gegenläufige Auswirkungen auf die Gesamtabbauraten des SOC haben. Während die absoluten SOC-Änderungen aufgrund von Bodenerwärmung und Trockenheit im Oberboden am stärksten sind, reagiert der SOC im Unterboden aufgrund der Wechselwirkungen zwischen der Halbsättigungskonstante, Temperatur- und Bodenfeuchtigkeitsänderungen und dem mineralassoziierten SOC empfindlicher auf Veränderungen.

Zusammenfassend lässt sich sagen, dass diese Arbeit neue Erkenntnisse über die komplexen Rückkopplungen zwischen Klimawandel und SOC-Dynamik liefert, die die weitere Entwicklung prozessbasierter Bodenmodelle unterstützen. Insbesondere zeigt die Arbeit, dass die nächste Generation von Modellen von der Einbeziehung vertikaler Darstellungen von Bodenprozessen mit mikrobieller Dynamik und Feuchtigkeitsfunktionen profitieren würde, die unser mechanistisches Verständnis der Auswirkungen von Bodentrocknung und -befeuchtung widerspiegeln. Die Einbindung solcher Modelle in gekoppelte Klima- oder Landoberflächenmodelle wird es uns ermöglichen, die Auswirkungen und potenziellen Rückkopplungen des Klimawandels auf die SOC-Bestände und die CO<sub>2</sub>-Freisetzung in die Atmosphäre zu untersuchen.

# Chapter 1 – General introduction

---

## 1.1 Importance of SOC stocks for the terrestrial C cycle

An increase in atmospheric carbon dioxide (CO<sub>2</sub>) has been identified as the main cause of global warming (IPCC, 2023). Soil organic carbon (SOC), as the largest terrestrial component in the global carbon (C) cycle, has a large influence on the accumulation of CO<sub>2</sub> in the atmosphere, and thereby on climate change. Soil respiration, the C flux from the soil into the atmosphere consisting of an autotrophic and a heterotrophic component, is currently estimated to be 68–101 Pg C yr<sup>-1</sup> globally (Jian et al., 2021a). This makes it the largest C flux from the land surface into the atmosphere, and up to 10 times greater than the current estimate of global anthropogenic atmospheric C emissions, which is around 9.6 Pg C yr<sup>-1</sup> (Friedlingstein et al., 2023). Heterotrophic respiration (R<sub>h</sub>) is produced by soil microbes, who feed on existing SOC stocks as well as fresh plant litter inputs to the soil. Global estimates of R<sub>h</sub> fluxes are highly uncertain, but considered the dominant C loss from soils at an estimated global mean loss of 47.2 - 58.9 Pg C yr<sup>-1</sup> (Hashimoto et al., 2015; Jian et al., 2021b; Tang et al., 2020; Warner et al., 2019).

Global SOC stock estimates range between ~650 to ~2400 Pg C until one meter depth (Fan et al., 2022). Given the enormous size of SOC stocks, especially in northern and equatorial regions (Crowther et al., 2019), even small relative SOC stock changes can have large consequences for future C release to or removal from the atmosphere (Davidson, 2020; Kirschbaum, 2006). Climate change is affecting SOC stocks by changing the complex balance between C inputs to and outputs from the soil. Therefore, understanding SOC dynamics and its sensitivities to ongoing global climate change is crucial to understand the Earth's current and future C balance. Whether soils will become a future C source or sink, is largely determined by changes in R<sub>h</sub>. Based on recent data-driven and modelled estimates, R<sub>h</sub> is expected to increase in the future mainly as a result of expected increases in plant gross primary productivity (GPP, causing increased soil C inputs), and as a result of higher C mineralisation rates by microbes (Bond-Lamberty et al., 2018). Soil microbes are the primary agents of SOC decomposition and heavily influence SOC stocks: On the one hand, they are responsible for the loss of SOC through R<sub>h</sub>, while on the other hand, microbial residues are recognised as important precursors for the formation of stable, mineral-associated SOC (Cotrufo et al., 2013; Liang et al., 2017; Xiao et al., 2023).

## 1.2 Importance of temperature and soil moisture for microbial SOC decomposition

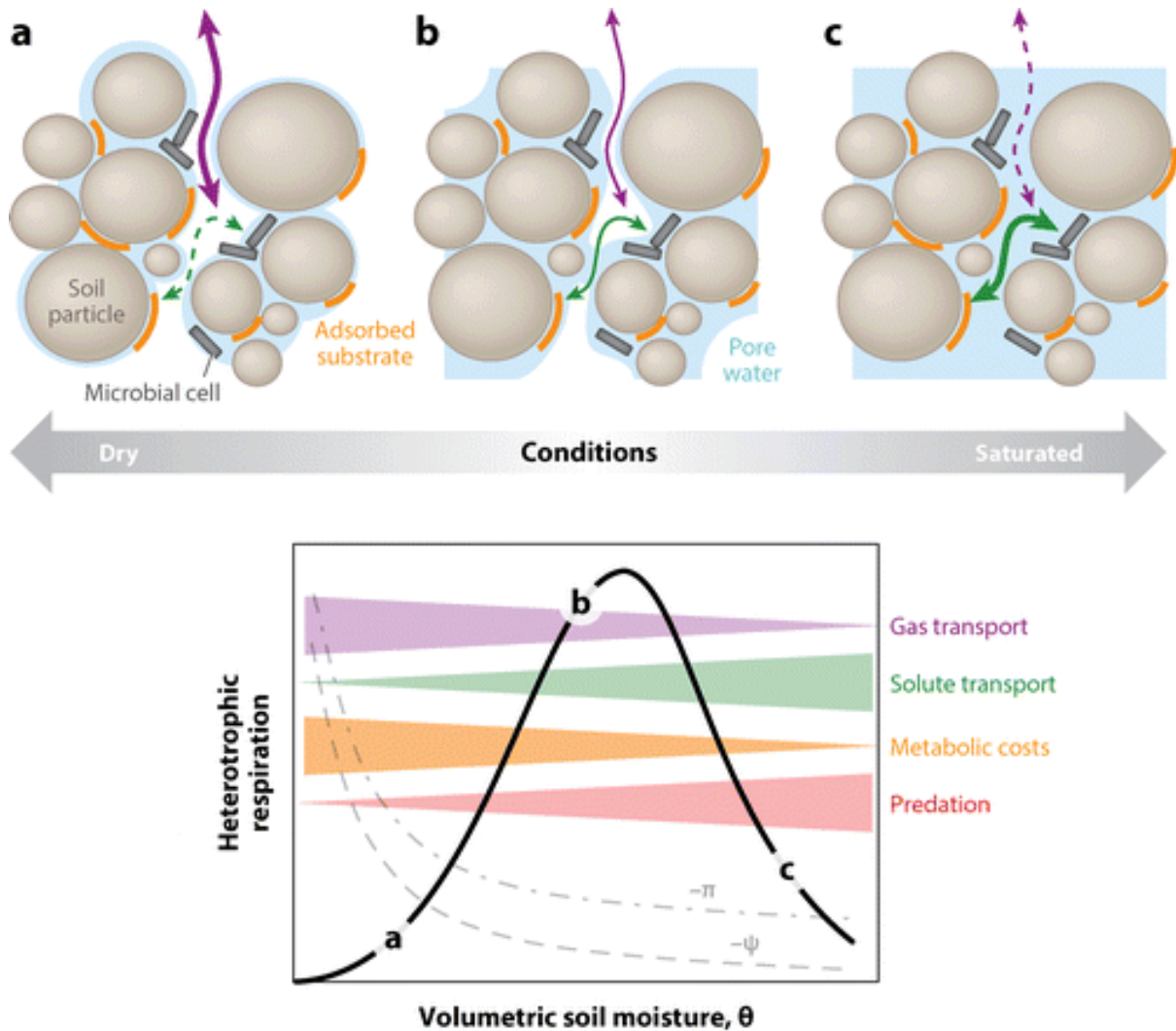
Warming is expected to increase SOC decomposition rates and lead to SOC losses through increased microbial activity (Walker et al., 2018). Microbial decomposition rates increase with temperature until a certain maximum where enzymes start to break down (Hochachka &

Somero, 2002; Nottingham et al., 2016), but only if sufficient soil moisture is available (Sierra et al., 2017). Soil moisture is extremely important for SOC dynamics as it affects soil physicochemical relationships in all phases: In solid form (e.g. reducing vertical transport and creating drought conditions in frozen soils), in liquid form (e.g. by reducing heat fluctuations, vertical transport, and by influencing soil microbes) and in gaseous form (e.g. many soil organisms depend on the high relative humidity of soil). Soil moisture also highly impacts microbial dynamics and thereby  $R_h$  (Fig. 1, Schimel, 2018; and Moyano et al., 2013): In dry soils, water connectivity in soil pores is poor and results in lower substrate availability for microbial decomposition. Additionally, microbes may experience osmotic stress under dry soil conditions and reduce their activity or die (Manzoni & Katul, 2014; Schimel, 2018). As a result,  $R_h$  rates are low ('a' in Fig. 1).

In very wet soils, soil pores become water-filled, restricting the diffusion of oxygen towards the microbial surface and decreasing  $R_h$  rates ('c' in Fig. 1), because oxygen diffusion in the gas phase is the main pathway to provide the necessary electron acceptor for organic C oxidation (Yan et al., 2016). Between very dry and very wet soil moisture conditions, an optimum exists where the availability of decomposable substrates as well as oxygen concentrations are ideal for microbial SOC decomposition, leading to high  $R_h$  rates ("b" in Fig. 1, Skopp et al., 1990). At this soil moisture optimum, temperature is the dominant driver of SOC decomposition rates (Sierra et al., 2017).

Earth system models (ESMs) predict that soils will warm by a global mean of  $\sim 4.5$  °C by the end of the century under the RCP 8.5 emission scenario (Soong et al., 2020), but projected future changes in soil moisture are more diverse (Berg et al., 2017) and highly dependent on anthropogenic greenhouse gas and aerosol emissions (Y. Wang et al., 2022). Uncertainty in soil moisture projections between ESMs is large, especially for near-surface soil moisture (Berg et al., 2017; Berg & Sheffield, 2018; Cheng et al., 2017; Lu et al., 2019; Yuan & Quiring, 2017). Additionally, soil moisture may not change in the same direction for surface and deeper soil layers (Fig. 2 in Berg et al., 2017). Until now, the temperature sensitivity of SOC decomposition has received a lot of attention, whereas the sensitivity to changes in soil moisture, especially in the deep soil, has been relatively understudied (Hicks Pries et al., 2023). Given the importance of soil moisture for SOC dynamics, and the considerable feedback for SOC stock changes to climate warming, it is imperative to improve our understanding of soil moisture and soil temperature controls on SOC decomposition, and to study their impacts separately as well as simultaneously.





Schimel JP. 2018. *Annu. Rev. Ecol. Evol. Syst.* 49:409–32

**Figure 1:** Moisture effects on soil microbial activity under conditions ranging from (a) dry to (c) saturated. Figure and caption taken directly from Schimel et al. (2018), who adapted it with permission from Moyano et al. (2013). Black rectangles represent microbial cells, and orange lines represent substrates adsorbed onto soil particles (grey spheres). The bottom panel shows the relationship between heterotrophic respiration ( $R_h$ , black line) and moisture results from interacting effects, including diffusion and physiological, biochemical, and ecological processes.  $\psi$  indicates the soil water potential, and  $\pi$  is the cell osmotic potential that would allow maintaining a stable turgor pressure as  $\psi$  declines.  $\psi$  and  $\pi$  have negative values; to plot them on a positive axis, they are plotted as their negative values. Reprinted with permission under a Copyright Clearance Center license agreement (ID 1448651-1). © 2018 Annual Reviews, Inc.

### 1.3 Process representation in SOC decomposition models

Earth system models are very important tools to understand and predict the global C cycle in light of climatic change. At the moment, the modelled response of SOC stocks to global change is diverse and the largest source of uncertainty in ESMs (Ito et al., 2020; Todd-Brown et al., 2013; Varney et al., 2023). Therefore, it is vital to improve our understanding and representation of the key processes determining SOC dynamics in models.

### 1.3.1 Traditional SOC decomposition models

Traditionally, SOC decomposition models are highly empirical and consist of various “fast”, “slow” and/or “passive” C pools with their own intrinsic turnover rates, using first-order decomposition rates adopted from the CENTURY approach (Parton et al., 1987). In these models, turnover is only proportional to the size of each respective SOC pool. They are still widely used; the majority of SOC models used in the Carbon Model Intercomparison Project (CMIP) 6 use a first-order representation of the soil with two or more C pools (Table 1 in Varney et al., 2023). The temperature sensitivity of these C pools is modelled using either a monotonic Arrhenius-type or a  $Q_{10}$  (the rate of increase for every 10 °C rise in temperature) function, so that respiration rates constantly rise with soil warming, and their soil moisture sensitivity is either not included at all, or modelled empirically with linear or optimum relationships (Sierra et al., 2015; Varney et al., 2023). Various models include an interaction with the nitrogen (N) cycle, but not all of them consider the vertical distribution of the soil carbon profile (Todd-Brown et al., 2013; Varney et al., 2023), which is important for long-term dynamics of SOC stabilisation (Ahrens *et al.*, 2015). So while these empirical analytical models could potentially match current-day observations, in particular with regard to long-term SOC dynamics (Parton *et al.*, 2015), there is a mismatch between these conceptual C pools and measurable SOC fractions (Abramoff et al., 2018). Additionally, due to the lack of process-based descriptions of SOC dynamics, it is difficult to assign the sensitivities of individual SOC decomposition processes to changes in climatic (e.g. temperature, soil moisture) and environmental (e.g. litter inputs) drivers.

### 1.3.2 Microbially explicit SOC models

Over the last decades, the recognition of soil microbes as active agents in SOC formation, preservation and loss (Cotrufo & Lavelle, 2022; Crowther et al., 2019), as well as advancements in process-understanding of SOC dynamics, have led to the development of soil models that take into account microbial (enzymatic) processes and sometimes organo-mineral interactions (e.g. Abramoff et al., 2017; Sulman et al., 2014; Wieder et al., 2014; Zhang et al., 2022). In these microbially explicit models, nonlinear kinetics describe the various feedbacks between microbes, SOC substrate availability, and sometimes mineral adsorption and desorption processes. Decomposition rates are limited as a function of SOC substrate availability (forward kinetics) or microbial biomass (reverse kinetics, Le Noë et al., 2023; Tang & Riley, 2019). The representation of temperature controls on microbial SOC decomposition rates is generally done using an Arrhenius-type function to describe a maximum reaction rate ( $V_{\max}$ ) with the use of an activation energy for the substrate of interest (Arrhenius, 1889). Moisture controls to describe the interactions between microbial activity and the diffusion of C substrates, extracellular enzymes, and/or oxygen are approached with e.g. forward and/or reverse Michaelis-Menten kinetics, Monod-type kinetics, or the Equilibrium Chemistry Approximation (ECA) kinetics (summarised in Tang & Riley, 2019).

Microbes produce extracellular enzymes to break down soil organic matter. Some models explicitly simulate the microbial production (and sometimes diffusion) of extracellular enzymes to degrade organic matter and maximise microbial growth (e.g. Abramoff et al.,

2017; Allison et al., 2010; Manzoni et al., 2016; Moorhead et al., 2012; Schimel & Weintraub, 2003; Tang & Riley, 2014). Other models simulate microbial enzyme production implicitly by calculating the amount of C substrates, proportional to the microbial biomass, which can diffuse to a microbial surface (e.g. Ahrens et al., 2015; Davidson et al., 2012; Robertson et al., 2019; Sihi et al., 2018a). The diffusion of substrates or enzymes through the soil matrix depends on soil moisture, which can be included as volumetric water content or soil matric potential (Ghezzehei et al., 2019; Runkles, 1956; Skopp et al., 1990). Many enzymes that break down substrates are assumed to follow Michaelis-Menten kinetics, where the reaction rate (V) is defined as:

$$V = V_{\max}[S]/(K_m + [S]) \quad (1)$$

Where  $V_{\max}$  is the maximum rate,  $[S]$  is the substrate concentration and  $K_m$  is the half-saturation constant, i.e. the value at which  $V$  is 50% of  $V_{\max}$ . Both  $V_{\max}$  and  $K_m$  are temperature sensitive (Atkin & Tjoelker, 2003; Berry & Raison, 1981). If, similar to  $V_{\max}$ ,  $K_m$  increases with temperature, the reaction rate would be reduced because  $K_m$  appears in the denominator of the equation. In other words, reaction rates may slow down with increasing temperatures, especially at lower  $[S]$ . This counteracting temperature effect has been identified as a potentially important factor for future SOC dynamics (Davidson et al., 2006; Davidson & Janssens, 2006). These modelling studies, however, did not consider a dynamic substrate pool, i.e. there is no interaction between the microbial pool (with its own growth and turnover rates) and the in- and outputs of different C substrate pools. A thorough search of the relevant literature on microbially explicit SOC decomposition models to date yielded no studies in which these interactions between the microbial pool and dynamic substrate pools were explored. Firstly, because of a lack of data on the temperature sensitivity of  $K_m$ , and secondly, because most models do not consider the temperature sensitivity of  $K_m$  and only assign a temperature sensitivity to  $V_{\max}$ , usually in the form of a  $Q_{10}$  value or activation energy (Wang et al., 2012).

A recent study reported the temperature sensitivities of different extracellular enzymes involved in the degradation of soil organic matter (Allison et al., 2018). In this study, the temperature sensitivities of the maximum reaction velocity ( $V_{\max}$ ) as well as the half-saturation constant ( $K_m$ ) were measured for nine different enzymes which are representative of degrading various SOC substrate types. Temperature sensitivities, expressed as  $Q_{10}$  values, ranged between 1.48 and 2.25 for  $V_{\max}$ , and between 0.71 and 2.80 for  $K_m$ . The latter values are particularly important, because values above 1 would lower the reaction rate (V) with increasing temperatures, whereas values below one would further accelerate them. This dataset allowed me to explore the interactions between temperature, soil moisture changes and SOC substrate concentration in a dynamic model in more detail for this PhD thesis.

### 1.3.3 Depth-dependent process representation of SOC dynamics

Carbon (C) is not distributed evenly within soil profiles: Globally, around 1500 Pg C is stored in the first metre, but roughly 50% of this C resides in the top 30 cm (e.g. Blume et al., 2016).

The vertical distributions of microbial biomass and SOC content are highly correlated, but the relative proportions of microbial biomass (compared to total microbial biomass down to 1 m) can be higher than that of SOC (compared to total SOC) in the top 10 cm (Sun et al., 2021). In general, the topsoil is more directly influenced by climate, land use and vegetation, whereas the deep soil is more influenced by mineral properties (Fig. 2, Hicks Pries et al., 2023). In what Hicks Pries et al. (2023) call the ‘wedge’ concept, it becomes apparent that the influence of biotic factors such as plant (root) litter inputs and microbial activity decreases with depth, whereas the importance of organo-mineral interactions increases with depth. The stabilisation of SOC on mineral surfaces is very important for SOC dynamics, because SOC may be protected from rapid microbial decomposition when associated with minerals. Microbes and mineral surfaces essentially compete for available SOC, and in the deep soil more SOC is mineral-associated and thereby less available to microbes. This is an additional C resource limitation on microbial decomposition, in addition to substrate diffusion limitation through soil moisture availability. The sorption and desorption rates of SOC to and from mineral surfaces are also sensitive to changes in temperature and soil moisture (Ahrens et al., 2020; Wang et al., 2013).

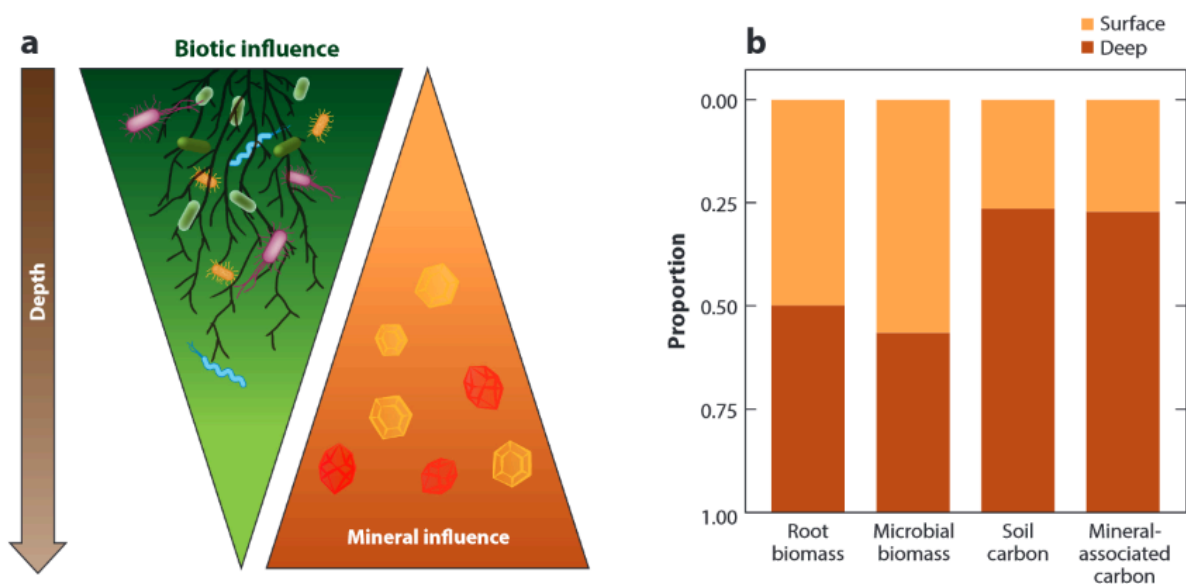


**Figure 2.** Changes in biotic versus mineral influences with soil depth, taken directly from Hicks Pries et al. (2023). a) Biotic influence (green wedge) declines with depth due to reduced plant (root) litter inputs and microbial activity with depth. Mineral influence (brown wedge) increases with depth as a larger proportion of SOC is associated with soil mineral surfaces (higher mineral-associated carbon (MAOC)). b) The different proportions of root and microbial biomass, and the amount of SOC and MAOC found in surface (0 - 20 cm depth) versus deep soils (> 20 cm depth). Reprinted with permission under the CC BY 4.0 licence: <https://creativecommons.org/licenses/by/4.0/deed.en#ref-appropriate-credit>.

Most SOC models in ESMs do not consider the vertical distribution of SOC stocks or mineral-organic associations, even though vertically explicit models have been around since the late 1970’s (summarised by Ahrens et al., 2015). As a result, the vertical distribution of root litter inputs, the vertical transport of C through leaching and bioturbation and their effects on SOC dynamics have been ignored. Furthermore, these models typically do not consider soil temperature and moisture interactions over a vertically resolved SOC profile,

and as a result fail to capture observed climate sensitivities of soil carbon turnover times (Koven et al., 2013, 2017). Even recently developed microbially explicit models (DAMM-MCNIP by Abramoff et al., 2017; e.g. CORPSE by Sulman et al., 2014; MIMICS by Wieder et al., 2014) typically only consider one soil depth, even though so many soil properties change with depth.

To improve our understanding of long-term SOC dynamics to climate change, models are needed that allow us to test the sensitivity of SOC to changes in soil moisture and temperature while considering the vertical soil profile. In the final study of this thesis, we used a newly developed SOC decomposition model which reconciles many of the mechanistic concepts introduced in this chapter. The Jena Soil Model (JSM, Yu et al., 2020) is vertically resolved, microbially explicit and includes representations of organo-mineral interactions, as well as mechanistic descriptions of the various physiological processes affecting microbial SOC decomposition. When calibrated for specific sites, the model simulates SOC stocks and microbial biomass well, and was tested for its ability to simulate the interactions of nutrient availability with SOC dynamics (Yu et al., 2020, 2023). As such, it provides a novel framework for this PhD thesis in which the individual and combined effects of soil moisture and temperature changes on microbial SOC dynamics can be studied.

## **1.4 Research objectives and questions**

The general aim of this thesis is to better understand the effects that temperature and soil moisture changes have on microbial SOC decomposition, and to explore what their potential individual and combined effects are on SOC dynamics in a changing climate. To aid the further development of process-based SOC models, different approaches suitable for model implementation were investigated to answer the following research questions:

- 1. Can soil moisture mitigate or exacerbate temperature-driven changes in SOC decomposition rates?*
- 2. How do soil moisture and temperature interact with SOC substrates and subsequently affect microbial SOC decomposition rates?*
- 3. How do soil moisture and soil temperature effects on SOC decomposition vary along a vertical soil gradient?*

Chapter 2 provides a detailed summary with the key findings of the three studies included in this PhD thesis, and highlights the connections between the individual studies. Chapter 3 answers the research questions and discusses the main findings of this thesis in a broader context, followed by an outlook on future research directions. Finally, an overview of author contributions for each study is provided, followed by the three full manuscripts including their supporting information.

# Chapter 2 – Study design and key findings

---

This chapter summarises the different modelling approaches and key findings from the three manuscripts that are part of this PhD thesis, and the connections between the respective studies are discussed.

To answer the research questions from Chapter 1, each study investigates the combined and individual effects of soil moisture and soil temperature on SOC dynamics from a different perspective: In study I, site-level measurements are used for a bulk soil column approach, without considering the vertical distributions of SOC over the soil profile. In the second study, global climate model outputs are considered, as well as the vertical differences in soil moisture, soil temperature and SOC content. In both studies, modelled changes are instantaneous and do not consider the past history of the soil's SOC content. The third study does consider this dynamic feedback between the different carbon pools and changes in temperature, soil moisture and temperature. For each study in this thesis, a figure is included with the conceptual representations of the different soil moisture and soil temperature controls for each modelling approach, highlighting the common thread between the three studies.

## **2.1 Study I: Modelling soil moisture controls on soil respiration through substrate and oxygen availability**

In Study I, we applied the Dual Arrhenius Michaelis-Menten (DAMM) model (Davidson et al., 2012) to site-level soil respiration measurements to disentangle how temperature and soil moisture affected the observed soil CO<sub>2</sub> efflux. The relative importance of substrate and oxygen limitations on soil respiration at different time periods (summer drought, winter flooding) were highlighted. We also compared and discussed our results in light of the original DAMM model development for the temperate site Harvard Forest, to demonstrate the model's suitability for application in semi-arid ecosystems.

The study site Las Majadas, a semi-arid dehesa ecosystem located in Extremadura of Spain, experiences strong temperature and soil moisture fluctuations throughout the year. We found that considering soil moisture controls was crucial to model the dynamics in the observed soil CO<sub>2</sub> efflux. Changes in substrate availability were the main driver of the observed soil respiration fluxes, and the DAMM model was able to reproduce the strong respiration pulses observed after a drying and subsequent rewetting event, also known as the "Birch effect" (Birch, 1958). If only soil temperature was considered as a driver of soil respiration, the model was not able to reproduce the observed CO<sub>2</sub> efflux well, and strongly overestimated the observations.

The DAMM model is based on the principle that at optimal soil moisture values, respiration rates are driven by soil temperature and exponentially increase with temperature following an Arrhenius function. This temperature-driven optimal maximum rate (often called  $V_{max}$ ), obtained at a certain optimal soil moisture level, is reduced when soil moisture either decreases or increases (Fig. 3): At low soil moisture, microbes are limited in the amount of accessible substrates to decompose, whereas at high soil moisture, oxygen availability limits microbial respiration rates.

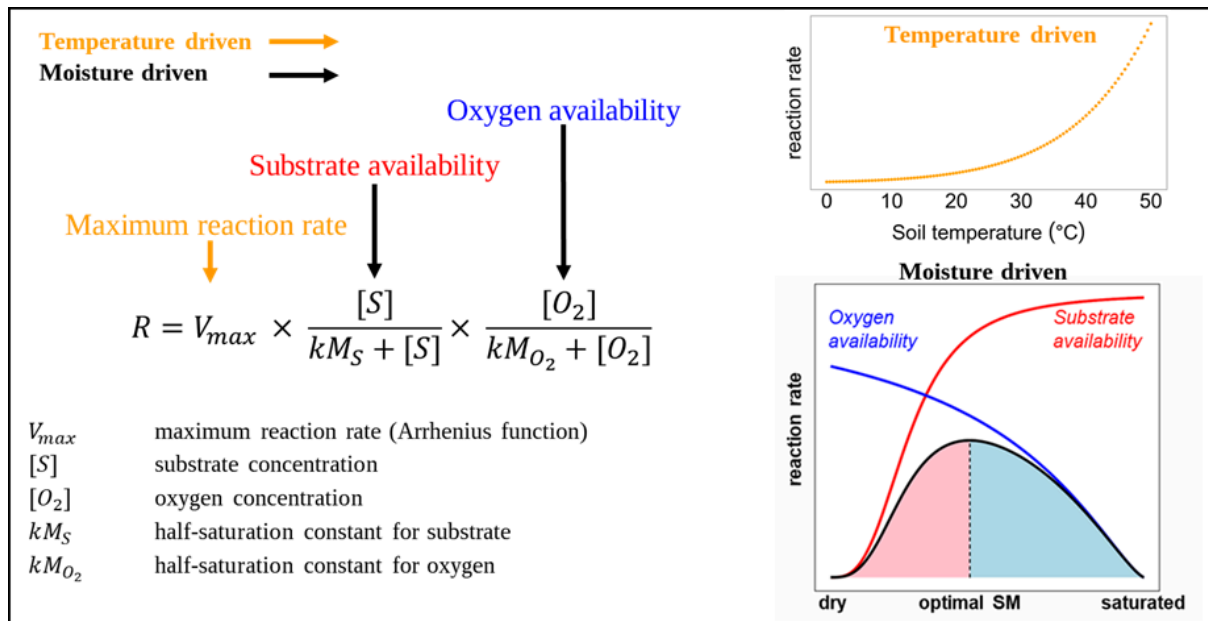


**Figure 3:** Conceptual representation of the effects of soil temperature and soil moisture on microbial respiration rates with the DAMM model (Davidson et al., 2012). The reaction rate ( $R$ ) consists of a maximum rate ( $V_{max}$ ) and two Michaelis-Menten terms to calculate substrate availability and oxygen availability. The figure on the top right depicts the temperature driven part of the equation:  $V_{max}$  increases with higher temperatures. The figure on the bottom right depicts the moisture driven part of the equation, with the two Michaelis-Menten terms of the DAMM model using the parameters from Davidson et al. (2012): When soils are dry, the availability of substrate (red line) to microbes is low, while oxygen availability (blue line) is high. When soils are saturated, oxygen availability is low while substrate availability increases. At optimal soil moisture (dotted vertical line), the reaction rate ( $R$ , solid black line) is governed by temperature and is at its maximum rate ( $V_{max}$ ).

The DAMM model requires information on soil temperature, soil moisture, soil C content, and soil porosity as inputs to calculate  $V_{max}$ , substrate availability, and oxygen availability (Study I, Eqs. 1–5). These data were measured at the study site. Substrate and oxygen availability were calculated as Michaelis-Menten terms (Fig. 3), where the half-saturation constants for oxygen and substrate were estimated from the data. Additionally, the activation energy and pre-exponential factor (a measure for the ‘base respiration’ at the site), required to calculate  $V_{max}$ , were estimated from the data: These four parameters in the DAMM model were calibrated to the soil  $\text{CO}_2$  efflux measurements at Las Majadas. The half-hourly measurements were taken over a 2.5 year period, with minimum soil temperatures at 5 cm depth between 3.8 and 31.2 °C, and water-saturation between 9.4% and 98.2% during the observation period (illustrated in Figs. 2b and 2c in Study I).

We found that soil respiration rates modelled with the calibrated DAMM model captured the observed fluxes at Las Majadas well (Fig. 4, green points). The observations repeatedly showed strong respiration pulses after a drying and subsequent rewetting event, which were well captured by the DAMM model. These soil respiration pulses could not be reproduced by the model when the Michaelis-Menten terms for substrate and oxygen diffusion were set to a fixed value of 1 (Fig. 4, pink points), i.e. by calculating the temperature-driven maximum rate ( $V_{max}$ ) only. This version of the DAMM model (“DAMM (MM = 1)”) strongly overestimated the observed soil CO<sub>2</sub> efflux at the site and explained less than 0.1% of the variance (Fig. 4). The demonstrated ability of the DAMM model to reproduce soil respiration pulses upon rewetting was a significant finding of Study I, as such CO<sub>2</sub> pulses can account for a large part of long-term carbon losses from the soil in dry and semi-arid ecosystems (e.g. Jarvis et al., 2007; Xu et al., 2004; Zhang et al., 2020).

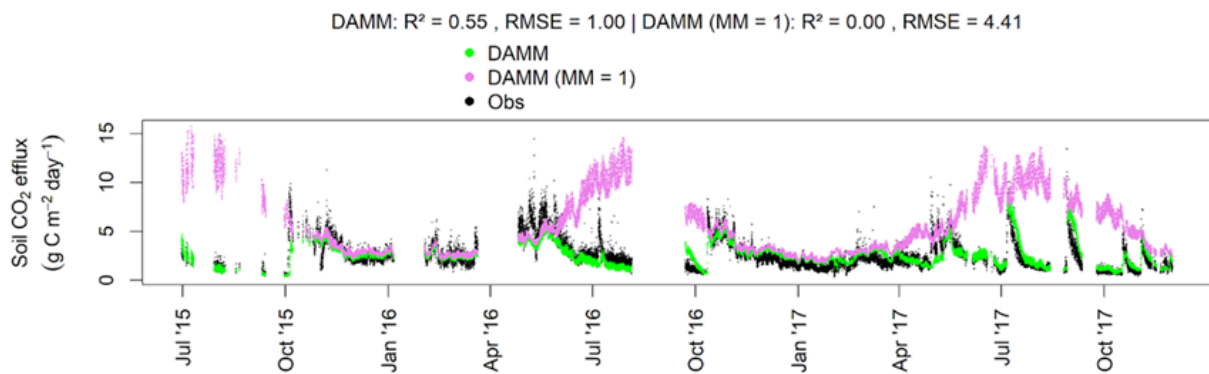


**Figure 4:** DAMM model fitted to  $R_{soil}$  observations at Las Majadas between July 2015 and December 2017. Observed (black) and modelled soil CO<sub>2</sub> efflux ( $\text{g C m}^{-2} \text{ day}^{-1}$ ) for the full DAMM model (green, DAMM) and DAMM model with both MM-terms set to 1 (pink, DAMM (MM = 1)). Goodness-of-fit values: Coefficient of determination ( $R^2$ ) and root mean squared error (RMSE,  $\text{g C m}^{-2} \text{ day}^{-1}$ ).

A detailed analysis of the Michaelis-Menten terms revealed that substrate diffusion limitation was the dominant driver of the observed soil respiration fluxes at Las Majadas (Fig. 3 in Study I), as the site experiences many drying and rewetting events. Significant CO<sub>2</sub> fluxes were observed during wintertime, even when the soil was highly saturated with soil moisture (> 90% saturation). The DAMM model with the Michaelis-Menten terms set to 1, could not reproduce the observed fluxes well under these conditions (Fig. 4 in Study I). Compared to this temperature only-driven model estimate, the full DAMM model matched the observations better by imposing oxygen diffusion limitation on the estimated respiration rates, but showed small mismatches (slight underestimation and overestimation) of the observed fluxes under these extremely wet conditions (Fig. 4 in Study I). Underestimation of the fluxes can be the result of ongoing autotrophic respiration, which is tightly coupled to photosynthetic activity (Hopkins et al., 2013) and not explicitly simulated by the DAMM model, as well as anaerobic CO<sub>2</sub> production (Fairbairn et al., 2023). Fairbairn et al. (2023) suggest that under these wet conditions, C substrate supply to microbes is high and provides



ideal circumstances for anaerobic CO<sub>2</sub> production. Additionally, the overestimation of the fluxes can be caused by a temporal mismatch between CO<sub>2</sub> production and the resulting soil CO<sub>2</sub> efflux, where water blocking the soil pores hinders the release of CO<sub>2</sub> from the soil to the atmosphere and can cause a drop in observed CO<sub>2</sub> efflux (Maier et al., 2011). As the DAMM model responds instantaneously to the temperature and soil moisture values at each model timestep by simulating respiration, such temporal shifts cannot be accurately captured. The results, however, showed that despite some temporal mismatches between the DAMM model and the observations, the total CO<sub>2</sub> release over the observational period was captured very well by the calibrated DAMM model (Table 2 in Study I). Additionally, the results indicate that substrate diffusion is extremely important to explain the observed variability in soil respiration, especially during long dry periods and subsequent rewetting events.

Since its development, the DAMM was successfully used at the temperate forest sites at which it was developed (e.g. Abramoff et al., 2017; Davidson et al., 2012; Sihi et al., 2018b). Temperature is the main driver of the measured heterotrophic fluxes at these sites, as soil moisture is close to optimal values most of the time. Overall, the results from this first study demonstrated that the DAMM model is also a suitable framework to model soil moisture controls on soil respiration rates at sites with highly dynamic changes in temperature and soil moisture such as Las Majadas (and see Oirkawa et al. (2014) and Drake et al. (2018) for applications in two extremely dry ecosystems).

Following these results, the scope of the second study moves from the instantaneous soil moisture and temperature changes and their effects on soil respiration at one site, to changes in future SOC decomposition rates using soil moisture and soil temperature projections simulated by different Earth system models (ESMs) at a global scale. Additionally, Study II considers the vertical distributions of the soil carbon content, as well as the vertical differences in soil temperature and soil moisture changes with depth.

## **2.2 Study II: Vertically divergent responses of SOC decomposition to soil moisture in a changing climate**

In the second study, the DAMM model was used to model the combined and individual impacts of projected temperature and soil moisture changes until the end of the century by comparing future SOC decomposition rates driven solely by temperature changes to SOC decomposition rates predicted by soil moisture and temperature changes. Study II was the first to use the DAMM model for a vertically discretized application, so the model results were successfully verified against independent observations.

The key finding of this study was that changes in soil moisture have the potential to not only mitigate, but also accelerate predicted decomposition rates driven by future soil warming. The analysis revealed that soil moisture changes have the potential to slow down or speed up these temperature-driven SOC decomposition rates by as much as 20%. We also found that the topsoil responded differently from the subsoil.

As outlined in Chapter 1, the role of soil moisture for organic matter decomposition remains poorly understood and represented in Earth system models (ESMs). In order to quantify the impacts of future soil moisture and temperature changes on SOC decomposition rates using a mechanistic model framework, we used historic and future soil moisture and soil temperature simulated by 4 different ESMs at a global scale from the Coupled Model Intercomparison Project 5 (CMIP5) model ensembles (Taylor et al., 2012). Additionally, a data-driven global dataset of SOC stocks and soil porosity was used from the SoilGrids database (Hengl et al., 2014, 2017) as inputs to the DAMM model (Fig. 5).

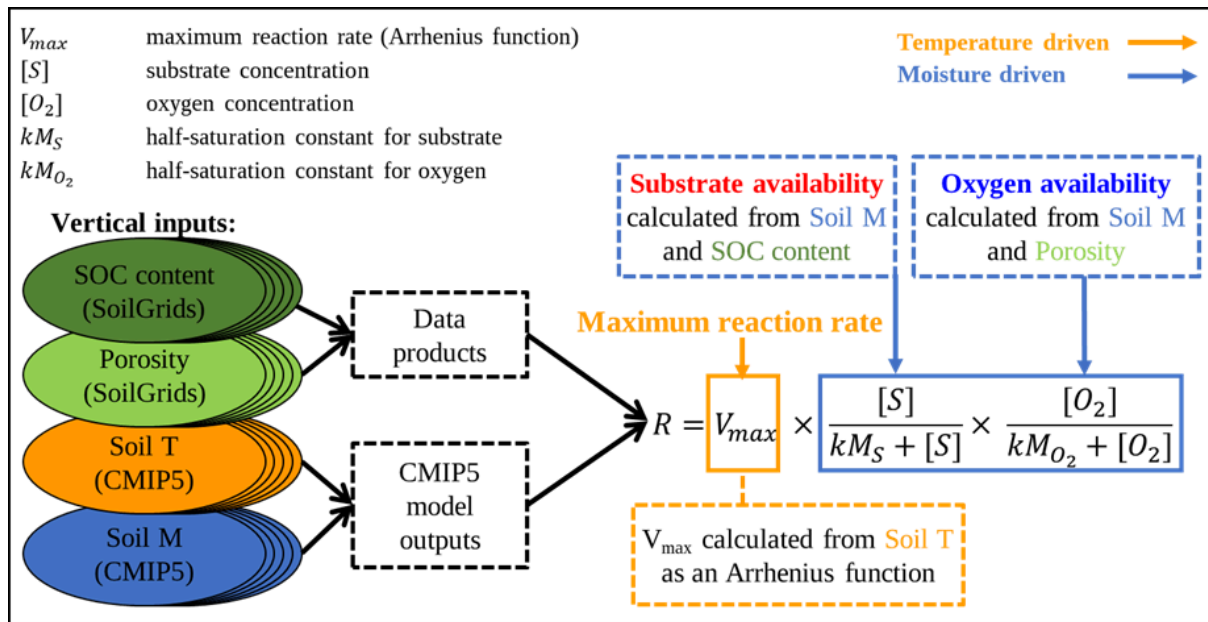


**Figure 5.** Conceptual representation of the temperature and soil moisture driven parts of the DAMM model, specifying the different data inputs that were used to calculate the SOC decomposition rate  $R$ . DAMM model inputs consisted of two data-driven products (SOC stocks and soil porosity from SoilGrids) and two CMIP5 model outputs (soil temperature and soil moisture) from four different ESMs, at multiple soil depths between 0 and 100 cm. SoilGrids data were spatially re-gridded to match the respective CMIP5 model’s spatial resolution. CMIP5 model outputs were vertically re-gridded to match the five soil depth intervals from the SoilGrids dataset: 0–5, 5–15, 15–30, 30–60, 60–100 cm depth, respectively.

A unique aspect of Study II is the consideration of SOC density, soil porosity and soil moisture and temperature changes at multiple soil depths until 1 m. To gain insight in SOC decomposition rate changes in a changing climate, we calculated the temperature- and soil moisture driven decomposition rate changes between a historic (1976–2005) simulation period and a future climate change period (2070–2099), following Representative Concentration Pathway 8.5 (RCP8.5). These calculations were done at global scale for each soil depth interval, so that the various temperature and soil moisture driven effects on SOC decomposition rates between the topsoil layer (0–5 cm depth) and a deep soil layer (60–100 cm depth) could be compared (Fig. 6).

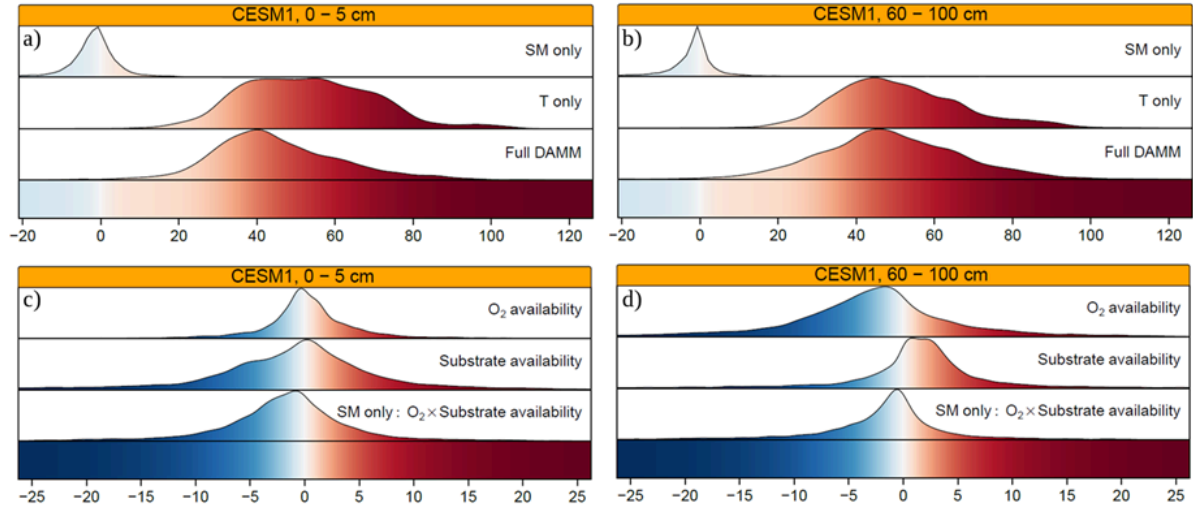


**Figure 6.** Probability density functions (PDFs) for global changes in decomposition rate in the topsoil (0–5 cm; a,c) and bottom soil layer (60–100 cm; c,d) for a single CMIP5 model (CESM1-BGC). The PDFs show changes (in %) in SOC decomposition rates between the historic and RCP8.5 simulation period. Each PDF shows the respective contribution of soil moisture (SM only); temperature (T only); soil moisture and temperature (Full DAMM); O<sub>2</sub> availability; and substrate availability. Blue cells indicate a slowdown, and red cells indicate an acceleration of the modelled decomposition rate between the two simulation periods.

Between the historic and future simulation period, the global mean soil temperature changed by 2.8 – 4.2 K between the different CMIP5 models. As a result, SOC decomposition rates accelerated by 20% – 120%, driven by rising soil temperatures alone (Fig. 6a,b). The analysis revealed that moisture has the potential to slow down or speed up these temperature-driven SOC decomposition rates by as much as 20% (Fig. 6, SM only).

Our finding that soil moisture has the ability to further accelerate temperature-driven decomposition rates contrasted with results from earlier modelling studies. For example, Falloon et al. (2011), reported that temperature-driven decreases in soil carbon by the year 2100 tended to be opposed by soil moisture, implying a slowdown of conventional SOC turnover rates in response to soil moisture. The work of this thesis, however, showed that the direction of change is very dependent on the initial soil moisture conditions, as well as the existing SOC content. These results hold particular significance: Firstly, initial soil moisture conditions are important to consider, because it implies that soil drying does not always lead to a slowdown of decomposition rates, but can also accelerate them. In such cases, a reduction in soil moisture moves the decomposition rates closer to the potential maximum rate ( $V_{max}$ ) under optimum soil moisture conditions, by increasing the availability of oxygen. Secondly, we found that considering the initial SOC content (which affects substrate availability) is important, as SOC content changes with soil depth and conventional SOC decomposition models generally do not consider this nonlinear feedback between soil moisture, soil temperature and SOC content across multiple soil depths.

Study II indeed revealed that the response to soil moisture changes in the topsoil was very different from the response of the deep soil layer. In the topsoil, the majority of the predicted SOC decomposition rate changes were driven by changes in substrate availability (Fig. 6c).

In the majority of cases, soil drying led to a decrease in substrate availability for decomposition and reduced the predicted decomposition rates (Table 2 in Study II). However, in more than 25% of the grid cells, an increase in soil moisture led to a further acceleration of the temperature driven decomposition rates. In the deep soil layer, this number increased to more than 34%, indicating that deep soil layers are very important in the feedback between SOC dynamics and climate warming.

While changes in substrate availability dominated the response to soil moisture in the top soil layers, Study II showed that changes in oxygen availability are increasingly important in the deeper soil layers (Fig. 6d). In particular, slowdown of the decomposition rates in the deeper soil corresponded with reductions in oxygen availability as a result of soil wetting (Table 2 in Study II).

It is important to note that within the full CMIP5 model ensemble there is a large spread in model results for both the initial (historic) soil model conditions, as well as in the projected soil moisture changes under the RCP8.5 scenario (Berg et al., 2017; Cheng et al., 2017; Lorenz et al., 2016; Orlowsky & Seneviratne, 2013). But while the four models considered in Study II varied in their soil moisture patterns (Fig. S4 in Study II), both spatially and vertically, the bi-directional nature of the modelled SOC decomposition rate response to soil moisture was found for all models and at all soil depths (Figs. S3 and S5 in the supporting information for Study II).

This study was the first to use the DAMM model in a depth-discretized application. Therefore, to demonstrate the DAMM model's suitability for a vertically resolved application, we compared the DAMM model to a set of soil respiration observations at different soil depths up to 1 m (Hicks Pries et al., 2017). Using the same parameters and sensitivities to soil moisture as in the DAMM model application on the CMIP5 model data, the DAMM model was able to match the observations well at each soil depth, but only when a vertically varying SOC content was used. Additionally, the robustness of the results for the DAMM model application on the CMIP5 model data was tested. As discussed previously, the model results were very sensitive to different initial soil moisture conditions, as well as the SOC content. The model results were neither sensitive to a  $\pm 20\%$  difference in parameter values, nor were they sensitive to a decline of oxygen concentration in air with soil depth.

Summarising, Study II showed that while future soil moisture changes are uncertain, they have strong potential to mitigate or accelerate SOC decomposition rates driven by soil warming by the end of this century. Changes in substrate availability will dominate the future SOC dynamics, especially in top soil layers. In the deeper soil layers, oxygen availability becomes increasingly important. Owing to the different soil moisture controls with soil depth, Study II also highlighted that the development of the next generation of SOC decomposition models would benefit from including vertical representations of soil processes, with moisture sensitivity functions that reflect our mechanistic understanding of the effects of soil drying (and a reduction in substrate availability) and soil wetting (and the reduction of oxygen availability).

In Study I and Study II of this thesis, the DAMM model was applied as a function where a fixed fraction of the existing SOC content determined substrate availability, without considering the dynamic changes in SOC content over time. As a next step, Study III focused on studying the interactions between soil moisture, soil temperature and substrate availability in a dynamic model, where the feedback between the different carbon pools and microbial dynamics affect the SOC dynamics over time.

### **2.3 Study III: Drought counteracts soil warming more strongly in the subsoil than in the topsoil according to a vertical microbial SOC model**

In the third study of this thesis, the dynamic interactions between soil moisture, soil temperature and substrate were investigated at different soil depths. Since SOC, microbial biomass and mineral-associated SOC are not distributed evenly within soil profiles, the interactions between soil moisture, microbes and substrates were expected to vary with depth. To test these interactions, we used a model with vertically resolved, mechanistic descriptions of microbially driven decomposition and organo-mineral interactions so that C substrate depletion by microbes or sorption could be explicitly simulated at different soil depths.

The main finding of the study was that soil warming leads to long-term SOC losses, but that depending on the SOC substrate composition and its associated temperature sensitivities, these losses could be either reduced or further accelerated, especially in the subsoil. We also showed that drought could alleviate the effects of soil warming and reduce SOC losses from the soil.

The model used in this study was the Jena Soil Model (JSM: developed by Ahrens et al., 2015, 2020; Yu et al., 2020), where we focussed on the depolymerisation of litter and microbial residues at different soil depths, and its sensitivities to soil warming and different drought intensities. Based on the theory and parameterisation of substrate kinetics for SOC decomposition (Tang & Riley, 2019), JSM represents microbial depolymerisation of the litter pools with reverse Michaelis-Menten (MM) kinetics. Effectively, this means that the depolymerisation rate of the litter pools is limited by the microbial biomass pool (Fig. 7). In JSM, microbial depolymerisation rates are also indirectly affected by the sorption and desorption of DOC and microbial residues onto mineral surfaces, as this affected the availability of microbial residues for depolymerisation and the amount of DOC available for microbial growth. In the model, the adsorbed DOC and adsorbed microbial residues (mineral-associated carbon, MAOC) are protected from microbial decomposition. We calculated SOC stocks (% increase or decrease) over a simulation period of 100 years between 0 and 50 cm depth, and compared results from a topsoil layer (0–6 cm) to those of a subsoil layer 36–50 cm.

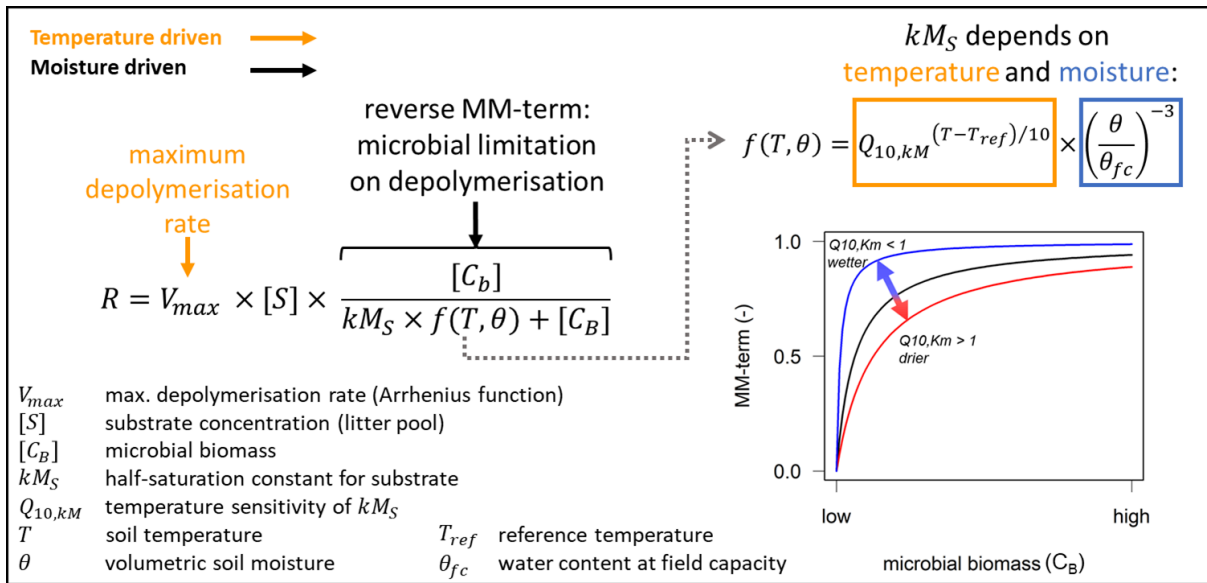


**Figure 7:** Conceptual representation of the effects of soil temperature and soil moisture on microbial depolymerisation rates within the Jena Soil Model. The depolymerisation flux ( $R$ ) consists of a maximum depolymerisation rate ( $V_{max}$ ) and a reverse MM-term to calculate microbial limitation on the depolymerisation rate of the two litter pools in JSM: polymeric litter and microbial residues. The figure on the right depicts the effects of soil moisture and different  $Q_{10, kM}$  values on the MM-term: When the soil gets drier or  $Q_{10, kM} > 1$ , the MM-term is reduced (red line), lowering the depolymerisation rate. When the soil gets wetter or  $Q_{10, kM} < 1$ , the MM-term is reduced (red line), lowering the depolymerisation rate. When soil moisture stays the same, or  $Q_{10, kM} = 1$ , the MM-term follows the black line. Overall, temperature and soil moisture effects on the MM-term are stronger at low microbial biomass.

Similar to Studies I and II, the maximum depolymerisation rate was driven by temperature (Fig. 7). Soil moisture affected the reverse MM-term for the depolymerisation through the half-saturation constant in the denominator of the MM-term (Fig. 7): Soil drying reduced the depolymerisation rate, reflecting microbial enzymatic diffusion limitation on the available SOC substrates (Tang & Riley, 2019). In the previous two studies of this thesis, the half-saturation constant ( $kM_s$ ) did not vary with temperature. A novel aspect of the third study in this thesis was the additional investigation of the effects of the half-saturation constant's sensitivity to soil temperature on SOC dynamics. Based on recent literature (Allison et al., 2018), different temperature sensitivities for the half-saturation constant, expressed as  $Q_{10}$  values, were tested in Study III. One value represented microbial depolymerisation of polymeric litter ( $Q_{10, kM, P} = 1.3$ ) and one value represented microbial depolymerisation of microbial residues ( $Q_{10, kM, R} = 0.7$ ).  $Q_{10}$  values above 1 lower the depolymerisation rate with increasing temperatures, whereas values below 1 further accelerate it (Fig. 7).

Prescribed litter inputs to the model were identical for each model experiment. This allowed us to individually test soil warming and drying effects on long-term SOC stocks, without the potentially confounding effects from changes in plant productivity. In line with the results from Study II, we found that soil warming accelerated SOC losses and that the topsoil responded differently from the subsoil (Fig. 8): Warming-induced SOC losses were

proportionally higher in the topsoil than in the subsoil when soil moisture was kept at ambient levels (Fig. 8a and 8b,  $SM * 1.0$ ).

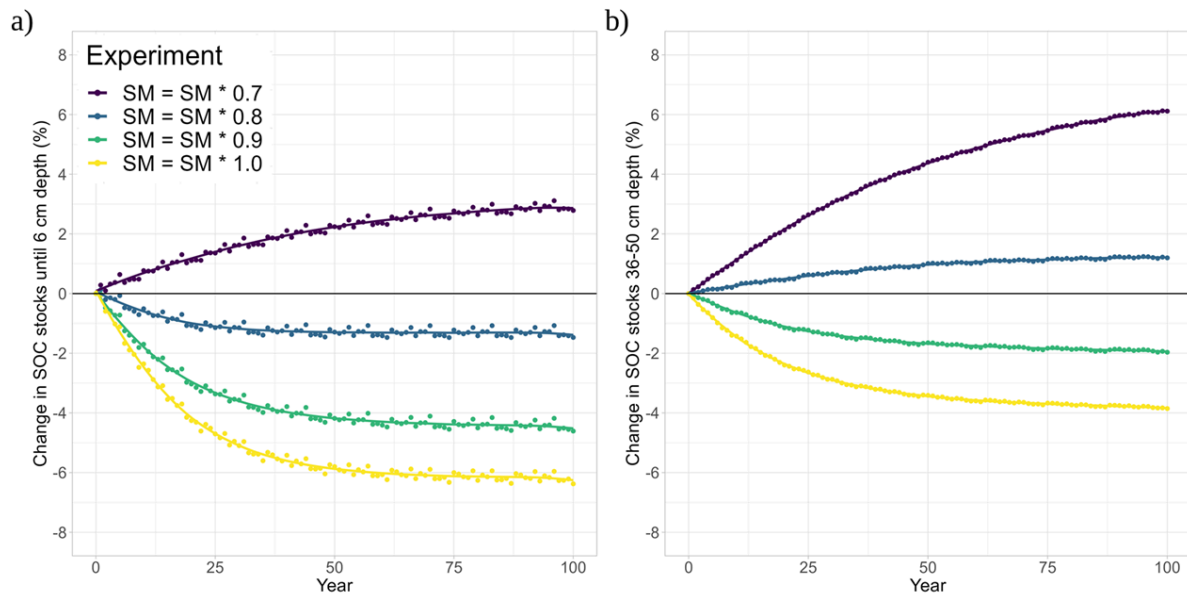


**Figure 8.** Combined temperature and soil moisture effects on long-term changes in modelled SOC stocks (% SOC lost since simulation year 0) for different model experiments in a) the topsoil layer (0 - 6 cm) and b) a subsoil layer (36 - 50 cm). In all model runs, the soil was warmed by 4.5 K and the half-saturation constants were sensitive to temperature changes:  $Q_{10,Km}$  was 1.3 for the depolymerisation of polymeric litter and  $Q_{10,Km}$  was 0.7 for depolymerisation of microbial residues.

We also found that drought could alleviate the effects of soil warming: when available soil moisture was reduced, less SOC was lost from the soil as a result of soil warming. With stronger drought intensity warming-induced SOC losses turned into SOC gains (Fig. 8), which occurred at less severe drying levels for the deep soil layer ( $SM * 0.8$ ) compared to the topsoil layer ( $SM * 0.7$ ).

Study III additionally revealed that the individual temperature sensitivities of the half saturation constants for polymeric litter and microbial residues counteracted each other, which led to SOC losses from the soil comparable to those found when the half-saturation constants were not sensitive to temperature. We also found, however, that the subsoil was more sensitive to different temperature sensitivities of the half-saturation constants than the topsoil. Given that the composition of SOC substrates likely differs between topsoils and subsoils, with topsoils receiving more polymeric litter inputs and subsoils containing a relatively larger proportion of microbial residues, our results indicated that the temperature sensitivity of the half-saturation constant can have a significant impact on deep SOC dynamics.

Study III demonstrated that in a vertically explicit, dynamic model system like JSM, complex feedbacks arise between microbial dynamics, organo-mineral interactions and substrate availability. Firstly, microbes and mineral surfaces compete for the same carbon substrates, dissolved organic carbon (DOC) and microbial residues. At lower depths, the amount of

mineral-associated SOC (MAOC) increased compared to the amount of particulate organic carbon (POC), which is not associated with mineral surfaces. Additionally, microbial biomass reduced with depth, which strongly increased the significance of the half-saturation constant for the depolymerisation rates (Fig. 7; Davidson et al., 2006; Davidson & Janssens, 2006). Overall, with our isolated experiments, we were able to demonstrate that subsoils are potentially more sensitive to soil warming and droughts.

The results from this study are important, as recent research has shown that the chances of drought coinciding with high soil temperatures will further increase in the future (García-García et al., 2023). As a result, the counteracting effects of the temperature sensitivities of the half-saturation constants and drought may be at their strongest, and ecosystems dominated by infrequent moisture inputs may show very strong sensitivities to soil warming and drought.



# Chapter 3 – Discussion and outlook

---

In this final discussion the research objectives and related research questions outlined in Chapter 1.4 are revisited. The aims of this PhD thesis were to: 1) better understand the effects that temperature and soil moisture changes have on microbial SOC decomposition; 2) explore what their potential individual and combined effects are on SOC dynamics in a changing climate; and 3) to aid the further development of process-based SOC models by investigating different approaches suitable for model implementation.

The following research questions were coupled to these three objectives:

*Q1: Can soil moisture mitigate or exacerbate temperature-driven changes in SOC decomposition rates?*

*Q2: How do soil moisture and temperature interact with SOC substrates and subsequently affect microbial SOC decomposition rates?*

*Q3: How do soil moisture and soil temperature effects on SOC decomposition vary along a vertical soil gradient?*

The contributions to these questions and the insights this thesis has provided are discussed, followed by an outlook on further research directions.

## **3.1 Changes in soil moisture can mitigate or accelerate SOC decomposition rates**

*Q1: Can soil moisture mitigate or exacerbate temperature-driven changes in SOC decomposition rates?*

This thesis demonstrated that changes in soil moisture have the potential to mitigate or further accelerate SOC decomposition rates in a warming climate through various mechanisms. All three studies contributed to finding the answer to this first research question. Firstly, Study I showed that low values of soil moisture could mitigate the temperature-driven soil respiration rates, primarily by limiting C substrate diffusion, especially during the summer period. Under highly water-saturated conditions, oxygen diffusion limited soil respiration rates, which mainly occurred in the winter period. Furthermore, we found that soil moisture not only restricted temperature-driven soil respiration rates, but also stimulated them: Upon rewetting after a period of drought, the observed high pulses in CO<sub>2</sub> efflux were captured by the DAMM model by lifting the substrate diffusion limitation, whereas a purely temperature-driven model estimate did not capture these dynamics.

Secondly, Study II found that the inclusion of soil moisture controls had diverging effects on both the speed and direction of projected decomposition rates (up to  $\pm 20\%$ ), compared to a temperature-only approach. In the topsoil, the majority of these changes were driven by substrate diffusion limitation. In deeper soil layers, oxygen availability played a relatively stronger role. This study also demonstrated that the initial soil moisture conditions were crucial to determine whether decomposition rates accelerate or slow down the projected temperature-driven rates. Depending on the initial soil moisture condition, the modelled decomposition rate can either increase or decrease for the same absolute change in water content (Fig. 9). The closer the initial soil moisture condition lies to an optimal soil moisture value, the smaller the impact of soil moisture changes will be on the overall decomposition rates (Fig. 9, 'SM only'). In soils, however, where soil moisture is already low or high, further drying or wetting will have very strong impacts on the decomposition rates.

The findings of Studies I and II are particularly important for drier ecosystems that experience strong drying-rewetting cycles, because both the initial moisture status, the strength of soil rewetting, as well as the length and frequency of drying-rewetting events affect how much C will be released into the atmosphere (Liang et al., 2021; Rousk & Brangarí, 2022). For wet ecosystems though, the reverse is true: If they wet further, oxygen availability would be further restricted, but drying could lead to higher SOC decomposition as oxygen becomes more easily available for microbial decomposition. E.g., in warming peatland soils, which store massive amounts of SOC, water table depth is extremely important to determine if they act as C sources or sinks. Peatland soils are rich in phenolic compounds, which are mainly degraded under aerobic conditions by the enzyme phenol-oxidase. As such, increased oxygen supply in drying peat soils could lead to substantial further SOC losses (Freeman et al., 2001), although these amplified warming effects can partly be mitigated by lower methane emissions (Kwon et al., 2022). Recently, the DAMM model framework was extended to simulate methane consumption and production (Sihi et al., 2020, 2021). Phenolic compounds could be added as an additional substrate (or as a lignified litter) pool, so that this framework provides further opportunities to explore peatland drying and wetting effects.

Thirdly, Study III found that soil warming led to SOC losses and that drought had the potential to mitigate warming losses considerably. Drought decreased microbial depolymerisation rates through decreased diffusion of enzymes, which led to a slowdown of the overall SOC decomposition rates. These results are in line with the first two studies of this thesis, as well as other modelling studies (e.g. Todd-Brown et al., 2014; Wieder et al., 2018) and data-driven studies (M. Wang et al., 2022). We also found that soil warming could have a mitigating effect on SOC decomposition rates through the temperature sensitivity of the half-saturation constants, especially in deeper soil layers where microbial biomass is low and the importance of the half-saturation constants is higher (Davidson et al., 2006; Davidson & Janssens, 2006).

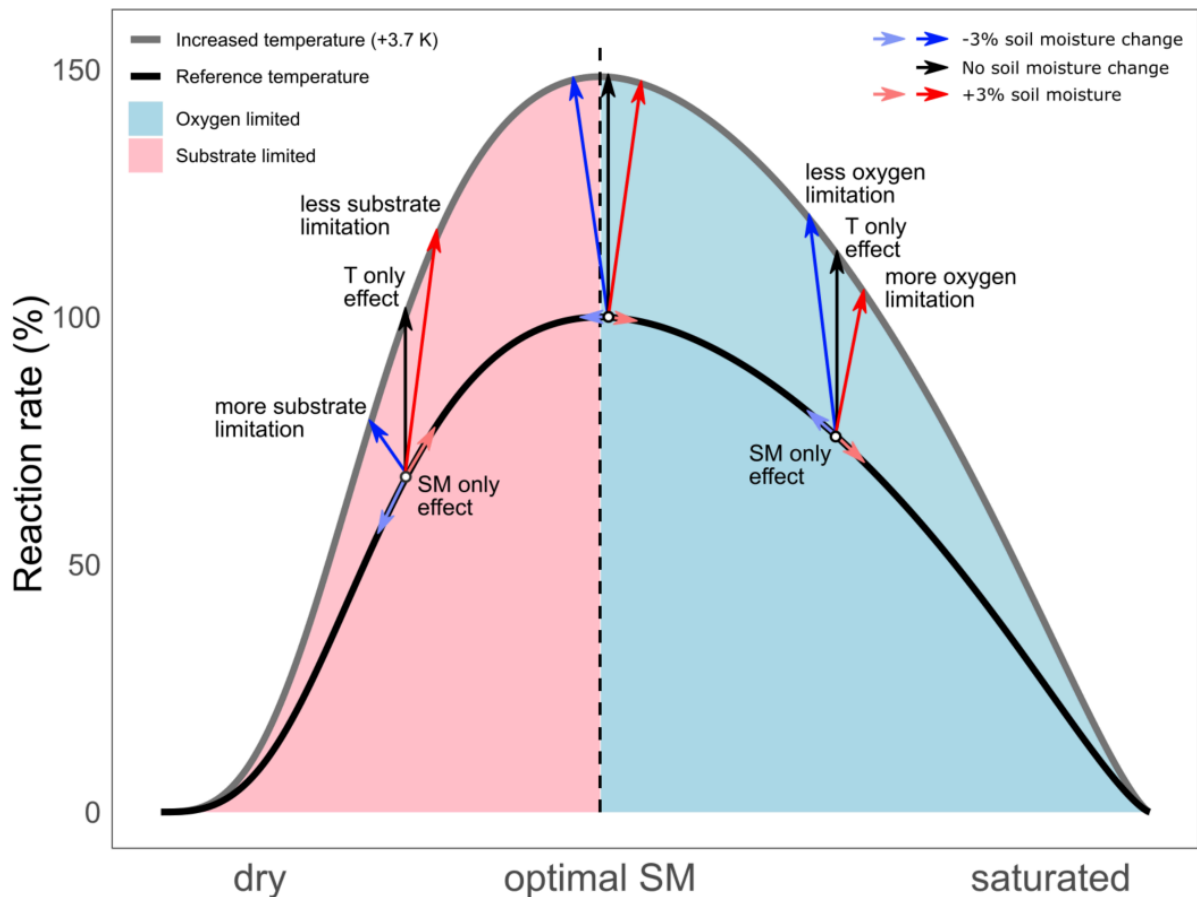


**Figure 9.** Importance of initial soil moisture conditions: Change in reaction rate (%) in response to soil moisture changes at reference temperature ( $T_{ref} = 283.15$  °K, black line) and increased temperature (+3.7 °K, grey line). Arrows indicate the change in reaction rate when soil moisture does not change (T only, black arrows), decreases by 3% (blue arrows), or increases by 3% (red arrows). The light blue and red arrows indicate the soil moisture (SM) only change (no temperature change) to a 3% decrease/increase in soil moisture, respectively. Around optimal SM (dotted line), temperature changes dominate the change in the reaction rate. The half-saturation constants of the MM-terms are not sensitive to temperature or soil moisture changes in this depiction. Figure included in this thesis as Fig. S1 (supplement of Study II), where a warming of +3.7 °K reflects the average mean soil warming projected by the different ESMs that were used in the study.

The findings of this thesis suggest that without better inter-model agreement of current and future soil moisture projections by ESMs (e.g. see Hsu & Dirmeyer, 2023; Lu et al., 2019), it will be difficult to determine future SOC dynamics and estimate the related carbon fluxes from the soil into the atmosphere that contribute to further warming. At present, however, soil moisture measurements are still sparse compared to soil temperature, and only representative of a smaller area (Berg et al., 2017). This also restricts the validation of satellite-derived soil moisture measurements (e.g. Gruber et al., 2020; O. & Orth, 2021), which can be useful as input for SOC decomposition models. Additionally, reliable simultaneous measurements of soil moisture, soil temperature and soil (heterotrophic) respiration rates from sites that cover a wide range of climatic conditions are needed to better estimate the shape of the soil moisture response curve. In Study I of this thesis, we showed that the range of soil moisture values for which the models are calibrated is important for their functional shape, and that it might be dangerous to extrapolate parameter values beyond calibration range. In Study II, we used the

parameter values from the original DAMM model study (Davidson et al., 2012), but a sensitivity analysis revealed that our model results were not very sensitive to large changes ( $\pm 20\%$ ) in these parameters. Rather than to the parameter values, the results were very sensitive to the projected relative changes in soil moisture, which are extremely uncertain (Berg et al., 2017). Therefore, the results demonstrated the importance of coherent soil moisture projections from ESMs and support a call for simultaneous measurements of soil moisture, soil temperature, and soil CO<sub>2</sub> fluxes.

## **3.2 Interactions between temperature, soil moisture and substrate availability in a dynamic system**

*Q2: How do soil moisture and temperature interact with SOC substrates and subsequently affect microbial SOC decomposition rates?*

In the first two studies, a fixed fraction of a static SOC pool was used to determine the substrate availability. While this provided insights in the ability of soil moisture and soil temperature to mitigate or accelerate SOC decomposition rates (Section 3.1), it was not possible to determine how the resulting changes in substrate availability over time would additionally affect SOC dynamics. Therefore, an important and novel aspect of the third study of this thesis was that within the Jena Soil Model, the dynamic feedback between the SOC substrate pools (dissolved organic C, polymeric litter, and microbial residues), microbial biomass, mineral sorption, and temperature and soil moisture could be studied.

In the third study, we found that soil warming led to long-term SOC losses, but that depending on the SOC substrate composition and its associated temperature sensitivities, these losses could be either reduced or further accelerated, especially in the subsoil. That temperature could potentially offset SOC losses through the temperature sensitivity of the half-saturation constant was previously theorised (Davidson et al., 2006; Davidson & Janssens, 2006), but never studied in a dynamic model as shown in this thesis. This temperature effect becomes increasingly important at low microbial biomass concentrations, as the depolymerisation rates are limited by the size of the microbial biomass pool (Fig. 7). Microbial biomass decreases with soil depth, while at the same time, the amount of SOC that is protected from decomposition by sorption to mineral surfaces increases. The latter is important because mineral-associated SOC has a lower temperature sensitivity than the particulate organic C pools: In JSM, the temperature sensitivities of the mineral-associated pools are implemented based on observations following Wang et al. (2013; Table 1 in Study III), which is supported by recent data-driven studies that have shown that unprotected SOC pools are more affected by temperature increases than mineral-protected SOC, so that temperature effects on SOC storage are higher in soils with higher proportions of unprotected carbon (Georgiou et al., 2024; Hartley et al., 2021). We demonstrated that this vertical gradient in microbial biomass and mineral-associated SOC led to different sensitivities of the overall SOC stocks to soil warming in the topsoil and subsoil layers: In the topsoil, there is more particulate SOC, and absolute SOC losses driven by soil warming were higher than in the subsoil. The subsoil contained a smaller proportion of particulate SOC, but the amount

that was there was found to be more sensitive to warming. Depending on the type of litter depolymerised by microbes (microbial residues or polymeric litter in this study) and its assigned temperature sensitivity, this mitigated (polymeric litter) or accelerated (microbial residues) the warming-induced SOC losses.

Study 3 also showed that drought could alleviate the effects of soil warming and reduce SOC losses from the soil. The drought led to such strong limitations on microbial depolymerisation that the effect of soil warming could be completely mitigated. In these simulations the litter inputs were not reduced in response to soil drying, so that the isolated effects of drought on SOC dynamics could be studied. It can be expected, though, that long-term soil drying reduces root and leaf litter inputs as plant productivity decreases (Deng et al., 2021).

Throughout the study, we observed stronger model responses to drought and the assigned temperature sensitivity values associated with the half-saturation constant for the depolymerisation of the litter pool in subsoils than in topsoils. This was related to the lower microbial biomass in subsoils, leading to stronger microbial limitation on depolymerisation in the subsoil than in the topsoil. Additionally, at low microbial biomass ( $C_B$ ) the value of the half-saturation constant became increasingly important (Fig. 7). At the same time, microbial depolymerisation rates only affected the POC pools (polymeric litter and microbial residues) and not the mineral-associated organic carbon pools (MAOC). Since the ratio of POC:MAOC was lower in the subsoil than the topsoil, total SOC losses were lower from the subsoil than the topsoil in our study, despite the higher sensitivity to the different  $Q_{10}$  values of the half-saturation constants for depolymerisation. When the  $Q_{10}$  value of the half-saturation constant was  $< 1$ , SOC losses were further accelerated in response to warming. In our study, this lower  $Q_{10}$  value was associated with the breakdown of proteins from the microbial residues pool. Data derived studies have shown that the contribution of microbial residues in the deep soil to total SOC is highly significant and can be up to 54% in grasslands (e.g. Wang et al., 2021). So, if free POC in deep soils is indeed more sensitive to warming as a result of low microbial biomass, our model results support the finding that deep soils rich in microbial residues are more temperature sensitive than those that contain less microbially-derived POC contents, due to the lower  $Q_{10}$  values of the half-saturation constants for the breakdown of polypeptides. However, compared to plant-derived POC, microbial residues have a high mineral sorption potential (Buckeridge et al., 2022; Liu et al., preprint) and could therefore be more protected from decomposition.

Study III demonstrated for the first time how the interplay between the half-saturation constants, temperature and soil moisture changes, and mineral-associated SOC, can affect SOC dynamics. While recently reported lab-based values for the temperature sensitivities of the half-saturation constants (Allison et al., 2018) were used, it remains unclear how these might change in field conditions, especially in the deep soil. Additionally, other enzymes with different temperature sensitivities may dominate microbial depolymerisation rates depending on the litter type and quality. For example, microbes in soils that are high in microbial necromass could also utilise a chitin-degrading enzyme, which was found to have a very high temperature sensitivity value of the half-saturation constant ( $Q_{10}$  value of 2.8, Allison et al.

(2018)). Overall, our results have shown that more research is needed on the response of deep soils to warming (and see Hicks Pries et al., 2023), in particular on the breakdown of deep soil particulate organic carbon, as the intricate interplay between microbes, mineral-associated carbon and changing climatic conditions affect the apparent  $Q_{10}$  values reported for deep soil studies (Gentsch et al., 2018). Zhang et al. (2024) recently showed that apparent  $Q_{10}$  values for SOC mineralisation are mainly dominated by the mineralisation of labile carbon, similar to what we observed in our study. They found that the apparent temperature response was governed by substrate availability under limited carbon availability, and was governed by substrate quality when carbon availability was not limiting. The work of this thesis opens up new possibilities to further explore these effects of different substrate types and substrate availability on microbial decomposition of SOC.

### **3.3 Importance of vertical process-representation in SOC decomposition models**

*Q3: How do soil moisture and soil temperature effects on SOC decomposition vary along a vertical soil gradient?*

A key outcome of the research in this PhD thesis was that SOC decomposition models should consider vertical representations of SOC dynamics because topsoil and subsoil layers respond differently to changes in soil temperature, soil moisture and the interlinked substrate changes. Studies II and III both showed that soil moisture modifies the temperature-driven decomposition rate differently in the topsoil compared to the subsoil. Study II showed that in the topsoil, a stronger slowdown of the decomposition rates was found as a result of stronger substrate diffusion limitation. If decomposition rates in the topsoil increased, this was also mainly driven by an increase in substrate availability. In the subsoil, however, a different pattern was found: Slowdowns were mostly caused by increased oxygen limitation, but acceleration happened both in response to lifting the oxygen limitation (drying) and by increased substrate availability (wetting), with large differences between different ESMs. While subsoil moisture will be less variable over time than topsoil moisture and has a smaller impact on the decomposition rates than topsoil moisture, this study showed that the impact of soil moisture in these lower layers was strongly bi-directional. Many existing SOC decomposition models, however, consider only one soil depth with an average temperature and soil moisture change (Koven et al., 2017), and there are large differences between reported soil moisture values and projections when only the top 10 cm of the soil are considered versus a "whole column" approach (Berg et al., 2017).

Besides soil moisture changes, the results from studies II and III in this thesis also showed that changes in substrate concentration are important along a vertical gradient. In study II, we found that the DAMM model results were very sensitive to the SOC content: When the model was confronted with vertically explicit measurements, it could only reproduce the observed  $CO_2$  fluxes well if a vertically varying SOC density was used. Furthermore, the amount of SOC that could go into solution was a static fraction within the DAMM model (Studies II and II). In reality, however, an increasing contribution of SOC is not dissolved but

sorbed to mineral surfaces with depth (Schrumpf et al., 2013), which can create a solubility gradient with depth and thereby modify the response to moisture. Therefore, Study III considered these dynamic links between substrate availability, microbial biomass and mineral sorption, and the response of SOC stocks to changes in temperature and soil moisture. The third study confirmed that the topsoil and subsoil displayed different responses to soil warming and drying: While absolute SOC changes driven by soil warming and drought were highest in the topsoil, SOC in the subsoil was more sensitive to the (sometimes counteracting) interplay between the half-saturation constants for depolymerisation, temperature and soil moisture changes, and mineral-associated SOC. Furthermore, this depth-resolved modelling approach had the advantage of representing other vital processes that drive substrate availability: Root litter inputs enter the soil at different depths, and organic matter is transported between soil layers through leaching and bioturbation.

This thesis showed that resolving vertical gradients in SOC models will be essential for representing future changes in SOC dynamics. This is especially the case for soils with strong depth gradients in temperature, such as permafrost soils, as well as with strong depth gradients in soil physical heterogeneity: E.g., mineralogical changes with depth will determine how much of SOC will be protected from microbial decomposition, and soil structure will be an important determinant for water connectivity through soil pores (Fisher & Koven, 2020). The studies in this thesis support the growing insight that deep soils can significantly contribute to the global carbon-climate feedback, and should be incorporated into both measurements and models to study SOC decomposition under climate change (Hicks Pries et al., 2023). The integration of new scientific knowledge can help build confidence in future soil carbon decomposition models (Wieder et al., 2019), even if increased model complexity comes with added uncertainty (Shi et al., 2018). Only in such modelling frameworks will it be possible to study and disentangle the individual and joint effects of soil moisture controls on SOC decomposition rates.

### **3.4 Conclusions**

This thesis and the three different studies included in it have shown that: (1) Soil moisture changes have the potential to either slow down or accelerate SOC decomposition rates under a warming climate. Additionally, increased soil temperatures can have a mitigating or further accelerating effect on SOC decomposition rates through the temperature sensitivity of the half-saturation constants for depolymerisation of SOC substrates (2) Soil moisture changes mainly impact SOC decomposition rates through changes in C substrate availability for microbes, although oxygen diffusion limitation can play a significant role too. (3) Vertically resolved model representations of SOC decomposition dynamics are very important, as topsoils and subsoils respond differently to changes in soil moisture and temperature. We showed that this is the result of a complex interplay between microbial biomass and mineral-associated SOC changes with depth, and the effects of temperature and soil moisture changes on the depolymerisation rates of different litter sources.

These insights were obtained by applying a mechanistic modelling framework, the DAMM model, on observations (Study I) and on vertically resolved Earth system model outputs (Study II), and then by studying the dynamic interactions between C substrate availability and climatic changes within a mechanistic, vertically resolved SOC decomposition model (Study III). We demonstrated that warming-induced decomposition rates can be mitigated by droughts as a result of C substrate limitation. Furthermore, by separating the effects of temperature and soil moisture driven changes on SOC decomposition, we were able to demonstrate that not only soil moisture, but also soil warming alone can partially mitigate SOC decomposition rates through the temperature sensitivities of the different enzymes involved in the breakdown of organic matter (Study III).

Overall, this thesis provided new insights into the complex feedback between climate change and SOC dynamics to aid the further development of process-based soil models. The work demonstrated that the next generation of models would benefit from including vertical representations of soil processes, with microbial dynamics and moisture functions that reflect our mechanistic understanding of the effects of soil drying and wetting. Incorporating such models into coupled climate or land surface models will enable us to study the effects and potential feedbacks of climate change on SOC stocks and CO<sub>2</sub>-release to the atmosphere.

### **3.5 Outlook**

The third study of this thesis showed that drought can mitigate warming-induced SOC losses and even result in SOC accumulation over the simulation period. The confounding effects of changes in litter inputs were eliminated from the study on purpose to isolate the effects of soil temperature and soil moisture changes on the modelled SOC stocks. While results from short-term data-driven studies support the model finding that SOC stocks can increase under drought (e.g. Brunn et al., 2023), long-term drought studies generally show a decline in SOC stocks, which can be mainly attributed to the effects of soil warming and decreased litter inputs (e.g. Deng et al., 2021; Meier & Leuschner, 2010). In this light, follow-up studies could focus on studying the feedback between a coupled soil and vegetation model. The model used in this work, JSM, is part of the land surface model QUINCY (Thum et al., 2019). For Study III, forcing files were generated by QUINCY for a static application of JSM. A dynamic coupling between the vegetation model in QUINCY with JSM is nearing completion at the writing of this thesis. In this coupled model, the feedbacks between climate change, vegetation functioning and SOC dynamics can be further explored mechanistically. For example, rising atmospheric CO<sub>2</sub> concentrations, warming, and drought will alter plant productivity, thereby altering the substrate-soil moisture dynamics in the soil system. Additionally, the effects of rising temperature and atmospheric CO<sub>2</sub> concentrations on plant productivity will be constrained by nutrient availability (Fleischer & Terrer, 2022; Terrer et al., 2019). Plants can plastically adapt their leaf nutrients, which is incorporated for nitrogen in the QUINCY model (Caldararu et al., 2020), so that in a coupled model simulation, plant litter inputs to the soil will change in quality and quantity under a changing climate.



The impacts of soil moisture on SOC decomposition can be further explored, as there are several other decomposition processes which are sensitive to soil moisture that were beyond the scope of this thesis, but may impact SOC dynamics. For example, in JSM the microbial turnover into the microbial residues pool is currently defined as a fixed fraction of the existing microbial biomass (Yu et al., 2020). Microbial activity and death, however, are both sensitive to soil moisture and could be linked through soil matric potential (Ghezzehei et al., 2019; Manzoni & Katul, 2014). As mortality increases with drought intensity, the microbial residue pool would increase under drought and store additional C substrates for microbes to access upon soil rewetting. Another process which depends on soil moisture is the solubilisation of DOC from litter. While this leaching rate is represented in JSM using a fixed loss fraction from the soluble litter pool, Yan et al (2018) describe a function where this loss term is multiplied with a soil moisture dependent optimum curve so that losses are highest at optimum soil moisture levels. Such a function, however, would need careful calibration, e.g. after Currie and Aber (1997).

Soils are extremely heterogeneous environments. In this thesis, the importance of including vertical heterogeneity of soils in model process representations was highlighted. In addition, the consideration of soil heterogeneity effects on microbial access to SOC substrates could be a focus of new research. Yan et al. (2018) introduce a collocation factor related to soil porosity and water-connectivity, which describes the physical separation of microbes from SOC associated with mineral surfaces. This factor depends linearly on soil clay content, so that soils with higher clay content have a stronger degree of separation between microbes and C substrates absorbed to mineral surfaces. As data on soil clay content are relatively well reported, such an additional microbial limitation on substrate accessibility could be explored in a follow-up study.

Another possible continuation of the work presented in this thesis would be the integration of different substrate types into nonlinear SOC decomposition models. In this thesis, microbes had access to two different kinds of litter to depolymerise: polymeric litter and microbial residues. The contents of the polymeric litter pool are driven by input from plant litter, and therefore, by the vegetation type used for the simulation. It would therefore be possible to, rather than having one polymeric litter pool, partition the plant litter into different subpools containing different substrates. Needle-leaf evergreen leaves would then enter a different subpool than for example a broadleaf summergreen leaf, and each subpool could be assigned its own temperature sensitivities based on the main chemical properties of the litter entering it.

Process-based non-linear microbial SOC models such as JSM provide opportunities to study the interactions between microbial communities, SOC and soil minerals independently of abiotic drivers (this thesis; Jian et al., 2021b). The difficulty, however, is that they require additional data from field or lab experiments to constrain their parameters which may not always be available, which is reflected by the low number of non-linear kinetic models which have been independently validated (Le Noë et al., 2023). Furthermore, inclusion of additional processes comes at the cost of higher model computational demands and model uncertainty,

so that a balance between model complexity and representation of key processes for SOC decomposition needs to be found (Shi et al., 2018). Therefore, it is important to test and compare different model formulations to advance the development of process-based SOC models based on the latest scientific insights. This remains a critical step in the advancement of our understanding of long-term SOC dynamics.

# References

---

- Abramoff, R., Davidson, E., & Finzi, A. C. (2017). A parsimonious modular approach to building a mechanistic belowground carbon and nitrogen model. *Journal of Geophysical Research: Biogeosciences*, *122*(9), 2418–2434. <https://doi.org/doi:10.1002/2017JG003796>
- Abramoff, R., Xu, X., Hartman, M., O'Brien, S., Feng, W., Davidson, E., et al. (2018). The Millennial model: in search of measurable pools and transformations for modeling soil carbon in the new century. *Biogeochemistry*, *137*(1), 51–71. <https://doi.org/10.1007/s10533-017-0409-7>
- Ahrens, B., Braakhekke, M. C., Guggenberger, G., Schrumpf, M., & Reichstein, M. (2015). Contribution of sorption, DOC transport and microbial interactions to the <sup>14</sup>C age of a soil organic carbon profile: Insights from a calibrated process model. *Soil Biology and Biochemistry*, *88*(Supplement C), 390–402. <https://doi.org/10.1016/j.soilbio.2015.06.008>
- Ahrens, B., Guggenberger, G., Rethemeyer, J., John, S., Marschner, B., Heinze, S., et al. (2020). Combination of energy limitation and sorption capacity explains <sup>14</sup>C depth gradients. *Soil Biology and Biochemistry*, *148*, 107912. <https://doi.org/10.1016/j.soilbio.2020.107912>
- Allison, S. D., Wallenstein, M. D., & Bradford, M. A. (2010). Soil-carbon response to warming dependent on microbial physiology. *Nature Geoscience*, *3*, 336. <https://doi.org/10.1038/ngeo846>  
<https://www.nature.com/articles/ngeo846#supplementary-information>
- Allison, S. D., Romero-Olivares, A. L., Lu, Y., Taylor, J. W., & Treseder, K. K. (2018). Temperature sensitivities of extracellular enzyme V<sub>max</sub> and K<sub>m</sub> across thermal environments. *Glob Chang Biol*, *24*(7), 2884–2897. <https://doi.org/10.1111/gcb.14045>
- Arrhenius, S. (1889). Über die Reaktionsgeschwindigkeit bei der Inversion von Rohrzucker durch Säuren. *Zeitschrift für Physikalische Chemie*, *4U*(1), 226–248. <https://doi.org/10.1515/zpch-1889-0416>
- Atkin, O. K., & Tjoelker, M. G. (2003). Thermal acclimation and the dynamic response of plant respiration to temperature. *Trends in Plant Science*, *8*(7), 343–351. [https://doi.org/10.1016/S1360-1385\(03\)00136-5](https://doi.org/10.1016/S1360-1385(03)00136-5)
- Berg, A., & Sheffield, J. (2018). Climate Change and Drought: the Soil Moisture Perspective. *Current Climate Change Reports*, *4*(2), 180–191. <https://doi.org/10.1007/s40641-018-0095-0>
- Berg, A., Sheffield, J., & Milly, P. C. D. (2017). Divergent surface and total soil moisture projections under global warming. *Geophysical Research Letters*, *44*(1), 236–244. <https://doi.org/10.1002/2016GL071921>
- Berry, J. A., & Raison, J. K. (1981). Responses of Macrophytes to Temperature. In O. L. Lange, P. S. Nobel, C. B. Osmond, & H. Ziegler (Eds.), *Physiological Plant Ecology I: Responses to the Physical Environment* (pp. 277–338). Berlin, Heidelberg: Springer. [https://doi.org/10.1007/978-3-642-68090-8\\_11](https://doi.org/10.1007/978-3-642-68090-8_11)
- Birch, H. F. (1958). The effect of soil drying on humus decomposition and nitrogen availability. *Plant and Soil*, *10*(1), 9–31. <https://doi.org/10.1007/BF01343734>
- Blume, H.-P., Brümmer, G. W., Fleige, H., Horn, R., Kandeler, E., Kögel-Knabner, I., et al. (2016). Soil Organic Matter. In H.-P. Blume, G. W. Brümmer, H. Fleige, R. Horn, E. Kandeler, I. Kögel-Knabner, et al. (Eds.), *Scheffer/Schachtschabel Soil Science* (pp.

- 55–86). Berlin, Heidelberg: Springer Berlin Heidelberg.  
[https://doi.org/10.1007/978-3-642-30942-7\\_3](https://doi.org/10.1007/978-3-642-30942-7_3)
- Bond-Lamberty, B., Bailey, V. L., Chen, M., Gough, C. M., & Vargas, R. (2018). Globally rising soil heterotrophic respiration over recent decades. *Nature*, *560*(7716), 80–83.  
<https://doi.org/10.1038/s41586-018-0358-x>
- Brunn, M., Krüger, J., & Lang, F. (2023). Experimental drought increased the belowground sink strength towards higher topsoil organic carbon stocks in a temperate mature forest. *Geoderma*, *431*, 116356. <https://doi.org/10.1016/j.geoderma.2023.116356>
- Buckeridge, K. M., Mason, K. E., Ostle, N., McNamara, N. P., Grant, H. K., & Whitaker, J. (2022). Microbial necromass carbon and nitrogen persistence are decoupled in agricultural grassland soils. *Communications Earth & Environment*, *3*(1), 1–10.  
<https://doi.org/10.1038/s43247-022-00439-0>
- Caldararu, S., Thum, T., Yu, L., & Zaehle, S. (2020). Whole-plant optimality predicts changes in leaf nitrogen under variable CO<sub>2</sub> and nutrient availability. *New Phytologist*, *225*(6), 2331–2346. <https://doi.org/10.1111/nph.16327>
- Cheng, S., Huang, J., Ji, F., & Lin, L. (2017). Uncertainties of soil moisture in historical simulations and future projections. *Journal of Geophysical Research: Atmospheres*, *122*(4), 2239–2253. <https://doi.org/10.1002/2016JD025871>
- Cotrufo, M. F., & Lavelle, J. M. (2022). Chapter One - Soil organic matter formation, persistence, and functioning: A synthesis of current understanding to inform its conservation and regeneration. In D. L. Sparks (Ed.), *Advances in Agronomy* (Vol. 172, pp. 1–66). Academic Press. <https://doi.org/10.1016/bs.agron.2021.11.002>
- Cotrufo, M. F., Wallenstein, M. D., Boot, C. M., Denef, K., & Paul, E. (2013). The Microbial Efficiency-Matrix Stabilization (MEMS) framework integrates plant litter decomposition with soil organic matter stabilization: do labile plant inputs form stable soil organic matter? *Global Change Biology*, *19*(4), 988–995.  
<https://doi.org/10.1111/gcb.12113>
- Crowther, T. W., van den Hoogen, J., Wan, J., Mayes, M. A., Keiser, A. D., Mo, L., et al. (2019). The global soil community and its influence on biogeochemistry. *Science*, *365*(6455), eaav0550. <https://doi.org/10.1126/science.aav0550>
- Currie, W. S., & Aber, J. D. (1997). Modeling Leaching as a Decomposition Process in Humid Montane Forests. *Ecology*, *78*(6), 1844–1860. <https://doi.org/10.2307/2266106>
- Davidson, E. A. (2020). Carbon dioxide loss from tropical soils increases on warming. *Nature*, *584*(7820), 198–199. <https://doi.org/10.1038/d41586-020-02266-9>
- Davidson, E. A., & Janssens, I. A. (2006). Temperature sensitivity of soil carbon decomposition and feedbacks to climate change. *Nature*, *440*, 165.  
<https://doi.org/10.1038/nature04514>
- Davidson, E. A., Janssens, I. A., & Luo, Y. (2006). On the variability of respiration in terrestrial ecosystems: moving beyond Q<sub>10</sub>. *Global Change Biology*, *12*(2), 154–164.  
<https://doi.org/10.1111/j.1365-2486.2005.01065.x>
- Davidson, E. A., Sudeep, S., Samantha, S. C., & Savage, K. (2012). The Dual Arrhenius and Michaelis–Menten kinetics model for decomposition of soil organic matter at hourly to seasonal time scales. *Global Change Biology*, *18*(1), 371–384.  
<https://doi.org/doi:10.1111/j.1365-2486.2011.02546.x>
- Deng, L., Peng, C., Kim, D.-G., Li, J., Liu, Y., Hai, X., et al. (2021). Drought effects on soil carbon and nitrogen dynamics in global natural ecosystems. *Earth-Science Reviews*, *214*, 103501. <https://doi.org/10.1016/j.earscirev.2020.103501>
- Drake, J. E., Macdonald, C. A., Tjoelker, M. G., Reich, P. B., Singh, B. K., Anderson, I. C., & Ellsworth, D. S. (2018). Three years of soil respiration in a mature eucalypt woodland exposed to atmospheric CO<sub>2</sub> enrichment. *Biogeochemistry*, *139*(1),

- 85–101. <https://doi.org/10.1007/s10533-018-0457-7>
- Fairbairn, L., Rezaeezhad, F., Gharasoo, M., Parsons, C. T., Macrae, M. L., Slowinski, S., & Van Cappellen, P. (2023). Relationship between soil CO<sub>2</sub> fluxes and soil moisture: Anaerobic sources explain fluxes at high water content. *Geoderma*, *434*, 116493. <https://doi.org/10.1016/j.geoderma.2023.116493>
- Falloon, P., Jones, C. D., Ades, M., & Paul, K. (2011). Direct soil moisture controls of future global soil carbon changes: An important source of uncertainty. *Global Biogeochemical Cycles*, *25*(3), n/a-n/a. <https://doi.org/10.1029/2010gb003938>
- Fan, K., Slater, L., Zhang, Q., Sheffield, J., Gentine, P., Sun, S., & Wu, W. (2022). Climate warming accelerates surface soil moisture drying in the Yellow River Basin, China. *Journal of Hydrology*, *615*, 128735. <https://doi.org/10.1016/j.jhydrol.2022.128735>
- Fisher, R. A., & Koven, C. D. (2020). Perspectives on the Future of Land Surface Models and the Challenges of Representing Complex Terrestrial Systems. *Journal of Advances in Modeling Earth Systems*, *12*(4). <https://doi.org/10.1029/2018ms001453>
- Fleischer, K., & Terrer, C. (2022). Estimates of soil nutrient limitation on the CO<sub>2</sub> fertilization effect for tropical vegetation. *Global Change Biology*, *28*(21), 6366–6369. <https://doi.org/10.1111/gcb.16377>
- Freeman, C., Ostle, N., & Kang, H. (2001). An enzymic “latch” on a global carbon store. *Nature*, *409*, 149. <https://doi.org/10.1038/35051650>
- Friedlingstein, P., O’Sullivan, M., Jones, M. W., Andrew, R. M., Bakker, D. C. E., Hauck, J., et al. (2023). Global Carbon Budget 2023. *Earth System Science Data*, *15*(12), 5301–5369. <https://doi.org/10.5194/essd-15-5301-2023>
- García-García, A., Cuesta-Valero, F. J., Miralles, D. G., Mahecha, M. D., Quaas, J., Reichstein, M., et al. (2023). Soil heat extremes can outpace air temperature extremes. *Nature Climate Change*, *13*(11), 1237–1241. <https://doi.org/10.1038/s41558-023-01812-3>
- Gentsch, N., Wild, B., Mikutta, R., Čapek, P., Diáková, K., Schrumpf, M., et al. (2018). Temperature response of permafrost soil carbon is attenuated by mineral protection. *Global Change Biology*, *24*(8), 3401–3415. <https://doi.org/10.1111/gcb.14316>
- Georgiou, K., Koven, C. D., Wieder, W. R., Hartman, M. D., Riley, W. J., Pett-Ridge, J., et al. (2024). Emergent temperature sensitivity of soil organic carbon driven by mineral associations. *Nature Geoscience*, *17*(3), 205–212. <https://doi.org/10.1038/s41561-024-01384-7>
- Ghezzehei, T. A., Sulman, B., Arnold, C. L., Bogie, N. A., & Berhe, A. A. (2019). On the role of soil water retention characteristic on aerobic microbial respiration. *Biogeosciences*, *16*(6), 1187–1209. <https://doi.org/10.5194/bg-16-1187-2019>
- Gruber, A., De Lannoy, G., Albergel, C., Al-Yaari, A., Brocca, L., Calvet, J.-C., et al. (2020). Validation practices for satellite soil moisture retrievals: What are (the) errors? *Remote Sensing of Environment*, *244*, 111806. <https://doi.org/10.1016/j.rse.2020.111806>
- Hartley, I. P., Hill, T. C., Chadburn, S. E., & Hugelius, G. (2021). Temperature effects on carbon storage are controlled by soil stabilisation capacities. *Nature Communications*, *12*(1), 6713. <https://doi.org/10.1038/s41467-021-27101-1>
- Hashimoto, S., Carvalhais, N., Ito, A., Migliavacca, M., Nishina, K., & Reichstein, M. (2015). Global spatiotemporal distribution of soil respiration modeled using a global database. *Biogeosciences*, *12*(13), 4121–4132. <https://doi.org/10.5194/bg-12-4121-2015>
- Hengl, T., de Jesus, J. M., MacMillan, R. A., Batjes, N. H., Heuvelink, G. B., Ribeiro, E., et al. (2014). SoilGrids1km--global soil information based on automated mapping. *PLOS ONE*, *9*(8), e105992. <https://doi.org/10.1371/journal.pone.0105992>

- Hengl, T., Mendes de Jesus, J., Heuvelink, G. B. M., Ruiperez Gonzalez, M., Kilibarda, M., Blagotić, A., et al. (2017). SoilGrids250m: Global gridded soil information based on machine learning. *PLOS ONE*, *12*(2), e0169748. <https://doi.org/10.1371/journal.pone.0169748>
- Hicks Pries, C., Ryals, R., Zhu, B., Min, K., Cooper, A., Goldsmith, S., et al. (2023). The Deep Soil Organic Carbon Response to Global Change. *Annual Review of Ecology, Evolution, and Systematics*, *54*(1), null. <https://doi.org/10.1146/annurev-ecolsys-102320-085332>
- Hicks Pries, C. E., Castanha, C., Porras, R., & Torn, M. S. (2017). The whole-soil carbon flux in response to warming. *Science*, eaa1319. <https://doi.org/10.1126/science.aal1319>
- Hochachka, P. W., & Somero, G. N. (2002). *Biochemical Adaptation: Mechanism and Process in Physiological Evolution*. New York: Oxford University Press.
- Hopkins, F., Gonzalez-Meler, M. A., Flower, C. E., Lynch, D. J., Czimczik, C., Tang, J., & Subke, J.-A. (2013). Ecosystem-level controls on root-rhizosphere respiration. *New Phytologist*, *199*(2), 339–351. <https://doi.org/10.1111/nph.12271>
- Hsu, H., & Dirmeyer, P. A. (2023). Uncertainty in Projected Critical Soil Moisture Values in CMIP6 Affects the Interpretation of a More Moisture-Limited World. *Earth's Future*, *11*(6), e2023EF003511. <https://doi.org/10.1029/2023EF003511>
- IPCC (Ed.). (2023). Global Carbon and Other Biogeochemical Cycles and Feedbacks. In *Climate Change 2021 – The Physical Science Basis: Working Group I Contribution to the Sixth Assessment Report of the Intergovernmental Panel on Climate Change* (pp. 673–816). Cambridge: Cambridge University Press. <https://doi.org/10.1017/9781009157896.007>
- Ito, A., Hajima, T., Lawrence, D. M., Brovkin, V., Delire, C., Guenet, B., et al. (2020). Soil carbon sequestration simulated in CMIP6-LUMIP models: implications for climatic mitigation. *Environmental Research Letters*, *15*(12), 124061. <https://doi.org/10.1088/1748-9326/abc912>
- Jarvis, P., Rey, A., Petsikos, C., Wingate, L., Rayment, M., Pereira, J., et al. (2007). Drying and wetting of Mediterranean soils stimulates decomposition and carbon dioxide emission: the “Birch effect”†. *Tree Physiology*, *27*(7), 929–940. <https://doi.org/10.1093/treephys/27.7.929>
- Jian, J., Vargas, R., Anderson-Teixeira, K., Stell, E., Herrmann, V., Horn, M., et al. (2021a). A restructured and updated global soil respiration database (SRDB-V5). *Earth System Science Data*, *13*(2), 255–267. <https://doi.org/10.5194/essd-13-255-2021>
- Jian, J., Bond-Lamberty, B., Hao, D., Sulman, B. N., Patel, K. F., Zheng, J., et al. (2021b). Leveraging observed soil heterotrophic respiration fluxes as a novel constraint on global-scale models. *Global Change Biology*, *27*(20). <https://doi.org/10.1111/gcb.15795>
- Kirschbaum, M. U. F. (2006). The temperature dependence of organic-matter decomposition—still a topic of debate. *Soil Biology and Biochemistry*, *38*(9), 2510–2518. <https://doi.org/10.1016/j.soilbio.2006.01.030>
- Koven, C. D., Riley, W. J., Subin, Z. M., Tang, J. Y., Torn, M. S., Collins, W. D., et al. (2013). The effect of vertically resolved soil biogeochemistry and alternate soil C and N models on C dynamics of CLM4. *Biogeosciences*, *10*(11), 7109–7131. <https://doi.org/10.5194/bg-10-7109-2013>
- Koven, C. D., Hugelius, G., Lawrence, D. M., & Wieder, W. R. (2017). Higher climatological temperature sensitivity of soil carbon in cold than warm climates. *Nature Climate Change*, *7*(11), 817–822. <https://doi.org/10.1038/nclimate3421>
- Kwon, M. J., Ballantyne, A., Ciais, P., Qiu, C., Salmon, E., Raoult, N., et al. (2022). Lowering water table reduces carbon sink strength and carbon stocks in northern

- peatlands. *Global Change Biology*, 28(22), 6752–6770.  
<https://doi.org/10.1111/gcb.16394>
- Le Noë, J., Manzoni, S., Abramoff, R., Bölscher, T., Bruni, E., Cardinael, R., et al. (2023). Soil organic carbon models need independent time-series validation for reliable prediction. *Communications Earth & Environment*, 4(1), 1–8.  
<https://doi.org/10.1038/s43247-023-00830-5>
- Liang, C., Schimel, J. P., & Jastrow, J. D. (2017). The importance of anabolism in microbial control over soil carbon storage. *Nature Microbiology*, 2(8), 1–6.  
<https://doi.org/10.1038/nmicrobiol.2017.105>
- Liang, J., Wang, G., Singh, S., Jagadamma, S., Gu, L., Schadt, C. W., et al. (2021). Intensified Soil Moisture Extremes Decrease Soil Organic Carbon Decomposition: A Mechanistic Modeling Analysis. *Journal of Geophysical Research: Biogeosciences*, 126(8), e2021JG006392. <https://doi.org/10.1029/2021JG006392>
- Liu, Y., Tian, J., He, N., & Tiemann, L. (preprint). Global microbial necromass contribution to soil organic matter. <https://doi.org/10.21203/rs.3.rs-473688/v1>
- Lorenz, R., Argüeso, D., Donat, M. G., Pitman, A. J., van den Hurk, B., Berg, A., et al. (2016). Influence of land-atmosphere feedbacks on temperature and precipitation extremes in the GLACE-CMIP5 ensemble. *Journal of Geophysical Research: Atmospheres*, 121(2), 607–623. <https://doi.org/10.1002/2015JD024053>
- Lu, J., Carbone, G. J., & Grego, J. M. (2019). Uncertainty and hotspots in 21st century projections of agricultural drought from CMIP5 models. *Sci Rep*, 9(1), 4922. <https://doi.org/10.1038/s41598-019-41196-z>
- Maier, M., Schack-Kirchner, H., Hildebrand, E. E., & Schindler, D. (2011). Soil CO<sub>2</sub> efflux vs. soil respiration: Implications for flux models. *Agricultural and Forest Meteorology*, 151(12), 1723–1730. <https://doi.org/10.1016/j.agrformet.2011.07.006>
- Manzoni, S., & Katul, G. (2014). Invariant soil water potential at zero microbial respiration explained by hydrological discontinuity in dry soils. *Geophysical Research Letters*, 41(20), 7151–7158. <https://doi.org/10.1002/2014gl061467>
- Manzoni, S., Moyano, F., Kätterer, T., & Schimel, J. (2016). Modeling coupled enzymatic and solute transport controls on decomposition in drying soils. *Soil Biology and Biochemistry*, 95, 275–287. <https://doi.org/10.1016/j.soilbio.2016.01.006>
- Meier, I. C., & Leuschner, C. (2010). Variation of soil and biomass carbon pools in beech forests across a precipitation gradient. *Global Change Biology*, 16(3), 1035–1045. <https://doi.org/10.1111/j.1365-2486.2009.02074.x>
- Moorhead, D. L., Lashermes, G., & Sinsabaugh, R. L. (2012). A theoretical model of C- and N-acquiring exoenzyme activities, which balances microbial demands during decomposition. *Soil Biology and Biochemistry*, 53, 133–141. <https://doi.org/10.1016/j.soilbio.2012.05.011>
- Moyano, F. E., Manzoni, S., & Chenu, C. (2013). Responses of soil heterotrophic respiration to moisture availability: An exploration of processes and models. *Soil Biology and Biochemistry*, 59, 72–85. <https://doi.org/10.1016/j.soilbio.2013.01.002>
- Nottingham, A. T., Turner, B. L., Whitaker, J., Ostle, N., Bardgett, R. D., McNamara, N. P., et al. (2016). Temperature sensitivity of soil enzymes along an elevation gradient in the Peruvian Andes. *Biogeochemistry*, 127(2), 217–230. <https://doi.org/10.1007/s10533-015-0176-2>
- O., S., & Orth, R. (2021). Global soil moisture data derived through machine learning trained with in-situ measurements. *Scientific Data*, 8(1), 170. <https://doi.org/10.1038/s41597-021-00964-1>
- Oikawa, P. Y., Grantz, D. A., Chatterjee, A., Eberwein, J. E., Allsman, L. A., & Jenerette, G. D. (2014). Unifying soil respiration pulses, inhibition, and temperature hysteresis

- through dynamics of labile soil carbon and O<sub>2</sub>. *Journal of Geophysical Research: Biogeosciences*, 119(4), 521–536. <https://doi.org/doi:10.1002/2013JG002434>
- Orlowsky, B., & Seneviratne, S. I. (2013). Elusive drought: uncertainty in observed trends and short- and long-term CMIP5 projections. *Hydrol. Earth Syst. Sci.*, 17(5), 1765–1781. <https://doi.org/10.5194/hess-17-1765-2013>
- Parton, W. J., Schimel, D. S., Cole, C. V., & Ojima, D. S. (1987). Analysis of Factors Controlling Soil Organic Matter Levels in Great Plains Grasslands. *Soil Science Society of America Journal*, 51(5), 1173–1179. <https://doi.org/10.2136/sssaj1987.03615995005100050015x>
- Robertson, A. D., Paustian, K., Ogle, S., Wallenstein, M. D., Lugato, E., & Cotrufo, M. F. (2019). Unifying soil organic matter formation and persistence frameworks: the MEMS model. *Biogeosciences*, 16(6), 1225–1248. <https://doi.org/10.5194/bg-16-1225-2019>
- Rousk, J., & Brangarí, A. C. (2022). Do the respiration pulses induced by drying–rewetting matter for the soil–atmosphere carbon balance? *Global Change Biology*, 28(11), 3486–3488. <https://doi.org/10.1111/gcb.16163>
- Runkles, J. R. (1956). *Diffusion, sorption and depth distribution of oxygen in soils*. Iowa State College, Digital Repository @ Iowa State University, <http://lib.dr.iastate.edu/>.
- Schimel, J. P. (2018). Life in Dry Soils: Effects of Drought on Soil Microbial Communities and Processes. *Annual Review of Ecology, Evolution, and Systematics*, 49(1), 409–432. <https://doi.org/10.1146/annurev-ecolsys-110617-062614>
- Schimel, J. P., & Weintraub, M. N. (2003). The implications of exoenzyme activity on microbial carbon and nitrogen limitation in soil: a theoretical model. *Soil Biology and Biochemistry*, 35(4), 549–563. [https://doi.org/10.1016/S0038-0717\(03\)00015-4](https://doi.org/10.1016/S0038-0717(03)00015-4)
- Schrumpf, M., Kaiser, K., Guggenberger, G., Persson, T., Kögel-Knabner, I., & Schulze, E. D. (2013). Storage and stability of organic carbon in soils as related to depth, occlusion within aggregates, and attachment to minerals. *Biogeosciences*, 10(3), 1675–1691. <https://doi.org/10.5194/bg-10-1675-2013>
- Shi, Z., Crowell, S., Luo, Y., & Moore, B. (2018). Model structures amplify uncertainty in predicted soil carbon responses to climate change. *Nat Commun*, 9(1), 2171. <https://doi.org/10.1038/s41467-018-04526-9>
- Sierra, C. A., Trumbore, S. E., Davidson, E. A., Vicca, S., & Janssens, I. (2015). Sensitivity of decomposition rates of soil organic matter with respect to simultaneous changes in temperature and moisture. *Journal of Advances in Modeling Earth Systems*, 7(1), 335–356. <https://doi.org/10.1002/2014MS000358>
- Sierra, C. A., Malghani, S., & Loescher, H. W. (2017). Interactions among temperature, moisture, and oxygen concentrations in controlling decomposition rates in a boreal forest soil. *Biogeosciences*, 14(3), 703–710. <https://doi.org/10.5194/bg-14-703-2017>
- Sihi, D., Davidson, E. A., Chen, M., Savage, K. E., Richardson, A. D., Keenan, T. F., & Hollinger, D. Y. (2018a). Merging a mechanistic enzymatic model of soil heterotrophic respiration into an ecosystem model in two AmeriFlux sites of northeastern USA. *Agricultural and Forest Meteorology*, 252, 155–166. <https://doi.org/10.1016/j.agrformet.2018.01.026>
- Sihi, D., Davidson, E. A., Chen, M., Savage, K. E., Richardson, A. D., Keenan, T. F., & Hollinger, D. Y. (2018b). Merging a mechanistic enzymatic model of soil heterotrophic respiration into an ecosystem model in two AmeriFlux sites of northeastern USA. *Agricultural and Forest Meteorology*, 252, 155–166. <https://doi.org/10.1016/j.agrformet.2018.01.026>
- Sihi, D., Davidson, E. A., Savage, K. E., & Liang, D. (2020). Simultaneous numerical representation of soil microsite production and consumption of carbon dioxide,



- methane, and nitrous oxide using probability distribution functions. *Global Change Biology*, 26(1), 200–218. <https://doi.org/10.1111/gcb.14855>
- Sihi, D., Xu, X., Salazar Ortiz, M., O’Connell, C. S., Silver, W. L., López-Lloreda, C., et al. (2021). Representing methane emissions from wet tropical forest soils using microbial functional groups constrained by soil diffusivity. *Biogeosciences*, 18(5), 1769–1786. <https://doi.org/10.5194/bg-18-1769-2021>
- Skopp, J., Jawson, M. D., & Doran, J. W. (1990). Steady-state aerobic microbial activity as a function of soil water content. *Soil Science Society of America Journal*, 54(6), 1619–1625. <https://doi.org/10.2136/sssaj1990.03615995005400060018x>
- Soong, J. L., Phillips, C. L., Ledna, C., Koven, C. D., & Torn, M. S. (2020). CMIP5 Models Predict Rapid and Deep Soil Warming Over the 21st Century. *Journal of Geophysical Research: Biogeosciences*, 125(2), e2019JG005266. <https://doi.org/10.1029/2019JG005266>
- Sulman, B. N., Phillips, R. P., Oishi, A. C., Shevliakova, E., & Pacala, S. W. (2014). Microbe-driven turnover offsets mineral-mediated storage of soil carbon under elevated CO<sub>2</sub>. *Nature Climate Change*, 4, 1099. <https://doi.org/10.1038/nclimate2436> <https://www.nature.com/articles/nclimate2436#supplementary-information>
- Sun, T., Wang, Y., Lucas-Borja, M. E., Jing, X., & Feng, W. (2021). Divergent vertical distributions of microbial biomass with soil depth among groups and land uses. *Journal of Environmental Management*, 292, 112755. <https://doi.org/10.1016/j.jenvman.2021.112755>
- Tang, J., & Riley, W. J. (2014). Weaker soil carbon–climate feedbacks resulting from microbial and abiotic interactions. *Nature Climate Change*, 5, 56. <https://doi.org/10.1038/nclimate2438> <https://www.nature.com/articles/nclimate2438#supplementary-information>
- Tang, J., & Riley, W. J. (2019). Competitor and substrate sizes and diffusion together define enzymatic depolymerization and microbial substrate uptake rates. *Soil Biology and Biochemistry*, 139, 107624. <https://doi.org/10.1016/j.soilbio.2019.107624>
- Tang, X., Fan, S., Du, M., Zhang, W., Gao, S., Liu, S., et al. (2020). Spatial and temporal patterns of global soil heterotrophic respiration in terrestrial ecosystems. *Earth System Science Data*, 12(2), 1037–1051. <https://doi.org/10.5194/essd-12-1037-2020>
- Taylor, K. E., Stouffer, R. J., & Meehl, G. A. (2012). An Overview of CMIP5 and the Experiment Design. *Bulletin of the American Meteorological Society*, 93(4), 485–498. <https://doi.org/10.1175/BAMS-D-11-00094.1>
- Terrer, C., Jackson, R. B., Prentice, I. C., Keenan, T. F., Kaiser, C., Vicca, S., et al. (2019). Nitrogen and phosphorus constrain the CO<sub>2</sub> fertilization of global plant biomass. *Nature Climate Change*, 9(9), 684–689. <https://doi.org/10.1038/s41558-019-0545-2>
- Thum, T., Caldararu, S., Engel, J., Kern, M., Pallandt, M., Schnur, R., et al. (2019). A new model of the coupled carbon, nitrogen, and phosphorus cycles in the terrestrial biosphere (QUINCY v1.0; revision 1996). *Geoscientific Model Development*, 12(11), 4781–4802. <https://doi.org/10.5194/gmd-12-4781-2019>
- Todd-Brown, K. E. O., Randerson, J. T., Post, W. M., Hoffman, F. M., Tarnocai, C., Schuur, E. A. G., & Allison, S. D. (2013). Causes of variation in soil carbon simulations from CMIP5 Earth system models and comparison with observations. *Biogeosciences*, 10(3), 1717–1736. <https://doi.org/10.5194/bg-10-1717-2013>
- Todd-Brown, K. E. O., Randerson, J. T., Hopkins, F., Arora, V., Hajima, T., Jones, C., et al. (2014). Changes in soil organic carbon storage predicted by Earth system models during the 21st century. *Biogeosciences*, 11(8), 2341–2356. <https://doi.org/10.5194/bg-11-2341-2014>
- Varney, R. M., Chadburn, S. E., Burke, E. J., Jones, S., Wiltshire, A. J., & Cox, P. M. (2023).

- Simulated responses of soil carbon to climate change in CMIP6 Earth system models: the role of false priming. *Biogeosciences*, 20(18), 3767–3790.  
<https://doi.org/10.5194/bg-20-3767-2023>
- Walker, T. W. N., Kaiser, C., Strasser, F., Herbold, C. W., Leblans, N. I. W., Wobken, D., et al. (2018). Microbial temperature sensitivity and biomass change explain soil carbon loss with warming. *Nature Climate Change*, 8(10), 885–889.  
<https://doi.org/10.1038/s41558-018-0259-x>
- Wang, B., An, S., Liang, C., Liu, Y., & Kuzyakov, Y. (2021). Microbial necromass as the source of soil organic carbon in global ecosystems. *Soil Biology and Biochemistry*, 162, 108422. <https://doi.org/10.1016/j.soilbio.2021.108422>
- Wang, G., Post, W. M., Mayes, M. A., Frerichs, J. T., & Sindhu, J. (2012). Parameter estimation for models of ligninolytic and cellulolytic enzyme kinetics. *Soil Biology and Biochemistry*, 48, 28–38. <https://doi.org/10.1016/j.soilbio.2012.01.011>
- Wang, G., Post, W. M., & Mayes, M. A. (2013). Development of microbial-enzyme-mediated decomposition model parameters through steady-state and dynamic analyses. *Ecological Applications*, 23(1), 255–272. <https://doi.org/10.1890/12-0681.1>
- Wang, M., Guo, X., Zhang, S., Xiao, L., Mishra, U., Yang, Y., et al. (2022). Global soil profiles indicate depth-dependent soil carbon losses under a warmer climate. *Nature Communications*, 13(1), 5514. <https://doi.org/10.1038/s41467-022-33278-w>
- Wang, Y., Mao, J., Hoffman, F. M., Bonfils, C. J. W., Douville, H., Jin, M., et al. (2022). Quantification of human contribution to soil moisture-based terrestrial aridity. *Nature Communications*, 13(1), 6848. <https://doi.org/10.1038/s41467-022-34071-5>
- Warner, D. L., Bond-Lamberty, B., Jian, J., Stell, E., & Vargas, R. (2019). Spatial Predictions and Associated Uncertainty of Annual Soil Respiration at the Global Scale. *Global Biogeochemical Cycles*, 33(12), 1733–1745. <https://doi.org/10.1029/2019GB006264>
- Wieder, W. R., Grandy, A. S., Kallenbach, C. M., & Bonan, G. B. (2014). Integrating microbial physiology and physio-chemical principles in soils with the MIMICs model. *Biogeosciences*, 11(14), 3899–3917. <https://doi.org/10.5194/bg-11-3899-2014>
- Wieder, W. R., Hartman, M. D., Sulman, B. N., Wang, Y.-P., Koven, C. D., & Bonan, G. B. (2018). Carbon cycle confidence and uncertainty: Exploring variation among soil biogeochemical models. *Global Change Biology*, 24(4), 1563–1579.  
<https://doi.org/10.1111/gcb.13979>
- Wieder, W. R., Sulman, B. N., Hartman, M. D., Koven, C. D., & Bradford, M. A. (2019). Arctic Soil Governs Whether Climate Change Drives Global Losses or Gains in Soil Carbon. *Geophysical Research Letters*, 46(24), 14486–14495.  
<https://doi.org/10.1029/2019gl085543>
- Xiao, K.-Q., Zhao, Y., Liang, C., Zhao, M., Moore, O. W., Otero-Fariña, A., et al. (2023). Introducing the soil mineral carbon pump. *Nature Reviews Earth & Environment*, 4(3), 135–136. <https://doi.org/10.1038/s43017-023-00396-y>
- Xu, L., Baldocchi, D. D., & Tang, J. (2004). How soil moisture, rain pulses, and growth alter the response of ecosystem respiration to temperature. *Global Biogeochemical Cycles*, 18(4). <https://doi.org/10.1029/2004GB002281>
- Yan, Z., Liu, C., Todd-Brown, K. E., Liu, Y., Bond-Lamberty, B., & Bailey, V. L. (2016). Pore-scale investigation on the response of heterotrophic respiration to moisture conditions in heterogeneous soils. *Biogeochemistry*, 131(1), 121–134.  
<https://doi.org/10.1007/s10533-016-0270-0>
- Yan, Z., Bond-Lamberty, B., Todd-Brown, K. E., Bailey, V. L., Li, S., Liu, CongQiang, & Liu, Chongxuan. (2018). A moisture function of soil heterotrophic respiration that incorporates microscale processes. *Nature Communications*, 9(1), 2562.

- <https://doi.org/10.1038/s41467-018-04971-6>
- Yu, L., Ahrens, B., Wutzler, T., Schrumf, M., & Zaehle, S. (2020). Jena Soil Model (JSM v1.0; revision 1934): a microbial soil organic carbon model integrated with nitrogen and phosphorus processes. *Geoscientific Model Development*, *13*(2), 783–803. <https://doi.org/10.5194/gmd-13-783-2020>
- Yu, L., Caldararu, S., Ahrens, B., Wutzler, T., Schrumf, M., Helfenstein, J., et al. (2023). Improved representation of phosphorus exchange on soil mineral surfaces reduces estimates of phosphorus limitation in temperate forest ecosystems. *Biogeosciences*, *20*(1), 57–73. <https://doi.org/10.5194/bg-20-57-2023>
- Yuan, S., & Quiring, S. M. (2017). Evaluation of soil moisture in CMIP5 simulations over the contiguous United States using in situ and satellite observations. *Hydrol. Earth Syst. Sci.*, *21*(4), 2203–2218. <https://doi.org/10.5194/hess-21-2203-2017>
- Zhang, S., Yu, Z., Lin, J., & Zhu, B. (2020). Responses of soil carbon decomposition to drying-rewetting cycles: A meta-analysis. *Geoderma*, *361*, 114069. <https://doi.org/10.1016/j.geoderma.2019.114069>
- Zhang, S., Wang, M., Xiao, L., Guo, X., Zheng, J., Zhu, B., & Luo, Z. (2024). Reconciling carbon quality with availability predicts temperature sensitivity of global soil carbon mineralization. *Proceedings of the National Academy of Sciences*, *121*(11), e2313842121. <https://doi.org/10.1073/pnas.2313842121>
- Zhang, X., Xie, Z., Ma, Z., Barron-Gafford, G. A., Scott, R. L., & Niu, G.-Y. (2022). A Microbial-Explicit Soil Organic Carbon Decomposition Model (MESDM): Development and Testing at a Semiarid Grassland Site. *Journal of Advances in Modeling Earth Systems*, *14*(1), e2021MS002485. <https://doi.org/10.1029/2021MS002485>

# Individual and co-author contributions to each study

---

Author contributions are described using the CRediT Taxonomy system: <https://credit.niso.org/> “CRediT (Contributor Roles Taxonomy) is a high-level taxonomy, including 14 roles, that can be used to represent the roles typically played by contributors to research outputs. The roles describe each contributor’s specific contribution to the scholarly output.”

## Study I

This study is included as a manuscript to be submitted as a journal article:

**Pallandt, M. , Lange, H., Meissner, H., Schrumpf, M. Reichstein, M. , and Ahrens, B.**

Modelling soil moisture controls on soil respiration through substrate and oxygen availability.

M. Pallandt wrote the original draft for the manuscript with contributions from B. Ahrens and H. Lange. M. Pallandt performed the model calibration and created all visualisations based on source code provided by B. Ahrens. This study was conceptualised by M. Pallandt, B. Ahrens, M. Schrumpf, and H. Lange. Formal analysis was carried out by M. Pallandt, B. Ahrens and H. Lange. Funding acquisition: B. Ahrens, H. Lange and M. Reichstein. H. Meissner conducted fieldwork and curated data for this study. Supervision of M. Pallandt by B. Ahrens, M. Schrumpf, H. Lange, and M. Reichstein.

## Study II

This study has been published as:

**Pallandt, M., Ahrens, B., Koirala, S., Lange, H., Reichstein, M., Schrumpf, M., & Zaehle, S.** (2022). Vertically divergent responses of SOC decomposition to soil moisture in a changing climate. *Journal of Geophysical Research: Biogeosciences*, 127, e2021JG006684. <https://doi.org/10.1029/2021JG006684>

M. Pallandt wrote the original draft for the manuscript with contributions from all co-authors. Conceptualization: M. Pallandt, B. Ahrens, S. Koirala, H. Lange, M. Reichstein, M. Schrumpf, S. Zaehle. Data curation: M. Pallandt, B. Ahrens. Formal analysis: M. Pallandt, B. Ahrens. Funding acquisition: B. Ahrens, H. Lange. Investigation: M. Pallandt, B. Ahrens, S. Koirala. Resources: B. Ahrens, S. Koirala. Supervision: B. Ahrens, H. Lange, M. Reichstein, M. Schrumpf, S. Zaehle. Validation: M. Pallandt, B. Ahrens. Visualisation: M. Pallandt, B. Ahrens.

## Study III

This study is under review with the journal Biogeosciences and available as a preprint:

**Pallandt, M., Schrumpf, M., Lange, H., Reichstein, M., Yu, L. and Ahrens, B.** Drought counteracts soil warming more strongly in the subsoil than in the topsoil according to a vertical microbial SOC model, EGUsphere [preprint], <https://doi.org/10.5194/egusphere-2024-186>, 2024.

M. Pallandt wrote the original draft for the manuscript with contributions from all co-authors. B. Ahrens and L. Yu wrote the original JSM model code (version 1.0, Yu et al. 2020), M. Pallandt and B. Ahrens wrote minor code modifications to run the model experiments as described in Study III, Section 2, and M. Pallandt performed the model simulations and created all visualisations. This study was conceptualised by M. Pallandt, B. Ahrens, M. Schrumpf, and H. Lange. Formal analysis was carried out by M. Pallandt and B. Ahrens. Funding acquisition: B. Ahrens, H. Lange and M. Reichstein. Supervision of M. Pallandt by B. Ahrens, H. Lange, M. Schrumpf, and M. Reichstein.

# Study I

---

## Modelling soil moisture controls on soil respiration dynamics through substrate and oxygen availability

This study is included as a manuscript to be submitted as a journal article:

*Pallandt, M. , Lange, H., Meissner, H., Schruppf, M. Reichstein, M. , and Ahrens, B.*  
Modelling soil moisture controls on soil respiration through substrate and oxygen availability.

### **Abstract**

Soil organic carbon losses through microbial respiration can create a considerable feedback on climate warming. As a result of climate change, soils are expected to warm considerably, with the potential of accelerating decomposition rates if sufficient soil moisture is available. In non-mesic ecosystems, however, soil moisture may mitigate these warming effects by limiting decomposition rates, by restricting the diffusion of carbon (C) substrates (in dry soils) or the diffusion of oxygen (in very wet soils). This study uses the Dual Arrhenius Michaelis-Menten (DAMM) model which mechanistically links simultaneous changes in soil temperature and soil moisture to estimate soil respiration. We calibrate the DAMM model to soil CO<sub>2</sub> efflux measurements collected at Las Majadas, a semi-arid site in Spain which experiences strong temperature and soil moisture fluctuations throughout the year. The calibrated DAMM model successfully captures observed temporal variability in soil respiration, highlighting its suitability for savanna ecosystems like Las Majadas. Our results demonstrate that soil moisture exerts very strong controls on observed soil CO<sub>2</sub> efflux at the site. The observed C flux dynamics cannot be accurately captured without including C substrate and oxygen diffusion limitations on the temperature-driven respiration rates. At Las Majadas, C substrate diffusion limitation is the dominant driver in explaining the observations, especially during the summer period. Additionally, we find that oxygen diffusion limitation affects respiration rates under very wet soil conditions, which is not accurately captured by temperature driven model estimates. Lastly, comparing our calibrated soil moisture control function with the original DAMM model calibration emphasises the need for careful parameter estimation, particularly when extrapolating beyond the model's calibration range. Overall, this study enhances our understanding of the complex interactions between soil temperature, moisture, and respiration rates, offering valuable insights to improve the modelling of soil C dynamics in non-mesic ecosystems.

# 1 Introduction

Soil respiration ( $R_{soil}$ ), the soil-to-atmosphere flux of carbon dioxide ( $\text{CO}_2$ ) generated by soil microbes and plant roots, is an important flux in the global carbon (C) cycle.  $R_{soil}$  reflects the linked processes of plant primary productivity, which generates the autotrophic respiration flux, and microbial mineralization of litter and soil organic matter, which generates the heterotrophic (microbial) respiration flux. Next to soil temperature, soil moisture is the most important climatic factor controlling  $R_{soil}$  (Davidson & Janssens, 2006; Moyano et al., 2013; Yan et al., 2018). As a result of climate change, it is expected that soils will warm by  $\sim 4.5$  degrees by the end of the century (Soong et al., 2020), but projected future changes in soil moisture are more diverse (Berg et al., 2017) and highly dependent on anthropogenic factors (Wang et al., 2022). At the same time, and despite long-standing evidence that soil moisture is an important driver of  $R_{soil}$  rates (Greaves & Carter, 1920; Skopp et al., 1990), biogeochemical models of soil organic matter decomposition, and the heterotrophic and autotrophic components of soil respiration are often highly empirical with a strong focus on temperature (e.g. through the use of  $Q_{10}$  functions) which reduces their predictive capabilities (Davidson et al., 2012; Moyano et al., 2013; Sierra et al., 2015; Yan et al., 2018).

Soil moisture variations confound temperature effects on  $R_{soil}$ , lowering the high apparent  $Q_{10}$  values that can be observed under optimal soil moisture conditions as soils dry out or get wetter (Davidson et al., 2014). So, to independently describe the effects of soil temperature and soil moisture changes on  $R_{soil}$ , Davidson et al. (2012) developed a simple modelling framework that mechanistically links simultaneous changes in soil temperature and soil moisture to the heterotrophic component of  $R_{soil}$ . Their Dual Arrhenius Michaelis-Menten (DAMM) model is based on the principle that at optimal soil moisture values, respiration rates are driven by soil temperature and exponentially increase with temperature following an Arrhenius function. This temperature-driven optimal maximum rate (often called  $V_{max}$ ) is reduced when soil moisture decreases or increases below this optimum (Fig. 1): At low soil moisture, microbes are limited in the amount of accessible substrates to decompose, whereas at high soil moisture, oxygen availability limits microbial respiration rates. The diffusion of solutes through the soil matrix in the liquid phase is the main pathway by which organic C substrates can reach microbial surfaces, and for substrate-degrading enzymes produced by microbes to reach the substrate. Low soil moisture impedes the diffusion of these solutes, thereby limiting microbial activity. Oxygen diffusion in the gas phase is the main pathway to provide the necessary electron acceptor for organic C oxidation (Yan et al., 2016). So when high soil moisture fills soil pores with water, oxygen diffusion through air to microbes is restricted and microbial respiration rates decrease.

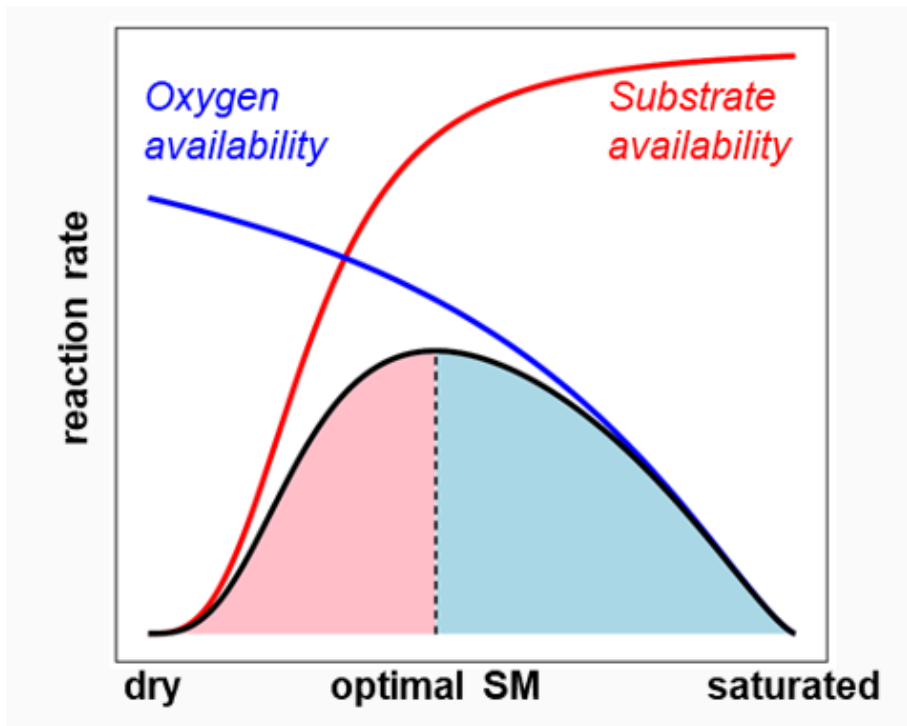


**Figure 1:** Conceptual representation of the combined effects of soil temperature and soil moisture on microbial respiration rates with the DAMM model (Davidson et al., 2012). When soils are dry, the availability of substrates to microbes is low, while oxygen availability is high. When soils are saturated, oxygen availability is low while substrate availability increases. At optimal soil moisture (dotted line), the reaction rate (solid black line) is governed by temperature and at its maximum ( $V_{max}$ ).

The DAMM model is developed to simulate changes in the heterotrophic component of  $R_{soil}$  and was successfully calibrated to data from field trenching experiments, where the autotrophic component from root respiration was experimentally excluded (Abramoff et al., 2017; Davidson et al., 2012; Sihi et al., 2018). Such trenching experiments, data-driven partitioning methods, and results from laboratory incubation experiments, however, suggest that heterotrophic respiration makes a large contribution to  $R_{soil}$  (Bond-Lamberty et al., 2018; Jian et al., 2021b, 2021a; Oikawa et al., 2014; Sihi et al., 2018). In this study, we calibrate the DAMM model directly to  $R_{soil}$  measurements, and assume that root respiration can be modelled as a function of soil temperature and moisture with the same functional form as in DAMM.

Since its development, the DAMM model is successfully used at the temperate forest sites at which it was developed (e.g. Abramoff et al., 2017; Davidson et al., 2012; Sihi et al., 2018). Temperature is the main driver of the measured heterotrophic fluxes there. When soil moisture controls dominate the response, for example during the summer, variations in substrate availability are the main driver, because the soil is very well drained and does not experience extremely wet conditions (Davidson et al., 2012). The DAMM model, with calibration of some of its parameters, was also successfully used at other ecosystems, e.g. at a



dry site in Australia with highly variable rainfall (Drake et al., 2018), and an irrigated agricultural site in a Californian desert climate (Oikawa et al., 2014).

In this study, we calibrate the DAMM model to soil respiration measurements with high temporal resolution from a semi-arid site in Spain which experiences strong seasonal variations in soil temperature and soil moisture to 1) demonstrate that soil moisture controls are very important to estimate  $R_{soil}$  in such dynamic systems; 2) highlight the relative importance of substrate and oxygen limitations on  $R_{soil}$  at different time periods (summer drought, winter flooding); and 3) compare and discuss our results from a semi-arid site in light of the original DAMM model development from the temperate site Harvard Forest (Davidson et al., 2012).

## 2 Methods

### 2.1 Study site and measurements

The research site Majadas de Tiétar, also known as ‘Las Majadas’, is located in a publicly accessible area in the Extremadura of Spain (39°56' N; 5°46' W, 258 m above sea level). The site is classified as a typical Iberian dehesa ecosystem and the main vegetation consists of widely spaced oak trees (mainly *Quercus ilex*, ~20 trees ha<sup>-1</sup>) and a highly diverse herbaceous layer on which cattle graze from early December to late June. The climate at the site is continental Mediterranean with mild winters and a mean annual temperature of 16.7 °C (El-Madany et al., 2018). Annual precipitation has large interannual variability but averages around 650 mm yr<sup>-1</sup>. Most rain falls between winter and early spring, occasionally flooding the site. In the summer the soil can get very dry as rain days are rare (only 5-10 days per summer) and usually with less than 10 mm rain day<sup>-1</sup> (El-Madany et al., 2018). The total soil profile is approximately 90-100 cm deep and classified as an Abruptic Luvisol (WRB 2015). The topsoil is sandy (6% clay, 20% silt, 74% sand, Morris et al. (2022)), followed by a horizon with higher clay contents starting at variable depths between 30 - 60 cm (El-Madany et al., 2020; Nair et al., 2023). The highest SOC contents are found in the upper 15 cm, and strongly decline with depth (Casals et al., 2011). The research site is part of the FLUXNET network of eddy-covariance measurements with three different towers. The eddy covariance measurements and further site characteristics are described in detail by El-Madany et al. (2018, 2020) and Morris et al. (2019, 2022). In May 2015, semi-automated soil respiration measurement chambers were installed at the site. Soil respiration measurements are taken every 30 minutes, and a more detailed description of the chamber design and experimental setup is summarised in Wutzler et al. (2020). Soil temperature and soil moisture are measured at 5, 10, and 20 cm depth, respectively (Paulus et al., 2022). Our time series includes half-hourly measurements recorded between 1 July 2015 until 30 November 2017 of soil temperature (°C) at 5 cm depth, soil moisture (volumetric, %) at 5 cm depth, and total CO<sub>2</sub> efflux (g C m<sup>-2</sup> d<sup>-1</sup>) from a soil respiration measurement chamber located in an open canopy grass area close to the northernmost eddy covariance flux tower. Gap-filled records or measurements with a poor data quality flag were removed from our dataset prior to analysis,

creating several gaps in the time series but increasing confidence in measurement accuracy (Wutzler et al., 2020).

## 2.2 The Dual Arrhenius Michaelis-Menten (DAMM) model

The Dual Arrhenius Michaelis-Menten (DAMM) model simulates the effects of soil temperature and soil moisture on soluble substrate supply for microbial decomposition of organic matter. For easy comparability of parameter estimates (Section 2.3), we follow the original units of the DAMM model by Davidson et al. (2012) to calculate the soil respiration rate ( $R$ , g C cm<sup>-3</sup> soil day<sup>-1</sup>):

$$R = V_{max} \times \frac{[S]}{kM_s + [S]} \times \frac{[O_2]}{kM_{O_2} + [O_2]} \quad (1)$$

where  $V_{max}$  is an Arrhenius function for the maximum reaction rate of  $R$  (g C cm<sup>-3</sup> soil day<sup>-1</sup>), which is multiplied by two Michaelis-Menten terms to represent the moisture controls on substrate ( $S$ ) and oxygen ( $O_2$ ) diffusion for microbial depolymerisation of plant litter and soil organic matter. The maximum reaction rate,  $V_{max}$ , depends on soil temperature and is expressed as:

$$V_{max} = \alpha \times \exp \left[ - \frac{Ea}{R_{gas} \times T_{soil}} \right] \quad (2)$$

where  $\alpha$  is a pre-exponential factor descriptive of the base respiration rate (mg C cm<sup>-3</sup> soil day<sup>-1</sup>; Sihi et al. 2018, 2020),  $Ea$  is the activation energy (kJ mol<sup>-1</sup>),  $R_{gas}$  is the universal gas constant (kJ K<sup>-1</sup> mol<sup>-1</sup>), and  $T_{soil}$  is the soil temperature (K).

To calculate the substrate concentration  $[S]$  at the reaction site:

$$[S] = p \times [S_{total}] \times D_{liq} \times \theta^3 \quad (3)$$

a fixed fraction  $p$  of the total soil C content ( $[S_{total}]$ , g C cm<sup>-3</sup> soil) can diffuse into the liquid phase, where  $D_{liq}$  is the diffusion coefficient of the substrate in liquid phase, and  $\theta$  (cm<sup>3</sup> H<sub>2</sub>O cm<sup>-3</sup> soil) is the volumetric soil moisture content. The oxygen concentration at the reaction site,  $[O_2]$ , is also calculated as a diffusivity function, using soil porosity and volumetric water content to calculate the air-filled pore space (Millington, 1959):

$$[O_2] = D_{gas} \times O_{2,airfrac} \times a^{\frac{4}{3}} \quad (4)$$

where  $D_{gas}$  is the diffusion coefficient for oxygen in air,  $O_{2,airfrac}$  is the fraction of oxygen in air (L O<sub>2</sub> L<sup>-1</sup> air), and  $a$  is the air-filled porosity which is calculated by subtracting the volumetric water content ( $\theta$ ) from total porosity as follows:

$$a = 1 - \frac{BD}{PD} - \theta \quad (5)$$

where total porosity is calculated from soil bulk density and particle density (1 -  $BD$  divided by  $PD$ ). When a site's total porosity is unknown, it can also be estimated from the observed maximum volumetric water content, provided that the soil reaches saturation during the observed time period. In Eq. 1,  $kM_s$  (g C cm<sup>-3</sup> soil) and  $kM_{O_2}$  (cm<sup>3</sup> O<sub>2</sub> cm<sup>-3</sup> air) are the corresponding half-saturation constants for substrate and oxygen diffusion limitation, respectively. Lastly, the calculated soil respiration rate ( $R$ , g C cm<sup>-3</sup> soil day<sup>-1</sup>, Eq. 1) is converted to a respiration flux (g C m<sup>-2</sup> day<sup>-1</sup>) using an effective soil depth of 10 cm (Davidson et al., 2012).

### 2.3 Model fitting and parameter estimation

The values for the input parameters discussed above are listed in Table 1. These were taken from Davidson et al. (2012), or taken from field measurements near the  $R_{soil}$  chamber (T. Hammer, personal communication, 2018): soil bulk density, particle density and soil C content. Four parameters were used to fit the DAMM model to the field data  $\alpha$ ,  $Ea$ ,  $kM_s$ , and  $kM_{O_2}$ . As the initial parameter values (prior to fitting) we used the values reported by Davidson et al. (2012, Table 1). We then run the DAMM model for a first estimate of  $R_{soil}$  and define a cost function where we try to minimise sum of squared residuals between modelled and observed  $R_{soil}$ :

$$cost = \sum (R_{soil,mod} - R_{soil,obs})^2 \quad (6)$$

where  $R_{soil,mod}$  is the soil CO<sub>2</sub> efflux modelled by the DAMM model using Eqs. 1-5 at an effective soil depth of 10 cm, and where  $R_{soil,obs}$  is the measured soil CO<sub>2</sub> efflux. We use the function `modFit` from the R package `FME` (Soetaert & Petzoldt, 2010, version 1.3.6.3) with its default ‘Nelder-Mead’ optimisation method to find the best set of parameter values that minimises the cost function (Eq. 6). We constrained our parameter estimates with a lower boundary of 0 to ensure no negative values could be fitted, but specified no upper boundary. Using the fitted parameter values, we calculated the goodness of fit metrics for the DAMM model as an R<sup>2</sup> value, and calculated the RMSE between modelled and observed  $R_{soil}$  using the function ‘`rsme`’ from the R package `ModelMetrics` (Hunt, 2022). To highlight the difference between the temperature and soil moisture controls on modelled  $R_{soil}$ , we also calculate values for the DAMM model while switching the soil moisture controls off, i.e. by

setting the two Michaelis-Menten terms from Eq. 1 to a value of 1. For plotting, we calculated the water-saturation of the soil as the ratio of the volumetric soil moisture content and the total porosity, i.e. as  $\theta/(1 - BD/PD)$ . All analyses were done in Rstudio (RStudio Team, 2018), using R version 4.3.2 (R Core Team, 2023) and latest versions of the additional R packages scales (Wickham et al., 2023) and ggplot2 (Wickham, 2016).

## 3 Results

### 3.1 Soil temperature and soil moisture dynamics at Las Majadas

Soil temperature at 5 cm depth follows a clear daily and seasonal cycle at Las Majadas (Fig. 2), varying between 3.8 and 31.2 °C, with a mean temperature of 16.0 °C (median 15.3 °C). Please note our observation period spans a little under 2.5 years from July 2015 until November 2017, which covers three summer and two winter periods. Soil moisture (SM) at 5 cm depth is highly variable at the site: The lowest observed mean volumetric SM is 0.043 and the maximum 0.448, with a mean of 0.193 (median 0.179). The site's total soil porosity, calculated from measured soil bulk density and particle density (Eq. 5, Table 1) is 0.456. As a result, the water-saturation of the soil is between 9.4% and 98.2% during the observation period (Fig. 2c) with a median and mean value of 39.3% and 42.4%, respectively. This illustrates that the site experiences both extremely dry and extremely wet soil moisture conditions throughout the year.

### 3.3 Soil temperature and soil moisture effects on $R_{soil}$

Soil respiration rates modelled with DAMM after fitting its parameters capture the observed fluxes at Las Majadas well (Fig. 2a, green points), explaining 55% of the variance in observed  $R_{soil}$  with an RMSE of 1.0 g C m<sup>-2</sup> day<sup>-1</sup> (Table 2). Periods with low  $R_{soil}$  rates coincide with low temperatures (Fig. 2b) or low water-saturation (Fig. 2c) at the site. The strength of the DAMM model's two moisture controls, substrate diffusion and oxygen diffusion, is calculated with the two MM-terms from Eq. 1 and shown in Fig. 2d: Values close to one indicate no diffusion limitation and values close to zero indicate severe diffusion limitation of either C substrate (red points) or oxygen (blue points). Our results show that substrate diffusion is extremely important to explain the observed variability in  $R_{soil}$ , especially during long dry periods and subsequent rewetting events. The importance of SM controls for explaining the observed variability is further confirmed by our results from a model simulation where soil moisture is not limiting modelled  $R_{soil}$  rates: We ran the DAMM model using a fixed value of 1 for both Michaelis-Menten terms for substrate and oxygen diffusion (Eq. 1), i.e. calculating the temperature-driven maximum rate ( $V_{max}$ ) only. This version of the DAMM model ("DAMM (MM = 1)", Fig. 2a, pink points) explained less than 0.1% of the variance in observed  $R_{soil}$  with an RMSE of 4.41 g C m<sup>-2</sup> day<sup>-1</sup> (Table 2). Additionally, the DAMM model with its MM-terms set to 1 clearly overestimates  $R_{soil}$  when soil temperature is high and SM is low. For example, in the period shortly before April 2017

and November 2017 the DAMM model with SM controls consistently reproduces the observed  $R_{soil}$  peaks, whereas it severely overestimates the fluxes when the MM-terms are set to 1. The DAMM model with its MM-terms set to 1 captures observed  $R_{soil}$  well when soil temperatures are low and SM is at intermediate levels (Fig. 2a). This indicates that when SM is not limiting the diffusion of C substrates or oxygen, temperature is the main driver of  $R_{soil}$  at our study site.

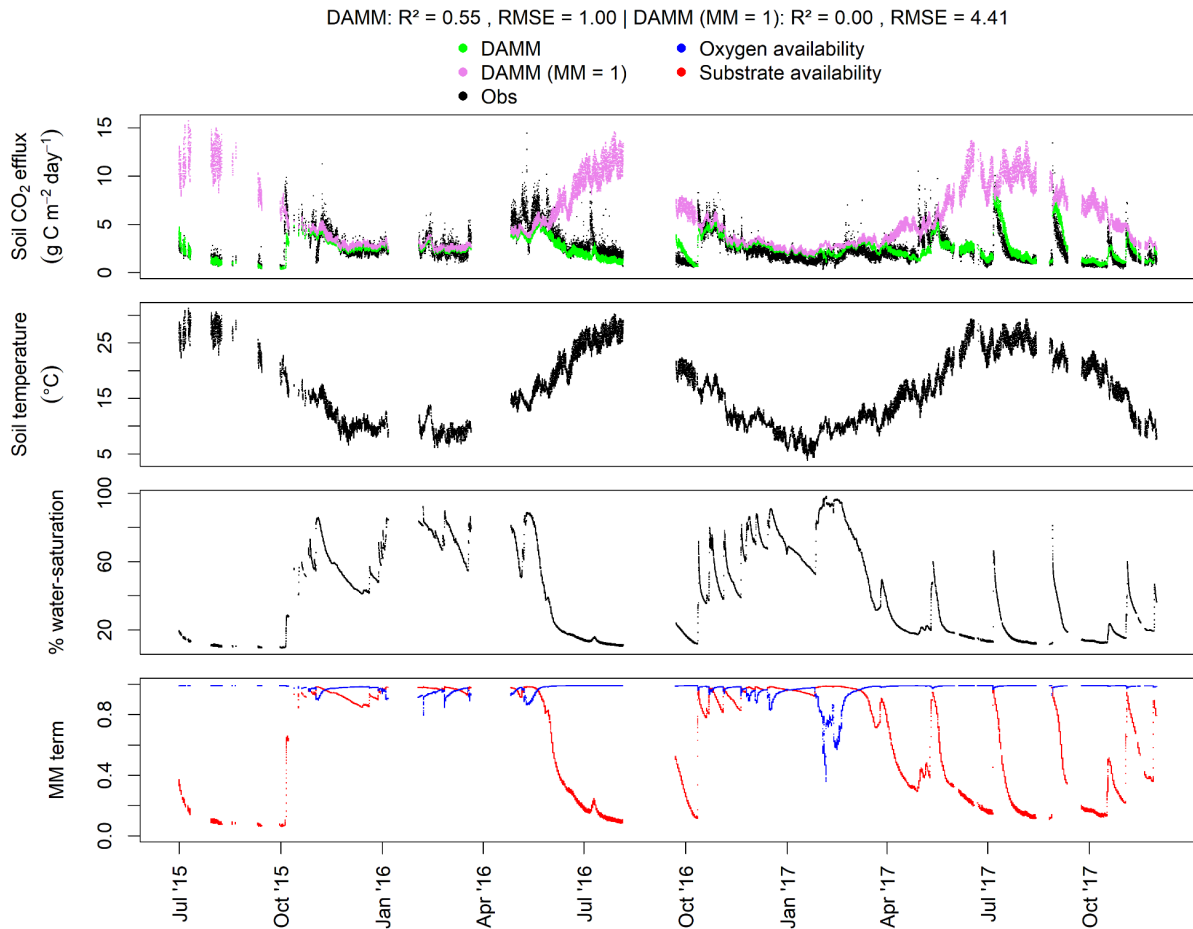


**Figure 2:** DAMM model fitted to  $R_{soil}$  observations at Las Majadas. a) Observed (black) and modelled soil  $CO_2$  efflux ( $g\ C\ m^{-2}\ day^{-1}$ ) for the full DAMM model (green, DAMM) and DAMM model with both MM-terms set to 1 (pink, DAMM (MM = 1)); b) Soil temperature ( $^{\circ}C$ ); c) Soil water-saturation (%); d) Michaelis-Menten (MM) terms for substrate availability (red) and oxygen availability (blue).

**Table 1:** Parameters and constants for the DAMM model. Four parameters were estimated in this study, we report their initial value before (default value) and after model fitting (fit value).

Parameter/ Constant	Units	Default value	Fit value	Description
$\alpha$	$\text{g C cm}^{-3} \text{ soil d}^{-1}$	$1.29 \times 10^{7a}$	$1.24 \times 10^6$	base rate (pre-exponential factor)
$Ea$	$\text{kJ mol}^{-1}$	72.76 <sup>a</sup>	57.67	activation energy for C substrate
$kM_S$	$\text{g C cm}^{-3} \text{ soil}$	$9.95 \times 10^{-7a}$	$4.34 \times 10^{-8}$	half-saturation constant for substrate
$kM_{O_2}$	$\text{cm}^3 \text{ O}_2 \text{ cm}^{-3} \text{ air}$	0.121 <sup>a</sup>	$1.06 \times 10^{-3}$	half-saturation constant for O <sub>2</sub>
BD	$\text{g cm}^{-3}$	1.37 <sup>b</sup>		bulk density
PD	$\text{g cm}^{-3}$	2.52 <sup>b</sup>		particle density
$S_{total}$	$\text{g cm}^{-3}$	0.027925 <sup>b</sup>		total soil C content
$p_{S_x}$	-	$4.14 \times 10^{-4a}$		soluble C substrate fraction
$D_{liq}$	-	3.17 <sup>a</sup>		diffusion coefficient for soil C substrate in liquid phase
$D_{gas}$	-	1.67 <sup>a</sup>		diffusion coefficient for O <sub>2</sub> in air
$R$	$\text{kJ K}^{-1} \text{ mol}^{-1}$	8.314 <sup>a</sup>		universal gas constant
$O_{2,airfrac}$	$\text{L O}_2 \text{ L}^{-1} \text{ air}$	0.209 <sup>a</sup>		fraction of oxygen in air

<sup>a</sup> Values from Davidson et al. (2012). <sup>b</sup> Values measured at Majadas (T. Hammer, personal communication 2018).

**Table 2:** Cumulative observed and modelled  $R_{soil}$  over the full simulation period with goodness of fit metrics.

	<b>Cumulative <math>R_{soil}</math> (kg C m<sup>-2</sup>)</b>	<b>R<sup>2</sup></b>	<b>RMSE (g C m<sup>-2</sup> d<sup>-1</sup>)</b>
<b>Observed</b>	1.43		
<b>DAMM</b>	1.41	0.551	1.00
<b>DAMM (MM = 1)</b>	3.02	0.001	4.41

The product of the two MM-terms for C substrate and oxygen diffusion (Eq. 1) indicates the strength of the soil moisture controls at the site (Fig. 3), because  $V_{max}$  is multiplied by substrate  $\times$  oxygen diffusion limitation. Strong SM controls (low substrate  $\times$  oxygen diffusion) often coincide with low water-saturation at the site, which indicates that C substrate diffusion limitation during dry soil conditions is the dominant SM control at Las Majadas. Oxygen diffusion limitation, however, also plays an important role during wintertime (Fig. 3). In February 2017, for example, the site's water-saturation was extremely high and reached values close to full saturation ( $> 98\%$ , Fig. 4c). As a result, in the DAMM model  $V_{max}$  is reduced by  $\sim 65\%$  due to oxygen diffusion limitation, posing a strong moisture control on modelled  $R_{soil}$  (Fig. 3). Despite slightly overestimating observed  $R_{soil}$  rates when water-saturation is above 90% at the beginning of the month, the DAMM model captures the observations much better than the DAMM model with the MM-terms set to 1 (Fig. 4). Overall, measured CO<sub>2</sub> efflux is low during this period but can still reach values up to 2 g C m<sup>-2</sup> day<sup>-1</sup>. As SM levels reduce in the last few days of February, the DAMM model with MM-terms set to 1 also captures the observations reasonably well again.

Besides the importance of SM controls to explain  $R_{soil}$  under extremely dry and wet soil moisture conditions at the site, our results further indicate that soil rewetting events are important in explaining  $R_{soil}$  peaks observed throughout the observation period (Fig. 2a): For example, in October 2015 and between May and December 2017, the DAMM model without soil moisture controls is not able to capture observed  $R_{soil}$  at all, while the DAMM model with SM controls follows the observations well.

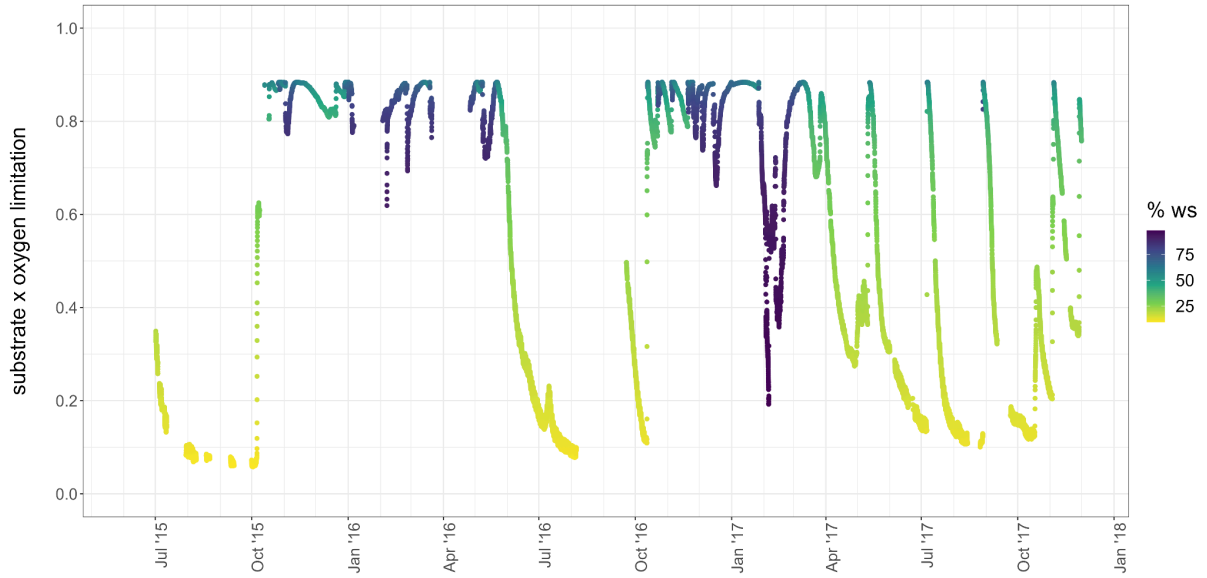


**Figure 3:** Strength of SM controls at Las Majadas, expressed as substrate x oxygen limitation, which is the product of the two Michaelis-Menten terms for C substrate and oxygen diffusion from Eq. 1. Points are coloured by % water-saturation (% ws), ranging from dry (9.4% ws) to very wet (98.2% ws) soil conditions.

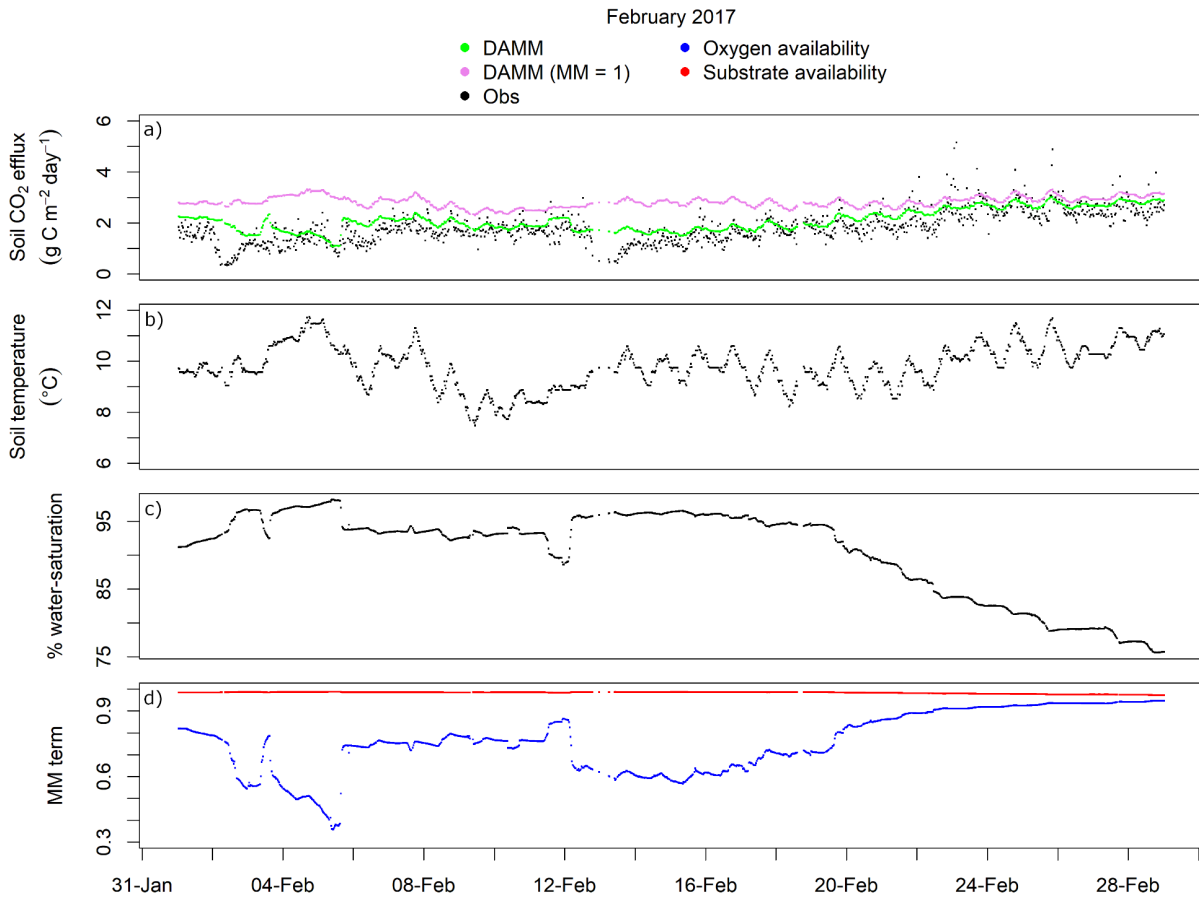


**Figure 4:** Subset of Fig. 2, from 1 - 28 Feb 2017. DAMM model fitted to  $R_{soil}$  observations at Las Majadas. a) Observed (black) and modelled soil CO<sub>2</sub> efflux (g C m<sup>-2</sup> day<sup>-1</sup>) for the full DAMM model (green, DAMM) and DAMM model with both MM-terms set to 1 (pink, DAMM (MM = 1)); b) Soil temperature (°C); c) Soil water-saturation (%); d) Michaelis-Menten (MM) terms for substrate availability (red) and oxygen availability (blue).



To further quantify the impact of soil moisture on  $R_{soil}$  fluxes at Las Majadas, we calculated the cumulative total soil CO<sub>2</sub> efflux during the observation period (1/7/2015 - 30/11/2017) with active measurements for 1) the observations; 2) the DAMM model; and 3) the DAMM model with both MM-terms set to one (Table 2). The observed cumulative total soil CO<sub>2</sub> efflux was 1.43 kg C m<sup>-2</sup>. The DAMM model closely captures the observed cumulative total soil CO<sub>2</sub> efflux at 1.41 kg C m<sup>-2</sup>, which is only 1% less than the observed value. Because the DAMM model is fitted on the data small deviations are expected, and can be caused by an underestimation of  $R_{soil}$  during periods with sufficient SM availability, where the DAMM model is not able to capture peaks in observed  $R_{soil}$  (Fig. 2a). Such peaks can be caused by variations in autotrophic respiration that are tightly coupled to plant photosynthetic activity (Hopkins et al., 2013), which is not explicitly simulated by the DAMM model. Another possible explanation is that the soil moisture and soil temperature measurements in our dataset are taken at 5 cm soil depth. Additional CO<sub>2</sub> is produced in deeper soil layers with different moisture and temperature. The DAMM model, however, closely matches the observed cumulative fluxes and observed temporal variations in  $R_{soil}$ . In contrast, the version of the DAMM model without SM controls (DAMM (MM = 1), Fig. 2a) would clearly overestimate  $R_{soil}$  rates when soil temperatures were high and the soil was dry. This large overestimation would result in a modelled cumulative total soil CO<sub>2</sub> efflux of 3.02 kg C m<sup>-2</sup>, which is more than double of the observations (112% overestimation). Overall, our results show that soil moisture poses a very strong control on soil respiration fluxes at Las Majadas and that the DAMM model is able to capture these dynamics well.

### 3.3 Parameter estimation and strength of soil moisture controls

To fit the DAMM model to the observations we estimated four parameters,  $\alpha$ ,  $Ea$ ,  $kM_S$ , and  $kM_{O_2}$ , using a cost function that minimises the sum of squared residuals between modelled and observed  $R_{soil}$  (Eq. 6). The fitted values for the pre-exponential factor ( $\alpha$ ), activation energy ( $Ea$ ), and the half-saturation constant for substrate diffusion ( $kM_S$ ) are lower than their initial values (Table 1). The estimated activation energy,  $Ea$ , is 57.67 kJ mol<sup>-1</sup>, a value comparable to measured activation energies reported for e.g.  $\beta$ -glucosidase which is involved in the breakdown of cellulose (Allison et al., 2018; Davidson et al., 2012). The fitted value for the half-saturation constant for oxygen diffusion ( $kM_{O_2}$ ) is  $1.06 \cdot 10^{-3}$  cm<sup>3</sup> O<sub>2</sub> cm<sup>-3</sup> air. This is much lower than the default value of 0.121 cm<sup>3</sup> O<sub>2</sub> cm<sup>-3</sup> air from Harvard forest, which was not calibrated against data in the original study by Davidson et al. (2012), but taken as the value of [O<sub>2</sub>] calculated from Eq. 4 at mean  $\theta$  observed at this site. To visually and quantitatively compare the difference between the moisture controls at Las Majadas and the original parameterisation from Harvard Forest, we plotted the individual substrate and oxygen diffusion terms as well as the product of both MM-terms along a 0 - 100% water-saturation gradient (Fig. 5), while correcting for each site's soil C content ( $S_{total}$ , Eq. 3) and total porosity (Eq. 5). At Las Majadas, substrate diffusion poses a gradual but strongly

increasing control on the modelled  $R_{soil}$  rates as water-saturation declines, while oxygen diffusion limitation only affects the modelled  $R_{soil}$  rates at very high water-saturation (>80%). Interestingly, there is a wide range of SM values during which modelled rates are not severely limited by SM. We have high confidence in the fitted parameters in our study, as the number of observations on which they were optimised is high (n= 26824): The median water-saturation at Las Majadas is 39.3%, so that the fitted value for  $kM_S$ , which imposes the strong decline in substrate diffusion under dry soil conditions, is constrained by at least 50% of all data points. For oxygen diffusion and the estimation of  $kM_{O_2}$  the number of data points is smaller, but still includes 22% of all observations where water-saturation is larger than the optimum SM value (marked with an asterisk in Fig. 5).

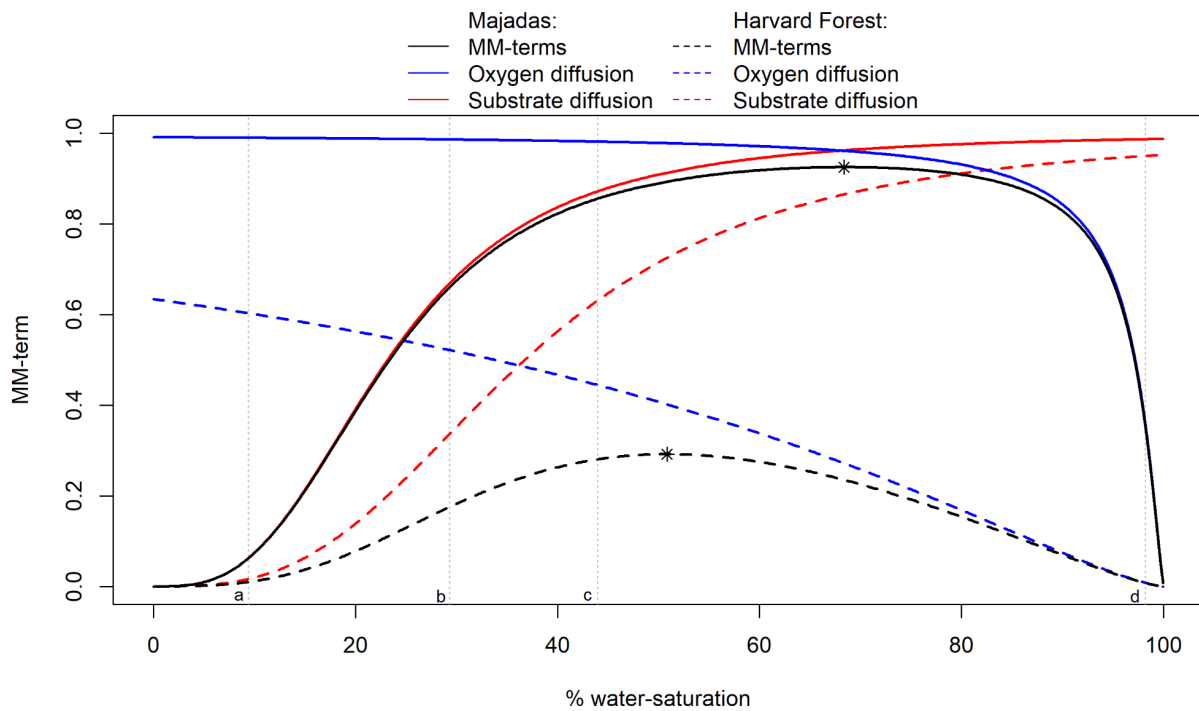


**Figure 5:** Difference between simulated SM controls in the DAMM model at Las Majadas (solid lines) and Harvard Forest (dashed lines) from 0 - 100% water-saturation. The MM-terms (black) are the product of the MM term for substrate diffusion (red) and the MM term for oxygen diffusion (blue) from Eq. 1, where optimal water-saturation is marked with an asterisk. The vertical dotted lines denote the respective SM ranges on which the parameters for the MM-terms are calibrated: Between ‘a’ and ‘d’ at Las Majadas, and between ‘b’ and ‘c’ at Harvard Forest.

At Harvard Forest, the substrate and oxygen diffusion MM-terms, as well as their product indicating the strength of the modelled SM controls, look very different from those at Las Majadas. Most striking is the strong oxygen diffusion limitation that affects modelled  $R_{soil}$  rates across the full SM range. Even when soil water-saturation is extremely low, oxygen

diffusion limits the rates by more than 35%. In their study, parameter  $kM_{O_2}$  was not calibrated against the observations, and its high value severely limits modelled respiration at this site. To place these results into context, we calculated the range of water-saturation values over which each site's parameters were estimated (Fig. 5, vertical lines with labels 'a' - 'd'). In our study at Las Majadas, parameters were estimated over data points between 9.4 and 94.2% water-saturation (Fig. 5, 'a' - 'd'). At Harvard Forest, parameters were estimated between a much smaller range from ~29 - 44% water-saturation (Fig 5, 'b' - 'c'; SM values were estimated from Fig. 5 in Davidson et al. (2012)). For both sites, the 'optimal SM value', i.e. where the product of the two MM-terms is at its maximum value, is denoted with an asterisk (Fig. 5). At Las Majadas, optimal SM is at ~68% water-saturation, and at 51% for Harvard forest. Please note that the optimum SM value for Harvard Forest falls outside of the model's calibration range.

The shape of the calibrated SM control function at Las Majadas (Fig. 5, MM-terms) shows a wide range of SM values during which modelled rates are not severely limited by SM. At optimum SM (denoted with an asterisk), the product of the MM-terms reaches a value close to 1 (0.99), so that the modelled soil CO<sub>2</sub> efflux is very close to  $V_{max}$ . Therefore, at SM values close to optimum SM, the model exercise where we set both MM-terms to 1 is a good indicator what the estimated fluxes would look like if the model was fitted as a 'temperature only model', i.e., only fitting the data to estimates of  $V_{max}$  (Eq. 1). At Harvard Forest, such a comparison would not be possible without recalibrating parameters  $\alpha$  and  $Ea$ , as the current parameters are fitted in such a way that the product of the MM-terms can never reach values close to 1.

## 4 Discussion

We calibrated the DAMM model to observed soil CO<sub>2</sub> efflux data at a semi-arid site with large temperature and soil moisture fluctuations. We show that this model, with its inclusion of soil temperature and soil moisture controls, captures the observed  $R_{soil}$  fluxes well at Las Majadas. Our results demonstrate that the inclusion of SM controls is essential for capturing the observed large temporal variability in  $R_{soil}$ , while temperature only dominates  $R_{soil}$  rates when sufficient soil moisture is available (usually during winter time). This adds to mounting scientific evidence that models of  $R_{soil}$  and subsequently, models of soil organic matter decomposition, should include soil moisture representations to accurately predict microbially driven soil CO<sub>2</sub> fluxes and subsequent changes in organic matter stocks (e.g. Liang et al., 2021; Wang et al., 2020; Zhang et al., 2022).

We show that changes in C substrate availability are the dominant soil moisture control at Las Majadas, and that moisture-driven reductions in C substrate availability need to be considered to correctly model  $R_{soil}$  rates during dry periods at this site. Such changes in C substrate availability are especially important upon rewetting after a dry period, when rapid increases in CO<sub>2</sub> efflux are observed at the site. This respiration pulse after rewetting is also known as

the “Birch effect” (Birch, 1958). Both the duration and frequency of drying and rewetting cycles (and the resulting stress on microbial communities) are important factors that determine the size of the observed soil CO<sub>2</sub> pulse following a rewetting event (Brangarí et al., 2021; Rousk & Brangarí, 2022). The DAMM model was able to capture these observed spikes in soil CO<sub>2</sub> efflux at Las Majadas, whereas the model estimates without SM controls did not capture such dynamics.

While C substrate diffusion is the dominant soil moisture control explaining  $R_{soil}$  rates at Las Majadas, oxygen availability also impacted  $R_{soil}$  rates, especially during winter time when SM values can get extremely high. Interestingly, the observations at Las Majadas show that even when the soil is close to full saturation, CO<sub>2</sub> soil efflux can still reach values as high as ~2 g C m<sup>-2</sup> day<sup>-1</sup>. This can be the result of continuing autotrophic respiration, which is closely linked to plant photosynthetic activity (Hopkins et al., 2013), although lower oxygen concentrations also inhibit autotrophic respiration rates (Ben-Noah & Friedman, 2018; Rankin et al., 2022). Substantial CO<sub>2</sub> efflux from fully saturated soils has been observed in earlier studies (e.g. Ghezzehei et al., 2019; Moyano et al., 2012, 2018; Wickland & Neff, 2008), but this is not what most mechanistic models linking volumetric SM with C diffusion of substrate and oxygen for microbial respiration, including the DAMM model, assume. In these models, oxygen diffusion (almost) fully restricts modelled respiration rates when soils are fully saturated with moisture (Fig. 5; Davidson et al. (2012); Yan et al. (2018), but see Ghezzehei et al. (2019) for an alternative formulation with a minimum aerobic respiration rate). Recent evidence from soil incubation experiments, however, suggests that anaerobic CO<sub>2</sub> production above 80% water-saturation is a significant contributor to soil CO<sub>2</sub> efflux, and that at 100% water-saturation observed values reached up to 1.9 g CO<sub>2</sub> m<sup>-2</sup> day<sup>-1</sup> (Fairbairn et al., 2023). The authors suggest that under these wet conditions, C substrate supply to microbes is high and provides ideal circumstances for anaerobic CO<sub>2</sub> production. In our study, the DAMM model slightly overestimated the observations under these very wet soil conditions in February 2017, in particular at the beginning of the month and following a gap in the input data. This is likely caused by a temporal mismatch between CO<sub>2</sub> production and the resulting soil CO<sub>2</sub> efflux, where water blocking the soil pores hinders the release of CO<sub>2</sub> from the soil to the atmosphere and can cause a drop in observed CO<sub>2</sub> efflux (Maier et al., 2011). As the DAMM model responds instantaneously to the temperature and SM values at each model timestep by simulating respiration, such temporal shifts cannot be accurately captured. Our results, however, show that despite some temporal mismatches between the DAMM model and the observations, the cumulative  $R_{soil}$  C budget over the observational period was captured very well by the calibrated model (Table 2). As a way to bridge the knowledge gap between the observed significant CO<sub>2</sub> fluxes under well-saturated soil moisture conditions and the functional shape of the soil moisture response curves which predict little to no CO<sub>2</sub> production when soils are saturated with moisture, we recommend that future research focuses on better constraining parameter  $kM_{O_2}$  at high water-saturation levels, especially in field conditions. For example, by applying the DAMM model, or similar mechanistic modelling frameworks, on respiration measurements from sites which regularly

experience water-saturated conditions: Three additional sites in Norway covering soil moisture and respiration measurements from 2016 to 2020 will be used in a further study to model the impact of moisture on respiration. Contrary to Majadas, they are mostly wet to very wet, so we expect limitation due to restricted oxygen diffusion to be an important process at these sites. To account for the effects of autotrophic respiration under saturated soil conditions, additional measurements would ideally also include heterotrophic respiration, e.g. from trenching experiments similar to those conducted at Harvard Forest. Such trenching experiments, data-driven partitioning methods, and results from laboratory incubation experiments, however, suggest that heterotrophic respiration makes a large contribution to  $R_{soil}$  and that variations in autotrophic respiration are mainly driven by changes in plant productivity (Bond-Lamberty et al., 2018; Jian et al., 2021b, 2021a; Oikawa et al., 2014; Sihi et al., 2018). Better constraints on parameter  $kM_{O_2}$  would be particularly important for understanding and modelling soil carbon dynamics in boreal regions, where soils are rich in soil organic carbon and soil warming is expected to be higher than the global average (Soong et al., 2020), while precipitation is expected to increase (Christensen et al., 2022).

Overall, our results confirm that the DAMM model is a suitable framework to model SM controls on  $R_{soil}$  at a site with highly dynamic changes in temperature and soil moisture such as Las Majadas. But our comparison to the original parameterisation at Harvard Forest reveals that it is important to estimate the parameters for the MM-terms, which determine the strength of the moisture control, over a wide range of SM values. At this site, soil moisture does not have a strong control on heterotrophic respiration and only explains a small additional part of the observed variability in C efflux compared to temperature (Abramoff et al., 2017; Davidson et al., 2012). Using parameter values outside of the SM range over which they were calibrated, could lead to over- or underestimation of soil moisture controls at more extreme soil moisture values. Additionally, it is known that SM can confound temperature-based parameters estimates (Davidson et al., 2006; Davidson & Janssens, 2006; Reichstein et al., 2005; Sierra et al., 2015). Our results demonstrate that the use of site-specific parameters for other model applications beyond the original calibration range should be done with care, especially in areas which experience extremely dry and/or wet soil moisture conditions.

## 5 Conclusions

Soil moisture, through the diffusion of C substrate and oxygen diffusion, strongly controls the observed soil CO<sub>2</sub> effluxes at Las Majadas. Our results demonstrate that considering temperature alone is not sufficient in capturing  $R_{soil}$  variability, especially under very dry and very wet soil moisture conditions. Furthermore, including soil moisture dynamics is essential to reproduce the observed spikes in soil CO<sub>2</sub> efflux during drying and rewetting events. We demonstrate that the DAMM model, calibrated against the observations, is a suitable framework to model soil respiration dynamics at a site which experiences extreme fluctuations in soil moisture and soil temperatures. Our study also identified a knowledge gap

in the understanding of the effects of oxygen limitation on modelled  $R_{soil}$  rates, which can be overcome by applying the DAMM model (or likewise mechanistic formulations) on observations from sites which experience very wet conditions throughout the year. This way, estimates for the control on oxygen diffusion through parameter  $kM_{O_2}$  can be better constrained, which can help modelling efforts in, for example, boreal regions with high soil organic carbon stocks, which are expected to become warmer and wetter.

## 6 Acknowledgements

The authors are grateful to Thomas Wutzler for processing the raw measurements at Las Majadas, and to the scientists and technicians from the MPI for Biogeochemistry and local partners for their fieldwork and maintenance at the site. Marleen Pallandt gratefully acknowledges funding support for this work from the Norwegian Research Council through grant no. RCN 255 061 (MOisture dynamics and CARbon sequestration in BOReal Soils) and the Max Planck Institute for Biogeochemistry.

## 7 References

- Abramoff, R., Davidson, E., & Finzi, A. C. (2017). A parsimonious modular approach to building a mechanistic belowground carbon and nitrogen model. *Journal of Geophysical Research: Biogeosciences*, 122(9), 2418–2434. <https://doi.org/doi:10.1002/2017JG003796>
- Allison, S. D., Romero-Olivares, A. L., Lu, Y., Taylor, J. W., & Treseder, K. K. (2018). Temperature sensitivities of extracellular enzyme Vmax and Km across thermal environments. *Glob Chang Biol*, 24(7), 2884–2897. <https://doi.org/10.1111/gcb.14045>
- Ben-Noah, I., & Friedman, S. P. (2018). Review and Evaluation of Root Respiration and of Natural and Agricultural Processes of Soil Aeration. *Vadose Zone Journal*, 17(1), 170119. <https://doi.org/10.2136/vzj2017.06.0119>
- Berg, A., Sheffield, J., & Milly, P. C. D. (2017). Divergent surface and total soil moisture projections under global warming. *Geophysical Research Letters*, 44(1), 236–244. <https://doi.org/10.1002/2016GL071921>
- Birch, H. F. (1958). The effect of soil drying on humus decomposition and nitrogen availability. *Plant and Soil*, 10(1), 9–31. <https://doi.org/10.1007/BF01343734>
- Bond-Lamberty, B., Bailey, V. L., Chen, M., Gough, C. M., & Vargas, R. (2018). Globally rising soil heterotrophic respiration over recent decades. *Nature*, 560(7716), 80–83. <https://doi.org/10.1038/s41586-018-0358-x>
- Brangarí, A. C., Manzoni, S., & Rousk, J. (2021). The mechanisms underpinning microbial resilience to drying and rewetting – A model analysis. *Soil Biology and Biochemistry*, 162, 108400. <https://doi.org/10.1016/j.soilbio.2021.108400>
- Casals, P., Lopez-Sangil, L., Carrara, A., Gimeno, C., & Nogués, S. (2011). Autotrophic and heterotrophic contributions to short-term soil CO<sub>2</sub> efflux following simulated summer precipitation pulses in a Mediterranean dehesa. *Global Biogeochemical Cycles*, 25(3). <https://doi.org/10.1029/2010GB003973>
- Christensen, O. B., Kjellström, E., Dieterich, C., Gröger, M., & Meier, H. E. M. (2022). Atmospheric regional climate projections for the Baltic Sea region until 2100. *Earth System Dynamics*, 13(1), 133–157. <https://doi.org/10.5194/esd-13-133-2022>
- Davidson, E. A., & Janssens, I. A. (2006). Temperature sensitivity of soil carbon decomposition and feedbacks to climate change. *Nature*, 440, 165. <https://doi.org/10.1038/nature04514>
- Davidson, E. A., Janssens, I. A., & Luo, Y. (2006). On the variability of respiration in terrestrial ecosystems: moving beyond Q<sub>10</sub>. *Global Change Biology*, 12(2), 154–164. <https://doi.org/10.1111/j.1365-2486.2005.01065.x>

- Davidson, E. A., Sudeep, S., Samantha, S. C., & Savage, K. (2012). The Dual Arrhenius and Michaelis–Menten kinetics model for decomposition of soil organic matter at hourly to seasonal time scales. *Global Change Biology*, *18*(1), 371–384. <https://doi.org/doi:10.1111/j.1365-2486.2011.02546.x>
- Davidson, E. A., Savage, K. E., & Finzi, A. C. (2014). A big-microsite framework for soil carbon modeling. *Global Change Biology*, *20*(12), 3610–3620. <https://doi.org/10.1111/gcb.12718>
- Drake, J. E., Macdonald, C. A., Tjoelker, M. G., Reich, P. B., Singh, B. K., Anderson, I. C., & Ellsworth, D. S. (2018). Three years of soil respiration in a mature eucalypt woodland exposed to atmospheric CO<sub>2</sub> enrichment. *Biogeochemistry*, *139*(1), 85–101. <https://doi.org/10.1007/s10533-018-0457-7>
- El-Madany, T. S., Reichstein, M., Perez-Priego, O., Carrara, A., Moreno, G., Pilar Martín, M., et al. (2018). Drivers of spatio-temporal variability of carbon dioxide and energy fluxes in a Mediterranean savanna ecosystem. *Agricultural and Forest Meteorology*, *262*, 258–278. <https://doi.org/10.1016/j.agrformet.2018.07.010>
- El-Madany, T. S., Carrara, A., Martín, M. P., Moreno, G., Kolle, O., Pacheco-Labrador, J., et al. (2020). Drought and heatwave impacts on semi-arid ecosystems' carbon fluxes along a precipitation gradient. *Philosophical Transactions of the Royal Society B: Biological Sciences*, *375*(1810), 20190519. <https://doi.org/10.1098/rstb.2019.0519>
- Fairbairn, L., Rezanezhad, F., Gharasoo, M., Parsons, C. T., Macrae, M. L., Slowinski, S., & Van Cappellen, P. (2023). Relationship between soil CO<sub>2</sub> fluxes and soil moisture: Anaerobic sources explain fluxes at high water content. *Geoderma*, *434*, 116493. <https://doi.org/10.1016/j.geoderma.2023.116493>
- Ghezzehei, T. A., Sulman, B., Arnold, C. L., Bogie, N. A., & Berhe, A. A. (2019). On the role of soil water retention characteristic on aerobic microbial respiration. *Biogeosciences*, *16*(6), 1187–1209. <https://doi.org/10.5194/bg-16-1187-2019>
- Greaves, J. E., & Carter, E. G. (1920). INFLUENCE OF MOISTURE ON THE BACTERIAL ACTIVITIES OF THE SOIL. *Soil Science*, *10*(5), 361.
- Hopkins, F., Gonzalez-Meler, M. A., Flower, C. E., Lynch, D. J., Czimczik, C., Tang, J., & Subke, J.-A. (2013). Ecosystem-level controls on root-rhizosphere respiration. *New Phytologist*, *199*(2), 339–351. <https://doi.org/10.1111/nph.12271>
- Hunt, T. (2022, October 12). ModelMetrics: Rapid Calculation of Model Metrics (Version R package version 1.2.2.2). Retrieved from <https://CRAN.R-project.org/package=ModelMetrics>
- Jian, J., Vargas, R., Anderson-Teixeira, K., Stell, E., Herrmann, V., Horn, M., et al. (2021a). A restructured and updated global soil respiration database (SRDB-V5). *Earth System Science Data*, *13*(2), 255–267. <https://doi.org/10.5194/essd-13-255-2021>
- Jian, J., Bond-Lamberty, B., Hao, D., Sulman, B. N., Patel, K. F., Zheng, J., et al. (2021b). Leveraging observed soil heterotrophic respiration fluxes as a novel constraint on global-scale models. *Global Change Biology*, *27*(20). <https://doi.org/10.1111/gcb.15795>
- Liang, J., Wang, G., Singh, S., Jagadamma, S., Gu, L., Schadt, C. W., et al. (2021). Intensified Soil Moisture Extremes Decrease Soil Organic Carbon Decomposition: A Mechanistic Modeling Analysis. *Journal of Geophysical Research: Biogeosciences*, *126*(8), e2021JG006392. <https://doi.org/10.1029/2021JG006392>
- Maier, M., Schack-Kirchner, H., Hildebrand, E. E., & Schindler, D. (2011). Soil CO<sub>2</sub> efflux vs. soil respiration: Implications for flux models. *Agricultural and Forest Meteorology*, *151*(12), 1723–1730. <https://doi.org/10.1016/j.agrformet.2011.07.006>
- Millington, R. J. (1959). Gas Diffusion in Porous Media. *Science*, *130*(3367), 100–102. <https://doi.org/10.1126/science.130.3367.100.b>
- Morris, K. A., Nair, R. K. F., Moreno, G., Schruppf, M., & Migliavacca, M. (2019). Fate of N additions in a multiple resource-limited Mediterranean oak savanna. *Ecosphere*, *10*(11), e02921. <https://doi.org/10.1002/ecs2.2921>
- Morris, K. A., Richter, A., Migliavacca, M., & Schruppf, M. (2022). Growth of soil microbes is not limited by the availability of nitrogen and phosphorus in a Mediterranean oak-savanna. *Soil Biology and Biochemistry*, *169*, 108680. <https://doi.org/10.1016/j.soilbio.2022.108680>
- Moyano, F. E., Vasilyeva, N., Bouckaert, L., Cook, F., Craine, J., Curiel Yuste, J., et al. (2012). The moisture response of soil heterotrophic respiration: interaction with soil properties.

- Biogeosciences*, 9(3), 1173–1182. <https://doi.org/10.5194/bg-9-1173-2012>
- Moyano, F. E., Manzoni, S., & Chenu, C. (2013). Responses of soil heterotrophic respiration to moisture availability: An exploration of processes and models. *Soil Biology and Biochemistry*, 59, 72–85. <https://doi.org/10.1016/j.soilbio.2013.01.002>
- Moyano, F. E., Vasilyeva, N., & Menichetti, L. (2018). Diffusion limitations and Michaelis–Menten kinetics as drivers of combined temperature and moisture effects on carbon fluxes of mineral soils. *Biogeosciences*, 15(16), 5031–5045. <https://doi.org/10.5194/bg-15-5031-2018>
- Nair, R., Luo, Y., El-Madany, T., Rolo, V., Pacheco-Labrador, J., Caldararu, S., et al. (2023). Nitrogen Availability and Summer Drought, but not N:P Imbalance Drive Carbon Use Efficiency of a Mediterranean Tree-Grass Ecosystem. *EGUsphere*, 1–38. <https://doi.org/10.5194/egusphere-2023-2434>
- Oikawa, P. Y., Grantz, D. A., Chatterjee, A., Eberwein, J. E., Allsman, L. A., & Jenerette, G. D. (2014). Unifying soil respiration pulses, inhibition, and temperature hysteresis through dynamics of labile soil carbon and O<sub>2</sub>. *Journal of Geophysical Research: Biogeosciences*, 119(4), 521–536. <https://doi.org/doi:10.1002/2013JG002434>
- Paulus, S. J., El-Madany, T. S., Orth, R., Hildebrandt, A., Wutzler, T., Carrara, A., et al. (2022). Resolving seasonal and diel dynamics of non-rainfall water inputs in a Mediterranean ecosystem using lysimeters. *Hydrology and Earth System Sciences*, 26(23), 6263–6287. <https://doi.org/10.5194/hess-26-6263-2022>
- R Core Team. (2023, June 16). R: A Language and Environment for Statistical Computing (Version 4.3.1). Vienna, Austria: R Foundation for Statistical Computing. Retrieved from <https://www.R-project.org>
- Rankin, T. E., Roulet, N. T., & Moore, T. R. (2022). Controls on autotrophic and heterotrophic respiration in an ombrotrophic bog. *Biogeosciences*, 19(13), 3285–3303. <https://doi.org/10.5194/bg-19-3285-2022>
- Reichstein, M., Subke, J.-A., Angeli, A. C., & Tenhunen, J. D. (2005). Does the temperature sensitivity of decomposition of soil organic matter depend upon water content, soil horizon, or incubation time? *Global Change Biology*, 11(10), 1754–1767. <https://doi.org/doi:10.1111/j.1365-2486.2005.001010.x>
- Rousk, J., & Brangarí, A. C. (2022). Do the respiration pulses induced by drying–rewetting matter for the soil–atmosphere carbon balance? *Global Change Biology*, 28(11), 3486–3488. <https://doi.org/10.1111/gcb.16163>
- RStudio Team. (2018). Rstudio: Integrated development environment for R. Retrieved from <http://www.rstudio.com/>
- Sierra, C. A., Trumbore, S. E., Davidson, E. A., Vicca, S., & Janssens, I. (2015). Sensitivity of decomposition rates of soil organic matter with respect to simultaneous changes in temperature and moisture. *Journal of Advances in Modeling Earth Systems*, 7(1), 335–356. <https://doi.org/10.1002/2014MS000358>
- Sihi, D., Davidson, E. A., Chen, M., Savage, K. E., Richardson, A. D., Keenan, T. F., & Hollinger, D. Y. (2018). Merging a mechanistic enzymatic model of soil heterotrophic respiration into an ecosystem model in two AmeriFlux sites of northeastern USA. *Agricultural and Forest Meteorology*, 252, 155–166. <https://doi.org/10.1016/j.agrformet.2018.01.026>
- Sihi, D., Davidson, E. A., Savage, K. E., & Liang, D. (2020). Simultaneous numerical representation of soil microsite production and consumption of carbon dioxide, methane, and nitrous oxide using probability distribution functions. *Global Change Biology*, 26(1), 200–218. <https://doi.org/10.1111/gcb.14855>
- Skopp, J., Jawson, M. D., & Doran, J. W. (1990). Steady-state aerobic microbial activity as a function of soil water content. *Soil Science Society of America Journal*, 54(6), 1619–1625. <https://doi.org/10.2136/sssaj1990.03615995005400060018x>
- Soetaert, K., & Petzoldt, T. (2010). Inverse Modelling, Sensitivity and Monte Carlo Analysis in R Using Package FME. *Journal of Statistical Software*, 33, 1–28. <https://doi.org/10.18637/jss.v033.i03>
- Soong, J. L., Phillips, C. L., Ledna, C., Koven, C. D., & Torn, M. S. (2020). CMIP5 Models Predict Rapid and Deep Soil Warming Over the 21st Century. *Journal of Geophysical Research: Biogeosciences*, 125(2), e2019JG005266. <https://doi.org/10.1029/2019JG005266>



- Wang, G., Huang, W., Zhou, G., Mayes, M. A., & Zhou, J. (2020). Modeling the processes of soil moisture in regulating microbial and carbon-nitrogen cycling. *Journal of Hydrology*, 585, 124777. <https://doi.org/10.1016/j.jhydrol.2020.124777>
- Wang, Y., Mao, J., Hoffman, F. M., Bonfils, C. J. W., Douville, H., Jin, M., et al. (2022). Quantification of human contribution to soil moisture-based terrestrial aridity. *Nature Communications*, 13(1), 6848. <https://doi.org/10.1038/s41467-022-34071-5>
- Wickham, H. (2016). *ggplot2*. Cham: Springer International Publishing. <https://doi.org/10.1007/978-3-319-24277-4>
- Wickham, H., Pedersen, T., & Seidel, D. (2023, November 23). scales: Scale Functions for Visualization (Version R package version 1.3.0).
- Wickland, K. P., & Neff, J. C. (2008). Decomposition of soil organic matter from boreal black spruce forest: environmental and chemical controls. *Biogeochemistry*, 87(1), 29–47. <https://doi.org/10.1007/s10533-007-9166-3>
- Wutzler, T., Perez-Priego, O., Morris, K., El-Madany, T. S., & Migliavacca, M. (2020). Soil CO<sub>2</sub> efflux errors are lognormally distributed – implications and guidance. *Geoscientific Instrumentation, Methods and Data Systems*, 9(1), 239–254. <https://doi.org/10.5194/gi-9-239-2020>
- Yan, Z., Liu, C., Todd-Brown, K. E., Liu, Y., Bond-Lamberty, B., & Bailey, V. L. (2016). Pore-scale investigation on the response of heterotrophic respiration to moisture conditions in heterogeneous soils. *Biogeochemistry*, 131(1), 121–134. <https://doi.org/10.1007/s10533-016-0270-0>
- Yan, Z., Bond-Lamberty, B., Todd-Brown, K. E., Bailey, V. L., Li, S., Liu, CongQiang, & Liu, Chongxuan. (2018). A moisture function of soil heterotrophic respiration that incorporates microscale processes. *Nature Communications*, 9(1), 2562. <https://doi.org/10.1038/s41467-018-04971-6>
- Zhang, X., Xie, Z., Ma, Z., Barron-Gafford, G. A., Scott, R. L., & Niu, G.-Y. (2022). A Microbial-Explicit Soil Organic Carbon Decomposition Model (MESDM): Development and Testing at a Semiarid Grassland Site. *Journal of Advances in Modeling Earth Systems*, 14(1), e2021MS002485. <https://doi.org/10.1029/2021MS002485>

## Study II

---

# Vertically divergent responses of SOC decomposition to soil moisture in a changing climate

This study has been published as:

**Pallandt, M., Ahrens, B., Koirala, S., Lange, H., Reichstein, M., Schrumpf, M., & Zaehle, S.** (2022). Vertically divergent responses of SOC decomposition to soil moisture in a changing climate. *Journal of Geophysical Research: Biogeosciences*, 127, e2021JG006684.  
<https://doi.org/10.1029/2021JG006684>

This is an open access article, reprinted with permission under the terms of the Creative Commons Attribution License: <http://creativecommons.org/licenses/by/4.0/>

# JGR Biogeosciences

## RESEARCH ARTICLE

10.1029/2021JG006684

### Key Points:

- Considering soil moisture effects can change modeled decomposition rates by up to  $\pm 20\%$  compared to considering only temperature effects
- The majority of these changes are driven by substrate availability, in particular in the top soil
- In the subsoil, oxygen availability becomes an increasingly important factor

### Supporting Information:

Supporting Information may be found in the online version of this article.

### Correspondence to:

M. Pallandt,  
mpalla@bgc-jena.mpg.de

### Citation:

Pallandt, M., Ahrens, B., Koirala, S., Lange, H., Reichstein, M., Schrupf, M., & Zaehle, S. (2022). Vertically divergent responses of SOC decomposition to soil moisture in a changing climate. *Journal of Geophysical Research: Biogeosciences*, 127, e2021JG006684. <https://doi.org/10.1029/2021JG006684>

Received 29 OCT 2021  
Accepted 27 DEC 2021  
Corrected 18 NOV 2023

This article was corrected on 18 NOV 2023. See the end of the full text for details.

### Author Contributions:

**Conceptualization:** Marleen Pallandt, Bernhard Ahrens, Sujan Koirala, Holger Lange, Markus Reichstein, Marion Schrupf, Sönke Zaehle  
**Data curation:** Marleen Pallandt, Bernhard Ahrens  
**Formal analysis:** Marleen Pallandt, Bernhard Ahrens  
**Funding acquisition:** Bernhard Ahrens, Holger Lange

© 2022. The Authors.

This is an open access article under the terms of the Creative Commons Attribution License, which permits use, distribution and reproduction in any medium, provided the original work is properly cited.

## Vertically Divergent Responses of SOC Decomposition to Soil Moisture in a Changing Climate

Marleen Pallandt<sup>1,2</sup>, Bernhard Ahrens<sup>1</sup>, Sujan Koirala<sup>1</sup>, Holger Lange<sup>3</sup>, Markus Reichstein<sup>1,2</sup>, Marion Schrupf<sup>1,2</sup>, and Sönke Zaehle<sup>1,2</sup>

<sup>1</sup>Max Planck Institute for Biogeochemistry, Jena, Germany, <sup>2</sup>International Max Planck Research School (IMPRS) for Global Biogeochemical Cycles, Jena, Germany, <sup>3</sup>Norwegian Institute of Bioeconomy Research, Ås, Norway

**Abstract** The role of soil moisture for organic matter decomposition rates remains poorly understood and underrepresented in Earth System Models (ESMs). We apply the Dual Arrhenius Michaelis-Menten (DAMM) model to a selection of ESM soil temperature and moisture outputs to investigate their effects on decomposition rates, at different soil depths, for a historical period and a future climate period. Our key finding is that the inclusion of soil moisture controls has diverging effects on both the speed and direction of projected decomposition rates (up to  $\pm 20\%$ ), compared to a temperature-only approach. In the top soil, the majority of these changes is driven by substrate availability. In deeper soil layers, oxygen availability plays a relatively stronger role. Owing to these different moisture controls along the soil depth, our study highlights the need for depth-resolved inclusion of soil moisture effects on decomposition rates within ESMs. This is particularly important for C-rich soils in regions which may be subject to strong future warming and vertically opposing moisture changes, such as the peat soils at northern high latitudes.

**Plain Language Summary** Soils contain a lot of carbon (C). Earth System Models (ESMs) predict that the amount of C released from soils into the atmosphere as CO<sub>2</sub> will increase in response to increased warming and microbial activity. Soil moisture also controls microbial C decomposition, but most ESMs do not yet describe this process very well. In this study we apply a simple equation to different ESMs, to see how both temperature and soil moisture change microbial decomposition under future climate. First, we show that the speed of C released into the atmosphere changes when we include soil moisture changes, compared to what is expected due to warming alone. Second, we found that the future speed at which carbon that can be decomposed in the topsoil mainly depends on how much carbon microbes have access to, but that in the deeper soil this process becomes much more affected by the absence/presence of oxygen. Including these soil moisture interactions in ESMs for different soil depths is important to predict whether soils will store more or less C in the future. Our findings are particularly relevant for high latitude soils which store large amounts of C, will warm fast, and experience frequent (re)wetting and drying.

## 1. Introduction

Soil organic carbon (SOC) is the largest terrestrial carbon pool, but it is still uncertain how it will respond to climate change in the 21st century (Bradford et al., 2016; Crowther et al., 2016; Gestel et al., 2018). Coupled climate modeling is a valuable tool to study climate–soil–carbon feedbacks, but there are large differences between existing model projections (e.g., Jones et al., 2013; Luo et al., 2016; Todd-Brown et al., 2013, 2014). This broad uncertainty partly reflects our lack of understanding and representation of the underlying processes (Sulman et al., 2018).

During the last decade, there has been a substantial shift in our perspective on the processes that determine the residence time of SOC in soils (Blankinship et al., 2018; Schmidt et al., 2011; Shi et al., 2020). Organic matter turnover is affected by several co-dependent factors and soil internal feedbacks (Davidson & Janssens, 2006; Heimann & Reichstein, 2008; Kirschbaum, 2006), such as temperature, soil moisture, oxygen availability, substrate availability and quality, stabilization of organic material by organo-mineral associations, and pH, with microbes as the main actors. This co-dependence of drivers of organic matter turnover can lead to non-linear system responses under future climate, a behavior which, due to their linear, first-order kinetics structure, conventional soil carbon decomposition models may not be able to capture (Falloon et al., 2011; Sierra et al., 2015;

**Investigation:** Marleen Pallandt, Bernhard Ahrens, Sujan Koirala  
**Resources:** Bernhard Ahrens, Sujan Koirala  
**Supervision:** Bernhard Ahrens, Holger Lange, Markus Reichstein, Marion Schrumpp, Sönke Zaehle  
**Validation:** Marleen Pallandt, Bernhard Ahrens  
**Visualization:** Marleen Pallandt, Bernhard Ahrens  
**Writing – original draft:** Marleen Pallandt  
**Writing – review & editing:** Marleen Pallandt, Bernhard Ahrens, Sujan Koirala, Holger Lange, Markus Reichstein, Marion Schrumpp, Sönke Zaehle

Wieder et al., 2018; Zhou et al., 2008). Yet, while these models do not reflect the latest scientific insights, they are actively used as coupled components within fully interacting ESMs.

The majority of coupled climate models currently in use include a soil component that uses a first-order decomposition rate for one or multiple carbon pools, generally sharing a similar mathematical structure (Sierra et al., 2012). The use of kinetic constants and response functions implicitly represents microbial interactions and nutrient dynamics (Schimel, 2001). Of particular importance are the dependencies of the decomposition rates on soil temperature and moisture, which, together with the biochemical recalcitrance of organic matter (and not explicit microbial interactions), determine the turnover rate of each carbon pool (Bradford & Fierer, 2012; Schimel, 2001; Schmidt et al., 2011; Todd-Brown et al., 2013). The temperature response functions generally prescribe faster decomposition at higher temperatures (Lloyd & Taylor, 1994; Sierra et al., 2015; Todd-Brown et al., 2018). However, the models' responses to moisture are less uniformly described: It is either not at all included, or only empirically described (Falloon et al., 2011; Sierra et al., 2015). Furthermore, classic soil carbon decomposition models typically do not consider soil temperature and moisture interactions over a vertically resolved SOC profile, and as a result fail to capture observed climate sensitivities of soil carbon turnover times (Ahrens et al., 2015; Braakhekke et al., 2011; Koven et al., 2013, 2017). Even recent microbially explicit models (e.g., CORPSE by Sulman et al., 2014, MIMICS by Wieder et al., 2014, DAMM-MCNIP by Abramoff et al., 2017) typically only consider one soil depth, even though many soil properties change with depth.

Data-driven studies clearly indicate that the feedback between climate and carbon turnover times strongly depends on temperature and the hydrological cycle on an ecosystem scale (Carvalhais et al., 2014; Jung et al., 2017; J. Wang et al., 2018). Locally, soil temperature and soil moisture are the two most important controlling factors of heterotrophic respiration rates, and thereby the carbon turnover rate of soils (Davidson & Janssens, 2006; Moyano et al., 2013; Yan et al., 2018). For temperature, it is generally accepted that the rate of decomposition increases as temperature increases, until a certain maximum where enzymes start to break down (Hochachka & Somero, 2002; Nottingham et al., 2016). For soil moisture, there is more uncertainty in both the functional shape and the extremes of the response curves (Sierra et al., 2017), that is, how decomposition rates are affected by very dry or very wet soil moisture conditions and the shape of the response during drying/(re)wetting events. Decomposition rates can reach a potential maximum at optimal soil moisture (Figure S1 in Supporting Information S1): At this point, both the availability of decomposable substrates (organic matter) and oxygen (as an electron acceptor) are optimal (Moyano et al., 2013; Sierra et al., 2015; Skopp et al., 1990). As a soil dries out, its structure and hydraulic conductivity changes so that microbes will reduce their activity or even die under extremely low water potentials (Manzoni & Katul, 2014; Schimel, 2018). As a soil becomes wetter, oxygen availability for aerobic decomposition becomes scarcer, slowing down decomposition.

At this moment, encouraging new SOC decomposition modelling developments are made: For example, Wieder et al. (2019) list several examples, and see Wutzler et al. (2017); Yu et al. (2020). These advances have not yet found their way into the coupled global climate models used in the Coupled Model Inter-comparison Project (CMIP) ensembles, nor do they explicitly deal with improving the soil moisture responses. Here we propose another method to gain insight into the potential effects of soil temperature and moisture changes on future SOC decomposition rates among a vertical soil profile using a simple, semi-mechanistic modelling approach. Davidson et al. (2012) provide such a framework, called the Dual Arrhenius Michaelis-Menten (DAMM) model. The process-based and empirically tested DAMM model consists of a set of three linked equations. The first term is an Arrhenius function to calculate a temperature dependent maximum decomposition rate ( $V_{max}$ ).  $V_{max}$  is multiplied with two moisture dependent Michaelis-Menten terms (MM-terms). Without explicitly simulating microbial biomass, the MM-terms describe the necessary diffusion of substrate and oxygen towards the microbial surface for decomposition. If substrate or oxygen availability are limiting, the decomposition rate is reduced.

Our goal is to quantify how under a changing climate, decomposition rates change in response to soil moisture changes, separate from the temperature-driven changes, as well as their combined effects. In addition, we investigate the effect of soil moisture along a vertical gradient and the implications for predicted decomposition rates. We run the DAMM model with vertically explicit SOC data, and vertically resolved CMIP5 model outputs for soil moisture and soil temperature. We calculate the temperature- and soil moisture driven decomposition rate changes between a historic (1976–2005) simulation period and a future climate change period (2070–2099), following Representative Concentration Pathway 8.5 (RCP8.5). This generates global maps that outline the various temperature and soil moisture driven effects on decomposition rates at different depths. Our study highlights

the possible magnitude of decomposition rate changes with projected soil moisture (and temperature) changes, in conjunction with spatially varying SOC content at different soil depths.

## 2. Data and Methods

### 2.1. The DAMM Model

The DAMM model by Davidson et al. (2012) uses a set of linked equations to study the simultaneous effects of soil temperature and soil moisture on organic matter decomposition. The DAMM models' functions are based on process concepts, and successfully developed and repeatedly tested using empirical data (Abramoff et al., 2017; Davidson et al., 2012; Drake et al., 2018; Sihi et al., 2018). We briefly summarize these equations here, but for full methods and references redirect the reader to the original paper. The DAMM model calculates the decomposition rate  $R_{S_x}$  of a substrate ( $S_x$ ):

$$R_{S_x} = V_{\max} \cdot MM_{S_x} \cdot MM_{O_2} \quad (1)$$

$V_{\max}$  is an Arrhenius function for the maximum reaction velocity of  $R_{S_x}$ , and two reverse MM-terms represent the reduction of  $R_{S_x}$  by either substrate diffusion limitation ( $MM_{S_x}$ ), or oxygen limitation ( $MM_{O_2}$ ).  $V_{\max}$  is affected by temperature, and the two MM-terms are affected by soil water content (Figure S1a in Supporting Information S1). With this relatively simple framework and without explicitly simulating microbial biomass or activity,  $MM_{S_x}$  represents substrate diffusion to a microbial surface, while  $MM_{O_2}$  represents oxygen availability. When either is limiting,  $R_{S_x}$  is reduced.

Following G. Wang et al. (2012), the Arrhenius function  $V_{\max}$  is expressed as:

$$V_{\max} = \alpha_{S_x} \cdot \exp \left[ -\frac{Ea_{S_x}}{R} \left( \frac{1}{T_{\text{soil}}} - \frac{1}{T_{\text{ref}}} \right) \right] \quad (2)$$

where  $\alpha_{S_x}$  is a base rate ( $\text{mg C cm}^{-3} \text{ soil h}^{-1}$ ; Sihi et al., 2018, 2020),  $Ea_{S_x}$  is the activation energy for substrate  $S_x$  ( $\text{kJ mol}^{-1}$ ),  $R$  is the universal gas constant ( $\text{kJ K}^{-1} \text{ mol}^{-1}$ ),  $T_{\text{soil}}$  and  $T_{\text{ref}}$  are soil temperature and reference temperature (K), respectively.

Substrate diffusion limitation is calculated as:

$$MM_{S_x} = \frac{[S_x]}{kM_{S_x} + [S_x]} \quad (3)$$

where  $[S_x]$  ( $\text{g cm}^{-3}$ ) is the soluble substrate concentration, calculated as a diffusivity function from  $S_{x,\text{tot}}$  ( $\text{g cm}^{-3}$ ), the total amount of substrate:

$$[S_x] = S_{x,\text{tot}} \cdot p_{S_x} \cdot D_{\text{liq}} \cdot \theta^3 \quad (4)$$

The substrate of interest ( $S_x$ ) for this study is the SOC density (Section 2.2),  $p_{S_x}$  is the fraction of carbon substrate which is soluble,  $D_{\text{liq}}$  is the diffusion coefficient of the substrate in liquid phase, and  $\theta$  is the volumetric soil moisture content.

Oxygen diffusion limitation ( $MM_{O_2}$ ) is calculated in a similar fashion:

$$MM_{O_2} = \frac{[O_2]}{kM_{O_2} + [O_2]} \quad (5)$$

where the oxygen concentration at the reaction site,  $[O_2]$ , is also calculated as a diffusivity function, using soil porosity and water content to calculate the air-filled pore space (Millington, 1959):

$$[O_2] = D_{\text{gas}} \cdot O_{2,\text{airfrac}} \cdot (\Phi - \theta)^{\frac{4}{3}} \quad (6)$$

where  $D_{\text{gas}}$  is the diffusion coefficient for oxygen in air,  $O_{2,\text{airfrac}}$  is the fraction of oxygen in air ( $\text{L O}_2 \text{ L}^{-1}$  air), and  $\Phi$  is the soil porosity.  $kM_{S_x}$  ( $\text{g C cm}^{-3} \text{ soil}$ ) and  $kM_{O_2}$  ( $\text{cm}^{-3} \text{ O}_2 \text{ cm}^{-3} \text{ air}$ ) are the half-saturation or Michaelis-Menten constants of the reactions with the substrate and oxygen, respectively. All climate and soil data input variables are described in Section 2.2, and all parameter values taken from the modeling script provided by

Davidson et al. (2012) are listed in Table S1 in Supporting Information S1. To verify that the DAMM model is not only suitable for the top soil layers but applicable throughout the whole soil column, we successfully applied the model on a set of monthly observations at multiple depth intervals up to 1 m (0–15, 15–30, 30–50, 50–70, 70–100 cm, Gomez et al., 2002; Hicks Pries et al., 2017). A detailed description of the data and methods is included in the Text S1 in Supporting Information S1.

## 2.2. Climate and Soil Input Data

The DAMM model (Section 2.1) requires the following variables and parameters: Soil temperature ( $T_{\text{soil}}$ ), soil moisture ( $\theta$ ), SOC density ( $S_{\text{x,soil}}$ ) and soil porosity ( $\Phi$ ). Variables  $T_{\text{soil}}$  and  $\theta$  are extracted from CMIP5 models (listed in Table S2 in Supporting Information S1). We analyze outputs for a historical period (1976–2005) and a future climate change period (RCP8.5; 2070–2099), similar to Berg et al. (2016). We select only those CMIP5 models with a spatial resolution of at least  $1^\circ \times 1.25^\circ$ , which contain layered monthly data for soil temperature and soil moisture for both simulation periods. SOC concentrations strongly decrease with soil depth (e.g., Section 3.2 in Blume et al., 2016), so for this study we assume that the majority of the microbial decomposition takes place in the top soil and limit our analysis to the first 100 cm of soil. To ensure sufficient climate information is available for each soil depth, we select only those CMIP5 models containing outputs for at least five soil layers between 0 and 1 m depth (Table S2 in Supporting Information S1).

Global SOC estimates and soil porosity data are taken from the global soil information database SoilGrids (<https://soilgrids.org>). In this study, we use SoilGrids v0.5.3 at 10 km spatial resolution (Hengl et al., 2014, 2017), taking the datasets' standard soil depths to 1 m (0–0.05, 0.05–0.15, 0.15–0.30, 0.30–0.60, 0.60–1, m depth respectively, Figure S2 in Supporting Information S1). SoilGrids' porosity is defined as saturated water content ( $tetaS$  in Hengl et al., 2019). Since both SoilGrids' porosity and the CMIP5 soil moisture values are model outputs, there are cases where the CMIP5 soil moisture value exceeds SoilGrids' porosity, which lead to numerical errors in Equation 6. Neither model output is considered correct or false, so in order to match these values the soil porosity is set to

$$\Phi = \max(tetaS, \max(\theta_{\text{histo}}, \theta_{\text{RCP8.5}})) \quad (7)$$

in each grid cell, where  $\theta_{\text{histo}}$  and  $\theta_{\text{RCP8.5}}$  are the monthly soil moisture contents during the historic and RCP8.5 simulation periods, respectively. In addition, a spatial mask is applied to exclude areas classified as hot or cold deserts, where the soil might be permanently dry or frozen and where SOC content and aboveground plant productivity are expected to be low. We mask grid cells following Carvalhais et al. (2014), excluding Köppen-classified hot and cold deserts and low GPP estimates (below  $10 \text{ g C m}^{-2} \text{ y}^{-1}$ ), as well as any grid cells containing NA's in one of the input datasets (soil moisture, soil temperature, porosity, SOC density).

## 2.3. Data Preprocessing

SOC stocks ( $\text{ton C ha}^{-1}$ ) were converted to densities ( $\text{g C cm}^{-3}$ ) at layer mid-point depth (0.025, 0.10, 0.225, 0.45, 0.8 m) after Hengl et al. (2017). SOC content, soil porosity and the mask were then spatially re-gridded to match the respective CMIP5 model spatial resolution (using `raster::aggregate` and `raster::resample`, `method = 'bilinear'`). Soil moisture (mrlsl) provided in  $\text{kg m}^{-2}$  was converted to volumetric water content ( $\theta$ ), using CMIP5 model soil layer thickness. Soil moisture and temperature data were vertically re-gridded to the midpoint depths of the five SoilGrids standardized depth intervals (0–5, 5–15, 15–30, 30–60, 60–100 cm), by computing the weighted average of the intersecting components of the CMIP5 model depth intervals. All analyses were done in RStudio (RStudio Team, 2018) using packages `raster`, `ncdf4`, `pals`, `plyr`, `plotrix`, and `rgdal`.

## 2.4. Model Experiment

We applied the DAMM model at five different depths (Section 2.2) and on each individual gridcell for the historical and RCP8.5 climate change scenario. Throughout the paper we investigate changes in  $R_{\text{d}}$  (a) considering the full DAMM model (Equation 1); (b) only considering the temperature-sensitive part of the DAMM model ( $V_{\text{max}}$ , Equation 2) and refer to this as the "T only" effect on the modeled decomposition rate; and (c) considering only the moisture-sensitive part of the DAMM model (the two MM-terms in Equations 3 and 5) and refer to this as the "SM only" effect on the modeled decomposition rate.

For each CMIP5 model, the changes in  $R_{Sx}$ ,  $V_{max}$  and the two individual MM-terms (substrate limitation,  $MM_{Sx}$ ; Equation 3 and oxygen limitation,  $MM_{O_2}$ ; Equation 4) are investigated further. First, to study the anticipated climate change effects (i.e., a warming and drying/wetting soil between locations and with depth), we calculate the relative change in modeled decomposition rates (change in  $R_{Sx}$ ) between the historical period and the RCP8.5 scenario for each soil depth for the full DAMM model. Following Equation 1, for soil layer  $i$ :

$$\Delta R_{Sx,i} = \left( \frac{[V_{max} \cdot MM_{Sx} \cdot MM_{O_2}]_{RCP8.5,i}}{[V_{max} \cdot MM_{Sx} \cdot MM_{O_2}]_{histo,i}} - 1 \right) \cdot 100\% \quad (8)$$

Then, modeled changes in  $V_{max,i}$  ("T only"),  $MM_{Sx,i}$ ,  $MM_{O_2,i}$  ("SM only"), and the two individual MM-terms are calculated in a similar fashion.

Throughout the paper we refer to drying or wetting of the soil between the two simulation periods as SM- or SM+, respectively. Similarly, decreases or increases in the modeled decomposition rates (Equation 8) are indicated as R- or R+, and changes in the MM terms for substrate and oxygen (Equations 4 and 5) as  $Sx-/Sx+$  or  $O_2-/O_2+$ , respectively. As conceptually outlined in Figure S1b in Supporting Information S1 (black line), a soil moisture driven decomposition rate increase (R+) can be caused by either an increase in available substrate ( $Sx+$ ) or an increase in oxygen availability ( $O_2+$ ). Conversely, a decrease in decomposition rate (R-) can be caused by lower substrate or oxygen availability ( $Sx-$  and  $O_2-$ , respectively). Therefore, apart from presenting the global figures, we also present the contribution of the MM-terms to the directional change in decomposition rate (R) as a ratio (R+ ratio as  $Sx+ : O_2+$  or the R-ratio as  $Sx- : O_2-$ ). A ratio of 1 indicates both MM-terms were equally important to the overall directional change in decomposition rate (R+ or R-); a value > 1 indicates a change in substrate availability was the dominant contributor; and a value < 1 indicates that oxygen availability was the dominant contributor. The global figures in this paper include a panel where the respective probability density distribution (PDF) of the modeled values is shown. Color bars are calculated using the 2nd to 98th percentile of the values (standardized across all four models).

## 2.5. Comparison of DAMM Model to Observations at Multiple Depths and Sensitivity Analyses

To demonstrate the applicability of the DAMM model for our modeling study, we compare the DAMM model to a set of soil respiration observations at different depths. Studies with a complete set of suitable data are extremely rare, but we found a deep mineral soil warming experiment in the USA which contained monthly measurements at multiple depths (up to 100 cm) needed as inputs for and validation of the DAMM model (Hicks Pries et al., 2017): Soil temperature, soil moisture, soil C content (measured once), and the observed soil C flux for comparison to modeled C fluxes. Soil porosity measurements at the site were additionally taken from Gomez et al. (2002). Hicks Pries et al. (2017) measured soil C flux ( $g C m^{-3} hr^{-1}$ ), soil temperature, soil moisture at five mid-point depths: 7.5, 22.5, 40, 60, 80 cm. Soil C properties were measured at 10 cm depth intervals from 0 to 100 cm. Gomez et al. (2002) measured porosity at 15 cm depth intervals from 0 to 45 cm. Similar to Section 2.3, soil C stocks were recalculated to densities ( $g C cm^{-3}$ ) and together with soil porosity calculated as a weighted average for each layer at the 5 midpoint depths.

To test the sensitivity of the DAMM model to different substrate and oxygen levels, we run the DAMM model on the observation data. We used the exact same moisture and temperature sensitivities as Davidson et al. (2012) (Table S1 in Supporting Information S1), only refitting the  $\alpha_{Sx}$  parameter, which describes the base rate at a site (Sihl et al., 2018, 2020). We performed three model experiments: (a) A standard model run using the measured soil C content ( $S_{x,tot}$ , Equation 4), and the time series of measured soil moisture ( $\theta$ ), soil temperature ( $T_{soil}$ ), and porosity ( $\Phi$ ) as inputs for each depth interval; (b) As run (a), but using a constant soil C content ( $S_{x,tot}$  is set to the mean soil C density between 0 and 100 cm) for each soil layer to test how sensitive the model is to changes in substrate availability; and (c) As run (a), but we let  $O_{2,airfrac}$  (Equation 6) decline from 0.21 to 0.04 to test how sensitive the model is to changes in oxygen availability. All analyses were done in RStudio (RStudio Team, 2018) using packages ModelMetrics and FME).

We also tested the sensitivity of the DAMM model with the CMIP5 model runs. As with the observation data set, we tested how sensitive the model is to changes in oxygen availability by letting  $O_{2,airfrac}$  (Equation 6) decline from 0.21 to 0.04. Furthermore, by generating 1000 parameter vectors through latin hypercube sampling from a range between 80% and 120% of the original parameters ( $\alpha_{Sx}$ ,  $Ea_{Sx}$ ,  $kM_{Sx}$  and  $kM_{O_2}$ , Table S1 in Supporting

Information S1) as reported by Davidson et al. (2012), we also tested the sensitivity of DAMM to changes in these parameters in conjunction with the sensitivity to changes in substrate availability ( $S_{x,tot}$ ) and to different initial soil moisture values (using constant  $O_{2,airfrac}$  and  $S_{x,tot}$  from Davidson et al. (2012)).

### 3. Results

#### 3.1. Soil Temperature Effects on Modeled Decomposition Rates

All four CMIP5 models predict an overall rise in soil temperatures between the historical and RCP8.5 simulation periods of 2.8–4.2 K ( $\Delta\overline{ST}$ , Table S2 in Supporting Information S1). As a direct result, the temperature only effect, that is, the modeled maximum decomposition rate ( $V_{max}$ ), increases between the two simulation periods (Figure 1 and S3 in Supporting Information S1, T only). For all models, the top soil layers (0–5 cm) are exposed to stronger warming than the deepest soil layers (60–100 cm), especially in northern latitudes. Overall, the T only model predicts an increase in decomposition rates of 10%–120%, driven by rising soil temperatures alone. The predicted mean change in soil temperature ( $\Delta\overline{ST}$ ) for models CESM1-BGC and NorESM-1M is 3.7 K, and Figure S1 in Supporting Information S1 conceptually shows how this mean temperature change affects the modeled decomposition rate. At optimum soil moisture, the T only effect is at its maximum.

#### 3.2. Soil Moisture Effects on Modeled Decomposition Rates

The soil moisture-sensitive part of the DAMM model (the two MM-terms in Equations 3 and 5) changes the modeled decomposition rates in both directions. In other words, inclusion of soil moisture slows down or speeds up the modeled decomposition rates by up to 20% at the end of the century for all models (Figure 1 and S3 in Supporting Information S1, SM only). For the topsoil (0–5 cm), drying (SM-) generally leads to a reduction of decomposition rates (R-), and wetting (SM+) to an increase in decomposition rates (R+, Table 1). For the deeper soil layers, there is a different pattern: First, drying leads to an acceleration of decomposition more often in the deep soil (i.e., SM-/R+ occurs more frequently in deep soil compared to the top soil); and second, wetting leads to a slowdown of decomposition more often in the deep soil (i.e., SM+/R- occurs more frequently in deep soil compared to the top soil). Three out of four models show these patterns in the top- and deep soil layers; only INM-CM4 does not. INM-CM4 predicts relatively high overall mean soil moisture ( $\overline{SM}$ ) and small changes ( $\Delta\overline{SM}$ ) between the two simulation periods (Table S2 and Figure S4 in Supporting Information S1). So with overall wetter conditions, a (small) decrease in moisture is more likely to lead to higher oxygen availability rather than induce substrate limitation (Figure S1 in Supporting Information S1, and see Section 3.3).

#### 3.3. Substrate and Oxygen Availability

In the top soil (0–5 cm), the modelled response of decomposition rates is mostly driven by changes in substrate availability (Figures 2 and S5 in Supporting Information S1, Table 2). The top- and middle panels of the figures show the individual effects of the two MM-terms (oxygen and substrate availability, Equations 5 and 3), as well as their combined effect on the modelled decomposition rate (SM only, bottom panel). In the deeper soil layers (60–100 cm), oxygen limitation plays an increasingly large role: Reduction of oxygen availability (blue cells) increasingly corresponds to grid cells showing a slowdown of the decomposition rates. Table 2 summarizes these results for each model by showing the relative contribution of each MM-term (i.e., a change in substrate/oxygen availability) to the overall change in the modeled decomposition rate (R+/R-). There is a clear pattern between the top- and deep soil for the slowdown of decomposition (R-): The dominant contributor in the topsoil (0–5 cm) is a decrease in substrate availability (ratio > 1), whereas in the deep soil layer (60–100 cm) a reduction in oxygen availability (R-ratio < 1) is the dominant contributor for three out of four models. For all models, the contribution of oxygen limitation ( $O_2^-$ ) becomes more important towards a slowdown of decomposition in the deep soil (60–100 cm). And for model INM-CM4, oxygen availability generally contributes more often towards an acceleration of decomposition rates. This is related to the relatively high overall mean soil moisture ( $\overline{SM}$ ) and small changes ( $\Delta\overline{SM}$ ) between the two simulation periods for this model (Table S2 and Figure S4 in Supporting Information S1): When soil moisture is high and possibly close to saturation, drying would lift oxygen limitation and accelerate decomposition rates (Table 1, INM-CM4: SM-/R+, Figure S1b in Supporting Information S1). The opposite is true for GFDL-ESM2M, where ( $\overline{SM}$ ) and ( $\Delta\overline{SM}$ ) are generally low (Table S2 and Figure S4 in Supporting Information S1), and therefore changes in substrate availability are always the dominant factor



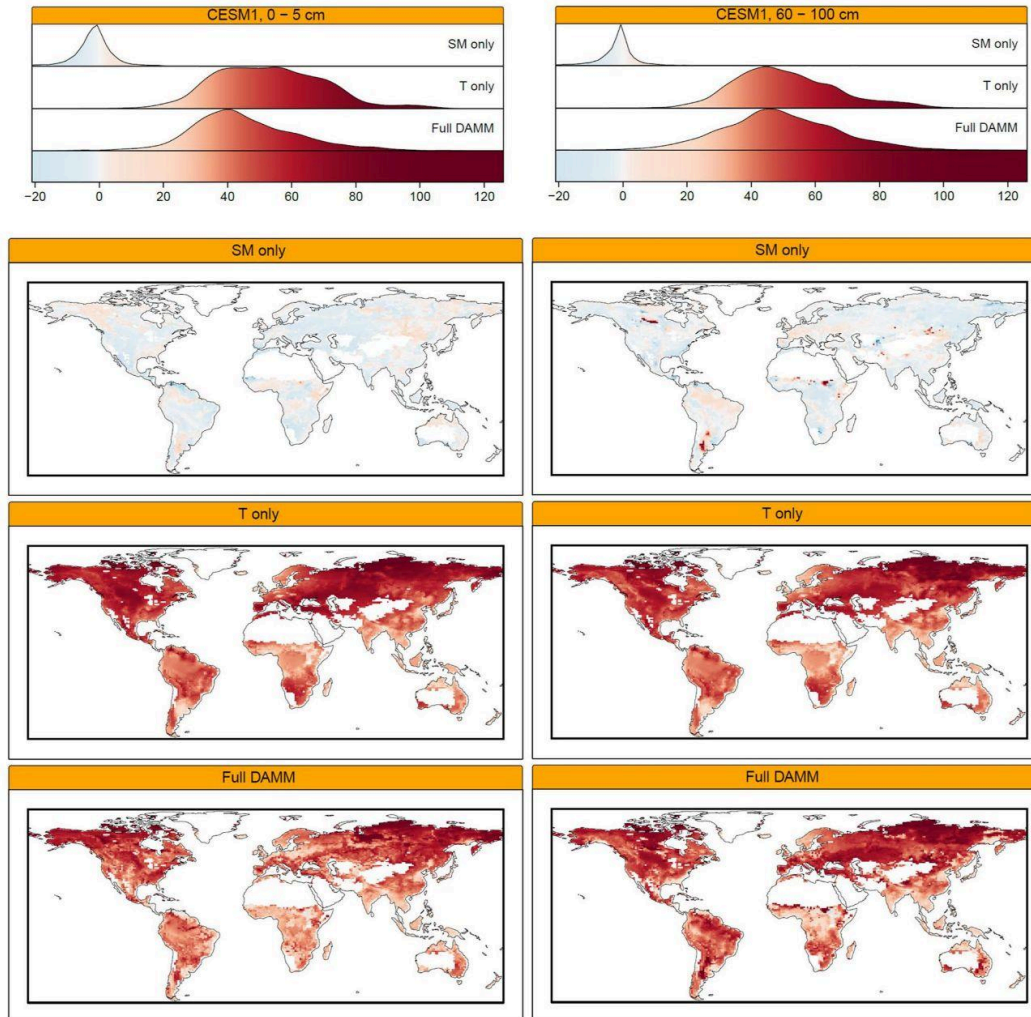


**Figure 1.** World maps showing changes in decomposition rate  $R_d$  in the topsoil (0–5 cm) and bottom soil layer (60–100 cm) for CIP5 model CESM1-BGC, due to soil moisture changes (SM only); due to temperature changes (T only); due to soil moisture and temperature changes (Full Dual Arrhenius Michaelis-Menten). All units are in % and calculated as the change between the historic and RCP8.5 simulation period (Equation 8). Blue cells indicate a slowdown, and red cells indicate an acceleration of the modeled decomposition rate between the two simulation periods. Color saturation indicates the relative speed of de-/acceleration. The top panels show the corresponding probability density functions for the values displayed in each world map. Breaks for the color scale are calculated using the inner 98 percentile of values.

determining the modelled change in decomposition rate (Table 2). Generally, the majority of the changes in the modelled decomposition rates are driven by changes in substrate availability, especially for modelled accelerations of the decomposition speed (Table 2, R+ ratio). In the deeper soil layers, however, changes in oxygen availability become increasingly important for the overall response of decomposition rates to soil moisture.

**Table 1**  
Summary of Soil Moisture Effects for All Four CMIP5 Models in the Topsoil (0–5 cm; 15–30 cm) and Subsoil (60–100 cm) Between the RCP8.5 and Historic Simulation Period

Model	Depth (cm)	SM-/R-	SM-/R+	SM+/R-	SM+/R+	no SM change
CESM1-BGC	0–5	46.4	6.4	19.5	27.7	0.0
	15–30	26.9	8.4	39.1	25.6	0.0
	60–100	16.6	13.2	50.0	20.2	0.0
INM-CM4	0–5	44.5	30.6	17.5	7.4	0.0
	15–30	30.5	34.9	25.2	9.4	0.0
	60–100	24.3	27.8	27.1	18.0	2.8
NorESM-1M	0–5	48.4	8.1	17.4	26.1	0.0
	15–30	29.7	11.1	35.7	23.5	0.0
	60–100	17.8	18.5	44.3	19.3	0.0
GFDL-ESM2M	0–5	47.1	19.0	9.0	24.9	0.0
	15–30	41.0	18.2	13.6	27.2	0.0
	60–100	41.7	21.4	14.4	22.3	0.2

Note. Numbers show the percentage of grid cells which became drier (SM-) or wetter (SM+) and whether this led to a slowdown (R-) or acceleration (R+) of the modelled decomposition rate (SM only). Two models predicted a small percentage of grid cells without soil moisture changes (no SM change).

### 3.4. Soil Moisture and Temperature Effects on Modeled Decomposition Rates

The full DAMM model (Figures 1 and S3 in Supporting Information S1, bottom panels), with the combined effects of soil temperature and soil moisture changes, generally follows the distribution of the T only response, but has a wider distribution of values that can be attributed to the soil moisture effect (top panels, SM only). In some cases, inclusion of soil moisture changes leads to a reversed direction of the predicted T only decomposition rates (Figures 1 and S3 in Supporting Information S1: Full DAMM, blue grid cells). All models show a wider PDF when soil moisture effects are included (Full DAMM): While this combined temperature and moisture effect still generally leads to a predicted acceleration of the decomposition rates at the end of this century, there is a shift toward more extreme values in both directions. For all models, and all depths, at least 52% of grid cells indicate a slowdown of decomposition in response to soil moisture changes (Table 2). A predicted slowdown occurs most frequently in the topmost soil layer (0–5 cm) lowering the overall mean predicted decomposition rate, often in response to soil drying (Table 2 and Figure S4 in Supporting Information S1). Typically, this also corresponds to soil layers where larger amounts of SOC are stored compared to the deeper layers (Figure S2 in Supporting Information S1). Deeper into the soil, the soil moisture response becomes more bi-directional, with increasing percentages of grid cells predicting an acceleration (Table 2).

### 3.5. Applicability and Sensitivity of the DAMM Model

To demonstrate the applicability of the DAMM model for our modeling study, we compared the DAMM model to a set of soil respiration observations at different depths. Our analysis shows that the DAMM model can be applied to vertically resolved respiration fluxes, using the same parameters and sensitivities to soil moisture as in our model experiment with the CMIP5 models (only calibrating  $\alpha_{SM}$ ). The DAMM model is very sensitive to changes in substrate concentrations: When ran with a constant SOC value for each soil depth, the model is no longer able to capture the respiration fluxes at any given soil depth. The model was not very sensitive to changes in the oxygen fraction in air. A full description of the site-level study and results can be found in the Supporting Informations, Text S1 and Figure S6 in Supporting Information S1.

The sensitivity tests with the CMIP5 model data reveal that the modeled changes in decomposition rate due to changes in soil moisture are sensitive to the initial soil moisture conditions (Figure 3). The sensitivity range of the reaction rate to a  $\pm 20\%$  change in the DAMM parameters is very small, and at most, falls between 2–5 percent change in reaction rate for larger changes in absolute water content. The potential for vertical divergence due to changes in soil moisture is visible: At low and high initial soil moisture content (ini.  $\theta$  of 0.15 and 0.4), the modeled changes in the decomposition rates are largest, but have relative small uncertainties. For example, in a soil column with a dry top soil and a moist deep soil layer (ini.  $\theta = 0.15$  and 0.4, respectively), the response of the modeled decomposition rate to a further drying or wetting would be opposing for both layers. As initial soil moisture comes closer to the DAMM model's optimum value (see Figure S1b in Supporting Information S1), there is less divergence in the modeled response of the reaction rate, but uncertainty increases slightly for larger changes in absolute water content (max.  $\pm 3\%$  change in absolute water content shown in Figure 3). The reported changes in modeled decomposition rates due to soil moisture changes in the CMIP5 models used for our study fall between  $-20\%$  and  $20\%$  ("SM only" in Figures 1, 2, S3 and S5 in Supporting Information S1). In other words, our results would not drastically change if we consider the added uncertainty from both the DAMM parameters and initial soil moisture conditions.

Depending on initial soil moisture content, our results can be sensitive to SOC content ( $S_{x,tot}$  from Equation 4, Figure S7 in Supporting Information S1). For dry and wet initial soil moisture conditions (ini.  $\theta$  0.15–0.2 and 0.35–0.4, respectively), there is little sensitivity of initial SOC content on the direction and magnitude of the modeled decomposition responses, but this increases for larger absolute changes in water content. Around the

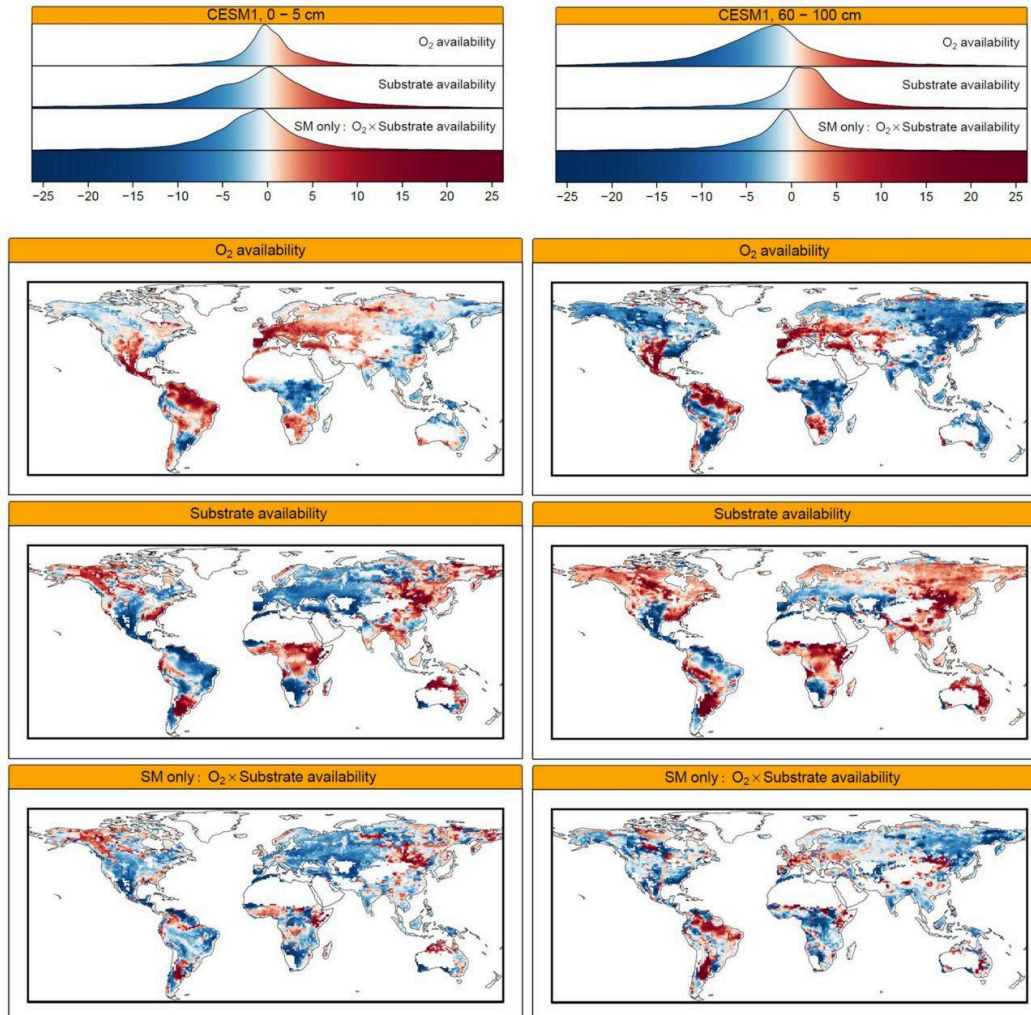


**Figure 2.** World maps showing changes in modeled decomposition rates  $R_{S_s}$  in the topsoil (0–5 cm) and bottom soil layer (60–100 cm) for CMIP5 model CESM1-BGC, due to changes in oxygen availability (top panel); due to changes in substrate availability (middle panel); and the combined soil moisture effect (SM only:  $O_2 \times$  Substrate availability, bottom panel). Units and calculation of breaks, colors and saturation similar to Figure 1.

soil moisture optimum (ini.  $\theta = 0.25\text{--}0.3$ ), there is a small additional vertical divergence visible due to changes in initial SOC content: For example, at an initial soil moisture content of 0.25, the decomposition rate is expected to decelerate in response to drying at low substrate levels ( $S_{s,tot} = 0.01\text{--}0.05 \text{ g C cm}^{-3}$ ), as a result of further restrictions of the substrate availability. But at higher substrate levels ( $S_{s,tot} = 0.09\text{--}0.11 \text{ g C cm}^{-3}$ ), the modeled decomposition rate accelerates in response to drying. So, depending on the initial soil moisture condition, future drying or wetting of a soil layer can lead to opposite effects depending on its SOC content. Generally, top soil layers have higher SOC contents than deeper layers, although this may be different in, for example, peat soils (blue areas in Figure S2 in Supporting Information S1, 60–100 cm).

**Table 2**  
Summary of Combined and Individual MM-Terms' Effects on Decomposition Rates for Four CMIP5 Models in the Topsoil (0–5 cm; 15–30 cm) and Subsoil (60–100 cm) Between the RCP8.5 and Historic Simulation Period

Model	Depth (cm)	slowdown (%)	acceleration (%)	R- ratio (Sx- : O2-)	R+ ratio (Sx+ : O2+)
CESM1-BGC	0–5	75	25	2.28	4.40
	15–30	66	34	0.69	3.01
	60–100	64	36	0.33	1.51
INM-CM4	0–5	62	38	2.56	0.28
	15–30	56	44	1.24	0.30
	60–100	52	48	0.91	0.65
NorESM-1M	0–5	74	26	2.74	3.23
	15–30	66	34	0.84	2.10
	60–100	60	40	0.40	1.04
GFDL-ESM2M	0–5	57	43	4.99	1.34
	15–30	56	44	2.94	1.52
	60–100	58	42	2.83	1.03

Note. Slowdown and acceleration are the percentage of grid cells where soil moisture changes slowed down or accelerated the decomposition rate compared to T-only (Full DAMM < T-only; or Full DAMM > T-only, respectively). The ratio  $S_x$ ;  $O_2$  represents the relative contributions of the individual terms towards a slowdown (R-)/acceleration (R+), respectively. A ratio of 1 represents an equal contribution of both MM-terms; values > 1 indicate that substrate availability ( $S_x$ ) contributed more often; values < 1 indicate that oxygen availability ( $O_2$ ) contributed more often.

The sensitivity test with the CMIP5 model data and a linearly declining  $O_{2,airfrac}$  from 0.21 to 0.04 at 1 m soil depth, indicates that our results have little sensitivity to such a steep decline in oxygen availability. Figure S8 in Supporting Information S1 shows the difference in percentage points between the standard CMIP5 model runs ( $O_{2,airfrac}$  constant at 0.21) and the runs with linearly declining oxygen gradient (Section 2.5). As expected, the top soil layer (0–5 cm) is hardly affected and the deep soil layer is most affected, but the changes are small. For all models, 90% of all data points did not change more than 2 percentage points from the model runs as presented in the manuscript, which means our results would not have drastically changed had we additionally assumed vertically decreasing oxygen levels in the DAMM model.

## 4. Discussion

### 4.1. Bi-Directional Response of Decomposition Rates to Soil Moisture

Our results show that changes in soil moisture have the potential to slow down or speed up the predicted decomposition rates by as much as 20%, compared to up to more than a doubling of the decomposition rate due to warming alone (20%–110%). This bi-directional behavior is a direct result of the interplay between the multiplicative substrate and oxygen availability terms in the DAMM model (Figure S1b in Supporting Information S1): Both a soil drying or wetting can direct the decomposition rate toward an optimum or a further decrease. Despite the strong overall temperature response, all CMIP5 model outputs considered in this study resulted not only in regions with a slowdown but also an acceleration of decomposition rates following soil moisture changes (Figures 1 and S3 in Supporting Information S1). This contrasts with earlier work by for example, Falloon et al. (2011), who reported that temperature-driven decreases in soil carbon by the year 2100 tended to be opposed by soil moisture, implying a slowdown of conventional turnover rates in response to soil moisture. The sensitivity analyses

of the DAMM model revealed that parameter uncertainty only influences the predicted decomposition rates by 2%–5% so that the observed trends are due to other factors discussed below. In our study the direction of expected changes in modeled decomposition rates at the end of this century depends on (a) the differences in the initial (historical) soil moisture levels in conjunction with (b) the projected soil moisture changes between CMIP5 models (Figure S4 in Supporting Information S1). Within the full CMIP5 model ensemble there is a large spread in model results for both, the initial soil model conditions, as well as the projected soil moisture changes under the RCP8.5 scenario (Berg et al., 2016; Cheng et al., 2017; Lorenz et al., 2016; Orlowsky & Seneviratne, 2013). We have shown the results for four different models of the CMIP5 ensemble to demonstrate the potential impacts of soil moisture on the modeled decomposition rates, where one model is on the drier end (GFDL-ESM2M), one on the wetter end (INM-CM4) and two models in the mid-range (CESM1-BGC and NorESM-1M). The bi-directional nature of the modeled decomposition rate response to soil moisture exists, however, for all models and at all soil depths.

Besides initial conditions, individual CMIP5 models also predicted different magnitudes and direction of soil moisture changes for each grid cell and also with depth, which was reported earlier by Berg et al. (2016). It is known that uncertainty in soil moisture projections between CMIP5 models is large, especially for near-surface soil moisture (Berg & Sheffield, 2018; Berg et al., 2016; Cheng et al., 2017; Lu et al., 2019; Yuan & Quiring, 2017). While climatic variability dominates differences in soil moisture predictions between CMIP5 models on shorter time scales, individual model formulations generally become the dominant source of model spread by the end of the 21st century (Orlowsky & Seneviratne, 2013). Our results show that for predicting future soil carbon it is also vital that the projections of soil moisture become better understood and constrained.

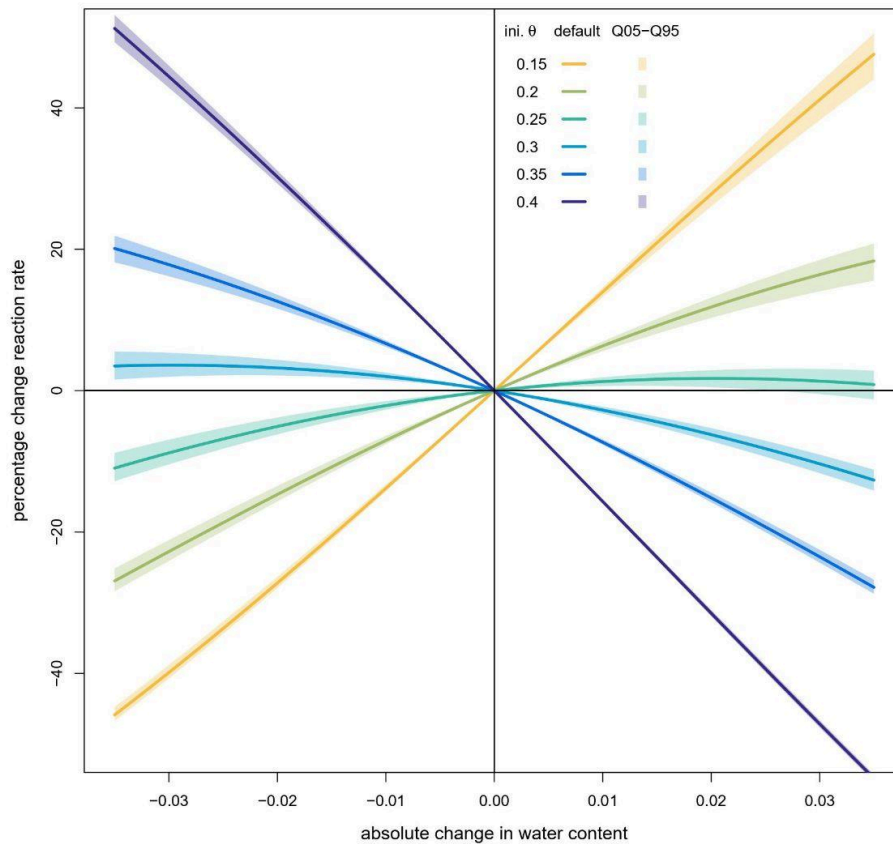


**Figure 3.** Sensitivity of Dual Arrhenius Michaelis-Menten (DAMM) model “SM only” to an absolute change in water content between the historic and RCP8.5 simulation period. Lines are colored for different initial soil moisture contents (ini.  $\theta$  from 0.15 to 0.4). Shading represents the sensitivity range (Q05–Q95: 5th–95th percentile) to  $\pm 20\%$  changes in the DAMM parameters used in this study ( $\alpha_{S_x}$ ,  $Ea_{S_x}$ ,  $kM_{S_x}$  and  $kM_{O_2}$ , Table S1 in Supporting Information S1). CMIP5 models’ historic mean soil moisture ranges from 0.24 to 0.29 (Table S2 in Supporting Information S1).

#### 4.2. Vertically Divergent Response of Decomposition Rates to Soil Moisture

By considering the vertical distribution of soil moisture, we find that soil moisture changes can further accelerate the temperature-driven decomposition rate in  $\geq 25\%$  of the gridcells in the topsoil of the four different models (Table 2). This number increases to  $\geq 34\%$  in deeper soil layers due to the interplay of substrate and oxygen availability (Figure S1 in Supporting Information S1). Especially in the upper soil layers, substrate availability is the dominant factor for the overall response of decomposition rates to soil moisture changes in this study. Our results additionally show that a vertically varying profile of soil moisture and SOC content is very important for determining the direction and magnitude of changes in the decomposition rate in response to soil moisture changes. The sensitivity tests in Figures 3 and S7 in Supporting Information S1 clearly demonstrate the potential for a divergent model response due to changes in initial soil moisture content: For different initial values of soil moisture, the modeled decomposition rate can change sign for the same absolute change in water content. But additionally, initial values of SOC content can impact the sign of the modeled decomposition rate for the same absolute changes in water content when soil moisture is close to the optimum value (Figure S1 in Supporting Information S1). When the DAMM model was confronted with measured data (Figure S6 in Supporting Information S1), it could only reproduce the observed  $\text{CO}_2$  fluxes well if a vertically varying SOC density was used.

Oxygen availability becomes increasingly important in the deeper soil layers. In our study we kept the amount of oxygen in the air-filled pore space ( $O_{2,airfrac}$ ) at atmospheric concentrations (21%), so that we might underestimate oxygen limitation if oxygen consumption in the soil profile was not replaced by diffusion. The diffusion of oxygen depends on soil texture, structure, and porosity and to a less-known degree on organic matter content through its influence on aggregate stability and pore size distribution (Neira et al., 2015). However, our model results showed little sensitivity to a linearly declining  $O_{2,airfrac}$  (Figure S8 in Supporting Information S1). As expected, the deepest soil layers were again the most affected: Soils that become wetter under future climate showed a possible, very small additional slowdown in response to reduced oxygen availability. The DAMM model does not explicitly simulate oxygen diffusion into and out of each soil layer, but indirectly simulates this by decreasing the decomposition rate due to water stagnation. Also, oxygen consumption during respiration could be an additional factor increasing anoxic conditions in soils, which is currently not considered in global scale SOC decomposition models. This possibly leads to an underestimation of the degree of anoxic conditions in soils, and would be a useful improvement when implementing DAMM into a SOC decomposition model.

Our results confirm the importance of including vertical gradients in SOC decomposition models, because top- and subsoil moisture projections can be highly divergent under future climate (Berg et al., 2016). Most existing SOC decomposition models consider only one soil depth with an average temperature and soil moisture change (Koven et al., 2017), and there are large differences between reported soil moisture values and projections when only the top 10 cm of the soil are considered versus a “whole column” approach (Berg et al., 2016). We demonstrate that SOC decomposition models which consider one soil depth with average SOC density, temperature, and moisture changes could poorly reflect the overall response of SOC turnover, because soil moisture at different depths can cause both accelerations and slowdowns of SOC turnover. So, while our study highlights the possible magnitude of decomposition rate changes with projected soil moisture (and temperature) changes, a quantitative assessment of the predicted changes in heterotrophic respiration and associated changes in SOC stocks additionally depends on the dynamic modeling of the feedback between climate change and SOC stocks (i.e., feedbacks of temperature and soil moisture on substrate availability, as well as fresh carbon inputs [NPP; Jian et al., 2021]).

#### 4.3. Future Directions

Our study shows that soil moisture can have divergent effects on SOC decomposition rates, both in different parts of the globe, as well as with soil depth. The non-linear behavior and importance of temperature and water availability for soil carbon dynamics has been repeatedly shown in global data-driven and modeling studies with regard to carbon turnover rates (Carvalhais et al., 2014), decomposition rates (this study, Falloon et al., 2011; Sierra et al., 2015) and heterotrophic respiration rates (Tang et al., 2020; Zhou et al., 2008). Our study again highlights the importance of representing soil moisture controls on decomposition, but perhaps more importantly, on developing vertically resolved SOC decomposition models. Most commonly applied soil biogeochemical models use empirical soil moisture rate modifiers (SMRF) to reduce SOC turnover rates (Figure 4c in Sierra et al., 2015), but these do not provide insight into the potential mechanisms involved (Abramoff et al., 2017; Davidson et al., 2012; Fatichi et al., 2019; Moyano et al., 2018; Yan et al., 2018). The DAMM model represents a more mechanistic framework to the soil moisture effects on decomposition. While it does not explicitly simulate microbial biomass and enzyme production, it is designed to mimic the behavior of microbial decomposition of soil substrates in what can be considered a “big microsite representation” in the soil (Davidson et al., 2012, 2014). Microbes are the main actors of SOC decomposition, and their dynamics are affected by soil moisture through water potential (controlling their survival and function), and as a physical transport medium for the resources they consume. Both soil texture and structure influence soil moisture, which in turn affects the (de)sorption potential of SOC. The DAMM model partly, but not completely, represents these microbial processes in the form of substrate limitation and by using soil porosity as a proxy for soil pore structure. As microbes continuously change their behavior in response to soil drying and re-wetting, they alter soil carbon cycling at the ecosystem level (Schimel, 2018). Representing these mechanisms in more detail inside SOC decomposition models is therefore very important for improved estimates of future SOC turnover times (Jian et al., 2021). The DAMM equations provide one model representation of the interactions between microbes, SOC decomposition and soil temperature and moisture. But there are other sets of equations available that allow us to separate the individual effects of temperature and moisture on decomposition rates in a modeling environment: For example, Yan et al. (2018) added a co-location factor to account for the amount of spatial segregation between microbes and their substrate, and Ghezzehei

et al. (2019) suggested a representation using soil matric potential instead of volumetric soil water content, which can be more easily connected to plant- and microbe specific moisture gradients.

Our study shows that adding the vertical dimension is necessary to properly account for changes in substrate and oxygen availability. In our application of the DAMM model, the amount of SOC varies for each soil depth, which is important for a good representation of the potentially available substrate for decomposition. In the DAMM model, the amount of SOC that can go into solution is represented as a fixed fraction. In reality, however, an increasing contribution of SOC is not dissolved but sorbed to mineral surfaces with depth (Schrumpf et al., 2013), which can create a solubility gradient with depth and thereby modify the response to moisture. Furthermore, a depth-resolved modelling approach presents the advantage of representing other vital processes driving substrate availability: For example, entering root litter inputs at different depths, and capturing movement of organic matter between soil layers through leaching and bioturbation. Therefore, a depth-dependent SOC decomposition model should not only represent the microbially driven processes such as the DAMM model captures, but also consider plant inputs and SOC (de)sorption with depth (Ahrens et al., 2020; Soong et al., 2020). The integration of new scientific knowledge into SOC decomposition models can help build confidence in future soil carbon decomposition models (Wieder et al., 2019), even if increased model complexity comes with added uncertainty (Shi et al., 2018). In such modelling frameworks it will be possible to study the individual and joint effects of soil moisture controls on decomposition rates and test a variety of functions. A new generation of soil models should therefore be built in such a way that they represent the latest scientific insights and are designed as modular as possible to allow for mechanistic hypothesis testing (Fisher & Koven, 2020).

## 5. Conclusions

Future soil moisture changes are uncertain, but have the potential to both slow down or accelerate the predicted SOC decomposition rates at the end of this century. These slowdowns or accelerations will be mostly driven by changes in substrate availability, especially in the top soil. In the deeper soil layers, oxygen availability becomes increasingly important. Our study highlights that the development of the next generation of SOC decomposition models would benefit from including vertical representations of soil processes, with moisture sensitivity functions that reflect our mechanistic understanding of the effects of soil drying (and a reduction in substrate availability) and soil wetting (and the reduction of oxygen availability). Given the importance of SOC stocks in the overall C cycle, it is important such dynamics are integrated into the next generation soil models embedded in coupled global climate models. This would enable us to study the effects and potential feedbacks of soil moisture on SOC stocks and CO<sub>2</sub>-release to the atmosphere under a changing climate.

## Data Availability Statement

Soil carbon and porosity data can be downloaded from <https://soilgrids.org>, climate data are available at <https://esgf-node.llnl.gov>. Supporting R-script including our use of the DAMM model can be downloaded from [https://gitlab.com/MarleenPallandt/pallandt\\_et\\_al2021\\_jgrbg\\_decomposition\\_sm\\_response](https://gitlab.com/MarleenPallandt/pallandt_et_al2021_jgrbg_decomposition_sm_response), which is permanently stored under a DOI: <https://doi.org/10.5281/zenodo.5654554>.

## References

- Abramoff, R., Davidson, E., & Finzi, A. C. (2017). A parsimonious modular approach to building a mechanistic belowground carbon and nitrogen model. *Journal of Geophysical Research: Biogeosciences*, 122(9), 2418–2434. <https://doi.org/10.1002/2017JG003796>
- Ahrens, B., Braakhekke, M. C., Guggenberger, G., Schrumpf, M., & Reichstein, M. (2015). Contribution of sorption, DOC transport and microbial interactions to the 14C age of a soil organic carbon profile: Insights from a calibrated process model. *Soil Biology and Biochemistry*, 88, 390–402. <https://doi.org/10.1016/j.soilbio.2015.06.008>
- Ahrens, B., Guggenberger, G., Rethemeyer, J., John, S., Marschner, B., Heinze, S., et al. (2020). Combination of energy limitation and sorption capacity explains 14C depth gradients. *Soil Biology and Biochemistry*, 148, 107912. <https://doi.org/10.1016/j.soilbio.2020.107912>
- Berg, A., & Sheffield, J. (2018). Climate change and drought: The soil moisture perspective. *Current Climate Change Reports*, 4(2), 180–191. <https://doi.org/10.1007/s40641-018-0095-0>
- Berg, A., Sheffield, J., & Milly, P. C. D. (2016). Divergent surface and total soil moisture projections under global warming. *Geophysical Research Letters*, 44(1), 236–244. <https://doi.org/10.1002/2016GL071921>
- Blankinship, J. C., Berhe, A. A., Crow, S. E., Druhan, J. L., Heckman, K. A., Keiluweit, M., et al. (2018). Improving understanding of soil organic matter dynamics by triangulating theories, measurements, and models. *Biogeochemistry*, 140(1), 1–13. <https://doi.org/10.1007/s10533-018-0478-2>

## Acknowledgments

We gratefully acknowledge funding support for this work from the Norwegian Research Council through grant no. RCN 255061 (MOisture dynamics and CArbon sequestration in BOREal Soils) and the Max Planck Institute for Biogeochemistry. We also acknowledge the World Climate Research Programme's Working Group on Coupled Modelling, which is responsible for CMIP, and thank the climate modeling groups (listed in Table S2 in Supporting Information S1 of this paper) for producing and making available their model output. For CMIP the U.S. Department of Energy's Program for Climate Model Diagnosis and Intercomparison provides coordinating support and led development of software infrastructure in partnership with the Global Organization for Earth System Science Portals. We thank Tea Thum for proof-reading an early draft of this manuscript.

- Blume, H.-P., Brümmer, G. W., Fleige, H., Horn, R., Kandeler, E., Kögel-Knabner, I., et al. (2016). Soil organic matter. In *Scheffer/Schachtschabel/Soil Science* (pp. 55–86). Springer. [https://doi.org/10.1007/978-3-642-30942-7\\_3](https://doi.org/10.1007/978-3-642-30942-7_3)
- Braakhekke, M. C., Beer, C., Hoosbeek, M. R., Reichstein, M., Kruijt, B., Schrumpp, M., & Kabat, P. (2011). SOMPROF: A vertically explicit soil organic matter model. *Ecological Modelling*, *222*(10), 1712–1730. <https://doi.org/10.1016/j.ecolmodel.2011.02.015>
- Bradford, M., & Fierer, N. (2012). The biogeography of microbial communities and ecosystem processes: Implications for soil and ecosystem models. In D. Wall et al. (Eds.), *Soil ecology and ecosystem services*. Oxford University Press. <https://doi.org/10.1093/acprof:oso/9780199575923.003.0017>
- Bradford, M. A., Wieder, W. R., Bonan, G. B., Fierer, N., Raymond, P. A., & Crowther, T. W. (2016). Managing uncertainty in soil carbon feedbacks to climate change. *Nature Climate Change*, *6*(8), 751–758. <https://doi.org/10.1038/nclimate3071>
- Carvalho, N., Forkel, M., Khomik, M., Bellarby, J., Jung, M., Migliavacca, M., et al. (2014). Global covariation of carbon turnover times with climate in terrestrial ecosystems. *Nature*, *514*(7521), 213–217. <https://doi.org/10.1038/nature13731>
- Cheng, S., Huang, J., Ji, F., & Lin, L. (2017). Uncertainties of soil moisture in historical simulations and future projections. *Journal of Geophysical Research: Atmospheres*, *122*(4), 2239–2253. <https://doi.org/10.1002/2016JD025871>
- Crowther, T. W., Todd-Brown, K. E. O., Rowe, C. W., Wieder, W. R., Carey, J. C., Machmuller, M. B., et al. (2016). Quantifying global soil carbon losses in response to warming. *Nature*, *540*(7631), 104–108. <https://doi.org/10.1038/nature20150>
- Davidson, E. A., & Janssens, I. A. (2006). Temperature sensitivity of soil carbon decomposition and feedbacks to climate change. *Nature*, *440*(7081), 165–173. <https://doi.org/10.1038/nature04514>
- Davidson, E. A., Samanta, S., Caramori, S. S., & Savage, K. (2012). The dual arrhenius and michaelis-menten kinetics model for decomposition of soil organic matter at hourly to seasonal time scales. *Global Change Biology*, *18*(1), 371–384. <https://doi.org/10.1111/j.1365-2486.2011.02546.x>
- Davidson, E. A., Savage, K. E., & Finzi, A. C. (2014). A big-microsite framework for soil carbon modeling. *Global Change Biology*, *20*(12), 3610–3620. <https://doi.org/10.1111/gcb.12718>
- Drake, J. E., Macdonald, C. A., Tjoelker, M. G., Reich, P. B., Singh, B. K., Anderson, I. C., & Ellsworth, D. S. (2018). Three years of soil respiration in a mature eucalypt woodland exposed to atmospheric CO<sub>2</sub> enrichment. *Biogeochemistry*, *139*(1), 85–101. <https://doi.org/10.1007/s10533-018-0457-7>
- Falloon, P., Jones, C. D., Ades, M., & Paul, K. (2011). Direct soil moisture controls of future global soil carbon changes: An important source of uncertainty. *Global Biogeochemical Cycles*, *25*(3). <https://doi.org/10.1029/2010gb003938>
- Faticchi, S., Manzoni, S., Or, D., & Paschalis, A. (2019). A mechanistic model of microbially mediated soil biogeochemical processes: A reality check. *Global Biogeochemical Cycles*, *33*(6), 620–648. <https://doi.org/10.1029/2018GB006077>
- Fisher, R. A., & Koven, C. D. (2020). Perspectives on the future of land surface models and the challenges of representing complex terrestrial systems. *Journal of Advances in Modeling Earth Systems*, *12*(4), e2018MS001453. <https://doi.org/10.1029/2018ms001453>
- Gestel, N. v., Shi, Z., Groenigen, K. J. v., Osenberg, C. W., Andresen, L. C., Dukes, J. S., et al. (2018). Predicting soil carbon loss with warming. *Nature*, *554*(7693), E4–E5. <https://doi.org/10.1038/nature25745>
- Ghezzehei, T. A., Sulman, B., Arnold, C. L., Bogie, N. A., & Berhe, A. A. (2019). On the role of soil water retention characteristic on aerobic microbial respiration. *Biogeosciences*, *16*(6), 1187–1209. <https://doi.org/10.5194/bg-16-1187-2019>
- Gomez, A., Powers, R. F., Singer, M. J., & Horwath, W. R. (2002). Soil compaction effects on growth of young ponderosa pine following litter removal in California's sierra Nevada. *Soil Science Society of America Journal*, *66*(4), 1334–1343. <https://doi.org/10.2136/sssaj2002.1334>
- Heimann, M., & Reichstein, M. (2008). Terrestrial ecosystem carbon dynamics and climate feedbacks. *Nature*, *451*(7176), 289–292. <https://doi.org/10.1038/nature06591>
- Hengl, T., de Jesus, J. M., MacMillan, R. A., Batjes, N. H., Heuvelink, G. B. M., Ribeiro, E., et al. (2014). Soilgrids1km—Global soil information based on automated mapping. *PLoS One*, *9*(8), 1–17. <https://doi.org/10.1371/journal.pone.0105992>
- Hengl, T., Kempen, B., Heuvelink, G., & Brendan, M. (2019). GSIF: Global Soil Information Facilities. R package version 0.5-5. Retrieved from <https://CRAN.R-project.org/package=GSIF>
- Hengl, T., Mendes de Jesus, J., Heuvelink, G. B. M., Ruiperez Gonzalez, M., Kilibarda, M., Blagotić, A., et al. (2017). Soilgrids250m: Global gridded soil information based on machine learning. *PLoS One*, *12*(2), 1–40. <https://doi.org/10.1371/journal.pone.0169748>
- Hicks Pries, C. E., Castanha, C., Porras, R. C., & Torn, M. S. (2017). The whole-soil carbon flux in response to warming. *Science*, *355*(6332), 1420–1423. <https://doi.org/10.1126/scien>
- Hochachka, P., & Somero, G. (2002). *Biochemical adaptation: Mechanism and process in physiological evolution*. Oxford University Press.
- Jian, J., Bond-Lamberty, B., Hao, D., Sulman, B. N., Patel, K. F., Zheng, J., et al. (2021). Leveraging observed soil heterotrophic respiration fluxes as a novel constraint on global-scale models. *Global Change Biology*, *27*, 5392–5403. <https://doi.org/10.1111/gcb.15795>
- Jones, C., Robertson, E., Arora, V., Friedlingstein, P., Sheviakova, E., Bopp, L., et al. (2013). Twenty-first-century compatible CO<sub>2</sub> emissions and airborne fraction simulated by cmip5 earth system models under four representative concentration pathways. *Journal of Climate*, *26*(13), 4398–4413. <https://doi.org/10.1175/jcli-d-12-00554.1>
- Jung, M., Reichstein, M., Schwalm, C. R., Huntingford, C., Sitch, S., Ahlström, A., et al. (2017). Compensatory water effects link yearly global land CO<sub>2</sub> sink changes to temperature. *Nature*, *541*(7638), 516–520. <https://doi.org/10.1038/nature20780>
- Kirschbaum, M. (2006). The temperature dependence of organic-matter decomposition—Still a topic of debate. *Soil Biology and Biochemistry*, *38*(9), 2510–2518. <https://doi.org/10.1016/j.soilbio.2006.01.030>
- Koven, C. D., Hugelius, G., Lawrence, D. M., & Wieder, W. R. (2017). Higher climatological temperature sensitivity of soil carbon in cold than warm climates. *Nature Climate Change*, *7*(11), 817–822. <https://doi.org/10.1038/nclimate3421>
- Koven, C. D., Riley, W. J., Subin, Z. M., Tang, J. Y., Torn, M. S., Collins, W. D., et al. (2013). The effect of vertically resolved soil biogeochemistry and alternate soil C and N models on C dynamics of CLM4. *Biogeosciences*, *10*(11), 7109–7131. <https://doi.org/10.5194/bg-10-7109-2013>
- Lloyd, J., & Taylor, J. A. (1994). On the temperature dependence of soil respiration. *Functional Ecology*, *8*(3), 315. <https://doi.org/10.2307/2389824>
- Lorenz, R., Argüeso, D., Donat, M. G., Pitman, A. J., van den Hurk, B., Berg, A., et al. (2016). Influence of land-atmosphere feedbacks on temperature and precipitation extremes in the GLACE-CMIP5 ensemble. *Journal of Geophysical Research: Atmospheres*, *121*(2), 607–623. <https://doi.org/10.1002/2015jd024053>
- Lu, J., Carbone, G. J., & Grego, J. M. (2019). Uncertainty and hotspots in 21st century projections of agricultural drought from CMIP5 models. *Scientific Reports*, *9*(1). <https://doi.org/10.1038/s41598-019-41196-z>
- Luo, Y., Ahlström, A., Allison, S. D., Batjes, N. H., Brovkin, V., Carvalho, N., et al. (2016). Toward more realistic projections of soil carbon dynamics by earth system models. *Global Biogeochemical Cycles*, *30*(1), 40–56. <https://doi.org/10.1002/2015GB005239>
- Manzoni, S., & Katul, G. (2014). Invariant soil water potential at zero microbial respiration explained by hydrological discontinuity in dry soils. *Geophysical Research Letters*, *41*(20), 7151–7158. <https://doi.org/10.1002/2014gl061467>
- Millington, R. J. (1959). Gas diffusion in porous media. *Science*, *130*(3367), 100–102. <https://doi.org/10.1126/science.130.3367.100-a>



- Moyano, F. E., Manzoni, S., & Chenu, C. (2013). Responses of soil heterotrophic respiration to moisture availability: An exploration of processes and models. *Soil Biology and Biochemistry*, *59*, 72–85. <https://doi.org/10.1016/j.soilbio.2013.01.002>
- Moyano, F. E., Vasilyeva, N., & Menichetti, L. (2018). Diffusion limitations and Michaelis–Menten kinetics as drivers of combined temperature and moisture effects on carbon fluxes of mineral soils. *Biogeosciences*, *15*(16), 5031–5045. <https://doi.org/10.5194/bg-15-5031-2018>
- Neira, J., Ortiz, M., Morales, L., & Acevedo, E. (2015). Oxygen diffusion in soils: Understanding the factors and processes needed for modeling. *Chilean Journal of Agricultural Research*, *75*, 35–44. <https://doi.org/10.4067/s0718-58392015000300005>
- Nottingham, A. T., Turner, B. L., Whitaker, J., Ostle, N., Bardgett, R. D., McNamara, N. P., et al. (2016). Temperature sensitivity of soil enzymes along an elevation gradient in the peruvian andes. *Biogeochemistry*, *127*(2–3), 217–230. <https://doi.org/10.1007/s10533-015-0176-2>
- Orlowsky, B., & Seneviratne, S. I. (2013). Elusive drought: Uncertainty in observed trends and short- and long-term CMIP5 projections. *Hydrology and Earth System Sciences*, *17*(5), 1765–1781. <https://doi.org/10.5194/hess-17-1765-2013>
- RStudio Team. (2018). *Rstudio: Integrated development environment for R*. Retrieved from <http://www.rstudio.com/>
- Schimel, J. (2001). 1.13—Biogeochemical models: Implicit versus explicit microbiology. In E. D. Schulze, M. Heimann, S. Harrison, J. Lloyd, I. C. Prentice & D. Schimel (Eds.), *Global biogeochemical cycles in the climate system* (pp. 177–183). Academic Press. <https://doi.org/10.1016/B978-012631260-7/50015-7>
- Schimel, J. P. (2018). Life in dry soils: Effects of drought on soil microbial communities and processes. *Annual Review of Ecology, Evolution, and Systematics*, *49*(1), 409–432. <https://doi.org/10.1146/annurev-ecolsys-110617-062614>
- Schmidt, M. W. I., Torn, M. S., Abiven, S., Dittmar, T., Guggenberger, G., Janssens, I. A., et al. (2011). Persistence of soil organic matter as an ecosystem property. *Nature*, *478*(7367), 49–56. <https://doi.org/10.1038/nature10386>
- Schrumpf, M., Kaiser, K., Guggenberger, G., Persson, T., Kögel-Knabner, I., & Schulze, E. D. (2013). Storage and stability of organic carbon in soils as related to depth, occlusion within aggregates, and attachment to minerals. *Biogeosciences*, *10*(3), 1675–1691. <https://doi.org/10.5194/bg-10-1675-2013>
- Shi, Z., Allison, S. D., He, Y., Levine, P. A., Hoyt, A. M., Beem-Miller, J., et al. (2020). The age distribution of global soil carbon inferred from radiocarbon measurements. *Nature Geoscience*, *13*(8), 555–559. <https://doi.org/10.1038/s41561-020-0596-z>
- Shi, Z., Crowell, S., Luo, Y., & Moore, B. (2018). Model structures amplify uncertainty in predicted soil carbon responses to climate change. *Nature Communications*, *9*(1). <https://doi.org/10.1038/s41467-018-04526-9>
- Sierra, C. A., Malghani, S., & Loescher, H. W. (2017). Interactions among temperature, moisture, and oxygen concentrations in controlling decomposition rates in a boreal forest soil. *Biogeosciences*, *14*(3), 703–710. <https://doi.org/10.5194/bg-14-703-2017>
- Sierra, C. A., Müller, M., & Trumbore, S. E. (2012). Models of soil organic matter decomposition: The SoilR package, version 1.0. *Geoscientific Model Development*, *5*(4), 1045–1060. <https://doi.org/10.5194/gmd-5-1045-2012>
- Sierra, C. A., Trumbore, S. E., Davidson, E. A., Vicca, S., & Janssens, I. (2015). Sensitivity of decomposition rates of soil organic matter with respect to simultaneous changes in temperature and moisture. *Journal of Advances in Modeling Earth Systems*, *7*(1), 335–356. <https://doi.org/10.1002/2014ms000358>
- Sih, D., Davidson, E. A., Chen, M., Savage, K. E., Richardson, A. D., Keenan, T. F., & Hollinger, D. Y. (2018). Merging a mechanistic enzymatic model of soil heterotrophic respiration into an ecosystem model in two AmeriFlux sites of northeastern USA. *Agricultural and Forest Meteorology*, *252*, 155–166. <https://doi.org/10.1016/j.agrformet.2018.01.026>
- Sih, D., Davidson, E. A., Savage, K. E., & Liang, D. (2020). Simultaneous numerical representation of soil microsite production and consumption of carbon dioxide, methane, and nitrous oxide using probability distribution functions. *Global Change Biology*, *26*(1), 200–218. <https://doi.org/10.1111/gcb.14855>
- Skopp, J., Jawson, M. D., & Doran, J. W. (1990). Steady-state aerobic microbial activity as a function of soil water content. *Soil Science Society of America Journal*, *54*(6), 1619–1625. <https://doi.org/10.2136/sssaj1990.03615995005400060018x>
- Soong, J. L., Fuchsliueger, L., Marañón-Jimenez, S., Torn, M. S., Janssens, I. A., Penuelas, J., & Richter, A. (2020). Microbial carbon limitation: The need for integrating microorganisms into our understanding of ecosystem carbon cycling. *Global Change Biology*, *26*(4), 1953–1961. <https://doi.org/10.1111/gcb.14962>
- Sulman, B. N., Moore, J. A. M., Abramoff, R., Averill, C., Kivlin, S., Georgiou, K., et al. (2018). Multiple models and experiments underscore large uncertainty in soil carbon dynamics. *Biogeochemistry*, *141*(2), 109–123. <https://doi.org/10.1007/s10533-018-0509-z>
- Sulman, B. N., Phillips, R. P., Oishi, A. C., Shevliakova, E., & Pacala, S. W. (2014). Microbe-driven turnover offsets mineral-mediated storage of soil carbon under elevated CO<sub>2</sub>. *Nature Climate Change*, *4*(12), 1099–1102. <https://doi.org/10.1038/nclimate2436>
- Tang, X., Fan, S., Du, M., Zhang, W., Gao, S., Liu, S., et al. (2020). Spatial and temporal patterns of global soil heterotrophic respiration in terrestrial ecosystems. *Earth System Science Data*, *12*(2), 1037–1051. <https://doi.org/10.5194/essd-12-1037-2020>
- Todd-Brown, K., Zheng, B., & Crowther, T. W. (2018). Field-warmed soil carbon changes imply high 21st-century modeling uncertainty. *Biogeosciences*, *15*(12), 3659–3671. <https://doi.org/10.5194/bg-15-3659-2018>
- Todd-Brown, K. E. O., Randerson, J. T., Hopkins, F., Arora, V., Hajima, T., Jones, C., et al. (2014). Changes in soil organic carbon storage predicted by Earth system models during the 21st century. *Biogeosciences*, *11*(8), 2341–2356. <https://doi.org/10.5194/bg-11-2341-2014>
- Todd-Brown, K. E. O., Randerson, J. T., Post, W. M., Hoffman, F. M., Tarnocai, C., Schuur, E. A. G., & Allison, S. D. (2013). Causes of variation in soil carbon simulations from CMIP5 Earth system models and comparison with observations. *Biogeosciences*, *10*(3), 1717–1736. <https://doi.org/10.5194/bg-10-1717-2013>
- Wang, G., Post, W. M., Mayes, M. A., Frerichs, J. T., & Sindhu, J. (2012). Parameter estimation for models of ligninolytic and cellulolytic enzyme kinetics. *Soil Biology and Biochemistry*, *48*, 28–38. <https://doi.org/10.1016/j.soilbio.2012.01.011>
- Wang, J., Sun, J., Xia, J., He, N., Li, M., & Niu, S. (2018). Soil and vegetation carbon turnover times from tropical to boreal forests. *Functional Ecology*, *32*(1), 71–82. <https://doi.org/10.1111/1365-2435.12914>
- Wieder, W. R., Grandy, A. S., Kallenbach, C. M., & Bonan, G. B. (2014). Integrating microbial physiology and physio-chemical principles in soils with the Microbial-Mineral Carbon Stabilization (MIMICS) model. *Biogeosciences*, *11*(14), 3899–3917. <https://doi.org/10.5194/bg-11-3899-2014>
- Wieder, W. R., Hartman, M. D., Sulman, B. N., Wang, Y.-P., Koven, C. D., & Bonan, G. B. (2018). Carbon cycle confidence and uncertainty: Exploring variation among soil biogeochemical models. *Global Change Biology*, *24*(4), 1563–1579. <https://doi.org/10.1111/gcb.13979>
- Wieder, W. R., Sulman, B. N., Hartman, M. D., Koven, C. D., & Bradford, M. A. (2019). Arctic soil governs whether climate change drives global losses or gains in soil carbon. *Geophysical Research Letters*, *46*(24), 14486–14495. <https://doi.org/10.1029/2019gl085543>
- Wutzler, T., Zaehle, S., Schrumpf, M., Ahrens, B., & Reichstein, M. (2017). Adaptation of microbial resource allocation affects modelled long term soil organic matter and nutrient cycling. *Soil Biology and Biochemistry*, *115*, 322–336. <https://doi.org/10.1016/j.soilbio.2017.08.031>
- Yan, Z., Bond-Lamberty, B., Todd-Brown, K. E., Bailey, V. L., Li, S., Liu, C., & Liu, C. (2018). A moisture function of soil heterotrophic respiration that incorporates microscale processes. *Nature Communications*, *9*(1), 2562. <https://doi.org/10.1038/s41467-018-04971-6>

- Yu, L., Ahrens, B., Wutzler, T., Schrupf, M., & Zaehle, S. (2020). Jena Soil Model (JSM v1.0; revision 1934): A microbial soil organic carbon model integrated with nitrogen and phosphorus processes. *Geoscientific Model Development*, *13*(2), 783–803. <https://doi.org/10.5194/gmd-13-783-2020>
- Yuan, S., & Quiring, S. M. (2017). Evaluation of soil moisture in CMIP5 simulations over the contiguous United States using in situ and satellite observations. *Hydrology and Earth System Sciences*, *21*(4), 2203–2218. <https://doi.org/10.5194/hess-21-2203-2017>
- Zhou, X., Weng, E., & Luo, Y. (2008). Modeling patterns of nonlinearity in ecosystem responses to temperature, CO<sub>2</sub>, and precipitation changes. *Ecological Applications*, *18*(2), 453–466. <https://doi.org/10.1890/07-0626.1>

### References From the Supporting Information

- Hu, S.-C., & Linnartz, N. E. (1972). *Variations in oxygen content of forest soils under mature loblolly pine stands*. Louisiana State University and Agricultural and Mechanical College, Agricultural Experiment Station. Retrieved from <http://digitalcommons.lsu.edu/agexp/105>
- Runkles, J. R. (1956). *Diffusion, sorption and depth distribution of oxygen in soils* (Thesis). <https://doi.org/10.31274/rtd-180813-16366>
- Silver, W. L., Lugo, A. E., & Keller, M. (1999). Soil oxygen availability and biogeochemistry along rainfall and topographic gradients in upland wet tropical forest soils. *Biogeochemistry*, *44*(3), 301–328. <https://doi.org/10.1007/bf00996995>

### Erratum

The originally published version of this article contained errors in the Author Contributions list. Marion Schrupf was incorrectly listed under Writing – original draft and has been corrected to Marleen Pallandt. Marleen Pallandt has also been added to Data curation, Formal analysis, Investigation, Validation, Visualization, and Writing – review & editing. In addition, Marleen Pallandt and Sujun Koirala have been added to Conceptualization. This may be considered the authoritative version of record.

# Supporting information for Study II

---



*JGR: Biogeoscience*

Supporting Information for

## **Vertically divergent responses of SOC decomposition to soil moisture in a changing climate**

Marleen Pallandt<sup>1,2</sup>, Bernhard Ahrens<sup>1</sup>, Sujan Koirala<sup>1</sup>, Markus Reichstein<sup>1,2</sup>, Holger Lange<sup>3</sup>,  
Marion Schrumpf<sup>1,2</sup>, Sönke Zaehle<sup>1,2</sup>

<sup>1</sup> Max Planck Institute for Biogeochemistry, Hans-Knöll Str. 10, 07745 Jena, Germany

<sup>2</sup> International Max Planck Research School (IMPRS) for Global Biogeochemical Cycles, Hans-Knöll Str. 10,  
07745 Jena, Germany

<sup>3</sup> Norwegian Institute of Bioeconomy Research, Høgskoleveien 8, 1433 Ås, Norway

## **Contents of this file**

Text S1: Comparison of DAMM model to observations at multiple depths

Figure S1: Conceptual graph for changes in Michaelis-Menten terms

Figure S2: SOC content from SoilGrids

Figure S3: Temperature- and moisture driven changes in modelled decomposition rates

Figure S4: Model mean historic soil moisture and soil moisture changes by the end of the century

Figure S5: Moisture driven changes in modelled decomposition rates

Figure S6: Comparison of different DAMM model runs to observations at different soil midpoint depths (cm)

Figure S7: Sensitivity of model results to different initial substrate concentrations Figure S8: Sensitivity of model results to declining oxygen gradient

Table S1: Parameter values and constants used in this study

Table S2: CMIP5 models used in this study

## Introduction

This supporting information file includes a conceptual visualization of the DAMM model (Fig. S1); parameters of the DAMM model used in this study (Table S1); a map of SOC content from SoilGrids at multiple depths (Fig. S2); CMIP5 mean historic soil moisture and mean soil moisture changes between the historic and RCP8.5 simulation period (Fig. S4); sensitivity of DAMM model to different total substrate concentrations ( $S_{x,total}$ ) and an absolute change in water content between the historic and RCP8.5 simulation period; and model results similar to Figs. 1 and 2 for the additional CMIP5 models in this study (Figs. S3 and S5, Table S2). All methods and data used to produce these figures and tables are described under “Data and Methods” (Section 2) of the main manuscript. R-code to run the DAMM model with CMIP5 data can be downloaded from [https://git.bgc-jena.mpg.de/mpalla/pallandt\\_et al2020\\_jgrbg\\_decomposition\\_sm\\_response.git](https://git.bgc-jena.mpg.de/mpalla/pallandt_et al2020_jgrbg_decomposition_sm_response.git). This supporting information file further includes a comparison of the DAMM model to site level observations from Hicks Pries et al. (2017) at multiple soil depth intervals to 1 m (Text S1 and Fig. S6). The methods and results are described in detail in the supporting information as they support, but are not essential to, the main manuscript. The data were downloaded with the original manuscript as provided by Hicks Pries et al. (2017).

## Text S1. Comparison of DAMM model to observations at multiple depths

### Methodology

Hicks Pries et al. (2017) measured soil C flux ( $\text{g C m}^{-3} \text{h}^{-1}$ ), soil temperature, soil moisture at the five following mid-point depths: 7.5, 22.5, 40, 60, 80 cm. Soil C properties were measured at 10 cm depth intervals from 0 – 100 cm. Gomez et al. (2002) measured porosity at 15 cm depth intervals from 0– 45 cm. Similar to Section 2.3, soil C stocks were recalculated to densities ( $\text{g C cm}^{-3}$ ) and together with soil porosity calculated as a weighted average for each layer at the 5 midpoint depths. The DAMM model was ran thrice: 1) Standard DAMM model run, using the measured SM, soil temperature, porosity and soil C content as inputs for each depth interval; 2) As the standard model run, but using a fixed soil C content (calculated as the mean measured soil C content between 0 – 100 cm) for each soil layer, to test how sensitive the model is to changes in substrate availability; 3) As the standard model run, but with a linearly declining value for the oxygen fraction in air ( $O_{2,airfrac}$  from 0.21 to 0.04 between 0 and 100 cm soil depth, to test the sensitivity of the model to a reduced oxygen gradient in the deeper soil. Reported measurements of oxygen concentrations at multiple depth intervals up to 100 cm depth are rare, and values vary highly with soil type, soil moisture content and time of measurement (Hu & Linnartz, 1972; Runkles, 1956; Silver et al., 1999). Our back of the envelope calculation, using a minimum value of 0.04, is based on some of the reported lower values. The parameter  $\alpha_{sx}$ , which describes the base respiration at the site, was refitted using the ‘modFit’ function of the R

package FME (methods “L-BFGS-B” and “Marq” to avoid local minima) by minimizing the residuals between the observed soil CO<sub>2</sub> fluxes and the values predicted by the DAMM model. DAMM model parameters  $Ea_{S_x}$ ,  $kM_{S_x}$ ,  $kM_{O_2}$ , and all constants (Table S1) were not refitted, but remained the same as in our application of the DAMM model on the CMIP5 data (values taken directly from Davidson et al. (2012)). All analyses were done in RStudio (RStudio Team, 2018) using packages ModelMetrics and FME).

## Results

When running the DAMM model with the same parameters as listed in Table S1, only refitting parameter  $\alpha_{S_x}$ , the model captures the observed fluxes relatively well (Fig. S6), with an R<sup>2</sup> of 0.52 and RMSE of 0.19. At lower depths, the model slightly overestimates the observed fluxes, but these are generally very small (close to zero). The model is very sensitive to changes in substrate availability: When using a constant value for C density (calculated as the mean C density between 0 and 100 cm depth), the DAMM model was no longer able to capture the observed fluxes at any given depth (Fig S6, R<sup>2</sup> = 0, RMSE is 0.27). The model was not at all sensitive to changes in the oxygen fraction in air ( $O_{2,airfrac}$  declining from 0.21 to 0.04), or other estimates of the half saturation constant for oxygen: Both model runs had the same rounded R<sup>2</sup> (0.58) and RMSE (0.18) as for the standard model run. Therefore, from this simple site-level exercise we can see that DAMM is capable of modeling the CO<sub>2</sub> efflux throughout the soil profile relatively well, and that substrate availability dominates the modeled response. A smaller role of the oxygen term at this site is in line with our expectations, as the soil seems to be well drained most of the time: The soil porosity at this site is high (0.62), but the maximum observed soil moisture is only 0.38. We did not find observations for this site’s soil porosity below 45 cm depth, but it is likely that porosity further declined with soil depth with lower SOC content and compaction (Maier et al., 2010). The slight overestimation of modeled fluxes from the two deepest soil layers might be related to uncertain estimates of the available C substrate. A deep analysis of the specific causes, however, falls outside of the scope of this paper.

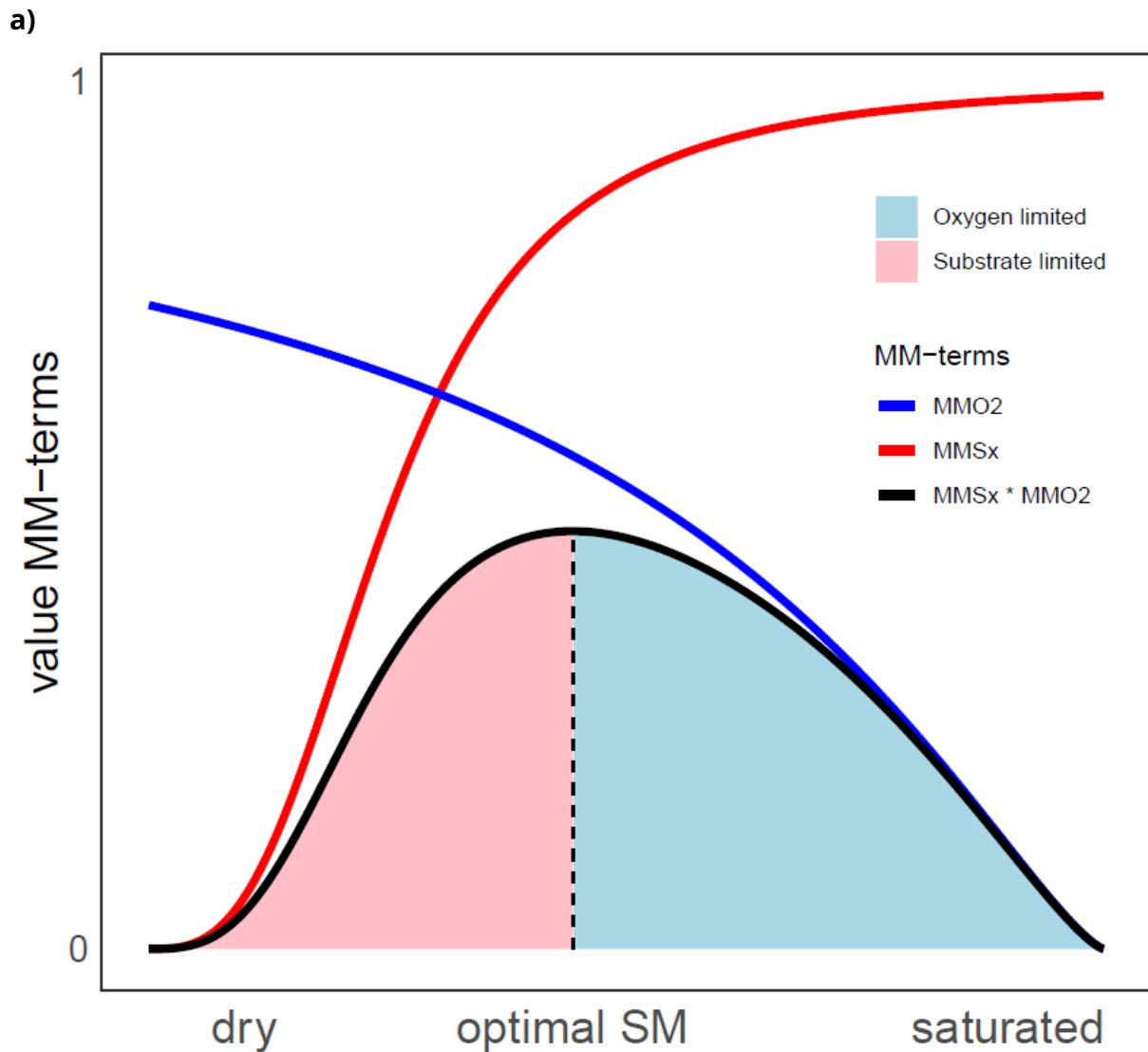


**Figure S1a.** Conceptual visualizations of the DAMM model. **a)** Change in Michaelis-Menten (MM) terms in response to soil moisture (SM). In a dry soil, substrate availability (MMSx , red line) increases with increases in soil moisture. As the soil gets wetter and more saturated, oxygen availability (MMO2, blue line) declines. The combined SM effect (MMSx \* MMO2 , black line) is a gradual, non-symmetrical change from a substrate limited domain (pink shade) into an oxygen-limited domain (light blue shade) as a soil becomes wetter. At optimal SM (dotted line), the SM-effect is at its maximum rate.

b)

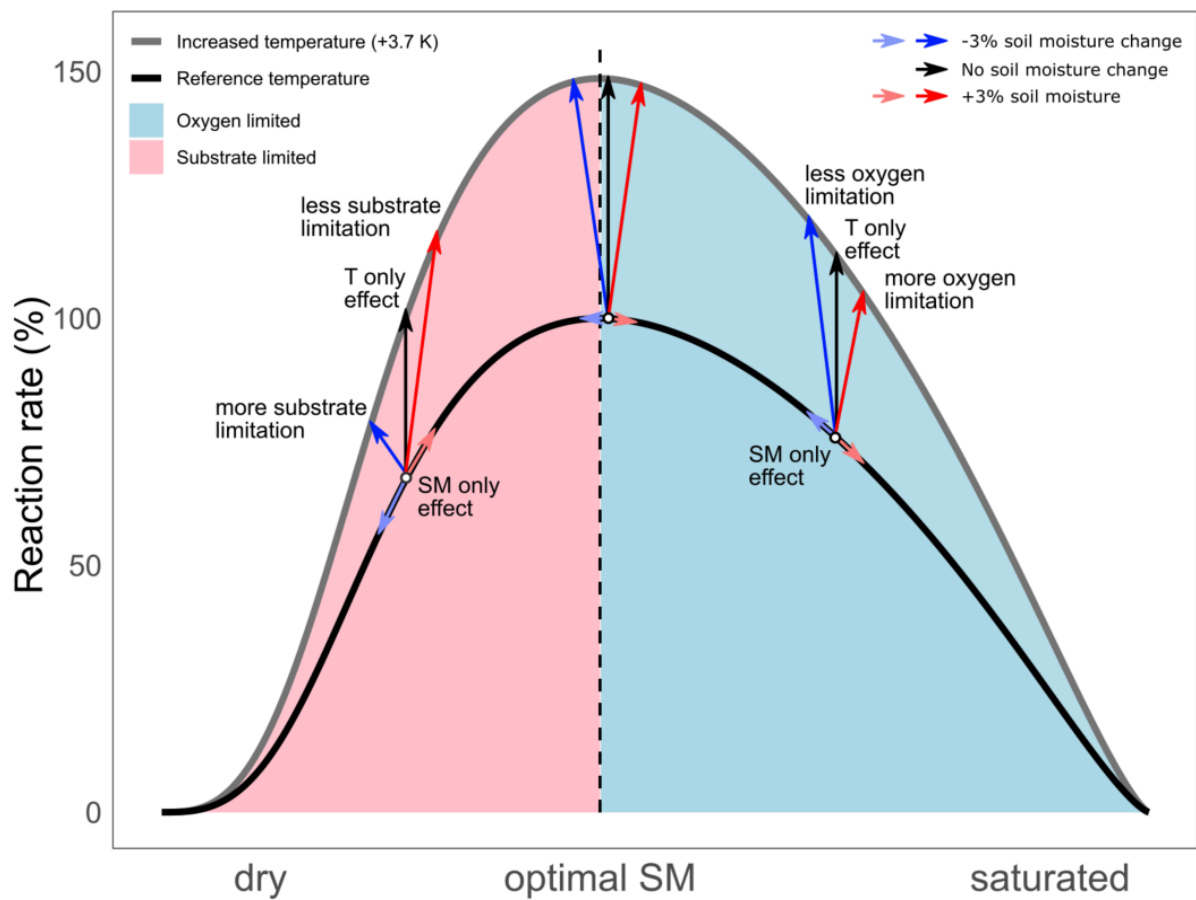


**Figure S1b.** Conceptual visualizations of the DAMM model. **b)** Change in reaction rate (%) in response to SM changes at reference temperature (Table S1:  $T_{ref} = 283.15$  °K, black line) and increased temperature (+3.7 °K, grey line). Arrows indicate the change in reaction rate when soil moisture does not change (T only, black arrows), decreases by 3% (blue arrows), or increases by 3% (red arrows). The light blue and red arrows indicate the SM only change (no temperature change) to a 3% decrease/increase in SM, respectively. Around optimal SM (dotted line), temperature changes dominate the change in the reaction rate.

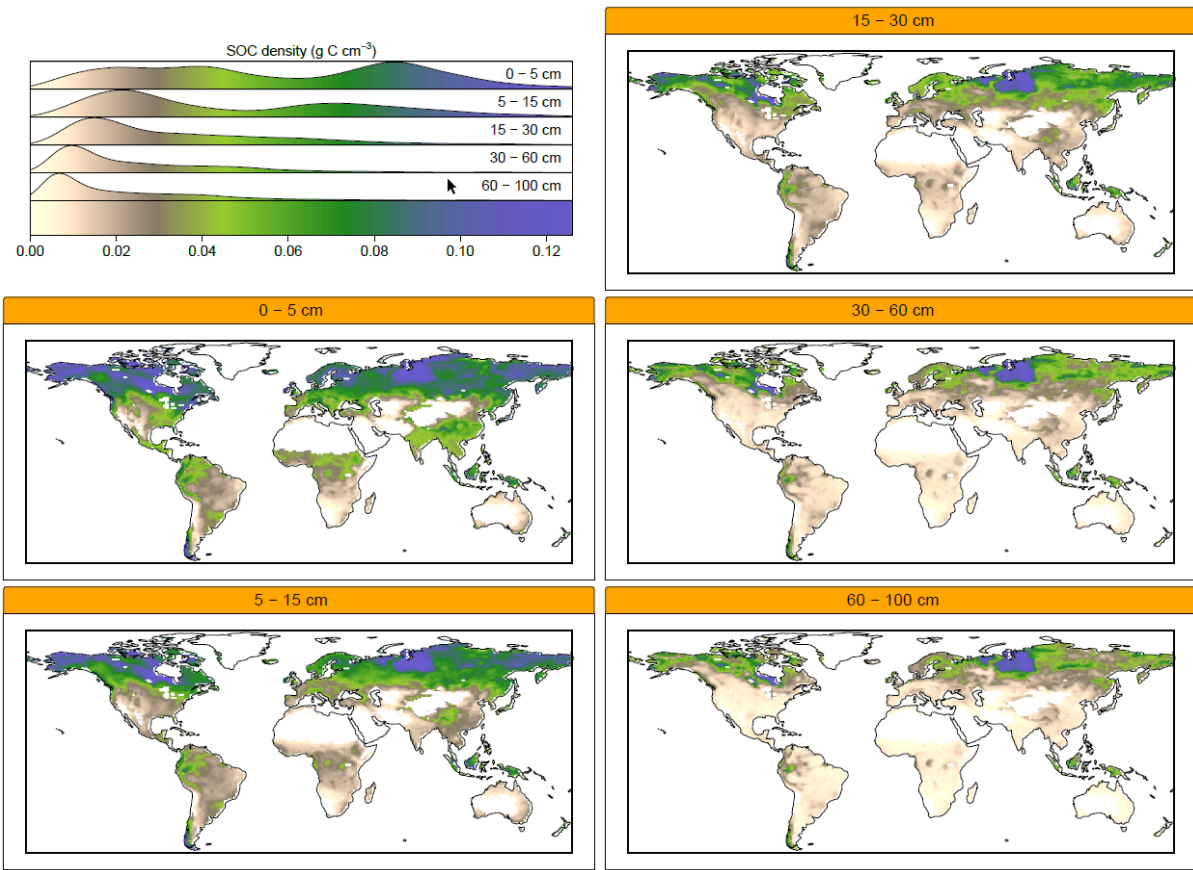


**Figure S2.** Soil organic carbon (SOC) content ( $S_{x,\text{tot}}$ , Eq. 4) in  $\text{g C cm}^{-3}$  from SoilGrids. Five depths until 1m are shown, at the spatial resolution of CMIP5 model CESM1-BGC.



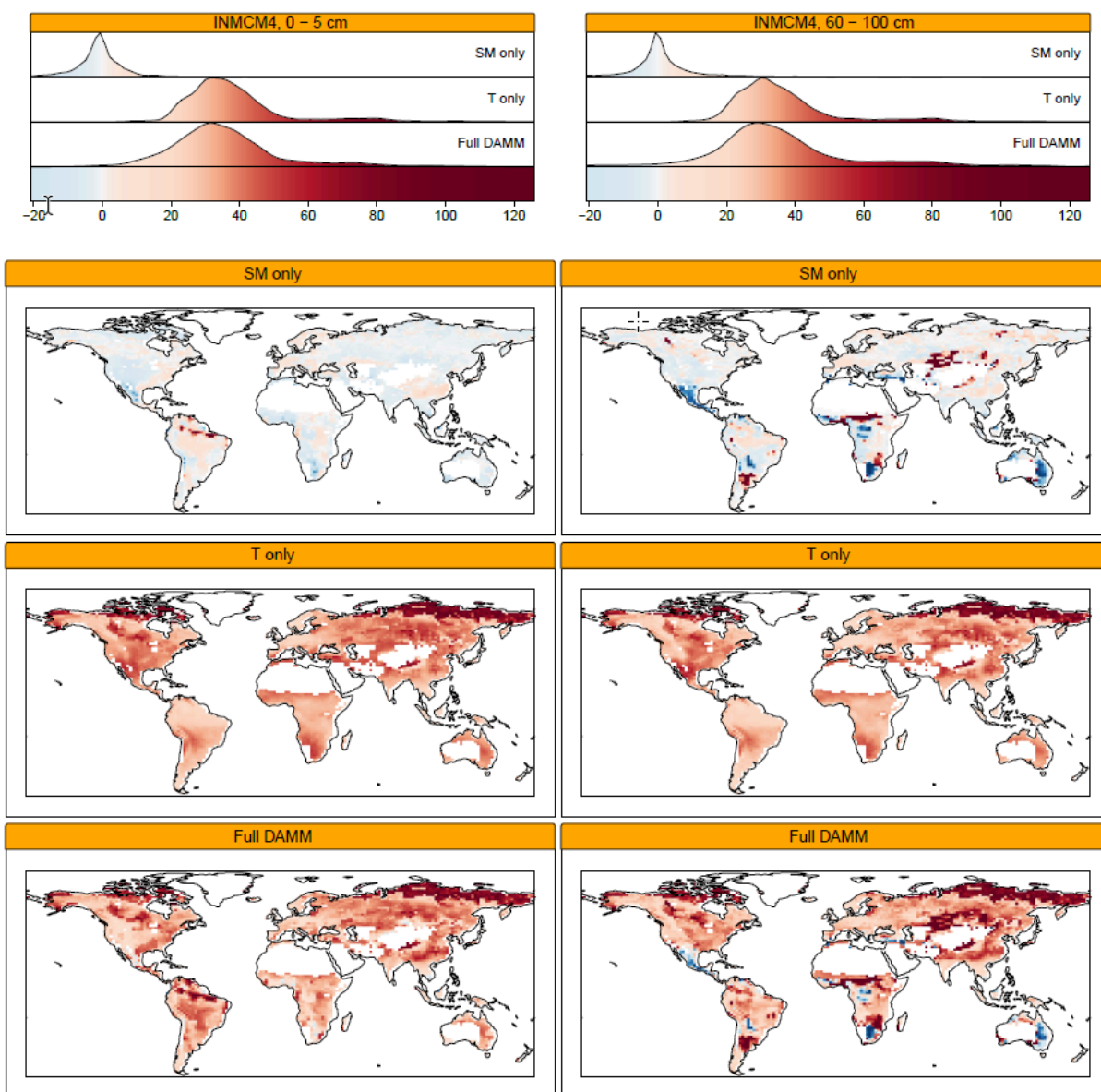


**Figure S3a.** Changes in modelled decomposition rates in top- and bottom soil layers for CMIP5 model INM-CM4, due to soil moisture changes (SM only); due to temperature changes (T-only); due to soil moisture and temperature changes (Full DAMM). Breaks and colors same as Fig. 1.

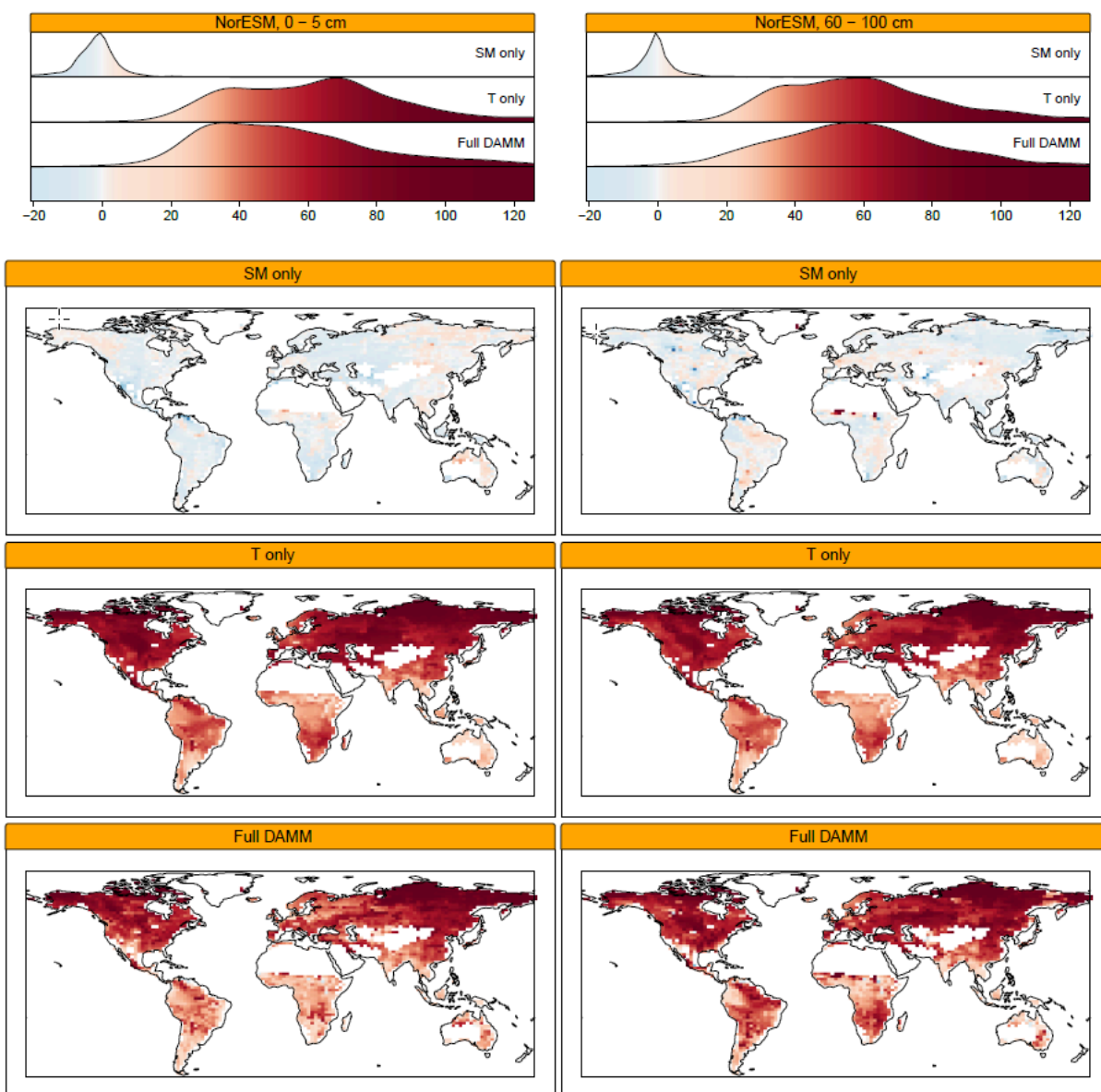


**Figure S3b.** Changes in modelled decomposition rates in top- and bottom soil layers for CMIP5 model NorESM-1M, due to soil moisture changes (SM only); due to temperature changes (T-only); due to soil moisture and temperature changes (Full DAMM). Breaks and colors same as Fig. 1.

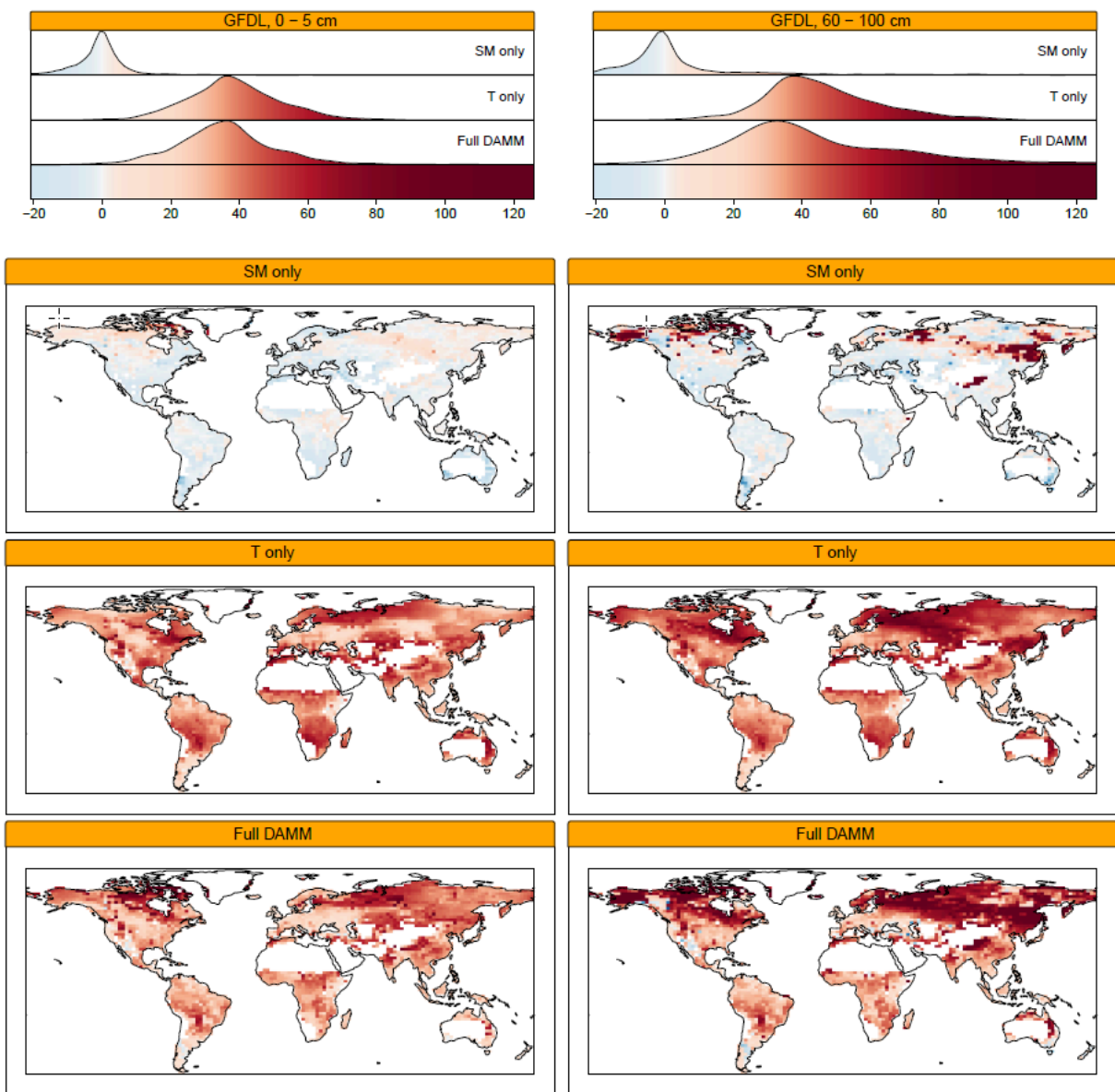


**Figure S3c.** Changes in modelled decomposition rates in top- and bottom soil layers for CMIP5 model GFDL-ESM2M, due to soil moisture changes (SM only); due to temperature changes (T-only); due to soil moisture and temperature changes (Full DAMM). Breaks and colors same as Fig. 1.

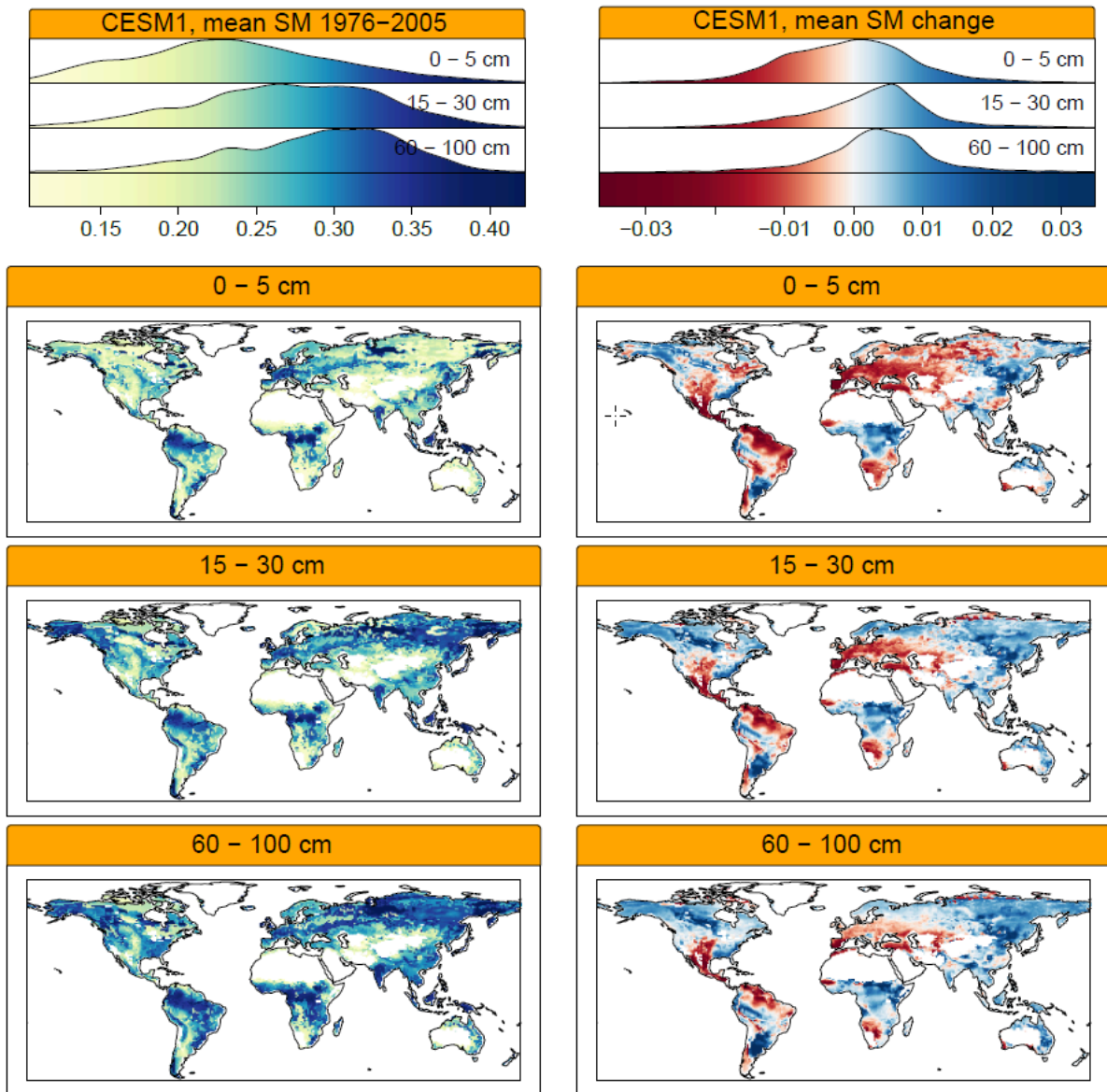


**Figure S4a.** Mean soil moisture ( $\overline{SM}$ ) for historic period (1976–2005) and mean soil moisture differences ( $\overline{\Delta SM}$ ) between historic and RCP8.5 (2070–2099) simulation period, for CESM1-BGC.

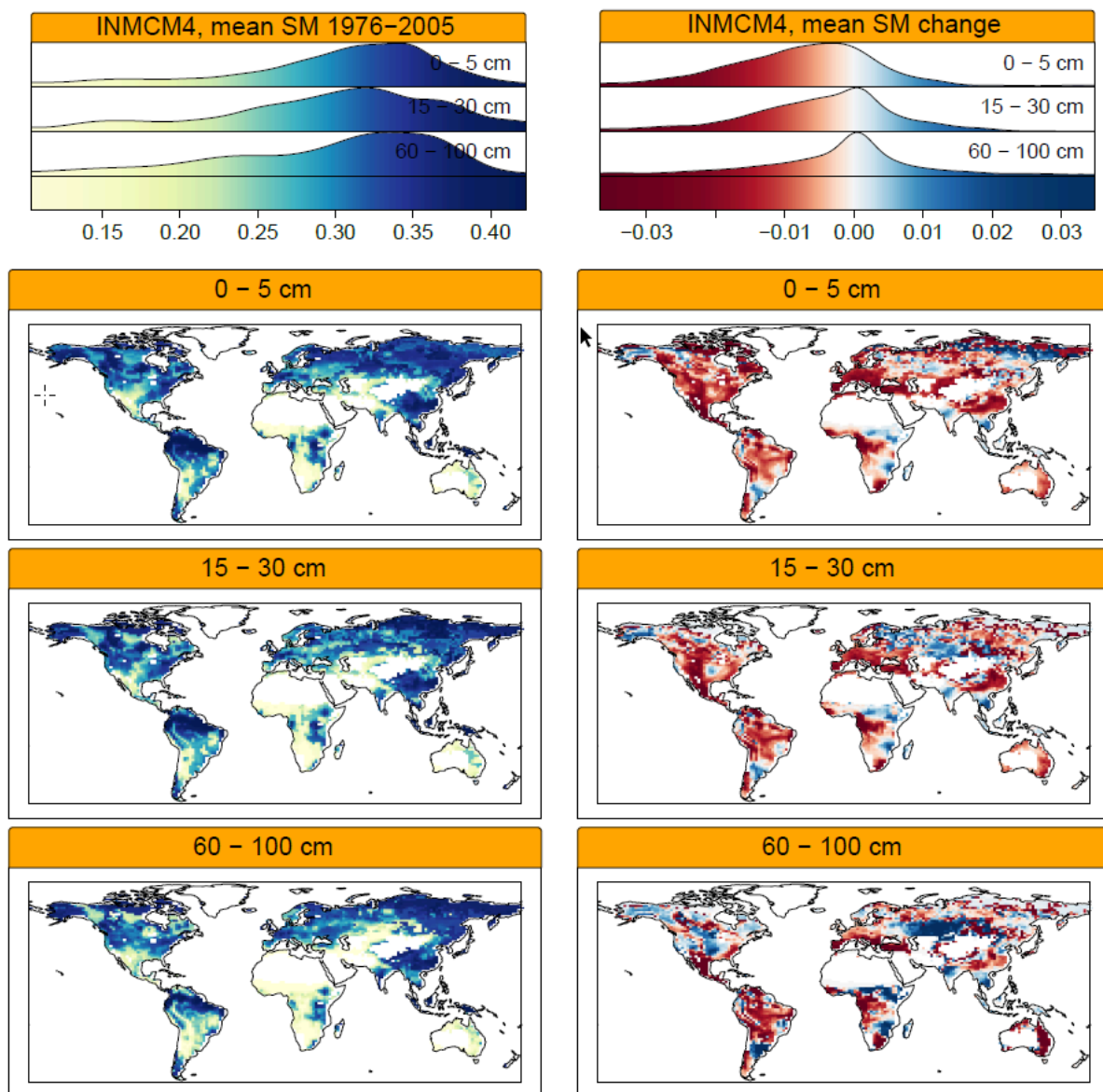


**Figure S4b.** Mean soil moisture ( $\overline{SM}$ ) for historic period (1976–2005) and mean soil moisture differences ( $\overline{\Delta SM}$ ) between historic and RCP8.5 (2070–2099) simulation period, for INM-CM4.

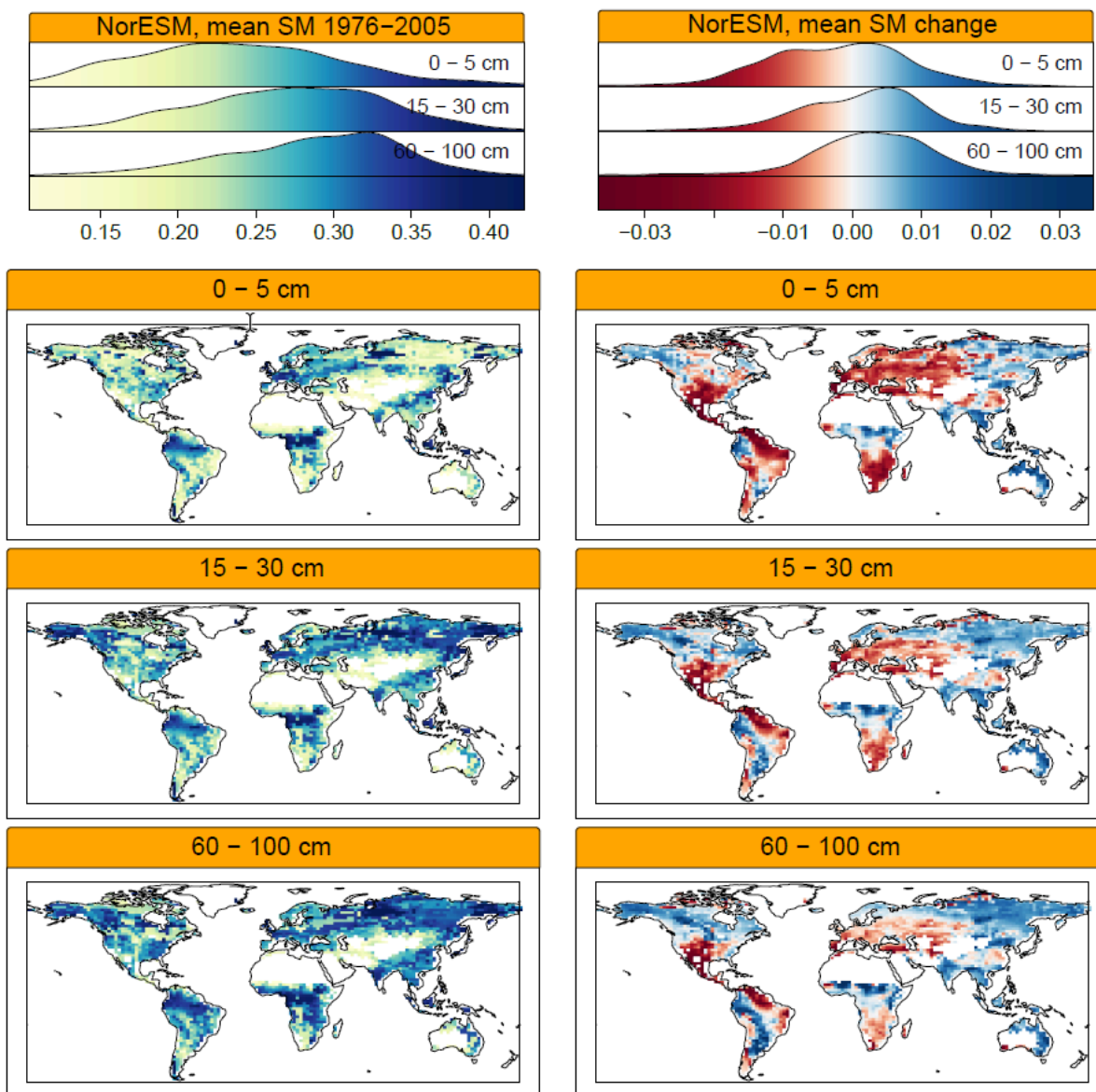


**Figure S4c.** Mean soil moisture ( $\overline{SM}$ ) for historic period (1976–2005) and mean soil moisture differences ( $\overline{\Delta SM}$ ) between historic and RCP8.5 (2070–2099) simulation period, for NorESM-1M.

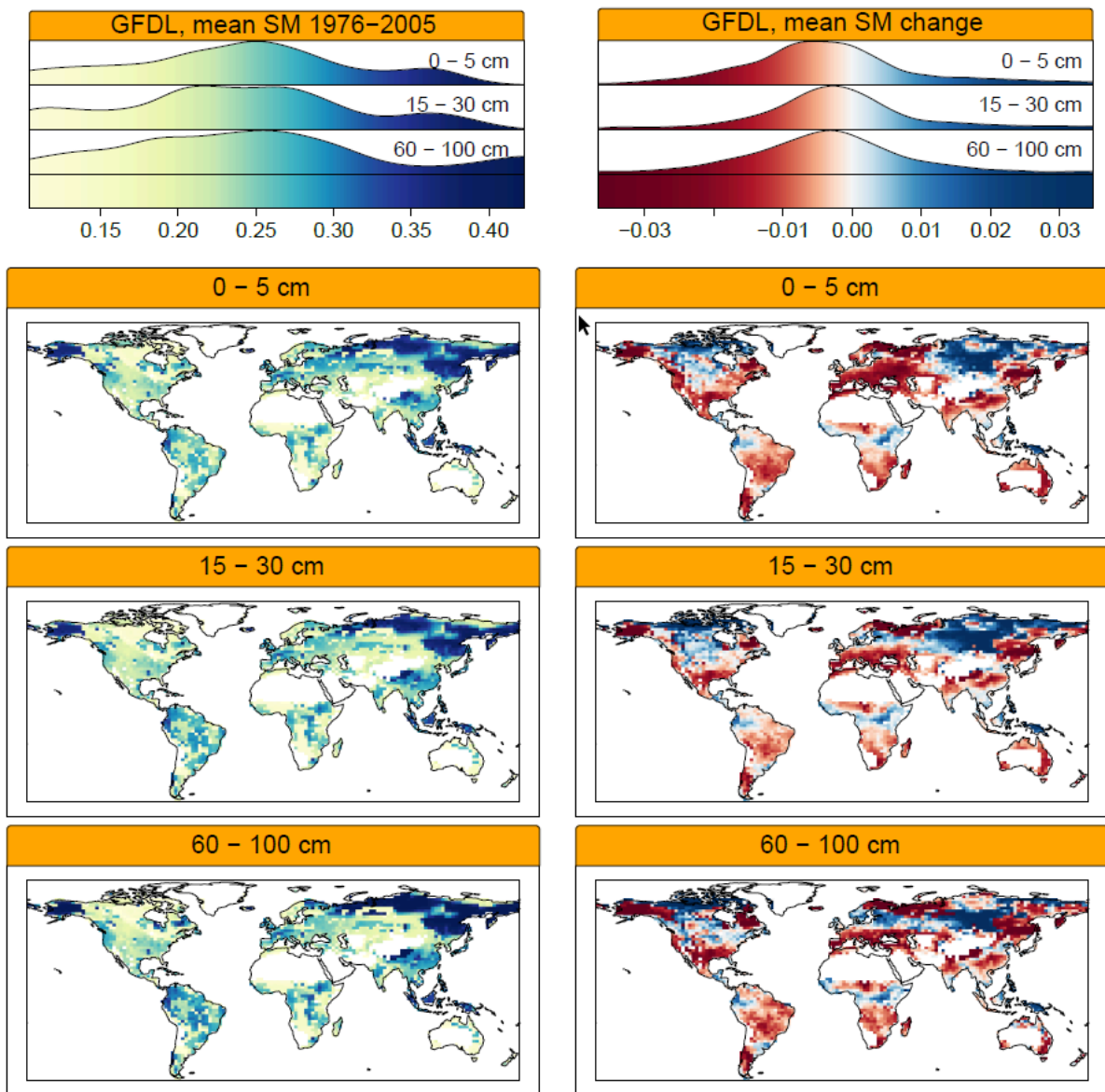


**Figure S4d.** Mean soil moisture ( $\overline{SM}$ ) for historic period (1976–2005) and mean soil moisture differences ( $\overline{\Delta SM}$ ) between historic and RCP8.5 (2070–2099) simulation period, for GFDL-ESM2M.

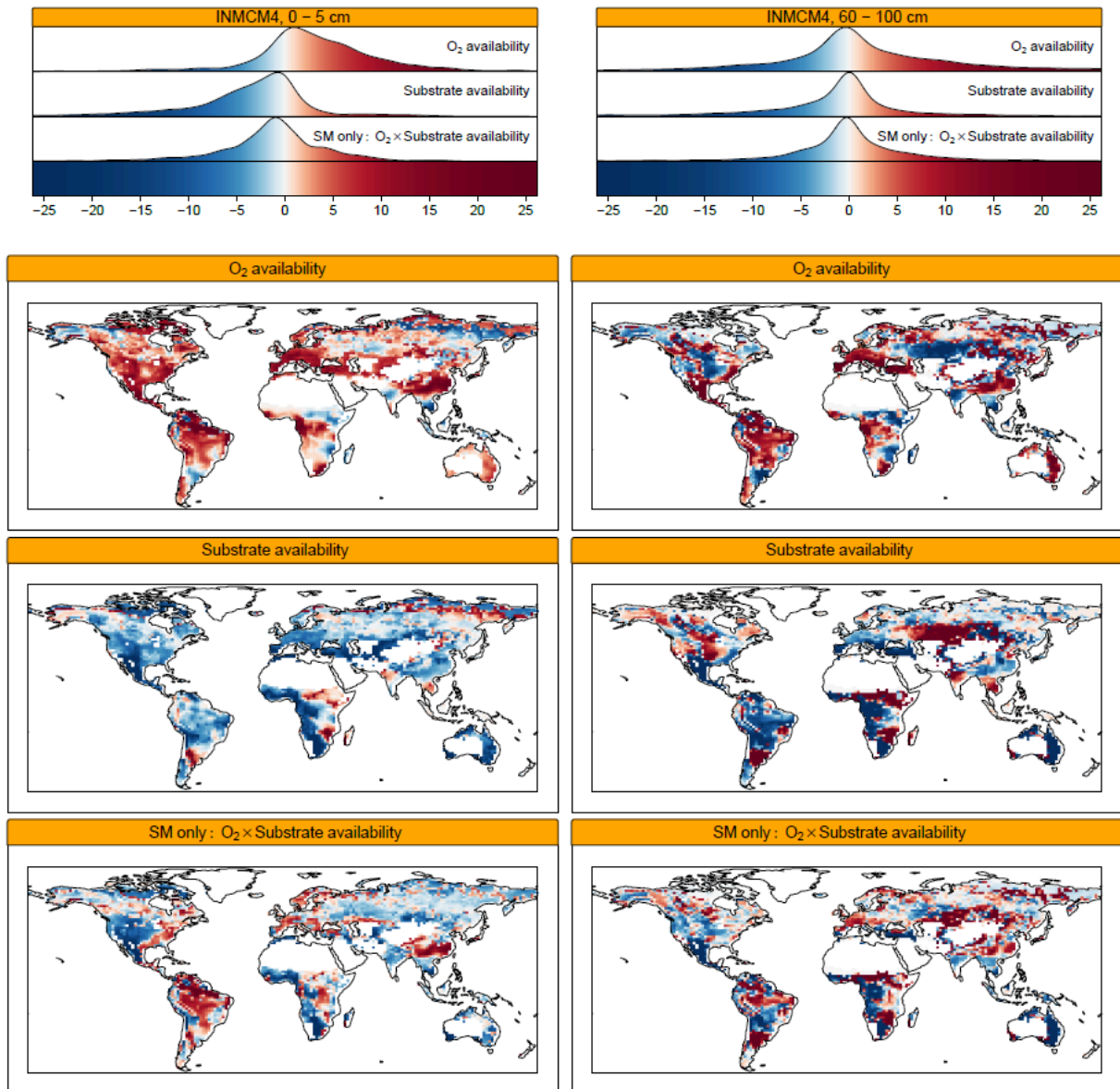


**Figure S5a.** Changes in modelled decomposition rates in top- and bottom soil layers for INM-CM4, due to changes in oxygen availability (top panel); due to changes in substrate availability (middle panel); and the combined soil moisture effect (SM only:  $O_2 \times$  Substrate availability, bottom panel). Breaks and colors same as Fig. 2.



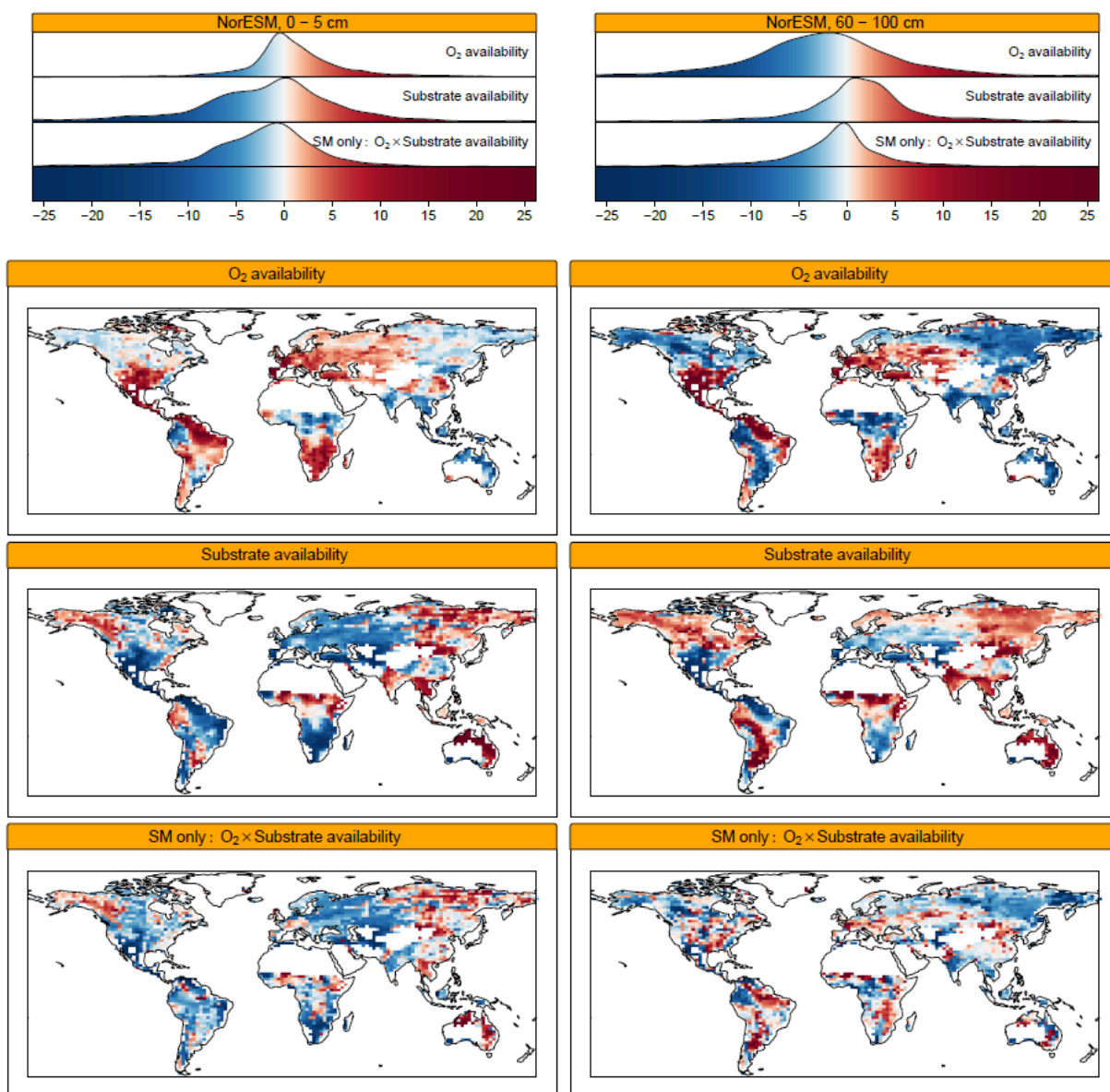


**Figure S5b.** Changes in modelled decomposition rates in top- and bottom soil layers for NorESM-1M, due to changes in oxygen availability (top panel); due to changes in substrate availability (middle panel); and the combined soil moisture effect (SM only: O<sub>2</sub> × Substrate availability, bottom panel). Breaks and colors same as Fig. 2.

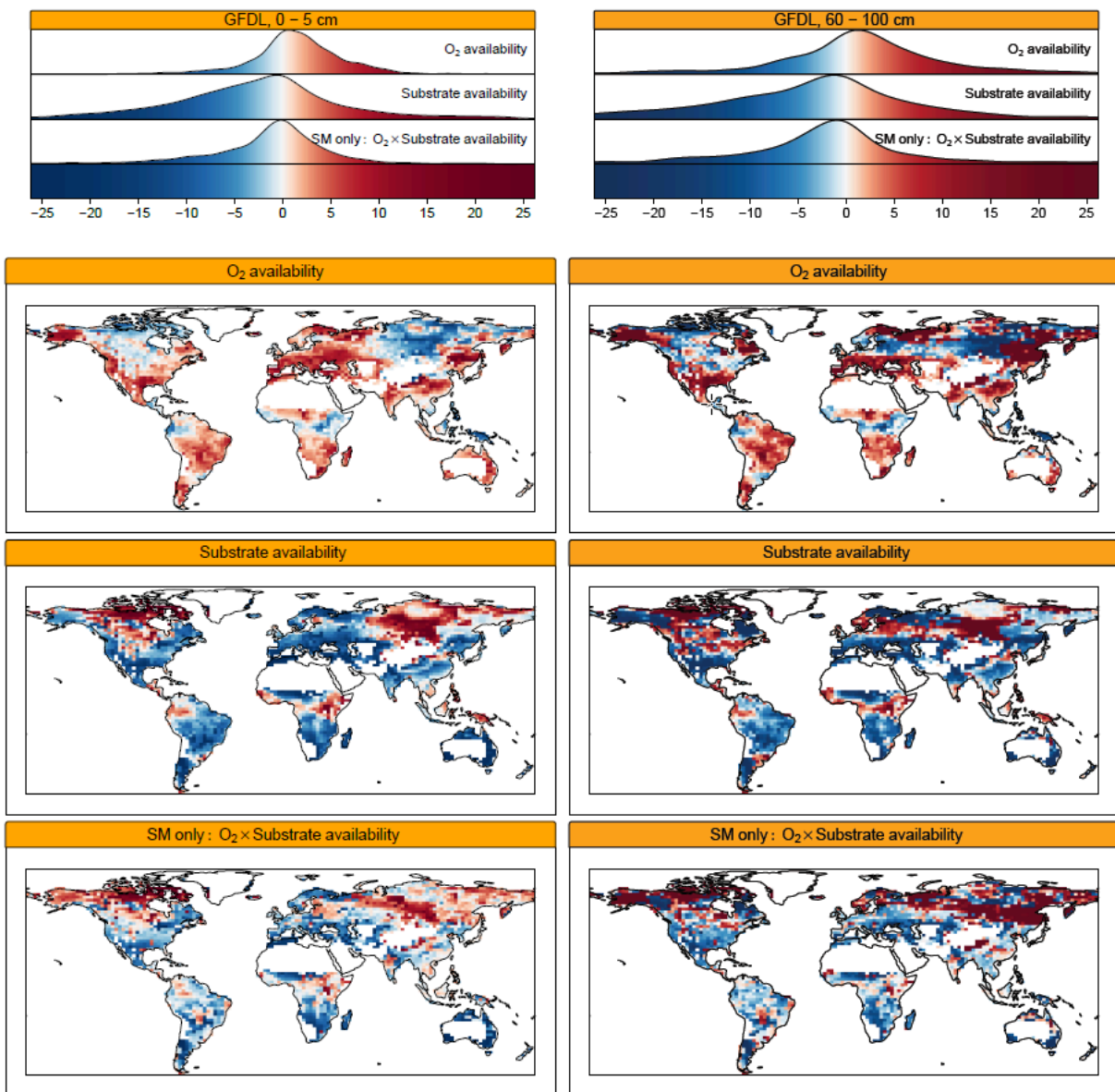


**Figure S5c.** Changes in modelled decomposition rates in top- and bottom soil layers for GFDL-ESM2M, due to changes in oxygen availability (top panel); due to changes in substrate availability (middle panel); and the combined soil moisture effect (SM only:  $O_2 \times$  Substrate availability, bottom panel). Breaks and colors same as Fig. 2.

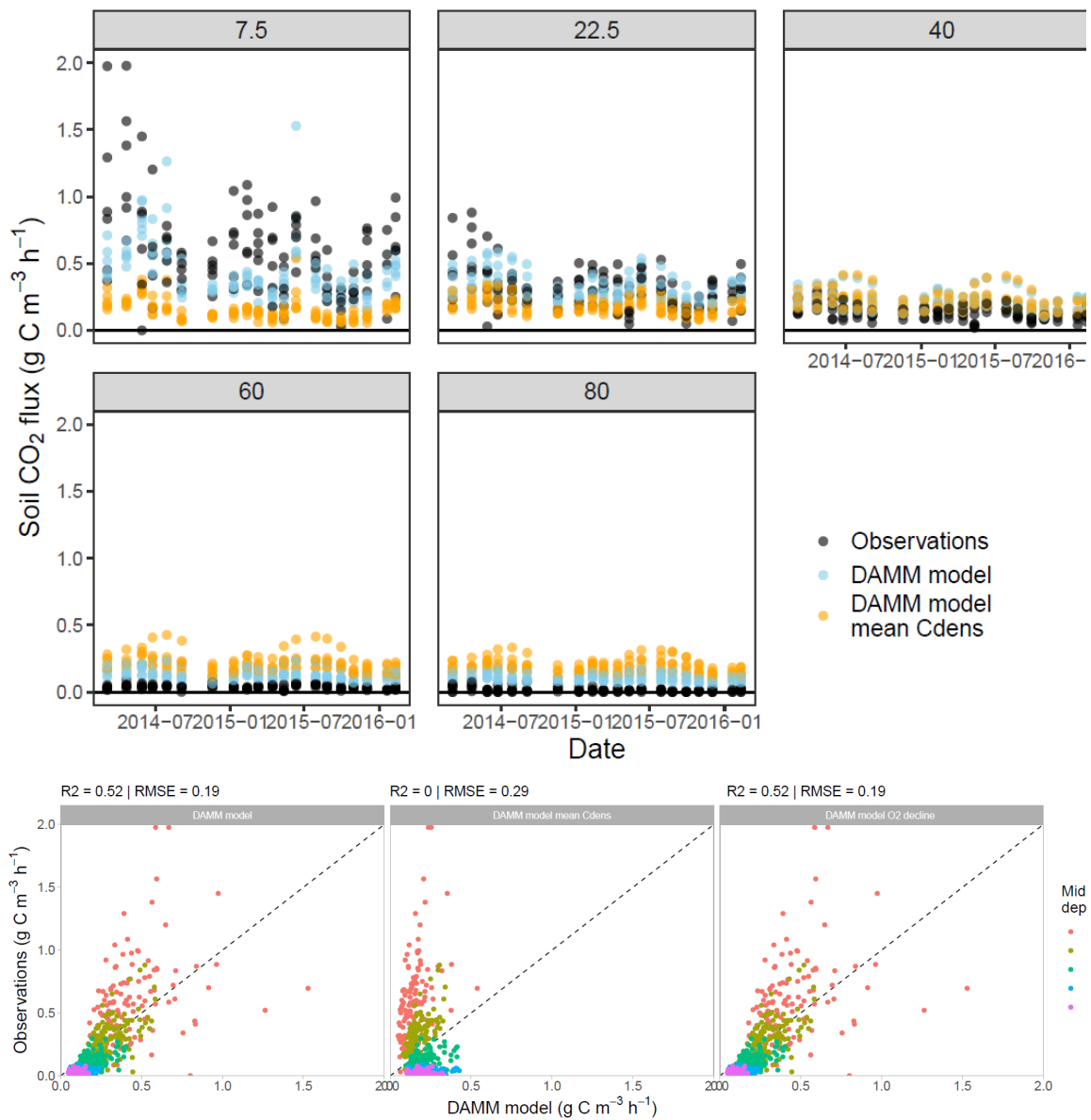


**Figure S6.** Comparison of different DAMM model runs to observations at different soil midpoint depths (cm). The top panel shows a time series with the observations (black points), the DAMM model run using measured C densities for each soil layer (DAMM model, blue points) and the DAMM model run using a constant C density for each soil layer (DAMM model mean Cdens, orange points). For figure clarity, the DAMM model run with declining oxygen (DAMM model O<sub>2</sub> decline) is not shown in the upper panel as the data points overlay with the standard model run. The bottom panel shows the goodness of fit between observations and all three DAMM model runs: DAMM model (using measured C densities per soil layer), DAMM model mean Cdens (using a constant mean C density per soil layer), and DAMM model O<sub>2</sub> decline (using a linearly declining O<sub>2</sub> gradient per soil layer). Points are colored by soil midpoint depth.

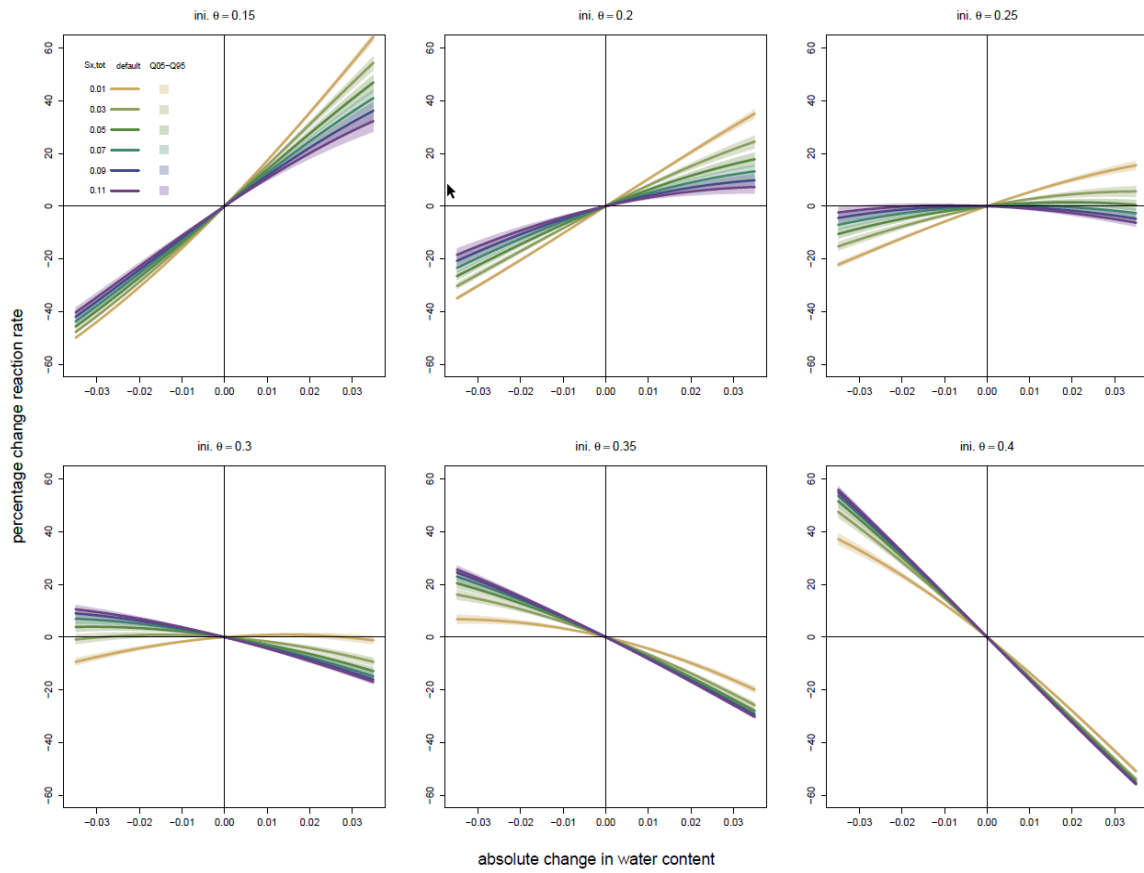


**Figure S7.** Sensitivity of DAMM model "SM only" to different total substrate concentrations ( $S_{x,total}$ ) and an absolute change in water content between the historic and RCP8.5 simulation period. Similar to Fig. 3, divergence in the reaction rate due to the initial soil moisture conditions is visible as initial soil moisture content (init.  $\theta$ ) increases from 0.15 to 0.4 in each sub panel. Shading represents the sensitivity range (Q05 – Q95: 5<sup>th</sup> – 95<sup>th</sup> percentile) to  $\pm 20\%$  changes in the DAMM parameters used in this study ( $\alpha_{Sx}$ ,  $Ea_{Sx}$ ,  $kM_{Sx}$  and  $kM_{O2}$ , Table S1). CMIP5 models' historic mean soil moisture ranges from 0.24 – 0.29 (Table S2).

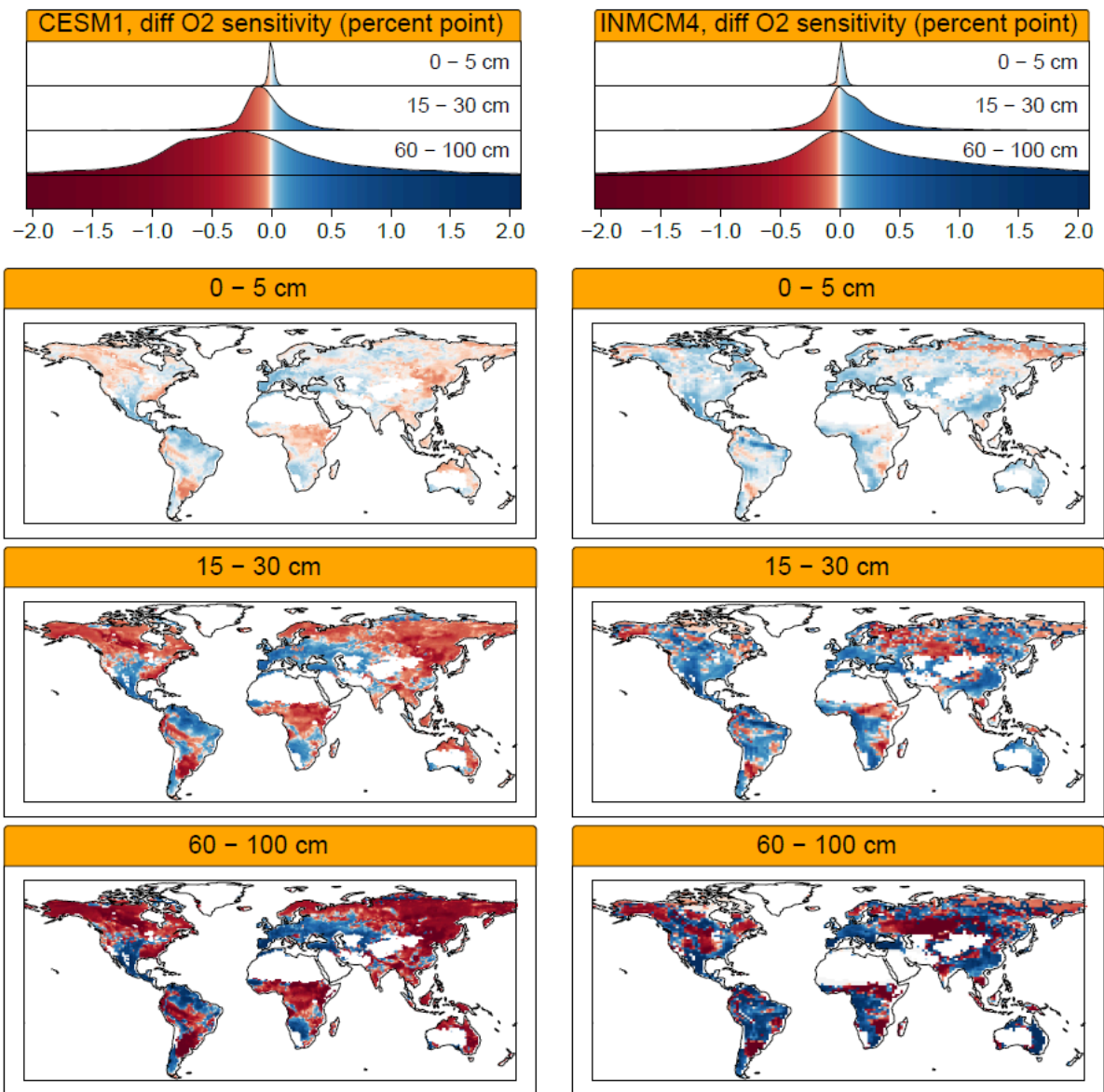


**Figure S8a.** Comparison of 'SM only' results between a model run with constant  $O_{2,airfrac}$  (at 0.21) and a run with linear oxygen decline (0.21 – 0.04 between 0 – 100 cm depth). Values are in percent point for three different soil depths, for model CESM1-BGC (left panel) and INM-CM4 (right panel).

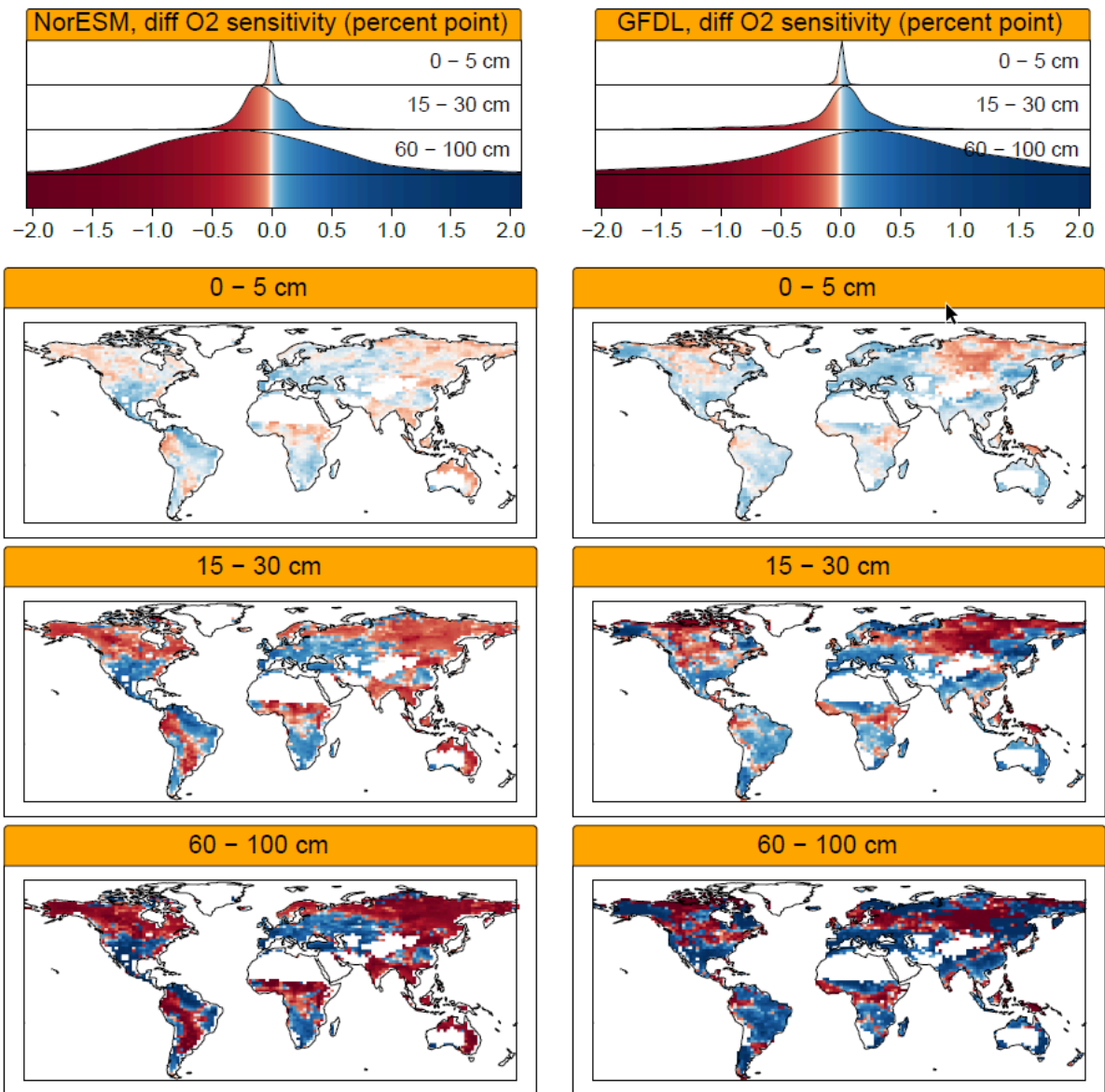


**Figure S8b.** Comparison of 'SM only' results between a model run with constant  $O_{2,airfrac}$  (at 0.21) and a run with linear oxygen decline (0.21 – 0.04 between 0 – 100 cm depth). Values are in percent point for three different soil depths, for model NorESM-1M (left panel) and GFDL-ESM2M (right panel).

Parameter/Constant	Description	Value	Units
$\alpha_{S_x}$	Base rate (pre-exponential factor)	5.38 E <sup>10</sup>	mg C cm <sup>-3</sup> soil h <sup>-1</sup>
$Ea_{S_x}$	Activation energy for substrate	72.76	kJ mol <sup>-1</sup>
$R$	Universal gas constant	8.314	kJ K <sup>-1</sup> mol <sup>-1</sup>
$T_{ref}$	Reference temperature	283.15	K
$kM_{S_x}$	Michaelis constant for C substrate	9.95 E <sup>-7</sup>	g C cm <sup>-3</sup> soil
$p_{S_x}$	Fraction of C substrate which is soluble	4.14 E <sup>-4</sup>	
$D_{liq}$	Diffusion coefficient of C substrate in liquid phase	3.17	
$kM_{O_2}$	Michaelis constant for oxygen	0.121	cm <sup>-3</sup> O <sub>2</sub> cm <sup>-3</sup> air
$D_{gas}$	Diffusion coefficient for oxygen in air	1.67	
$O_{2,airfrac}$	Fraction of oxygen in air	0.209	L O <sub>2</sub> L <sup>-1</sup> air

**Table S1.** Parameter values and constants used in this study. Values are identical to Davidson et al. (2012) except for  $T_{ref}$ , following Wang et al. (2012).

<b>Model name</b>	<b>Model Centre or Model Groups</b>	<b>Number of soil layers</b>	<b>Spatial resolution</b>	$\overline{ST}$	$\Delta\overline{ST}$	$\overline{SM}$	$\Delta\overline{SM}$
<b>CESM1-BGC</b>	Community Earth System Model Contributors	7	192 x 228	284.6 ± 10.7	3.7 ± 1.0	0.27 ± 0.08	0.0017 ± 0.01
<b>INM-CM4</b>	Institute for Numerical Mathematics	13	120 x 180	280.8 ± 10.4	2.8 ± 1.1	0.29 ± 0.08	-0.006 ± 0.01
<b>NorESM-1M</b>	Norwegian Climate Centre	7	96 x 144	283.3 ± 11.3	4.2 ± 1.6	0.27 ± 0.07	0.0005 ± 0.01
<b>GFDL-ESM2M</b>	NOAA Geophysical Fluid Dynamics Laboratory	10	90 x 144	282.0 ± 13.3	3.7 ± 1.2	0.24 ± 0.08	-0.002 ± 0.02

**Table S2.** CMIP5 models used in this study. Models were selected for their availability of layered soil moisture (mrlsl) and soil temperature (tsl) data, and their vertical resolution in the first meter ( $\geq 5$  soil layers).  $\overline{ST}$  and  $\overline{SM}$  are the global mean soil temperature and soil moisture values predicted for the historical simulation period (1976 – 2005).  $\Delta\overline{ST}$  and  $\Delta\overline{SM}$  are the predicted mean soil temperature and soil moisture changes between the RCP8.5 (2070 – 2099) and historical simulation period.



## References

- Davidson, E. A., Sudeep, S., Samantha, S. C., & Savage, K. (2012). The Dual Arrhenius and Michaelis–Menten kinetics model for decomposition of soil organic matter at hourly to seasonal time scales. *Global Change Biology*, 18(1), 371–384. <https://doi.org/doi:10.1111/j.1365-2486.2011.02546.x>
- Gomez, A., Powers, R. F., Singer, M. J., & Horwath, W. R. (2002). Soil Compaction Effects on Growth of Young Ponderosa Pine Following Litter Removal in California’s Sierra Nevada. *Soil Science Society of America Journal*, 66(4), 1334–1343. <https://doi.org/10.2136/sssaj2002.1334>
- Hicks Pries, C. E., Castanha, C., Porras, R., & Torn, M. S. (2017). The whole-soil carbon flux in response to warming. *Science*, eaal1319. <https://doi.org/10.1126/science.aal1319>
- Hu, S.-C., & Linnartz, N. E. (1972). Variations in oxygen content of forest soils under mature loblolly pine stands (LSU Agricultural Experiment Station Reports). Louisiana State University: LSU AgCenter.
- Maier, M., Schack-Kirchner, H., Hildebrand, E. E., & Holst, J. (2010). Pore-space CO<sub>2</sub> dynamics in a deep, well-aerated soil. *European Journal of Soil Science*, 61(6), 877–887. <https://doi.org/10.1111/j.1365-2389.2010.01287.x>
- RStudio Team. (2018). Rstudio: Integrated development environment for R. Retrieved from <http://www.rstudio.com/>
- Runkles, J. R. (1956). Diffusion, sorption and depth distribution of oxygen in soils. Iowa State College, Digital Repository @ Iowa State University, <http://lib.dr.iastate.edu/>.
- Silver, W. L., Lugo, A. E., & Keller, M. (1999). Soil oxygen availability and biogeochemistry along rainfall and topographic gradients in upland wet tropical forest soils. *Biogeochemistry*, 44(3), 301–328. <https://doi.org/10.1007/BF00996995>
- Wang, G., Post, W. M., Mayes, M. A., Frerichs, J. T., & Sindhu, J. (2012). Parameter estimation for models of ligninolytic and cellulolytic enzyme kinetics. *Soil Biology and Biochemistry*, 48, 28–38. <https://doi.org/10.1016/j.soilbio.2012.01.011>

## Study III

---

# Drought counteracts soil warming more strongly in the subsoil than in the topsoil according to a vertical microbial SOC model

This study is under review with the journal Biogeosciences and available as a preprint:

**Pallandt, M., Schrumpf, M., Lange, H., Reichstein, M., Yu, L. and Ahrens, B.** Drought counteracts soil warming more strongly in the subsoil than in the topsoil according to a vertical microbial SOC model, EGUsphere [preprint], <https://doi.org/10.5194/egusphere-2024-186>, 2024.

This is an open access preprint article, reprinted with permission under the terms of the Creative Commons Attribution License: <http://creativecommons.org/licenses/by/4.0/>



## Drought counteracts soil warming more strongly in the subsoil than in the topsoil according to a vertical microbial SOC model

Marleen Pallandt<sup>1,2</sup>, Marion Schrumpf<sup>1</sup>, Holger Lange<sup>3</sup>, Markus Reichstein<sup>1</sup>, Lin Yu<sup>4</sup> and Bernhard Ahrens<sup>1</sup>

- 5 1. Max Planck Institute for Biogeochemistry, Jena, Germany  
2. International Max Planck Research School (IMPRS) for Global Biogeochemical Cycles, Jena, Germany  
3. Norwegian Institute of Bioeconomy Research, Ås, Norway  
4. Department of Earth System Sciences, Hamburg University, Hamburg

*Correspondence to:* Marleen Pallandt (marleen.pallandt@natgeo.su.se)

- 10 **Abstract.** Soil organic carbon (SOC) is the largest terrestrial carbon pool, but it is still uncertain how it will respond to climate change. Especially the fate of SOC due to concurrent changes in soil temperature and moisture is uncertain. It is generally accepted that microbially driven SOC decomposition will increase with warming, provided that sufficient soil moisture, and hence enough C substrate, is available for microbial decomposition. We use a mechanistic, microbially explicit SOC decomposition model, the Jena Soil Model (JSM), and focus on the depolymerisation of litter and microbial residues by  
15 microbes at different soil depths, and its sensitivities to soil warming and different drought intensities. In a series of model experiments we test the effects of soil warming and droughts on SOC stocks, in combination with different temperature sensitivities ( $Q_{10}$  values) for the half-saturation constant  $K_m$  ( $Q_{10,Km}$ ) associated with the breakdown of litter or microbial residues. Microbial depolymerisation rates of litter and residues are proportional to microbial biomass (reverse kinetics), so that at low microbial biomass, the temperature sensitivity of  $K_m$  plays a more prominent role. We find that soil warming leads  
20 to long-term SOC losses, but depending on SOC composition and its associated  $Q_{10,Km}$  values, these losses can be either reduced or further accelerated, especially in the subsoil where microbial biomass is low. Droughts can alleviate the effects of soil warming and reduce SOC losses, and even lead to SOC gains, provided unchanged litter inputs. Furthermore, a combination of drought and different  $Q_{10,Km}$  values associated with the breakdown of litter or microbial residues can have counteracting effects on the overall decomposition rates. In this study, we show that while absolute SOC changes driven by  
25 soil warming and drought are highest in the topsoil, SOC in the subsoil is more sensitive to the (sometimes counteracting) interplay between  $K_m$ , temperature and soil moisture changes, and mineral-associated SOC.

### 1 Introduction

- Soils are an important component of the global carbon (C) cycle as they store large quantities of C. Soils can act as C sources or sinks, depending on the balance between C inputs and outputs over time. Apart from plant litter inputs, microbial residues  
30 are recognised as important precursors for the formation of stable, mineral-associated soil organic carbon (Cotrufo et al., 2013; Liang et al., 2017; Xiao et al., 2023). Therefore, to determine whether soils are a net C source or sink, the speed at which soil organisms decompose litter inputs and existing soil organic carbon (SOC) stocks including microbial residues is of particular importance (Kallenbach et al., 2016). Soil temperature and soil moisture are the two most important controlling factors of  
35 microbial decomposition rates, and thereby the carbon turnover rate of soils (Davidson and Janssens, 2006; Moyano et al., 2013; Yan et al., 2018). The interaction between microbial SOC decomposition and (de)stabilisation of SOC to mineral surfaces is another important factor determining the fate of SOC stocks (Ahrens et al., 2020; Dwivedi et al., 2017; Sokol et al., 2022). As SOC decomposition and its future variations depend on soil properties as well as climate, understanding and



representing the complex feedbacks between climate change and SOC decomposition in models is extremely important for future climate projections.

40 Microbes process SOC by depolymerizing a wide array of C substrates such as plant litter and microbial residues that greatly differ in their chemistry (Buckeridge et al., 2022; Cotrufo and Lavelle, 2022). In models, the microbial depolymerisation rate can be described using reverse Michaelis-Menten (MM) kinetics (Tang and Riley, 2019), where a maximum depolymerisation rate ( $V_{max}$ ) is multiplied with a MM-term that describes the diffusion of extracellular enzymes to a C substrate. A simple formulation of the MM-term is depicted in conceptual Fig. 1 with the term  $C_B/(K_m + C_B)$ , where  $C_B$  is the microbial biomass and  $K_m$  is the half-saturation constant for the reaction. Both  $V_{max}$  and  $K_m$  are temperature sensitive, where  $V_{max}$  increases with higher temperatures. The temperature sensitivity of  $K_m$ , however, has been shown to be negative or positive depending on which enzymes are involved in the breakdown of C substrates: Allison et al. (2018b) reported  $Q_{10,V_{max}}$  values between 1.48 - 2.24, and  $Q_{10,K_m}$  values between 0.7 - 2.8., where a value below denotes a negative temperature sensitivity.  $Q_{10,K_m}$  can modify  $K_m$  by the relationship:

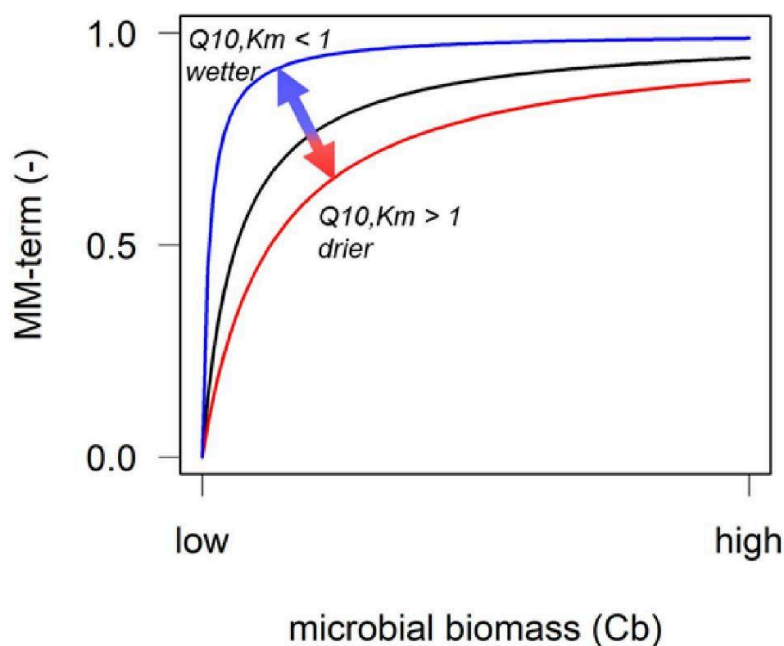
$$50 \quad K_m = K_{m,ref} \times Q_{10,K_m}^{(T - T_{ref})/10} \quad (1)$$

Where  $T$  and  $T_{ref}$  are the soil temperature and a reference temperature, respectively. The MM-term also depends on soil moisture, where lower soil moisture values result in stronger microbial limitation on enzymatic depolymerisation (Zhang et al., 2022).

$$K_m = K_{m,ref} \times \left(\frac{\theta}{\theta_{fc}}\right)^{-3} \quad (2)$$

55 Where  $\theta$  and  $\theta_{fc}$  are volumetric soil moisture and volumetric soil moisture at field capacity, respectively. Additionally, high soil moisture values result in lower oxygen availability - which can be described by a second MM-term (Skopp et al., 1990; Davidson et al., 2012). Global mean soil warming is expected to be  $4.5 \text{ °C} \pm 1.1 \text{ °C}$  by the end of this century (Soong et al., 2020), but for projected soil moisture changes there is much more uncertainty. While in mediterranean climates and desert ecosystems temperature and soil moisture may be inversely correlated (e.g. Garcia-Garcia et al., 2023; Zhang et al., 2020), projected global lateral and vertical distributions of future soil moisture are more diverse (Berg et al., 2017) and highly depend on anthropogenic greenhouse gas and aerosol emissions (Wang et al., 2022b).

The effect of soil moisture on substrate availability, and thus on the MM kinetics under a warming climate, depends on the value of  $Q_{10,K_m}$ . This interplay between different  $Q_{10,K_m}$  values and soil moisture has the potential to lead to counteracting effects on the overall decomposition rates, where the short-term responses on heterotrophic respiration have been shown in modelling studies (Davidson et al., 2006; Davidson and Janssens, 2006; Sierra et al., 2015). More specifically, at low microbial biomass and  $Q_{10,K_m}$  values  $> 1$ , an increase in  $K_m$  as a result of warming can 'compensate' or counteract the expected increase in SOC decomposition rates through  $Q_{10,V_{max}}$  (Davidson et al., 2006). These model studies, however, highly simplify the system as they do not consider a dynamic substrate pool, i.e. there is no interaction between the microbial pool (with its own growth and turnover rates) and the in- and outputs of different C substrate pools. To understand changes in SOC stocks on longer time scales, however, the microbial dynamics have to be included as well.



75 **Figure 1:** Conceptual depiction of the relationship between microbial biomass ( $C_B$ ) and the Michaelis-Menten (MM) term  $C_B/(K_m + C_B)$  to represent microbial limitation of depolymerisation. Soil moisture & temperature effects on half-saturation constant  $K_m$  can increase or decrease the MM-term through Eqs. 1 and 2. The black line shows the MM-term when  $Q_{10,Km} = 1$  and soil moisture is unchanged. The MM-term decreases when the soil gets drier or when  $Q_{10,Km} > 1$  (red line), and increases when the soil gets wetter or  $Q_{10,Km} < 1$  (blue line).

80 Besides the inclusion of microbial dynamics, it is important to consider soil moisture and temperature changes along a vertical gradient (Pallandt et al., 2022), because projected soil moisture may not change in the same direction for surface and deeper soil layers (Fig. 2 in Berg et al., 2017). As SOC, microbial biomass and mineral-associated SOC are also not distributed evenly within soil profiles, the interactions between soil moisture, microbes and substrates will vary with depth. This requires a model which includes vertically resolved, mechanistic descriptions of microbially driven decomposition and organo-mineral  
85 interactions so that C substrate depletion by microbes or sorption can be explicitly simulated. However, the vast majority of SOC decomposition models integrated in coupled climate models are highly empirical and have very simple process representation using first-order decomposition rates adopted from the CENTURY approach (Parton et al., 1987). Recent insights have led to the development of SOC decomposition models which take into account microbial (enzymatic) processes and sometimes organo-mineral interactions (e.g. Abramoff et al., 2017; Sulman et al., 2014; Wieder et al., 2014; Zhang et al.,  
90 2022). Another limitation of these models as well as the classic ones is that they generally only consider one soil depth (Wieder et al., 2015) and as a result, can fail to capture observed climate sensitivities of soil carbon turnover times (Ahrens et al., 2015; Braakhekke et al., 2011; Koven et al., 2013, 2017; Pallandt et al., 2022).



In this study, we bridge these gaps by applying the C cycle version of the Jena Soil Model (JSM, Yu et al., 2020) to investigate the interplay between microbial depolymerisation and climate change. JSM is a vertically resolved, mechanistic SOC decomposition model. It includes organo-mineral interactions, is microbially explicit, and uses mechanistic descriptions of the various physiological processes affecting microbial SOC decomposition affected by temperature and soil water content, such as substrate and oxygen availability. JSM's modular structure offers the opportunity to study the various soil temperature and soil moisture controls on SOC decomposition either individually or simultaneously. We focus on the following research questions: 1) How do temperature and soil moisture changes affect modelled SOC decomposition through  $V_{max}$  and the Michaelis-Menten term?; and 2) Do top- and subsoil layers respond differently to warming and drought? In a series of model experiments we test the effects of soil warming and droughts on SOC stocks, in combination with different  $Q_{10,Km}$  values which are associated with the depolymerisation of the polymeric litter pool or of microbial residues.

## 2 Methods

### 2.1 Model description

JSM is a vertically explicit soil organic matter (SOM) decomposition model with microbial interactions on SOM decomposition, and representation of organic matter (de)sorption to mineral surfaces. For this study, we represent and describe the C cycle, but JSM is also capable of simulating the coupled C,N and P cycles and isotope ( $^{13}\text{C}$ ,  $^{14}\text{C}$ ,  $^{15}\text{N}$ ) tracking. A full mathematical description of JSM and its coupled nutrient cycles can be found in the supplement material of Yu et al. (2020). Here, we summarise the most important C cycle processes relevant to this study, with a conceptual overview in Fig. 2 and parameters and units listed in Table 1.

Above- and belowground non-woody litter inputs are partitioned into soluble and polymeric litter following Parton et al. (1993). JSM does not explicitly simulate enzyme production, but these are implicitly described using Michaelis-Menten (MM) kinetics. For the depolymerisation steps reverse Michaelis-Menten kinetics are used, as Tang and Riley (2019) found these to be more appropriate than traditional, forward MM-kinetics. The depolymerisation of litter or microbial residues to the dissolved organic carbon (DOC) pool is described as:

$$f_{depoly,X} = V_{max,X} \times f_{V_{max,X}}(T_{soil}) \times C_X \times \frac{C_B}{K_{mX} \times f_{K_{mX}}(T_{soil}, \theta) + C_B} \quad (3)$$

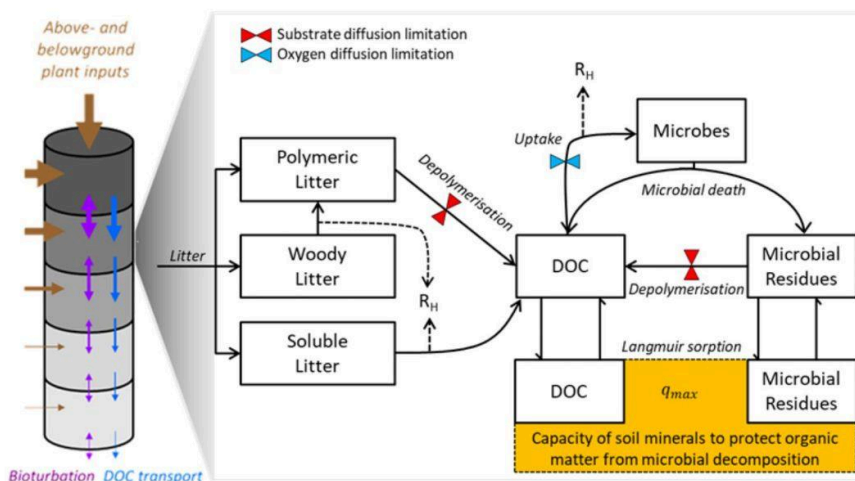
so that the depolymerisation rate is limited by the size of the microbial biomass pool ( $C_B$ ).  $X$  is either the polymeric litter pool ( $P$ ) or the microbial residues pool ( $R$ ),  $V_{max,X}$  is the maximum specific depolymerisation rate of  $X$ ,  $C_X$  is the respective litter pool  $X$ , and  $C_B$  is the microbial biomass pool.  $f_{V_{max,X}}(T_{soil})$  is an exponential function expressed with a  $Q_{10}$  base (Wang et al., 2012):

$$f_{V_{max,X}}(T_{soil}) = Q_{10,V_{max,X}} \frac{T_{soil} - T_{ref}}{10} \quad (4)$$

where  $Q_{10,V_{max,X}}$  is the temperature sensitivity of the maximum specific depolymerisation rate of litter pool  $X$ , and  $T_{soil}$  and  $T_{ref}$  are the soil temperature or reference temperature, respectively.

125

4



130 **Figure 2:** Schematic representation of the C cycle in JSM, after Yu et al. (2020), showing C pools (rectangles) and C fluxes (line arrows) between pools. DOC: Dissolved Organic Carbon,  $q_{max}$ : maximum sorption capacity for sorption of DOC and microbial residues to mineral surfaces. The dotted lines are heterotrophic respiration ( $R_H$ ) fluxes. The coloured hourglasses represent different soil moisture controls on SOC decomposition steps: microbial limitation of depolymerisation (red), and oxygen limitation (blue) on microbial uptake.

**Table 1:** Parameter values related to temperature sensitive processes in JSM.

Parameter	Value	Unit	Reference
$V_{max,P}$	0.1849	$yr^{-1}$	Yu et al. 2020
$V_{max,R}$	0.2317	$yr^{-1}$	Yu et al. 2020
$V_{max,U}$	95.76	$day^{-1}$	Yu et al. 2020
$K_{m,P}$ and $K_{m,R}$	3.70	$mmol\ C\ m^{-3}$	Yu et al. 2020
$K_{m,U}$	85.26	$mol\ C\ m^{-3}$	Yu et al. 2020
$Q_{10,Vmax,U}$	1.98		Allison et al. (2010)
$Q_{10,Vmax,P}$ and $Q_{10,Vmax,R}$	2.16		Wang et al. (2012)
$Q_{10,Km,P}$	1.31*		Allison et al. (2018b)
$Q_{10,Km,R}$	0.7*		Allison et al. (2018b)
$Q_{10,adsorption}$	1.08		Wang et al. (2013)
$Q_{10,desorption}$	1.34		Wang et al. (2013)
R	8.314	$J\ K^{-1}\ mol^{-1}$	
$T_{ref}$	293.15	K	Wang et al. (2012)

135

5



The  $Q_{10}$  coefficient is the ratio of reaction rates when temperature increases by 10 °C. For use within JSM, all  $Q_{10}$  values were converted to activation energies ( $E_a$ ) following Eq. (7) from Wang et al. (2012):

$$Q_{10} = \exp \left[ \frac{E_a}{R \times T_{ref}} \times \frac{10}{T_{soil}} \right] \quad (5)$$

where  $R$  is the universal gas constant, and  $T_{soil}$  and  $T_{ref}$  are the soil temperature and reference temperature, respectively.

140 Inclusion of soil moisture is done through Eq. (6):

$$f_{K_{m,X}}(T_{soil}, \theta) = Q_{10, K_{m,X}} \frac{T_{soil} - T_{ref}}{10} \times \left( \frac{\theta}{\theta_{fc}} \right)^{-3} \quad (6)$$

This is a function to describe the sensitivity of the half-saturation constant ( $K_{m,X}$ ) to soil moisture and temperature, where  $Q_{10, K_{m,X}}$  is the temperature sensitivity of the half-saturation constant of  $C_X$ , and where  $\theta$  and  $\theta_{fc}$  are the volumetric water content and water content at field capacity, respectively.

145 Microbial C uptake for growth is described using traditional, forward MM-kinetics (Tang and Riley, 2019):

$$f_{Uptake} = V_{max,U} \times f_{v_{max,X}}(T_{soil}) \times C_B \times \frac{C_{DOC}}{K_{m,U} + C_{DOC}} \times \frac{a^{4/3}}{K_{m,O_2} + a^{4/3}} \quad (7)$$

so that the uptake rate is limited by the size of the available substrate ( $C_{DOC}$ ) and by the air-filled pore space ( $a$ ), which is calculated as

$$a = \frac{\theta_{fc} - \theta}{\theta_{fc}} \quad (8)$$

150 and functions as a proxy to describe the amount of oxygen available for the reaction (Davidson et al., 2012).  $V_{max,U}$  is the maximum uptake rate of DOC by  $C_B$ ,  $C_{DOC}$  is the dissolved organic C pool,  $K_{m,U}$  is the half-saturation constant for the uptake of DOC by  $C_B$  and  $K_{m,O_2}$  is the half-saturation constant of the reaction with oxygen. DOC and microbial residues can be protected from microbial decomposition by sorption to mineral surfaces (Fig. 2). In JSM, adsorption and desorption rates are temperature sensitive ( $Q_{10}$  values reported in Table 1), with a full description of the process implementation in Ahrens et al.  
 155 (2020). \*  $Q_{10}$  values are reported for the model's reference temperature ( $T_{ref}$ ) of 20 °C, and their respective activation energies were calibrated for JSM in an earlier study (Yu et al., 2020), or taken from literature by Ahrens et al. (2020). Values marked with \* are unique to this study and taken from Allison et al. (2018b), and measured at a reference temperature of 16 °C. Activation energies for JSM were adjusted accordingly using Eq. (5).

## 2.2 Modelling protocol

160 The stand-alone application of JSM requires depth-specific soil temperature, soil moisture and litterfall forcing data at a half hourly time step as input. These were generated by running the QUINCY model for 500 years beforehand using meteorological forcing data from 1901 - 1930, and then starting a transient simulation in combination with FLUXNET3 forcing data from 1901 - 2012 as described in Thum et al. (2019), for a temperate forest site in Germany (DE-Hai). These site-specific soil forcing data are then used for model spinup for 500 years, where soil forcing data from 2000 - 2012 are used repeatedly. After  
 165 spinup, JSM is run for 100 simulation years for each model experiment (Section 2.4).





### 2.3 Choice of $Q_{10,Km}$ values for polymeric litter and microbial residues

Microbes process SOC by depolymerizing a wide array of C substrates derived from plant litter or microbial residues, which greatly differ in their chemistry (Buckeridge et al., 2022; Cotrufo and Lavelle, 2022). In JSM, the polymeric litter and microbial residues pool are depolymerised by extracellular enzymes produced by the microbial pool ( $C_B$ ) to enter the DOC pool (Fig. 2, Eq. (3)). Enzyme production is not explicitly simulated, but assumed to be proportional to the size of the microbial biomass pool. The half-saturation constants for depolymerisation of polymeric litter and microbial residues ( $K_{m,X}$ , Eq. (3)) are sensitive to temperature, but knowledge about their value is restricted to laboratory studies of individual enzymes. In this study, we explore different temperature sensitivities, expressed as  $Q_{10}$  values, for our model's half-saturation constants for microbial depolymerisation of polymeric litter ( $K_{m,P}$ ) and microbial residues ( $K_{m,R}$ ). We base these  $Q_{10}$  values on a study from Allison et al. (2018b), who give an extensive overview of the temperature sensitivities of different enzymes and their substrate targets. We chose values from this study that would likely be, or closely resemble, the main enzymes involved in the breakdown of our model's polymeric litter ( $C_P$ ) and microbial residue ( $C_R$ ) pools. For the depolymerisation of  $C_P$  we targeted a  $Q_{10,Km,P}$  value measured for the enzymes  $\beta$ -xylosidase and total oxidase, as these are involved in the degradation of hemicellulose, lignin and phenolics. For the depolymerisation of  $C_R$  we selected a  $Q_{10,Km,R}$  value measured for the enzyme leucine aminopeptidase, which is involved in the degradation of polypeptides, the main component of microbial cell walls. In the various model experiments (described in more detail in section 2.4), we explore the effects of these different temperature sensitivities on SOC decomposition individually, or combined.

### 2.4 Model experiments

During the first model run, ambient soil moisture and soil temperature are used repeatedly for a 100-year simulation. We do this to check whether the SOC pools between 0 - 50 cm depth still increase/decrease over the simulation period, i.e. to verify that the SOC pools reached steady state after the 500 year spinup period. Then, to investigate the effects of soil warming on SOC decomposition, we run the first set of soil warming experiments. Soils, including the deep soil up to 1m, are expected to warm by 4.5°C by the end of the century under representative concentration pathway (RCP) 8.5 (Soong et al., 2020), so we increased all ambient soil temperatures by 4.5 K throughout the 100 year simulation period, keeping the original seasonality in the ambient input data intact without altering the ambient soil moisture (SM) values. To test the sensitivity of SOC decomposition to warming and to investigate the potential feedbacks through the temperature sensitivity of the Michaelis-Menten term, we ran each warming experiment using different values for  $Q_{10,Km,P}$  and  $Q_{10,Km,R}$  (Table 1): Both  $Q_{10,Km,P}$  and  $Q_{10,Km,R}$  values are 1 (i.e. not temperature sensitive); Individual  $Q_{10}$  values for the breakdown of the microbial residue pool and the polymeric litter pool, where  $Q_{10,Km,R}$  is set to 0.7 and  $Q_{10,Km,P}$  is set to 1.3; Both  $Q_{10,Km,P}$  and  $Q_{10,Km,R}$  are 0.7 (representing the breakdown of microbial residues); Both  $Q_{10,Km,P}$  and  $Q_{10,Km,R}$  are 1.3 (representing the breakdown of the litter pool);. All model experiment settings are summarised in Table 2.

Then, to investigate the effects of soil warming and drying on SOC decomposition, we run the first set of drought experiments, where we keep all  $Q_{10,Km,X}$  values at 1 and use ambient soil temperature + 4.5 K. Soil drying is expected for most of the globe (Wang et al., 2022b and references therein), but drought intensity is uncertain and may vary locally (Cook et al., 2020; Hsu and Dirmeyer, 2023). Therefore, we compare three simple model drought scenarios, where the model's ambient SM inputs are reduced by 10% : In three model experiments, each ambient SM value is multiplied by 0.9, 0.8 or 0.7, respectively (Table 2). As with the warming experiment, the original seasonality in the ambient SM input values is kept intact.



As a last step, we investigate the combined effects of soil warming and drying on SOC decomposition including the feedback through the half-saturation constants' temperature sensitivities. Similar to the first set of 3 drought experiments, ambient soil temperature is raised by 4.5 K, and three different drought intensities are simulated (SM \* 0.9, SM \* 0.8 and SM \* 0.7). Reflecting the most likely realistic combination of  $Q_{10,Km}$  values for microbial depolymerisation, as soil will contain both microbial residues as well as polymeric litter for microbes to depolymerise, we used the two individual  $Q_{10}$  values from Allison et al. (2018b) for the breakdown of the microbial residue pool and the polymeric litter pool ( $Q_{10,Km,R} = 0.7$  and  $Q_{10,Km,P} = 1.3$ ).

## 2.5 Model output analyses

Each model experiment was run for 100 simulation years, yielding daily output files for different soil variables. We calculate SOC stocks as the sum of the soluble litter, polymeric litter, DOC, microbial residues, adsorbed DOC and adsorbed microbial residues pools (Fig. 2). Woody litter is excluded as it is considered part of the aboveground litter layer. To calculate the annual changes in SOC stocks, expressed as percentage change (%) since the start of the simulation, we used SOC values from the last day of each simulation year. All analyses and plots were done using packages "tidyverse", "ggplot2" and "viridis" under R version 4.3.1 in Rstudio (Garnier et al., 2023; R Core Team, 2023; RStudio Team, 2018; Wickham, 2016; Wickham et al., 2019).

## 3 Results

### 3.1 Warming effects on SOC decomposition

#### 3.1.1 Modelled SOC stock changes at ambient and elevated soil temperatures

To check whether JSM reached steady state after spinup, one model run was continued with ambient soil temperatures and soil moisture, and with  $Q_{10,Km,X}$  values of 1 (not temperature sensitive), i.e., the same setup as during spinup. The first 6 soil layers (0 - 50 cm) are in steady state at Hainich forest, as there is no SOC loss or gain over the complete simulation period (Fig. 3, dark blue). The small interannual variability in modelled SOC stocks reflects the interannual variability in the litter inputs and other forcing. Warming the soil by 4.5 K in a model experiment leads to SOC losses for all simulation years (Fig. 3, purple) until 5.1% of initial stocks are lost by the end of the simulation period (Table 2). The topsoil loses more SOC (- 6.2%) than the subsoil (- 3.9%), which is related to the fact that mineral-associated organic C (MAOC) increases with depth which leaves less available substrates for microbes to depolymerise in the subsoil (Fig. A1), as well as the lower microbial biomass in these layers which strongly reduces the Michaelis-Menten term for the depolymerisation rates (Fig. 1). Additionally, the processes of adsorption and desorption have lower temperature sensitivities than microbial processes in JSM so that warming affects the topsoil layers more strongly than the deeper layers where more SOC is mineral-associated. The soil warming effect is strongest at the beginning of the simulation period, but reduces as the model returns to a new steady state after roughly 100 simulation years.



**Table 2: Model experiments and settings with simulated changes (%) in SOC stocks at three different depth intervals**

Experiment	ST	SM	$Q_{10,Km,R}$	$Q_{10,Km,P}$	$\Delta$ SOC (%) 0 - 50 cm	$\Delta$ SOC (%) 0 - 6 cm	$\Delta$ SOC (%) 36 - 50 cm
1. Ambient model run	+ 0.0 K	SM * 1.0	1	1	0	0	0
2. Warming experiments	+ 4.5 K	SM * 1.0	1	1	-5.1	-6.2	-3.9
	+ 4.5 K	SM * 1.0	0.7	0.7	-6.8	-7.3	-5.6
	+ 4.5 K	SM * 1.0	1.3	1.3	-4.0	-5.5	-2.8
3. Drought experiments	+ 4.5 K	SM * 1.0	0.7	1.3	-5.2	-6.4	-3.9
	+ 4.5 K	SM * 0.9	1	1	-3.0	-4.4	-1.9
	+ 4.5 K	SM * 0.8	1	1	+1.0	-1.1	+1.6
4. Combined experiments	+ 4.5 K	SM * 0.7	1	1	+6.8	+3.8	+7.1
	+ 4.5 K	SM * 0.9	0.7	1.3	-3.1	-4.6	-2.0
	+ 4.5 K	SM * 0.8	0.7	1.3	+0.5	-1.5	+1.2
	+ 4.5 K	SM * 0.7	0.7	1.3	+5.8	+3.1	+6.1

235

### 3.1.2 Temperature sensitivity of half-saturation constants

To study the effects of temperature on SOC decomposition through the half-saturation constant for depolymerisation ( $Q_{10,Km,X}$ ), the model was run using three different combinations of  $Q_{10,Km,X}$  values for the depolymerisation of the polymeric litter and microbial residues pools (Table 2): Both  $Q_{10,Km,X}$  are 0.7; both  $Q_{10,Km,X}$  are 1.3; or  $Q_{10,Km,R}$  is 0.7 and  $Q_{10,Km,P}$  is 1.3. Using a  $Q_{10}$  value for half-saturation constants  $K_{m,P}$  and  $K_{m,R}$  of 0.7 (reflecting the temperature sensitivity of the depolymerisation of microbial residues) substantially accelerates SOC losses in response to warming. SOC losses until 50 cm depth reach 6.8% (Fig. 3, pink points). The topsoil loses more SOC than the subsoil (-7.3 % and -5.6 %, respectively), but when comparing with the run that uses  $Q_{10,Km,X}$  values of 1 the relative difference in the subsoil is larger than in the topsoil.

240



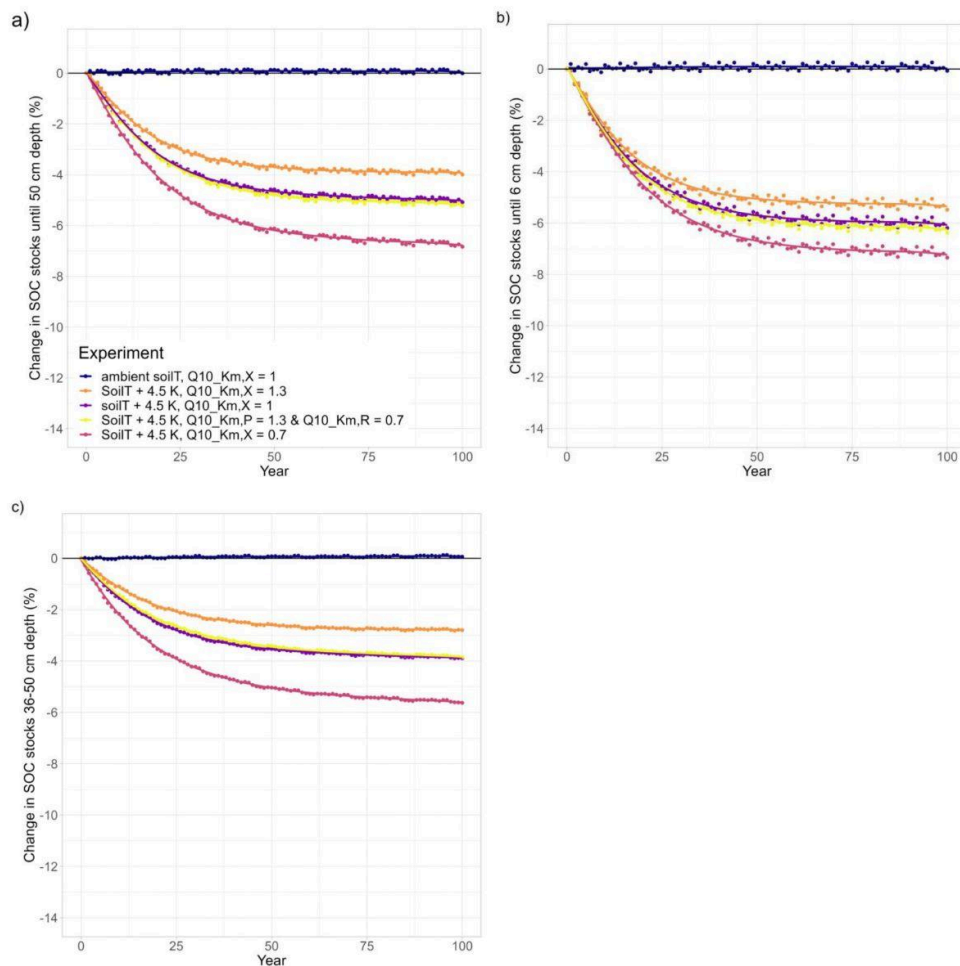
245 This indicates that in the subsoil, where microbial biomass is lower, the relative importance of  $Q_{10,Km,X}$  is larger than in the topsoil.

Contrastingly, using a  $Q_{10}$  value for half-saturation constants  $K_{m,P}$  and  $K_{m,R}$  of 1.3 (reflecting the temperature sensitivity of the depolymerisation of the polymeric litter pool) counteracts the warming effect and reduces SOC losses from the soil. The result is still a net loss: SOC stocks in the top 50 cm deplete by 4%, with higher SOC losses from topsoil compared to the subsoil (- 5.5 and - 2.8%, respectively, Fig. 3, orange points). Similar to the model run where  $Q_{10,Km,X}$  is 0.7, the temperature sensitivity of  $K_m$  in the model run where both  $Q_{10,Km,P}$  and  $K_{m,R}$  are 1.3 has a relatively larger impact in the subsoil than the topsoil.

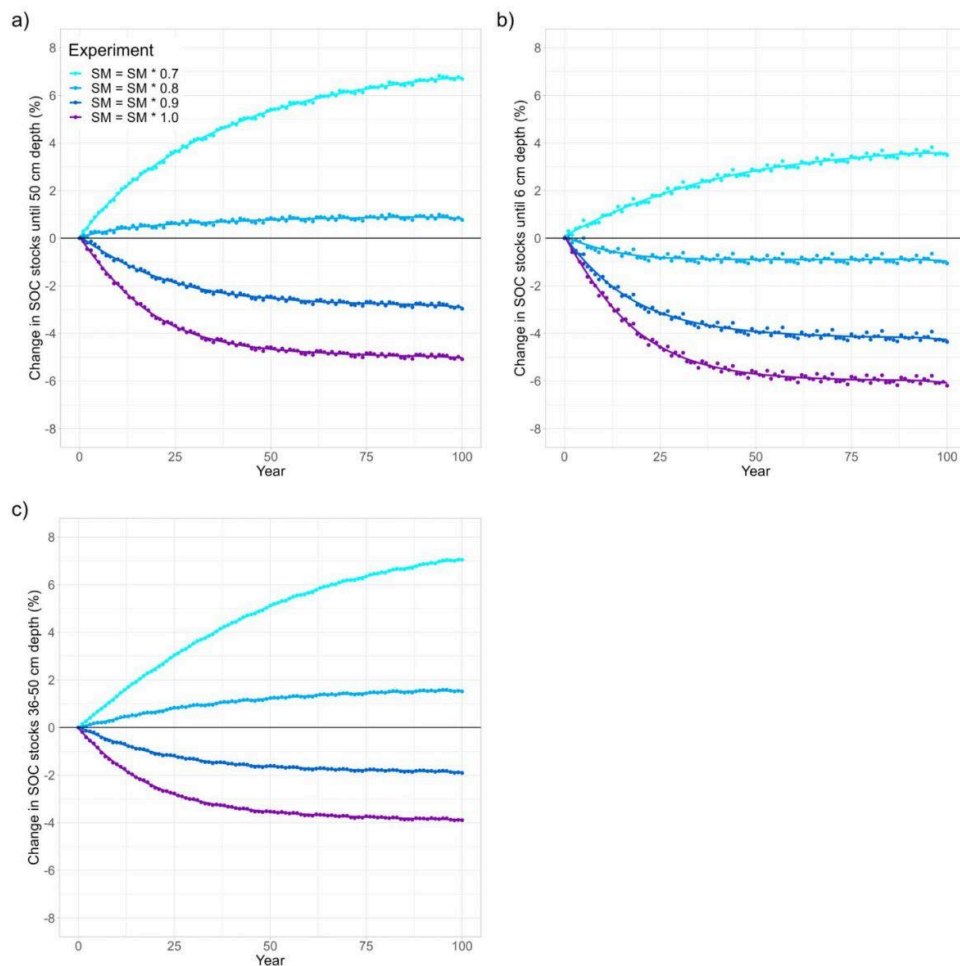
250 Using individual  $Q_{10}$  values for the half-saturation constant for the depolymerisation of microbial residues ( $K_{m,R}$ ) of 0.7 and of 1.3 for the polymeric litter pool ( $K_{m,P}$ ) results in SOC losses from the top 50 cm (- 5.2%, Fig.3, yellow). In comparison to the run where  $Q_{10,Km,X} = 1$  this result is very similar (5.1% loss from warming alone), indicating that the opposing temperature sensitivities of depolymerisation of microbial residues and polymeric litter pool cancel each other out. The topsoil loses more SOC (- 6.4%) than the subsoil (- 3.9%), but in comparison the run where  $Q_{10,Km,X} = 1$  the losses from the topsoil layer are slightly higher in the subsoil (-0.2%) similar in subsoil (0% difference).

### 3.2 Drought effects on SOC decomposition

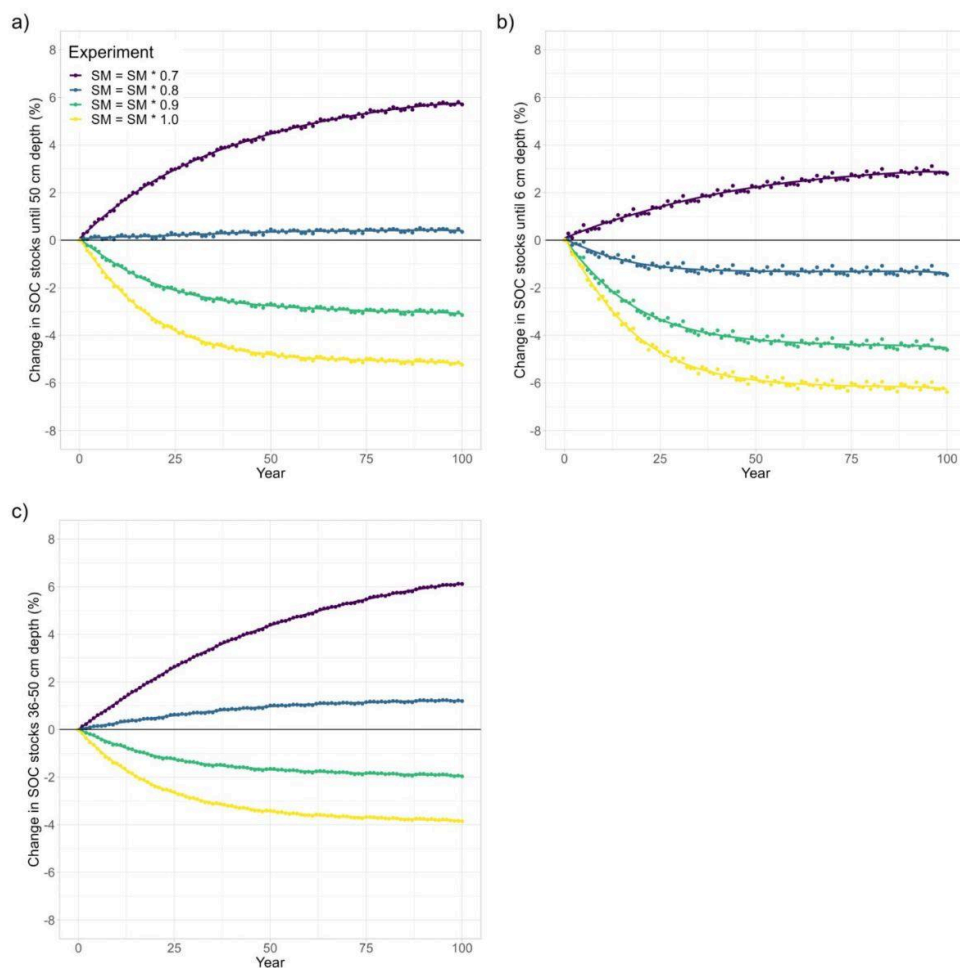
260 Inducing a drought strongly dampens the warming effect on SOC (Fig. 4). Depending on the drought intensity, the top 50 cm loses less SOC, or even acts as a sink and starts accumulating SOC over the course of the simulation period. A 10% reduction in SM results in a SOC loss of 3%, whereas at 80% and 70% SM, the soil column accumulates 1.0% or 6.8% SOC, respectively (Table 2). Stronger drought intensity led to a larger difference in modelled SOC stocks at 0-50 cm, from -5.1% at the original SM, to + 6.8% at 70% SM, a difference of 11.9 percentage points. This increased drought response on SOC decomposition is a direct result of the increase in the value of  $f_{Km,X}(T_{soil}, \theta)$  with decreasing SM ( $\theta$ , Eq. (4)). Again, the topsoil and subsoil layers show a different response: In the topsoil, there is high microbial biomass and therefore, the effect of the drought on microbial depolymerisation is not as strong as in the subsoil. Additionally, drought decreases the amount of MAOC in the subsoil, while POC accumulates (Fig. A1). As a result, the ratio of POC:MAOC increases, especially in the topsoil (Fig. A2). In 0 - 6 cm, SOC losses are 4.4% at 90% SM, 1.1% at 80% SM, and a 3.8% SOC gain at 70% SM. In the subsoil layer between 36 - 50 cm, there is a loss of 1.9% SOC at 90% SM, and 1.6% and 7.1% SOC gains at 80% and 70% SM, respectively. At 80% SM the drought has an opposite effect in the topsoil (a net source) than in the subsoil (a net sink). The whole column response, however, is a net sink, highlighting the strong contribution of the subsoil to the overall response.



275 **Figure 3: Temperature effects on long-term changes in modelled SOC stocks (% SOC lost since simulation year 0) for different model experiments in a) a whole soil column (0 - 50 cm), b) the topsoil layer (0 - 6 cm) and c) a subsoil layer (36 - 50 cm). In all runs, ambient SM (SM \* 1.0) was used.**



280 **Figure 4:** SM effects on long-term changes in modelled SOC stocks (% SOC lost since simulation year 0) for different model experiments in a) a whole soil column (0 - 50 cm), b) the topsoil layer (0 - 6 cm) and c) a subsoil layer (36 - 50 cm). Soil moisture is reduced in 10% steps from ambient (SM \* 1.0) to 70% (SM \* 0.7). In all runs,  $Q_{10,Km,X} = 1$  (not temperature sensitive).



285 **Figure 5: Combined temperature and SM effects on long-term changes in modelled SOC stocks (% SOC lost since simulation year 0) for different model experiments in a) a whole soil column (0 - 50 cm), b) the topsoil layer (0 - 6 cm) and c) a subsoil layer (36 - 50 cm). In all model runs, the soil was warmed by 4.5 K and  $Q_{10,Km,D}$  was 1.3 for depolymerisation of litter and  $Q_{10,Km,R}$  was 0.7 for depolymerisation of microbial residues.**



### 3.3 Combined effects of drought and temperature sensitivity of half-saturation constants on SOC decomposition

290 To investigate the potentially counteracting responses of temperature sensitivity of  $K_m$  and droughts, we also run the model for the three different drought intensities in conjunction with a  $Q_{10,Km,P}$  value of 1.3 for the polymeric litter pool and a  $Q_{10,Km,R}$  value of 0.7 for the microbial residues pool. At ambient SM conditions, the temperature sensitivity of both  $K_{m,X}$  values only marginally amplified the warming effects (Figs. 3 and 5, yellow points). When SM is reduced, however, this slows down the decomposition rates (Fig. 5, Table 2): At a 10% reduction in available SM, less SOC is lost from the top 50 cm (-3.1%) than when SM is kept at ambient levels (-5.2%). At 80 and 70% SM the soil starts gaining SOC (+0.5% and 5.8%, respectively). Generally, modelled SOC stocks for this combination of temperature sensitivities of  $K_m$  and different drought intensities closely resemble the simulated drought response (Fig. 4), with the temperature sensitivity of  $K_m$  counteracting the drought effects: when  $K_m$  is temperature sensitive, SOC losses are always higher, and SOC gains are always smaller than when  $K_m$  is not temperature sensitive (Table 2). Similar to the drought experiments (Section 3.2), the differences in modelled SOC stocks at 0-50 cm increase with stronger drought intensity. Interestingly, the temperature sensitivity effect through  $Q_{10,Km,P}$  and  $Q_{10,Km,R}$  also increases with stronger drought intensity: For example, at ambient SM, SOC stocks decreased by 5.1% when both  $Q_{10,Km,X}$  are 1, and decreased by 5.2% when  $Q_{10,Km,R} = 0.7$  and  $Q_{10,Km,P} = 1.3$ , a difference of 0.1 percentage point (Table 2). But at 70% SM, SOC stocks increase to 6.8% when both  $Q_{10,Km,X}$  are 1, and increase to 5.8% when  $Q_{10,Km,R} = 0.7$  and  $Q_{10,Km,P} = 1.3$ , a difference of 1.0 percentage point. The same trend is also visible for both the topsoil (relative difference from 0.2 percentage point at SM = 1.0 to 0.7 percentage point difference at SM = 0.7) and the subsoil (no difference at SM = 1.0 to 1.0 percentage point difference at SM = 1.0). At the same time, the ratio POC:MAOC did not change much compared to the model run where  $K_{m,X}$  was not temperature sensitive (Fig. A2, yellow and pink). This indicates that rather than causing a shift in the litter and microbial residues C pools, microbial limitation is strong under dry conditions (low  $C_B$ , Fig. 1), which in turn increases the importance of  $Q_{10,Km,R}$  and  $Q_{10,Km,P}$  for the overall SOC decomposition rates. Contrasting to the results from the isolated warming and drought experiments, the differences in SOC stock changes between the topsoil and subsoil are not very large: From a -6.4% SOC loss to +3.1% SOC gain, which is a 9.5 percent point change in the topsoil, to -3.9 to +6.1, which is a 10 percentage point change in the subsoil (Table 2). These results indicate that the combined sensitivity of SOC stocks to moisture and temperature in topsoil and subsoil is similar due to the counteracting effects of temperature and soil moisture on  $K_m$  (Eq. (6)): higher temperatures promote SOC decomposition rates due to the stronger influence of depolymerisation of microbial residues (which has a  $Q_{10,Km,R}$  value of 0.7), whereas drought decreases SOC decomposition rates.

## 320 4 Discussion

### 4.1 Warming effects on SOC decomposition

We find that warming the soil by 4.5 K accelerates SOC losses, and these losses are proportionally higher in the topsoil than in the subsoil. This is expected, as higher soil temperature increase maximum depolymerisation rates and microbial growth rates through  $Q_{10,Vmax,X}$  (Eq. (4)). Our findings are also consistent with other modelling studies that investigate isolated soil warming effects (e.g. Pallandt et al., 2022; Todd-Brown et al., 2014; Wieder et al., 2018), as well as with results from a recent large meta-analysis of SOC profiles (Wang et al., 2022a), which reports higher losses of SOC stock and SOC content from topsoil (0-30 cm) than subsoils (0.3 - 1m). In our study, during the warming experiments, the topsoil almost always loses more





SOC than the subsoil, except when  $Q_{10,Km,P}$  and  $Q_{10,Km,R}$  are both set to 0.7 and SOC losses are accelerated in the subsoil (-5.6% loss). Two depth-dependent model processes play an important role in these top- and subsoil differences. Firstly, microbial biomass ( $C_b$ ) decreases with depth, and as microbial biomass declines, the Michaelis-Menten term for depolymerisation decreases (Fig. 1, Eq. (3)), thereby limiting the depolymerisation rates at lower depths. Secondly, SOC is protected from microbial decomposition by sorption to mineral surfaces, and mineral-associated organic carbon (MAOC, consisting of adsorbed DOC and microbial residues) strongly increases with soil depth (Fig. A1). In JSM, the  $Q_{10}$  value of the mineral-associated C pools are 1.08 for adsorption and 1.34 for desorption, which is much lower than the  $Q_{10}$  values of the particulate organic carbon (POC) pools: The  $Q_{10}$  value for microbial depolymerisation of polymeric litter and microbial residues is 2.16, and 1.98 for microbial C uptake (Table 1, Allison et al., 2010; Wang et al., 2012, 2013). As the ratio of MAOC to POC strongly increases in the subsoil, this leads to an overall lower apparent temperature sensitivity of SOC pools in the subsoil. Total SOC losses consist of DOC, POC, and MAOC from the 36 - 50 cm subsoil layer, so the overall SOC losses may be relatively small as the majority of SOC in this layer consists of protected MAOC - which decreases its overall temperature sensitivity.

Whether or not the apparent temperature sensitivity of SOC declines with depth, as we observe in this study, is still a topic of debate. According to kinetic theory subsoils may have lower apparent  $Q_{10}$  values when they contain less complex, necromass derived substrates (Davidson and Janssens, 2006; Hicks Pries et al., 2023). Contrastingly, the same argument is used to explain higher temperature sensitivities in subsoils when they may contain molecules with higher activation energies (e.g. Li et al., 2020). These observed higher temperature sensitivities could be the result of deriving the apparent  $Q_{10}$  values from bulk soil samples containing both POC and MAOC, whereas several other studies demonstrated that this trend can be counteracted by the strong mineral protection of SOC in subsoils (Gentsch et al., 2018; Gillabel et al., 2010; Qin et al., 2019) and that reported high apparent  $Q_{10}$  values originate from the decomposition of POC (Soong et al., 2021). In a recent review, Hicks Pries et al. (2023) conclude that the temperature response of deep soils is likely to be context dependent, and that subsoils with high POC content, or with low reactive mineral content are likely to be more susceptible to warming than soils with limited POC or with highly reactive mineral surfaces which protect SOC from microbial decomposition. In our model experiments, MAOC strongly increased with soil depth, which resulted in smaller total SOC losses from the topsoil than the subsoil layer in response to warming.

We observe stronger model responses to different  $Q_{10,Km,X}$  values in subsoils than in topsoils, firstly, because microbial limitation is stronger in subsoils than in topsoils. At low microbial biomass ( $C_b$ ), the value of  $K_{m,X}$  becomes increasingly important (Fig. 1, Eq. (3)). At the same time, depolymerisation rates only affect the POC pools ( $C_p$  and  $C_r$ ) and not the MAOC pools (adsorbed DOC and adsorbed microbial residues). Since the ratio of POC:MAOC is low in subsoils (Fig. A2), the total SOC losses from subsoils are lower from the subsoil than the topsoil, despite the higher sensitivity to different  $Q_{10,Km,X}$  values. So, when  $Q_{10,Km,X} < 1$ , SOC losses can be further accelerated, especially in the deep soil. In our study, this lower  $Q_{10}$  was associated with the breakdown of proteins from the microbial residues pool. The contribution of microbial residues in the deep soil to total SOC is highly significant and can be up to 54% in grasslands (Wang et al., 2021). So if free POC in deep soils is indeed more sensitive to warming as a result of low microbial biomass, our model results support the finding that deep soils rich in microbial residues are more temperature sensitive than those that contain less microbially-derived POC contents, due to the lower  $Q_{10,Km}$  value of the breakdown of polypeptides. However, compared to plant-derived POC, microbial residues have a high mineral sorption potential (Liu et al., preprint; Buckeridge et al., 2022) and could therefore be more protected from decomposition.



#### 4.2 Drought effects on SOC decomposition

Our results show that soil drying can alleviate the losses of SOC from soil warming. In our model, this is the result of the soil moisture sensitivity of the half-saturation constants for microbial depolymerisation ( $K_{m,R}$  and  $K_{m,P}$ , Eq. (6)): Lower soil moisture reduces the Michaelis-Menten term for depolymerisation (Fig. 1), which lowers the SOC decomposition rates. Microbial C uptake for growth is also sensitive to changes in soil moisture through changes in the air-filled pore space (Eqs. 7 and 8), but this would result in faster SOC decomposition rates as microbial growth is less affected by oxygen limitation, which was not the case for any of the modelled drought experiments. Generally, SOC decomposition peaks at intermediate soil moisture, but most soils are below these optimal soil moisture levels and as a result, drying leads to reduced decomposition rates due to stronger microbial limitation, whereas wetting the soil leads to an acceleration of the decomposition rates until oxygen limitation limits SOC decomposition rates (Davidson et al., 2012; Moyano et al., 2018; Pallandt et al., 2022; Skopp et al., 1990). In our model framework, substrate and oxygen limitation is split between two processes: we simulate moisture-driven diffusion limitation on the microbial depolymerisation rates (reverse MM-kinetics, Eq. (6)), and oxygen and DOC availability affect microbial growth (forward MM-kinetics, Eq. (7)). We found that soil drying consistently reduced modelled SOC losses compared to SOC losses due to soil warming alone, indicating that microbial limitation of depolymerisation is more important than oxygen limitation on microbial growth in our study. Additional support for strong microbial limitation on SOC decomposition comes from our observation that particulate organic C (POC) accumulates in both the topsoil and subsoil layers in response to the most intense drought scenario ( $SM = SM * 0.7$ , Fig. A1). If microbes were not limited by the drought, they would degrade POC quickly in response to warming.

Our finding that microbial SOC decomposition consistently declines in response to drought is in agreement with other studies that explore drought effects on SOC decomposition using microbially explicit models (Liang et al., 2021; Wang et al., 2020; Zhang et al., 2022). In the topsoil, we find that the impact of each 10% reduction in SM has a relatively small impact on alleviating SOC losses through warming, compared to the subsoil (Fig. 4). These observed differences in the drought response between top- and subsoil can mainly be explained by the vertical differences in microbial biomass concentration ( $C_B$ ), which is higher in the topsoil than the subsoil. Therefore, at low  $C_B$ , the relative impact of drought on the MM-term for depolymerisation is larger in the subsoil than the topsoil, making the modelled subsoil SOC stocks more sensitive to drought. For example, at 80% SM, modelled SOC stocks in the topsoil reduce in response to soil warming (from -6.2% to -1.1% as SM reduces to 80%, a net difference of 5.1 percent points), whereas subsoil SOC stocks decrease at ambient SM but increase at 80% SM (from -3.9% to +1.6%, a difference of 5.5 percent points). As discussed in section 4.1, the relatively higher sensitivity of the subsoil to not only warming but also to drought, is also related to the strong increase in MAOC with depth and its lower temperature sensitivity compared to that of the POC pools. In order to focus completely on drought effects on microbial SOC decomposition, adsorption and desorption rates were not sensitive to changes in soil moisture during our experiments. Drought favours the stabilisation of SOC on mineral surfaces (Blankinship and Schimel, 2018), thereby protecting it from microbial depolymerisation. Therefore, if we would consider the moisture sensitivity of adsorption and desorption rates in our model, we expect a further decrease in the SOC decomposition rates in response to drought. The formulation of moisture sensitivity of adsorption and desorption, however, is not well established to our knowledge.

Overall, our model results indicate a potential for net SOC gains in 0 - 50 cm depth when SM is reduced to 80% or 70% of its original values, and that a large part of the whole soil column response is driven by the subsoil. While data-driven deep soil drying studies are rare, our simulation results are supported by a recent study (Brunn et al., 2023), where total annual precipitation throughfall was reduced by 70% for 5 consecutive years and both SOC stocks and SOC stability increased between 0 - 30 cm. They found that the majority of the SOC stock increase occurred in the top 5 cm as a result of higher root exudates, but we do not consider this in our experiment. We found that the largest SOC stock increase occurred in the subsoil,



because of the higher sensitivity of subsoil to drought at low microbial biomass concentrations and the strong protection of  
410 MAOC from microbial depolymerisation. Our finding that SOC stocks can potentially increase with drought despite the  
expected losses through warming, is mainly the result of lower microbial depolymerisation (Eq. (6), Fig. 1). Indeed, short term  
studies indicate that SOC stocks may increase under drought, as a strong reduction in microbial activity may dominate over  
the effect of reduced litter and root inputs (Brunn et al., 2023; Deng et al., 2021; Moyano et al., 2013). While results from  
415 short-term data-driven studies support our modelling results, long-term drought studies generally show a decline in SOC  
stocks, which can be mainly attributed to the effects of soil warming and decreased litter inputs (e.g. Deng et al., 2021; Meier  
and Leuschner, 2010). An advantage of our stand-alone soil model environment with prescribed litter inputs is that it allows  
us to individually test soil warming and drying effects on long-term SOC stocks, while eliminating the potentially confounding  
effects from changes in plant productivity. Recent research has shown that the chances of drought coinciding with high soil  
temperatures will further increase in the future (García-García et al., 2023). As a result, the counteracting effects of  $K_m$  and  
420 drought may be at their strongest, and ecosystems dominated by infrequent moisture inputs may show strong sensitivities to  
soil warming and drought.

#### 4.3 Combined effects of drought and temperature sensitivity of half-saturation constants on SOC decomposition

We show that soil drying in combination with temperature sensitivity of the half-saturation constants for depolymerisation of  
polymeric litter and microbial residues, can both increase or decrease SOC stocks, and that the direction and magnitude of the  
425 effect on SOC stocks depends on drought intensity. The combined effects of soil drying and temperature sensitivity of the half-  
saturation constants for depolymerisation on SOC stocks closely resembled that of the drought response, which indicates that  
microbial limitation on depolymerisation poses a strong control on modelled SOC stocks and that drought can indeed alleviate  
SOC losses in response to soil warming. While the effect of drought on modelled SOC stocks is strong, the temperature  
sensitivity of  $K_{m,x}$  can counteract these effects: Compared to the model runs without temperature sensitivity of  $K_{m,x}$ , SOC  
430 losses are higher and SOC gains are smaller. This indicates that the breakdown of microbial residues, which had a  $Q_{10,K_{m,R}}$   
value of 0.7, is important for the overall results because a  $Q_{10}$  value lower than 1 increases the MM-term for depolymerisation,  
and accelerates SOC decomposition. Furthermore, this counteracting effect of  $Q_{10,K_{m,x}}$  is stronger with increased drought  
intensity while the ratio POC:MAOC does not change much when compared to the model run where  $Q_{10,K_{m,x}}$  is not  
temperature sensitive. In line with our results from the isolated drought experiments (Section 4.2), this supports the conclusion  
435 that microbial limitation increases under drought, so that  $Q_{10,K_{m,x}}$  becomes more important for the overall depolymerisation  
rates.

Unlike the individual warming and drought experiments, we only find small differences in SOC stock changes between the  
top- and subsoil for the combination of drought and temperature sensitivity of  $K_{m,R}$  and  $K_{m,P}$ . This shows that drought and  
temperature sensitivity can both play a strong role, and counteract each other so that the overall changes in SOC stocks appear  
440 similar. This is an important result, because long-term warming can accelerate soil drying, especially at the soil surface (Berg  
and Sheffield, 2018; Fan et al., 2022; García-García et al., 2023). Our results show divergent responses of top and subsoil SOC  
stocks to concurrent soil warming and drying, in particular at a 20% SM reduction, where modelled SOC stocks in the topsoil  
increase but decrease in the subsoil. While we only explored the effects of evenly drying out the soil column in this study, the  
long-term response of SOC stocks to soil moisture changes could be even more non-linear as top- and subsoils may not dry  
445 out evenly (Berg et al., 2017). Using multi-model predictions, Berg et al. (2017) show that surface soil moisture decreases by  
the end of the century, while subsoils, especially in the northern hemisphere, diverge with either less severe drying or wetter  
conditions. On top of soil warming, such dynamic vertical changes in soil moisture have a strong potential of further  
accelerating or slowing down SOC decomposition rates in the deep soil by microbial limitation or oxygen diffusion limitation



(Pallandt et al., 2022). We call for modelling studies that address such changes simultaneously by running ‘new generation’  
450 models with future climate forcing datasets.

#### 4.4 Microbial response to substrate changes in the POC/MAOC framework

The duration of our experiments is 100 simulation years, but the values of  $Q_{10,Vmax}$  and  $Q_{10,Km,X}$  may not stay constant over  
time, as the environment changes and microbial communities adapt. However, in light of our long-term warming experiments  
we feel confident with the choice of  $Q_{10,Km}$  values, as they were measured in microorganisms that showed no sensitivity to a  
455 6 °C increase in average temperature - but did show a strong response to changes in substrate types (Allison et al., 2018a). In  
our model experiment, microbes have access to both litter inputs and microbial residues to depolymerise, which have  
counteracting  $Q_{10,Km}$  values and therefore the possibility to simultaneously accelerate and slow down microbial SOC  
decomposition rates. In this light, it is important that modellers have access to data sources that help connect model  $Q_{10}$  values  
460 for  $K_{m,X}$  and  $V_{max}$  to the dominant C sources that microbes could depolymerise. For example, information on soils that are  
high in POC versus soils that are high in MAOC: Soils with high MAOC contents and low POC inputs can have lower apparent  
 $Q_{10}$  values because  $Q_{10,sorption}$  is much lower than the  $Q_{10}$  values of unprotected organic carbon (Table 1; Wang et al., 2012,  
2013). Secondly, such soils would have necromass rather than fresh litter inputs as the dominant C substrate for microbes.  
New datasets such as global maps of necromass C contributions to total SOC stocks (e.g. Liu et al., preprint) can inform  
465 modellers on substrate type or SOC stabilisation mechanisms, and thereby help identify the climate sensitivities of SOC stocks  
in different regions of the world. At the moment, though, there are no clear answers as to which values we should use for  
 $Q_{10,Km,X}$  because SOC consists of many different molecules, which all have their own specific temperature sensitivities  
(Allison et al., 2018b). One possibility to investigate the potential climate-substrate feedbacks with a model like JSM, would  
be a further partitioning of the litter pools into functional groups related to their main degrading enzymes. Our current study,  
470 which explores different values for  $Q_{10,Km,X}$  already provides valuable insights into what might be possible. For example, soils  
with high POC contents, i.e. with a developed organic layer as a result of high litter inputs, low SOC losses and low  
bioturbation, are likely to have  $Q_{10,Km,X}$  values  $> 1$ , which has the potential to counteract soil warming effects through  
 $Q_{10,Vmax}$ , especially in deeper layers where microbial biomass is low and the temperature sensitivity of the half-saturation  
constant will have a stronger impact. In combination with soil drought, this would further enhance microbial limitation for  
475 depolymerisation and could dampen SOC losses in such organic soil layers over time - if litter inputs stay constant over time.  
Peat soils could be an exception, as they usually have high volumetric water contents and drought can lift oxygen limitation,  
thereby increasing SOC decomposition rates. It can be expected though, that long-term soil drying reduces root and leaf litter  
inputs as plant productivity decreases (Deng et al., 2021). Therefore, we recommend future research focuses on further studying  
climate-substrate interactions within a fully coupled soil-plant model, such as the coupling between land surface model  
QUINCY (Thum et al., 2019) with JSM, which is nearing completion.

#### 480 5 Conclusions

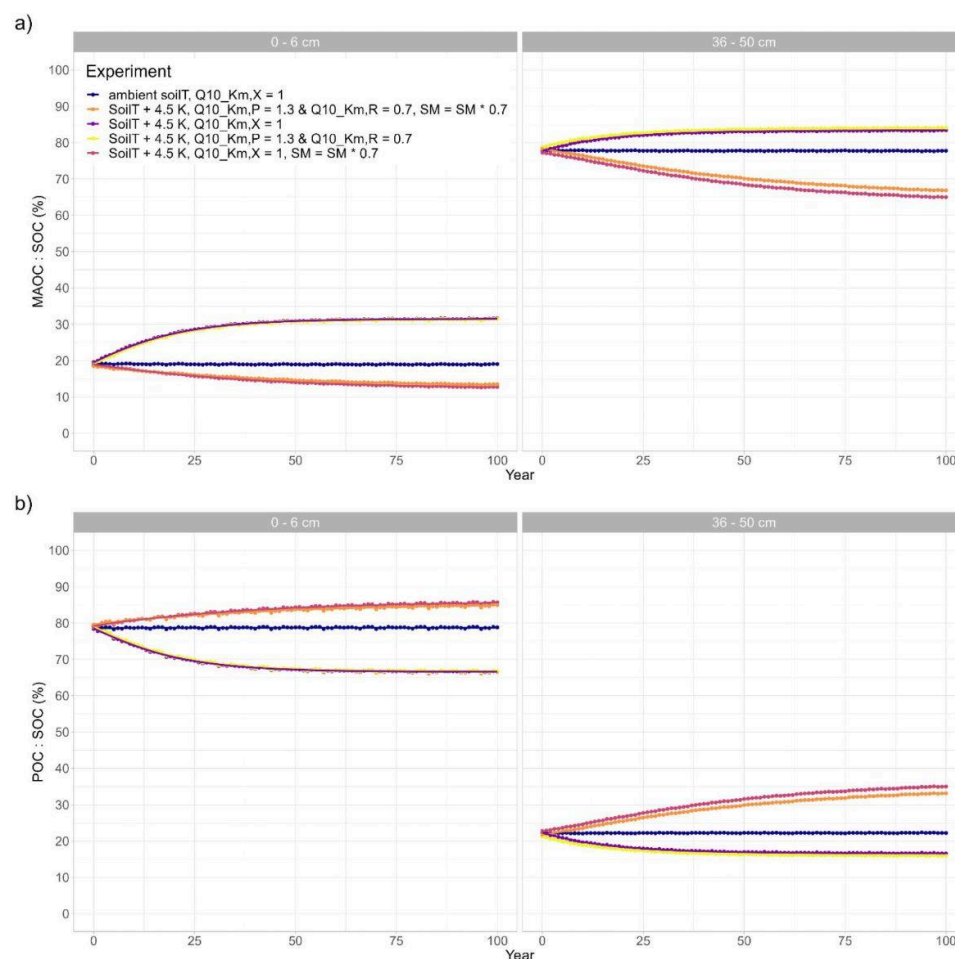
With JSM we show that both soil drying and warming pose strong controls on SOC decomposition. The vertically explicit  
model structure allows us to demonstrate that subsoil SOC stocks respond differently to warming and drought through a  
combination of processes. First of all, we show that SOC association to mineral surfaces plays an important role in reducing  
the overall sensitivity of SOC stocks to microbial decomposition: MAOC strongly increases with soil depth and has a low  
485 apparent temperature sensitivity, which results in smaller total SOC losses from the subsoil than the topsoil. At the same time,  
our model results indicate that unprotected subsoil SOC is more sensitive to soil warming and drought. Secondly, we show  
that drought can alleviate the effects of soil warming through microbial limitation on depolymerisation rates. As drought gets  
stronger, microbially mediated depolymerisation rates become severely limited so that less SOC is lost from the soil. In the



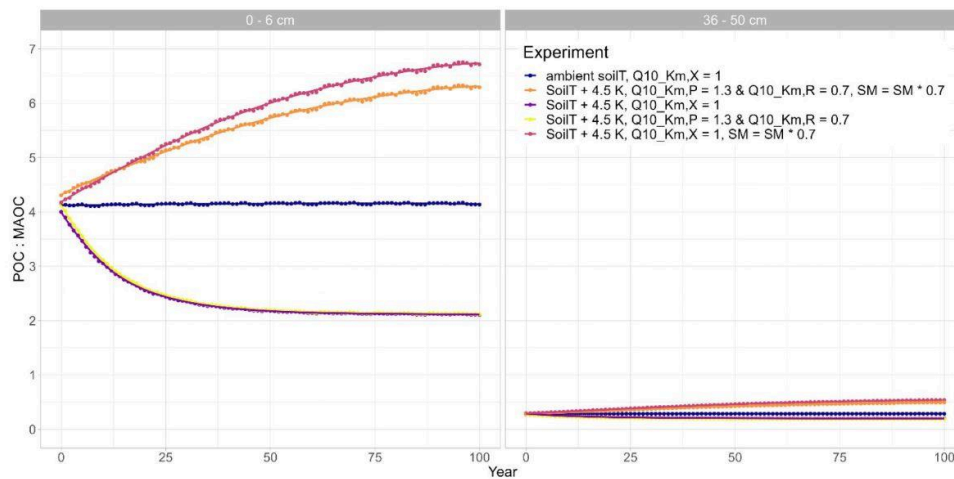
490 model experiments with constant litter inputs in this study this can even lead to SOC accumulation over time, despite soil  
warming. Thirdly, we show that considering the temperature sensitivities of the half-saturation constants for different C  
substrates (litter and microbial residues) is important, as they can both slow down and accelerate microbial SOC decomposition  
rates. Our results highlight the importance of representing SOC decomposition processes in a vertically resolved model, which  
includes carbon stabilisation on mineral surfaces. We recommend that future model development focuses on further identifying  
the (un)importance of temperature sensitivities of  $V_{max}$  and  $K_{m,x}$  for different C substrates and moisture sensitivities of all  
495 microbial-mineral interactions in the new class of soil organic carbon models.



Appendix A



500 **Figure A1:** a) Ratio of mineral associated organic carbon (MAOC) to SOC (%) and b) particular organic carbon (POC) to SOC (%) for different model runs at two different soil depths: Topsoil (0 - 6 cm) and subsoil (36-50 cm). If not indicated otherwise, SM = SM \* 1.0 in the experiment.



505 **Figure A2:** Ratio of particular organic carbon (POC) to mineral-associated carbon (MAOC) for different model runs at two different soil depths: Topsoil (0 - 6 cm) and subsoil (36-50 cm). If not indicated otherwise,  $SM = SM * 1.0$  in the experiment.



#### Code availability

The Jena Soil Model (JSM) - release01 is fully described and published under <https://doi.org/10.5194/gmd-13-783-2020>. The JSM source code is available online (<https://git.bgc-jena.mpg.de/quincy/quincy-model-releases>, branch “jsm/release01”), but access is restricted to registered users. Readers interested in running the model should request a username and password from S. Zaehle or via the git repository. JSM is developed using the framework of the QUINCY model. The QUINCY model is free software: It can be distributed and/or modified under the terms of the GNU GPL version 3 (<https://www.gnu.org/licenses/gpl-3.0.en.html>, last access 10 January 2024). The use of the QUINCY model relies on the application of software developed by the MPI for Meteorology, which is subject to the MPI-M ICON software licence (see ICON section: “By using ICON, the user accepts the individual licence (<https://code.mpimet.mpg.de/attachments/download/20888/MPI-M-ICONLizenzvertragV2.6.pdf>, last access 10 January 2024). Where software is supplied by third parties such as the MPI for Meteorology, it is indicated in the header of the file. Model users are strongly encouraged to follow the fair-use policy stated at <https://www.bgc-jena.mpg.de/en/bsi/projects/quincy/software> (last access: 10 January 2024).

#### Author contribution

MP wrote the original draft for the manuscript with contributions from all co-authors. BA and LY wrote the original JSM model code (version 1.0, see code availability), MP and BA wrote minor code modifications to run the model experiments as described in Section 2, and MP performed the model simulations and created all visualisations. This study was conceptualised by MP, BA, MS, and HL. Formal analysis was carried out by MP and BA. Funding acquisition: BA, HL and MR. Supervision of MP by BA, HL, MS, and MR.

#### Acknowledgements

MP is grateful for discussions with Prof. S. Zaehle in the early phases of this study as well as technical support from J. Nabel and J. Engel from the QUINCY modelling team at the Max Planck Institute for Biogeochemistry in Jena. MP received funding support for this work from the Norwegian Research Council through grant no. RCN 255 061 (MOisture dynamics and CArbon sequestration in BOREal Soils) and the Max Planck Institute for Biogeochemistry.

#### Competing interests

The authors declare that they have no conflict of interest.

#### References

- Abramoff, R., Davidson, E., and Finzi, A. C.: A parsimonious modular approach to building a mechanistic belowground carbon and nitrogen model, *Journal of Geophysical Research: Biogeosciences*, 122, 2418–2434, <https://doi.org/doi:10.1002/2017JG003796>, 2017.
- Ahrens, B., Braakhekke, M. C., Guggenberger, G., Schrupf, M., and Reichstein, M.: Contribution of sorption, DOC transport and microbial interactions to the 14C age of a soil organic carbon profile: Insights from a calibrated process model, *Soil Biology and Biochemistry*, 88, 390–402, <https://doi.org/10.1016/j.soilbio.2015.06.008>, 2015.
- Ahrens, B., Guggenberger, G., Rethemeyer, J., John, S., Marschner, B., Heinze, S., Angst, G., Mueller, C. W., Kögel-Knabner, I., Leuschner, C., Hertel, D., Bachmann, J., Reichstein, M., and Schrupf, M.: Combination of energy limitation and sorption capacity explains 14C depth gradients, *Soil Biology and Biochemistry*, 148, 107912, <https://doi.org/10.1016/j.soilbio.2020.107912>, 2020.





- Allison, S. D., Wallenstein, M. D., and Bradford, M. A.: Soil-carbon response to warming dependent on microbial physiology, *Nature Geoscience*, 3, 336, <https://doi.org/10.1038/ngeo846> [https://www.nature.com/articles/ngeo846#supplementary-](https://www.nature.com/articles/ngeo846#supplementary-information)  
545 information, 2010.
- Allison, S. D., Romero-Olivares, A. L., Lu, L., Taylor, J. W., and Treseder, K. K.: Temperature acclimation and adaptation of enzyme physiology in *Neurospora discreta*, *Fungal Ecology*, 35, 78–86, <https://doi.org/10.1016/j.funeco.2018.07.005>, 2018a.
- Allison, S. D., Romero-Olivares, A. L., Lu, Y., Taylor, J. W., and Treseder, K. K.: Temperature sensitivities of extracellular enzyme Vmax and Km across thermal environments, *Glob Chang Biol*, 24, 2884–2897, <https://doi.org/10.1111/gcb.14045>,  
550 2018b.
- Berg, A. and Sheffield, J.: Climate Change and Drought: the Soil Moisture Perspective, *Curr Clim Change Rep*, 4, 180–191, <https://doi.org/10.1007/s40641-018-0095-0>, 2018.
- Berg, A., Sheffield, J., and Milly, P. C. D.: Divergent surface and total soil moisture projections under global warming, *Geophysical Research Letters*, 44, 236–244, <https://doi.org/10.1002/2016GL071921>, 2017.
- 555 Blankinship, J. C. and Schimel, J. P.: Biotic versus Abiotic Controls on Bioavailable Soil Organic Carbon, *Soil Systems*, 2, 10, <https://doi.org/10.3390/soilsystems2010010>, 2018.
- Braakhekke, M. C., Beer, C., Hoosbeek, M. R., Reichstein, M., Kruijt, B., Schrumpf, M., and Kabat, P.: SOMPROF: A vertically explicit soil organic matter model, *Ecological Modelling*, 222, 1712–1730, <https://doi.org/10.1016/j.ecolmodel.2011.02.015>, 2011.
- 560 Brunn, M., Krüger, J., and Lang, F.: Experimental drought increased the belowground sink strength towards higher topsoil organic carbon stocks in a temperate mature forest, *Geoderma*, 431, 116356, <https://doi.org/10.1016/j.geoderma.2023.116356>, 2023.
- Buckeridge, K. M., Mason, K. E., Ostle, N., McNamara, N. P., Grant, H. K., and Whitaker, J.: Microbial necromass carbon and nitrogen persistence are decoupled in agricultural grassland soils, *Commun Earth Environ*, 3, 1–10, <https://doi.org/10.1038/s43247-022-00439-0>, 2022.
- 565 Cook, B. I., Mankin, J. S., Marvel, K., Williams, A. P., Smerdon, J. E., and Anchukaitis, K. J.: Twenty-First Century Drought Projections in the CMIP6 Forcing Scenarios, *Earth's Future*, 8, e2019EF001461, <https://doi.org/10.1029/2019EF001461>, 2020.
- Cotrufo, M. F. and Lavelle, J. M.: Chapter One - Soil organic matter formation, persistence, and functioning: A synthesis of current understanding to inform its conservation and regeneration, in: *Advances in Agronomy*, vol. 172, edited by: Sparks, D. L., Academic Press, 1–66, <https://doi.org/10.1016/bs.agron.2021.11.002>, 2022.
- Cotrufo, M. F., Wallenstein, M. D., Boot, C. M., Deneff, K., and Paul, E.: The Microbial Efficiency-Matrix Stabilization (MEMS) framework integrates plant litter decomposition with soil organic matter stabilization: do labile plant inputs form stable soil organic matter?, *Global Change Biology*, 19, 988–995, <https://doi.org/10.1111/gcb.12113>, 2013.
- 575 Davidson, E. A. and Janssens, I. A.: Temperature sensitivity of soil carbon decomposition and feedbacks to climate change, *Nature*, 440, 165, <https://doi.org/10.1038/nature04514>, 2006.
- Davidson, E. A., Janssens, I. A., and Luo, Y.: On the variability of respiration in terrestrial ecosystems: moving beyond Q10, *Global Change Biology*, 12, 154–164, <https://doi.org/10.1111/j.1365-2486.2005.01065.x>, 2006.
- Davidson, E. A., Sudeep, S., Samantha, S. C., and Savage, K.: The Dual Arrhenius and Michaelis–Menten kinetics model for decomposition of soil organic matter at hourly to seasonal time scales, *Global Change Biology*, 18, 371–384, <https://doi.org/doi:10.1111/j.1365-2486.2011.02546.x>, 2012.
- 580 Deng, L., Peng, C., Kim, D.-G., Li, J., Liu, Y., Hai, X., Liu, Q., Huang, C., Shangguan, Z., and Kuzyakov, Y.: Drought effects on soil carbon and nitrogen dynamics in global natural ecosystems, *Earth-Science Reviews*, 214, 103501, <https://doi.org/10.1016/j.earscirev.2020.103501>, 2021.



- 585 Dwivedi, D., Riley, W. J., Torn, M. S., Spycher, N., Maggi, F., and Tang, J. Y.: Mineral properties, microbes, transport, and plant-input profiles control vertical distribution and age of soil carbon stocks, *Soil Biology and Biochemistry*, 107, 244–259, <https://doi.org/10.1016/j.soilbio.2016.12.019>, 2017.
- Fan, K., Slater, L., Zhang, Q., Sheffield, J., Gentine, P., Sun, S., and Wu, W.: Climate warming accelerates surface soil moisture drying in the Yellow River Basin, China, *Journal of Hydrology*, 615, 128735, <https://doi.org/10.1016/j.jhydrol.2022.128735>, 2022.
- 590 García-García, A., Cuesta-Valero, F. J., Miralles, D. G., Mahecha, M. D., Quaas, J., Reichstein, M., Zscheischler, J., and Peng, J.: Soil heat extremes can outpace air temperature extremes, *Nat. Clim. Chang.*, 13, 1237–1241, <https://doi.org/10.1038/s41558-023-01812-3>, 2023.
- Garnier, S., Ross, N., BoB Rudis, Filipovic-Pierucci, A., Galili, T., Timelyportfolio, O’Callaghan, A., Greenwell, B., Sievert, C., Harris, D. J., Sciaini, M., and JJ Chen: *sjmgarnier/viridis: CRAN release v0.6.3*, <https://doi.org/10.5281/ZENODO.4679423>, 2023.
- 595 Gentsch, N., Wild, B., Mikutta, R., Čapek, P., Diáková, K., Schruppf, M., Turner, S., Minnich, C., Schaarschmidt, F., Shibistova, O., Schnecker, J., Urich, T., Gittel, A., Šantrůčková, H., Bárta, J., Lashchinskiy, N., Fuß, R., Richter, A., and Guggenberger, G.: Temperature response of permafrost soil carbon is attenuated by mineral protection, *Global Change Biology*, 24, 3401–3415, <https://doi.org/10.1111/gcb.14316>, 2018.
- 600 Gillabel, J., Cebrian-Lopez, B., Six, J., and Merckx, R.: Experimental evidence for the attenuating effect of SOM protection on temperature sensitivity of SOM decomposition, *Global Change Biology*, 16, 2789–2798, <https://doi.org/10.1111/j.1365-2486.2009.02132.x>, 2010.
- Hicks Pries, C., Ryals, R., Zhu, B., Min, K., Cooper, A., Goldsmith, S., Pett-Ridge, J., Torn, M., and Asefaw Berhe, A.: The Deep Soil Organic Carbon Response to Global Change, *Annual Review of Ecology, Evolution, and Systematics*, 54, null, <https://doi.org/10.1146/annurev-ecolsys-102320-085332>, 2023.
- Hsu, H. and Dirmeyer, P. A.: Uncertainty in Projected Critical Soil Moisture Values in CMIP6 Affects the Interpretation of a More Moisture-Limited World, *Earth’s Future*, 11, e2023EF003511, <https://doi.org/10.1029/2023EF003511>, 2023.
- Kallenbach, C. M., Frey, S. D., and Grandy, A. S.: Direct evidence for microbial-derived soil organic matter formation and its ecophysiological controls, *Nat Commun*, 7, 13630, <https://doi.org/10.1038/ncomms13630>, 2016.
- 610 Koven, C. D., Riley, W. J., Subin, Z. M., Tang, J. Y., Torn, M. S., Collins, W. D., Bonan, G. B., Lawrence, D. M., and Swenson, S. C.: The effect of vertically resolved soil biogeochemistry and alternate soil C and N models on C dynamics of CLM4, *Biogeosciences*, 10, 7109–7131, <https://doi.org/10.5194/bg-10-7109-2013>, 2013.
- Koven, C. D., Hugelius, G., Lawrence, D. M., and Wieder, W. R.: Higher climatological temperature sensitivity of soil carbon in cold than warm climates, *Nature Climate Change*, 7, 817–822, <https://doi.org/10.1038/nclimate3421>, 2017.
- 615 Li, J., Pei, J., Pendall, E., Reich, P. B., Noh, N. J., Li, B., Fang, C., and Nie, M.: Rising Temperature May Trigger Deep Soil Carbon Loss Across Forest Ecosystems, *Advanced Science*, 7, 2001242, <https://doi.org/10.1002/adv.202001242>, 2020.
- Liang, C., Schimel, J. P., and Jastrow, J. D.: The importance of anabolism in microbial control over soil carbon storage, *Nat Microbiol*, 2, 1–6, <https://doi.org/10.1038/nmicrobiol.2017.105>, 2017.
- 620 Liang, J., Wang, G., Singh, S., Jagadamma, S., Gu, L., Schadt, C. W., Wood, J. D., Hanson, P. J., and Mayes, M. A.: Intensified Soil Moisture Extremes Decrease Soil Organic Carbon Decomposition: A Mechanistic Modeling Analysis, *Journal of Geophysical Research: Biogeosciences*, 126, e2021JG006392, <https://doi.org/10.1029/2021JG006392>, 2021.
- Liu, Y., Tian, J., He, N., and Tiemann, L.: Global microbial necromass contribution to soil organic matter, <https://doi.org/10.21203/rs.3.rs-473688/v1>, preprint.
- 625 Meier, I. C. and Leuschner, C.: Variation of soil and biomass carbon pools in beech forests across a precipitation gradient, *Global Change Biology*, 16, 1035–1045, <https://doi.org/10.1111/j.1365-2486.2009.02074.x>, 2010.



- Moyano, F. E., Manzoni, S., and Chenu, C.: Responses of soil heterotrophic respiration to moisture availability: An exploration of processes and models, *Soil Biology and Biochemistry*, 59, 72–85, <https://doi.org/10.1016/j.soilbio.2013.01.002>, 2013.
- 630 Moyano, F. E., Vasilyeva, N., and Menichetti, L.: Diffusion limitations and Michaelis–Menten kinetics as drivers of combined temperature and moisture effects on carbon fluxes of mineral soils, *Biogeosciences*, 15, 5031–5045, <https://doi.org/10.5194/bg-15-5031-2018>, 2018.
- Pallandt, M., Ahrens, B., Koirala, S., Lange, H., Reichstein, M., Schrumpp, M., and Zaehle, S.: Vertically Divergent Responses of SOC Decomposition to Soil Moisture in a Changing Climate, *JGR Biogeosciences*, 127, <https://doi.org/10.1029/2021JG006684>, 2022.
- 635 Parton, W. J., Schimel, D. S., Cole, C. V., and Ojima, D. S.: Analysis of Factors Controlling Soil Organic Matter Levels in Great Plains Grasslands, *Soil Science Society of America Journal*, 51, 1173–1179, <https://doi.org/10.2136/sssaj1987.03615995005100050015x>, 1987.
- Parton, W. J., Scurlock, J. M. O., Ojima, D. S., Gilmanov, T. G., Scholes, R. J., Schimel, D. S., Kirchner, T., Menaut, J.-C., Seastedt, T., Garcia Moya, E., Kamnalrut, A., and Kinyamario, J. I.: Observations and modeling of biomass and soil organic  
640 matter dynamics for the grassland biome worldwide, *Global Biogeochemical Cycles*, 7, 785–809, <https://doi.org/10.1029/93GB02042>, 1993.
- Qin, S., Chen, L., Fang, K., Zhang, Q., Wang, J., Liu, F., Yu, J., and Yang, Y.: Temperature sensitivity of SOM decomposition governed by aggregate protection and microbial communities, *Science Advances*, 5, eaau1218, <https://doi.org/10.1126/sciadv.aau1218>, 2019.
- 645 R Core Team: R: A Language and Environment for Statistical Computing, 2023.
- RStudio Team: Rstudio: Integrated development environment for R., 2018.
- Sierra, C. A., Trumbore, S. E., Davidson, E. A., Vicca, S., and Janssens, I.: Sensitivity of decomposition rates of soil organic matter with respect to simultaneous changes in temperature and moisture, *Journal of Advances in Modeling Earth Systems*, 7, 335–356, <https://doi.org/10.1002/2014MS000358>, 2015.
- 650 Skopp, J., Jawson, M. D., and Doran, J. W.: Steady-state aerobic microbial activity as a function of soil water content, *Soil Science Society of America Journal*, 54, 1619–1625, <https://doi.org/10.2136/sssaj1990.03615995005400060018x>, 1990.
- Sokol, N. W., Whalen, E. D., Jilling, A., Kallenbach, C., Pett-Ridge, J., and Georgiou, K.: Global distribution, formation and fate of mineral-associated soil organic matter under a changing climate: A trait-based perspective, *Functional Ecology*, 36, 1411–1429, <https://doi.org/10.1111/1365-2435.14040>, 2022.
- 655 Soong, J. L., Phillips, C. L., Ledna, C., Koven, C. D., and Torn, M. S.: CMIP5 Models Predict Rapid and Deep Soil Warming Over the 21st Century, *Journal of Geophysical Research: Biogeosciences*, 125, e2019JG005266, <https://doi.org/10.1029/2019JG005266>, 2020.
- Soong, J. L., Castanha, C., Hicks Pries, C. E., Ofiti, N., Porras, R. C., Riley, W. J., Schmidt, M. W. I., and Torn, M. S.: Five years of whole-soil warming led to loss of subsoil carbon stocks and increased CO<sub>2</sub> efflux, *Science Advances*, 7, eabd1343, <https://doi.org/10.1126/sciadv.abd1343>, 2021.
- 660 Sulman, B. N., Phillips, R. P., Oishi, A. C., Shevliakova, E., and Pacala, S. W.: Microbe-driven turnover offsets mineral-mediated storage of soil carbon under elevated CO<sub>2</sub>, *Nature Climate Change*, 4, 1099, <https://doi.org/10.1038/nclimate2436> <https://www.nature.com/articles/nclimate2436#supplementary-information>, 2014.
- Tang, J. and Riley, W. J.: Competitor and substrate sizes and diffusion together define enzymatic depolymerization and  
665 microbial substrate uptake rates, *Soil Biology and Biochemistry*, 139, 107624, <https://doi.org/10.1016/j.soilbio.2019.107624>, 2019.
- Thum, T., Caldararu, S., Engel, J., Kern, M., Pallandt, M., Schnur, R., Yu, L., and Zaehle, S.: A new model of the coupled carbon, nitrogen, and phosphorus cycles in the terrestrial biosphere (QUINCY v1.0; revision 1996), *Geoscientific Model Development*, 12, 4781–4802, <https://doi.org/10.5194/gmd-12-4781-2019>, 2019.



- 670 Todd-Brown, K. E. O., Randerson, J. T., Hopkins, F., Arora, V., Hajima, T., Jones, C., Shevliakova, E., Tjiputra, J., Volodin, E., Wu, T., Zhang, Q., and Allison, S. D.: Changes in soil organic carbon storage predicted by Earth system models during the 21st century, *Biogeosciences*, 11, 2341–2356, <https://doi.org/10.5194/bg-11-2341-2014>, 2014.
- Wang, B., An, S., Liang, C., Liu, Y., and Kuzyakov, Y.: Microbial necromass as the source of soil organic carbon in global ecosystems, *Soil Biology and Biochemistry*, 162, 108422, <https://doi.org/10.1016/j.soilbio.2021.108422>, 2021.
- 675 Wang, G., Post, W. M., Mayes, M. A., Frerichs, J. T., and Sindhu, J.: Parameter estimation for models of ligninolytic and cellulolytic enzyme kinetics, *Soil Biology and Biochemistry*, 48, 28–38, <https://doi.org/10.1016/j.soilbio.2012.01.011>, 2012.
- Wang, G., Post, W. M., and Mayes, M. A.: Development of microbial-enzyme-mediated decomposition model parameters through steady-state and dynamic analyses, *Ecological Applications*, 23, 255–272, <https://doi.org/10.1890/12-0681.1>, 2013.
- Wang, G., Huang, W., Zhou, G., Mayes, M. A., and Zhou, J.: Modeling the processes of soil moisture in regulating microbial and carbon-nitrogen cycling, *Journal of Hydrology*, 585, 124777, <https://doi.org/10.1016/j.jhydrol.2020.124777>, 2020.
- 680 Wang, M., Guo, X., Zhang, S., Xiao, L., Mishra, U., Yang, Y., Zhu, B., Wang, G., Mao, X., Qian, T., Jiang, T., Shi, Z., and Luo, Z.: Global soil profiles indicate depth-dependent soil carbon losses under a warmer climate, *Nat Commun*, 13, 5514, <https://doi.org/10.1038/s41467-022-33278-w>, 2022a.
- Wang, Y., Mao, J., Hoffman, F. M., Bonfils, C. J. W., Douville, H., Jin, M., Thornton, P. E., Ricciuto, D. M., Shi, X., Chen, H., Wullschlegel, S. D., Piao, S., and Dai, Y.: Quantification of human contribution to soil moisture-based terrestrial aridity, *Nat Commun*, 13, 6848, <https://doi.org/10.1038/s41467-022-34071-5>, 2022b.
- 685 Wickham, H.: *ggplot2*, Springer International Publishing, Cham, <https://doi.org/10.1007/978-3-319-24277-4>, 2016.
- Wickham, H., Averick, M., Bryan, J., Chang, W., McGowan, L., François, R., Golemund, G., Hayes, A., Henry, L., Hester, J., Kuhn, M., Pedersen, T., Miller, E., Bache, S., Müller, K., Ooms, J., Robinson, D., Seidel, D., Spinu, V., Takahashi, K.,
- 690 Vaughan, D., Wilke, C., Woo, K., and Yutani, H.: Welcome to the Tidyverse, *JOSS*, 4, 1686, <https://doi.org/10.21105/joss.01686>, 2019.
- Wieder, W. R., Grandy, A. S., Kallenbach, C. M., and Bonan, G. B.: Integrating microbial physiology and physio-chemical principles in soils with the Microbial-Mineral Carbon Stabilization (MIMICS) model, *Biogeosciences*, 11, 3899–3917, <https://doi.org/10.5194/bg-11-3899-2014>, 2014.
- 695 Wieder, W. R., Allison, S. D., Davidson, E. A., Georgiou, K., Hararuk, O., He, Y., Hopkins, F., Luo, Y., Smith, M. J., Sulman, B., Todd-Brown, K., Wang, Y.-P., Xia, J., and Xu, X.: Explicitly representing soil microbial processes in Earth system models, *Global Biogeochemical Cycles*, 29, 1782–1800, <https://doi.org/10.1002/2015GB005188>, 2015.
- Wieder, W. R., Hartman, M. D., Sulman, B. N., Wang, Y.-P., Koven, C. D., and Bonan, G. B.: Carbon cycle confidence and uncertainty: Exploring variation among soil biogeochemical models, *Global Change Biology*, 24, 1563–1579, <https://doi.org/doi:10.1111/gcb.13979>, 2018.
- 700 Xiao, K.-Q., Zhao, Y., Liang, C., Zhao, M., Moore, O. W., Otero-Fariña, A., Zhu, Y.-G., Johnson, K., and Peacock, C. L.: Introducing the soil mineral carbon pump, *Nat Rev Earth Environ*, 4, 135–136, <https://doi.org/10.1038/s43017-023-00396-y>, 2023.
- Yan, Z., Bond-Lamberty, B., Todd-Brown, K. E., Bailey, V. L., Li, S., Liu, C., and Liu, C.: A moisture function of soil heterotrophic respiration that incorporates microscale processes, *Nature Communications*, 9, 2562, <https://doi.org/10.1038/s41467-018-04971-6>, 2018.
- 705 Yu, L., Ahrens, B., Wutzler, T., Schrupf, M., and Zaehle, S.: Jena Soil Model (JSM v1.0; revision 1934): a microbial soil organic carbon model integrated with nitrogen and phosphorus processes, *Geoscientific Model Development*, 13, 783–803, <https://doi.org/10.5194/gmd-13-783-2020>, 2020.
- 710 Zhang, X., Xie, Z., Ma, Z., Barron-Gafford, G. A., Scott, R. L., and Niu, G.-Y.: A Microbial-Explicit Soil Organic Carbon Decomposition Model (MESDM): Development and Testing at a Semiarid Grassland Site, *Journal of Advances in Modeling Earth Systems*, 14, e2021MS002485, <https://doi.org/10.1029/2021MS002485>, 2022.

<https://doi.org/10.5194/egusphere-2024-186>  
Preprint. Discussion started: 29 January 2024  
© Author(s) 2024. CC BY 4.0 License.



Zhang, Z., Pan, Z., Pan, F., Zhang, J., Han, G., Huang, N., Wang, J., Pan, Y., Wang, Z., and Peng, R.: The Change Characteristics and Interactions of Soil Moisture and Temperature in the Farmland in Wuchuan County, Inner Mongolia, China, *Atmosphere*, 11, 503, <https://doi.org/10.3390/atmos11050503>, 2020.

# List of publications

---

**Pallandt, M.**, Lange, H., Meissner, H., Schrumpf, M. Reichstein, M. , and Ahrens, B (in preparation). Soil moisture controls on soil respiration through substrate and oxygen availability.

**Pallandt, M.**, Schrumpf, M., Lange, H., Reichstein, M., Yu, L. and Ahrens, B. Drought counteracts soil warming more strongly in the subsoil than in the topsoil according to a vertical microbial SOC model, EGU sphere [preprint], <https://doi.org/10.5194/egusphere-2024-186>, 2024.

**Pallandt, M.**, Ahrens, B., Koirala, S., Lange, H., Reichstein, M., Schrumpf, M., & Zaehle, S. (2022). Vertically Divergent Responses of SOC Decomposition to Soil Moisture in a Changing Climate. *Journal of Geophysical Research: Biogeosciences*, 127(2). <https://doi.org/10.1029/2021JG006684>

\* Thum, T., Caldararu, S., Engel, J., Kern, M., **Pallandt, M.**, Schnur, R., Yu, L., and Zaehle, S. (2019). A new terrestrial biosphere model with coupled carbon, nitrogen, and phosphorus cycles (QUINCY v1.0; revision 1996). *Geoscientific Model Development* 12, <https://doi.org/10.5194/gmd-12-4781-2019>.

\* **Vermeulen, M.**, Kruijt, B., Hickler, T., Kabat, P., 2015. Modelling short-term variability in carbon and water exchange in a temperate Scots pine forest. *Earth System Dynamics* 6, <https://doi.org/10.5194/esd-6-485-2015>

\* Mücher, C.A., Kooistra, L., **Vermeulen, M.**, Vanden Borre, J., Haest, B., Haveman, R., 2013. Quantifying structure of Natura 2000 heathland habitats using spectral mixture analysis and segmentation techniques on hyperspectral imagery. *Ecological Indicators* 33, <https://doi.org/10.1016/j.ecolind.2012.09.013>

\* These publications were not part of this PhD thesis.

A complete publication record including conference proceedings, reports and peer-review activities can be found here: <https://orcid.org/0000-0002-0645-7269>

# Eidesstattliche Versicherungen und Erklärungen

---

(§ 8 Satz 2 Nr. 3 PromO Fakultät)

Hiermit versichere ich eidesstattlich, dass ich die Arbeit selbstständig verfasst und keine anderen als die von mir angegebenen Quellen und Hilfsmittel benutzt habe (vgl. Art. 97 Abs. 1 Satz 8 BayHIG).

(§ 8 Satz 2 Nr. 3 PromO Fakultät)

Hiermit erkläre ich, dass ich die Dissertation nicht bereits zur Erlangung eines akademischen Grades eingereicht habe und dass ich nicht bereits diese oder eine gleichartige Doktorprüfung endgültig nicht bestanden habe.

(§ 8 Satz 2 Nr. 4 PromO Fakultät)

Hiermit erkläre ich, dass ich Hilfe von gewerblichen Promotionsberatern bzw. –vermittlern oder ähnlichen Dienstleistern weder bisher in Anspruch genommen habe noch künftig in Anspruch nehmen werde.

(§ 8 Satz 2 Nr. 7 PromO Fakultät)

Hiermit erkläre ich mein Einverständnis, dass die elektronische Fassung der Dissertation unter Wahrung meiner Urheberrechte und des Datenschutzes einer gesonderten Überprüfung unterzogen werden kann.

(§ 8 Satz 2 Nr. 8 PromO Fakultät)

Hiermit erkläre ich mein Einverständnis, dass bei Verdacht wissenschaftlichen Fehlverhaltens Ermittlungen durch universitätsinterne Organe der wissenschaftlichen Selbstkontrolle stattfinden können.

---

Ort, Datum, Unterschrift

